Spring 2019

Ecohydrology of aspen and eucalyptus plantations: considerations for management

Jose Antonio Gutierrez Lopez
University of New Hampshire, Durham

ECOHYDROLOGY OF ASPEN AND EUCALYPTUS PLANTATIONS: CONSIDERATIONS FOR MANAGEMENT

By:

Jose Antonio Gutierrez Lopez

BS, Technological Institute of the Oaxaca Valley, 2007

MS, Iowa State University, 2012

DISSERTATION

Submitted to the University of New Hampshire

in Partial Fulfillment of the Requirements for the Degree of

Doctor of Philosophy

In

Earth and Environmental Sciences

May, 2019

This thesis/dissertation has been examined and approved in partial fulfillment of the requirements for the degree of PhD in Earth and Environmental Sciences by:

Dissertation Director, Heidi Asbjornsen,
Associate Professor. Natural Resources and the Environment

Thomas Pypker, Associate Professor, Forest Hydrology
Thompson Rivers University, Canada

Julian Licata. Adjunct Professor, Forest Ecophysiology
Michigan Technological University

Michael Palace, Associate Professor, Geospatial analysis
Associate Professor. Natural Resources and the Environment

Mark Ducey, Professor. Forest Biometrics
Associate Professor. Natural Resources and the Environment

On May 6, 2019

Original approval signatures are on file with the University of New Hampshire Graduate School.

ABSTRACT

ECOHYDROLOGICAL IMPACTS OF BIOENERGY PRODUCTION IN ASPEN AND EUCALYPTUS PLANTATIONS

By

Jose Gutierrez Lopez

University of New Hampshire, May, 2019

Forecast scenarios predict an increase in the demand of alternative sources of energy during the coming decades, such as woody biomass crops (**WBC**). WBC have the potential to become a major challenge for the next generation of researchers, policymakers and land managers. However, the current rationale for promoting plant-based over petroleum-based energy sources emphasizes the benefits of reduced carbon dioxide and other emissions, while giving less attention to potential impacts to water resources.

It is well documented in the scientific literature that trees use large amounts of water for metabolic needs. Water use at the tree and ecosystem level has always been of scientific interest, however, the potential impact of water use in bioenergy plantations is often considered a "possible environmental impact". Thus, understanding the ecological implications of water use in WBC is essential for their sustainable development.

The general goal of my research was to assess potential ecohydrological impacts associated with the production of biomass for bioenergy from aspen (*Populus tremuloides* Mich.) in Wisconsin, USA, and eucalyptus (*Eucalyptus grandis*) plantations in Entre Rios, Argentina. My doctoral research was part of a large international interdisciplinary NSF-PIRE research project that examined the impacts, barriers and opportunities related to bioenergy production across the Americas (USA, Mexico, Brazil, Argentina).

We selected plantation ages within the most common rotation cycles for each species. In Wisconsin, we studied three sites, a 10- and a 24-year-old (YO) coppice plantations, and a reference 34 YO mature forest. In Argentina, we studied two 1 YO plantations one at high and one at regular density, a 4 YO, a 10 YO plantation, and a reference grassland. This was a unique study to determine annual water use based on a combination of tree-level measurements of water use using sap flow sensors, and deterministic models of potential evapotranspiration.

We validated two sap flow methods (heat dissipation and heat ratio), and validated a third method (maximum heat ratio) that is capable of measuring with precision high and low sap flux densities (F_d, $cm^3\ cm^{-2}\ cm^1$). According to the results from the validation studies, we were able to estimate tree-level water use within a 7% error margin (estimated as the difference between observed and estimated sap flow in $L\ h^{-1}$) using heat ratio and maximum heat ratio methods, without generating species-specific parameters. However, using the heat dissipation method, the average estimation error without species-specific parameters was -53%, and improved to 5% once species-specific parameters were generated. Validating the maximum heat ratio method, allowed us to estimate F_d in young trees, which are often excluded from chronosequence studies due to their high F_d. Our estimates of F_d at different plantation ages, allowed us to extrapolate from the tree to the site level, using real tree-level response to various environmental variables.

Our analysis of *P. tremuloides* and *E. grandis* offered contrasting results. In *P. tremuloides* plantations, water use at the site level generally increased with age, even when site density decreased over time (from approx. 6500 to 1900 from 10 to 34 YO). We observed that young plantations (10 YO) used 80% of the annual water early in the growing season, compared to a 45% for the same period in the Mid-aged and Mature plantations. Site effects, specifically soil type and the resulting soil saturation (***S***), had a significant effect on *T* estimates. After modeling the effects of *S*, creating two artificial scenarios (e.g. limited and non-limited *S*) the 10 YO site

showed the highest sensibility to changes in *S*, while the 34 YO mature site was the least affected. Average stand transpiration by site considering the effects of *S* increased with age, which supported our hypothesis regarding the relationship between stand age and stand *T*. However, the relationship between stand *T* was not constant across seasons, which according to our results might be caused by a higher hydraulic stress observed in the 10YO site, compared to the other two sites.

On eucalyptus plantations, when the density remained constant, stand *T* decreased with plantation age, reaching maximum water use rates at around 4 YO and declining afterwards for the remainder of the typical 15 YO rotation cycles. Due to similar site conditions in terms of soil characteristics, we did not observe a strong site effect. Our experimental site at high density (e.g., double of a regular site) showed an increase in average site *T* of 50%, and both 1 YO sites presented an opportunistic pattern in water use, increasing when soil water was available, but decreasing significantly when soil moisture was limiting. Finally, in both plantations we observed that reference evapotranspiration, estimated with the Penman-Monteith equation, was a poor predictor of water use in young plantations. We associate these results to the seasonal patterns of water use in young plantations.

Within the context of bioenergy production, our results provide ample evidence for the importance of water use in bioenergy plantations in the early stages of feedstock production. We also show that plantation density in fast and slow growing species, impacts the way trees respond to water availability in the soil.

Dedication

To my family

My friends

To all members, past, current and future, of the ecohydrology Lab, at UNH

To Juana Inés de Asbaje y Ramírez de Santillana (1648-1695)

Acknowledgements

All the members of my committee, for their support, patience and constructive feedback

To the Natural Resources and Earth Systems Sciences at UNH

To all the INTA (Concordia, Argentina) personal

The owners and managers of BEyGa Humaitá

The NSF-PIRE program. The grant number: 1243444

To all PIRE collaborators

Table of contents

List of Tables

List of Figures

CHAPTER I

GENERAL INTRODUCTION

National trends and major research advancements

The increasing demand for alternative sources of energy has expanded the research frontiers of production and processing systems for bioenergy (Perlack et al. 2005). However, unlike algae or agricultural crops (e.g., corn, soybean, grass biomass) woody bioenergy crops (**WBC**) or short rotation woody crops (**SRWC**) (e.g., poplar or eucalyptus plantations) are still behind in technological advancements. Some of the reasons behind this lag are the complexity of management strategies, systems and practices that would be required for sustainable large-scale production of bioenergy derived from WBC or SRWC; practices that need to be adaptable to a variety of local conditions (BRDB 2011, White 2010). In other words, sustainable development of WBC is largely dependent on local or regional-based studies. In Argentina, fast-growing plantations of the *Eucalyptus* genus (and other WBC) tends to focus on timber production, and the debate over national bioenergy development is limited to small trials, primarily on small crops (Perry 2009, van Dam et al. 2009) as will be shown in Chapter IV. As a result, this introduction will not discuss the development of the section in Argentina. Conversely, in the USA, the bioenergy sector has received more attention and among various topics, it deals with the complex debate of the feasibility of feedstock production to meet national demands.

Despite its complexity, specific areas within the WBC field and important research advancements have been conducted, such as: the development of policies (Molony 2011), financial analysis (El Kasmioui and Ceulemans 2013), production and harvesting (Abbas et al. 2011), technological advancements for storage, refinement, yield (Dillen et al. 2013) and the impacts to the hydrologic balance (Babel et al. 2011). At the national level, the United States

Department of Energy (USDE), through the Bioenergy Technologies Office (BETO) published in 2005 an extensive review on the feasibility of the required supply for bioenergy for a variety of sources including crops and WBC (Perlack et al. 2005), which covered several potential concerns, including transportation, access, costs associated with biomass removal, transportations costs, labor availability, among others. In May 2013, the same office published a five-year program of research, development, demonstrations and deployment of activities aimed to achieve large scale production of bioenergy (BETO 2013). However, both reports (from 2005 and 2013) give little attention to the potential ecohydrological impacts of bioenergy production.

Other documents published by the USDE, the United States Department of Agriculture (USDA), and the BETO indicate that at the federal level, the complexity of the bioenergy industry is such, that issues regarding the impacts to hydrological services or water balance are often disregarded as mere "possible environmental impacts" and are not fully addressed (BETO 2013, BRDB 2011, Perlack et al. 2005, White 2010). The multi-year program released in May of 2013 by the BETO establishes the objective "(to) maintain or improve water quality, reduce consumptive water use, and improve water use efficiency" as the main strategy to deal with sustainability issues associated with ecohydrological impacts of bioenergy production. However, in this 170+ page document, this is the only mention of a strategy to address hydrologic concerns of biomass production (BETO 2013).

It can be argued then, that the development of national level policies can speed or halt the development of projects aimed at understanding the ecohydrological impacts of the establishment of WBC or SRWC. This is something the BETO acknowledges, stating that the key issues of this year (2015) in the global bioenergy race are: (a) local manufacturing, (b) emerging pathways and innovative technologies and (c) national and state policies. Despite the

influence of policies, our understanding of the impacts of WBC on local water balance has progressed substantially.

A few examples of important research advancements related to, or that complement ecohydrological impacts of bioenergy production and WBC/SRWC, that have not yet been fully reflected in national-scale programs are: selection of potential forest species (Christersson 2010, Dougherty and Wright 2012, Evans et al. 2010, Tharakan et al. 2003), suitable areas for production (Cartisano et al. 2013, Headlee et al. 2013), yields based on stand composition (Nelson et al. 2012), guidelines for harvesting (Abbas et al. 2011), hydrological impacts (Babel et al. 2011) impacts to soil properties (Baum et al. 2013), environmental impacts (Rowe et al. 2009, Wu et al. 2013), and nutrient amendments (Li et al. 2012) among others.

Other research advancements related to WBC within the biotechnology field that are also worth mentioning are: the genetic manipulation of trees to increase branch production and total biomass in poplar and chestnut trees, which found positive results modifying the CsRAV1 gene to induce sylleptic[1] branches (Moreno-Cortes et al. 2012). Pilate et al (2012) reported, based on 20 years of field trials of transgenic trees, that it is possible to reduce lignin in cell walls (to increase cellulose yield), but with negative effects on plant growth. Conversely, Wang et al (2011) reported increased rates of growth and development in hybrid poplars after the reduction of the expression of the SHORT-ROOT gene. Also within this field, the *Eucalyptus grandis* genome was recently published by Myburg et al (2014), which has been considered a landmark that will redefine and improve breeding programs oriented towards the production of bioenergy, in a similar way the genome of Populus trichocarpa (Torr & Gray) revolutionized breeding poplar programs (Tuskan et al. 2006).

[1] Growth in which branches develop from a lateral meristem, without the formation of a bud or period of dormancy, when the lateral meristem is split from a terminal meristem.

Water-related research gaps in bioenergy production

To understand potential ecohydrological impacts of bioenergy production, it is important to review first water use at the plant level and the driving factors. Dynamics of plant water use vary with age and it is greatly influenced by environmental factors (Gochis and Cuenca 2000, Muller and Lambs 2009). For example, a single mature poplar tree can vary from 50 to 100 L of sap per day during the peak of the growing season (Wullschleger et al. 1998b), the same tree growing under a different set of management or environmental conditions (e.g., high density or extended periods of drought) can change drastically its water use patterns and have completely different seasonal patterns of water use. Inter-annual (i.e., seasonal) environmental changes, and species-specific structural changes within the tree, like leaf area and total biomass have similar effects (Forrester et al. 2010a, Hubbard et al. 2010).

The scientific literature that focus on the driving factors that influence water use patterns in forest ecosystems, particularly plantations, can be grouped into two categories: (a) the physiological response of plants to changes in resource availability and environmental conditions (e.g., light, soil moisture, nutrients, light, temperature), and (b) changes in plant structure and growth patterns that result from adaptation to changes in the available growing space and subsequent changes in horizontal and vertical stand structure caused by plant interactions (e.g., canopy closure, abrasion, etc.), disturbance, or other factors. From this classification, it is possible to identify areas where our current scientific understanding is limited.

Both physiological changes and structural adaptations in plantations start at the canopy and leaf level. Research has shown that LAI and transpiration (or canopy conductance) are linearly related in several tree species, including aspen and eucalyptus (Allen et al. 1999, Blanken et al. 1997, Forrester et al. 2010a, Kull and Tulva 2000, Wilske et al. 2009). However,

the seasonal changes between these two variables due to the response of trees to resource availability or phenology, is often ignored or assumed to be constant. Studies have found that as a plantation ages, the portion of the canopy that is shaded, or under constant indirect light, increases over time until the stand reaches canopy closure, and the amount of light that reaches lower branches is significantly reduced. Lower leaves that are not able to photosynthesize (or maintain a positive carbon balance) at reduced light levels, die off, reducing the total photosynthetic surface of the canopy (Kozlowski et al. 1991), thus decreasing transpiration and water use rates.

These patterns of canopy reduction over time and other structural adaptations and subsequent impacts on stand water use, are undoubtedly different among species and even within the same species growing in different regions. Studies on species specific patterns have found that depending on light assimilation, leaf shape and photosynthetic rates (Salisbury and Ross 1992), trees can continue developing leaves past canopy closure. Clear examples are pine plantations, which due to the relative smaller area of individual needles, allow for more light to pass through the canopy (high canopy transmittance) (Ewers et al. 2007, Stenberg et al. 1994), increasing the amount of light that reaches lower branches. Another advantage of pine needles over broad-leaved trees is their ability to photosynthesize at lower light intensities (red and far-red frequencies (656-714 nm)), typical of the understory (Kozlowski et al. 1991, Taiz and Zeiger 2002), this allows several conifer species to continue canopy development past canopy closure.

Returning to aspen and eucalyptus, given their larger leaf area, low shadow tolerance and high water demands, it is highly unlikely for shaded aspen leaves to maintain positive carbon balances under these conditions (Pallardy and Kozlowski 1979), reducing the total leaf area and the active photosynthetic surface. However, studies looking at the effects of structural adaptations (e.g., canopy adaptation to growing space and self-thinning crowns as a result of

negative carbon balances) over time of aspen or eucalyptus trees growing in plantations at different stand ages are not very common (Forrester et al. 2010a, Kull and Tulva 2000). We know however, is that the factors affecting specific canopy closure patterns in plantations, are unique, and different from those affecting natural stands of the same species. A clear example for plantations is crown abrasion, the reduction in crown size, and the increment of inter-crown openings, resulting from sway action, where the altered vertical structure of trees species lowers their structural integrity, potentially reducing crown size as the plantation matures (Peltola 1996, Sellier and Fourcaud 2009).

Physiological changes and structural adaptations have been also observed in eucalyptus plantations. In a recent study on eucalyptus plantations varying from 2 to 8 years old, Forrester et al (2010a), reported that as trees aged, their sap velocities decreased (observed in 8 YO trees). They argue that trees compensate water requirements by modifying their LAI to sapwood area ratios. While allometric relationships have long been developed and the growth dynamics are well understood for major eucalyptus and poplar varieties, this self-regulation process (by which trees balance water requirements with the required area of conductive tissue for water transport) (i.e., sapwood area), can have major impacts on water use in WBC where growing patterns are modified due to management practices oriented to increase biomass productivity (i.e., high density, or short rotations).

Belowground dynamics are not the exception; access to soil moisture and nutrients also plays an important role in defining canopy shape, LAI and transpiration rates. Research in eucalyptus trees has shown that water limitation can reduce canopy development (Beadle in (Sandanandan and Brown 1997)), particularly leaf area. Similarly, deficiencies in nitrogen have been shown to reduce photosynthetic rates in melaleuca and eucalyptus species (Nguyen et al. 2003). Conversely, if water and nutrient limitations are eliminated by fertilizing and irrigating,

studies in poplar plantations have observed increments in total stand growth of up to 18% (Kim et al. 2008). These results were similar to observations on transgenic poplar trees using enriched ^{15}N as a tracer of nutrient uptake, where it was found a higher nitrogen assimilation and overall growth when nutrient limitations were eliminated (Man et al. 2005).

Unlike natural forests or plantations for timber production, WBC of eucalyptus and poplar are often planted at high densities to increase site productivity (Almeida et al. 2007, Tullus et al. 2009). In these sites, canopy closure, maximum LAI, etc., and the subsequent effects on water use -as previously discussed- may occur much earlier than in regular unmanaged stands, which in turn, can have consequences for the stand water budget (Fernández and Gyenge 2009, Oguntunde 2007) not fully documented or understood.

The timing at which these plant, and stand processes occur, can potentially impact the water balance in completely different ways (i.e., early depletion of soil moisture, reduced outflows and runoff) in unforeseeable ways. However, due to the relatively new development of methods to reliably estimate water use at the plant level (i.e., high precision sap flow methods), our current scientific understanding is strongly focused on stand growth dynamics and biomass accumulation under various management conditions (Kauter et al. 2003, Tullus et al. 2009, Werner et al. 2012), giving less attention to the ecohydrological impacts of WBC (Bungart et al. 2001, Jassal et al. 2013).

Considering then the reduction in water use with age in WBC, caused by previously discussed physiological changes and structural adaptations, the often-attributed negative impacts of increased water use in these plantations, can be potentially managed or regulated with longer rotation cycles. The logic behind this argument is that, if a production system is constantly running at its maximum capacity (i.e., rotation cycles focused on high productivity), the stress on water resources should be similarly intensive. Then increasing rotation cycles will by default,

include periods of time when water use requirement for plant growth is not as intensive. The later will in turn allow plantations to function as natural regulators of water flows (e.g., reducing runoff and increasing infiltration) and, hence, improve impacts on water resource sustainability. Understanding how water use changes over time in a plantation or managed forest, can be of great value to propose long-term forecasting scenarios of water use and biomass accumulation, as shown in Figure I-1.

Finally, considering that most eucalyptus and aspen plantations are harvested at or before 15 years of age (Forrester et al. 2010a, Tullus et al. 2009), and some use even shorter rotation cycles, studies of water use dynamics in bioenergy plantations of 15+ years-old, are rare and highly important to understanding the implications of water use in WBC plantations of aspen and eucalyptus on the overall stability of the ecosystem.

Hydrological services and biomass accumulation tradeoffs

Hydrological services (**HS**) are part of the various environmental services that society requires from forests, and in many regions of the world represent the base of livelihood of local communities. Given that water quality and quantity are considered the most important of services forests provide to society (Hamilton et al. 2008), understanding the impacts of WBC have on hydrological services is essential for their sustainable development, but most importantly, to guarantee that the livelihoods of local communities are not compromised.

At the ecosystem level, impacts of WBC on HS has been addressed at the national level (Cartisano et al. 2013, Davis et al. 2012, White 2010, Zalesny et al. 2012, Zamora et al. 2013), and around the world in various environmental conditions in Australia (Sochacki et al. 2007), the United Kingdom (Rowe et al. 2009), France (Toillon et al. 2013), Canada (Jassal et al. 2013), among several others. The goal of these studies is often to understand direct impacts of biomass

production on HS, to provide policy-makers and land managers science-based information to achieve sustainable management. Regionally and at the state level, in the USA, several publications make evident that steps are being taken to address potential impacts of bioenergy production to HS (Indiana: (IDNR 2007); Virginia: (Jackson 2007); South Carolina: (SCFC 2012); and Wisconsin: (Herrick et al. 2009, Radloff et al. 2012), among others).

Nonetheless, despite the increasing scientific interest and research initiatives on bioenergy-water relationships, much work still needs to be done to fully address the ecohydrological impacts of the production of bioenergy using various species and growing conditions (BETO 2013, Perlack et al. 2005). The important issue at hand is that intensive production of bioenergy, will likely impact HS that provide direct benefits to society through HS (e.g., water infiltration, outflows and water yield). Forest management for HS alone is inherently complex, which combined with management that aims to maximize biomass production, results in conflicting management strategies due to the constant overlap in goals. Since the primary object of bioenergy production of to maximize crop yield, biomass production often leads to higher water use at the stand level, reducing water outflows and thus creating direct negative impacts to the ecosystem and its HS (e.g., water yield, water balance).

The dynamics of biomass accumulation (e.g., potential yield, mean annual increment (**MAI**), periodic annual increment (**PAI**)) are well documented for a variety of softwood species, in part due to the strong importance of these studies, which are required to elaborate energy scenarios at the national level, as previously mentioned (Perlack et al. 2005). At this point, the scientific literature has focused on the most common management systems for WBC, such as: (a) short rotations; (b) short rotation with coppice; (c) harvest residues and (f) hazard-fuel reduction (White 2010). Short rotation woody crops (**SRWC**) of softwood species such as hybrid poplars (Populus spp.), willow (Salix spp.), Sycamore (Platanus spp.) and silver maple (Acer

saccharinum L.) have received the greatest attention (White 2010), in part due to their ability to achieve high biomass production over short time spans and with low production inputs, as well as their wood properties, known for a relatively easy conversion to fuel (Lasch et al. 2010). Coppice systems have also been used in some eucalyptus species (e.g., Eucalyptus grandis), which are also commonly managed under short rotations of varying lengths (Dougherty and Wright 2012, Mizrachi et al. 2012, Sochacki et al. 2007).

Previous research on SRWC in poplars and willows has provided evidence on the potential impacts to HS under future climate change conditions (Lasch et al. 2010), potential nitrogen and CO_2 fluxes and greenhouse gas mitigations associated to their production (Balasus et al. 2012, Hansen et al. 2013, Verlinden et al. 2013), the impacts of their production to water quality, soil organic matter and microbial communities (Baum et al. 2013), and the quality and quantity of the biomass that can be harvested (Kauter et al. 2003). However, despite the current state of knowledge on SRWC, there are several questions that remain unanswered regarding water use patterns and impacts on HS of WBC.

Water use in plantations

Trees are grown in managed plantations to produce desirable characteristics across the stand (bole height and diameter). In WBC, the goal is often to maximize production per unit of land (Forrester 2013, Nelson et al. 2012, Tullus et al. 2009). Each year thousands of hectares are added to these artificial ecosystems by either managing naturally occurring forests (e.g., aspen stands (Tullus et al. 2009)), or by replacing existing land covers (e.g., eucalyptus plantations (Forrester et al. 2010a)). In both natural forest under coppice management, and plantations that replace existing vegetation, understanding their water use dynamics is fundamental in order to foresee potential negative impacts.

Establishing a plantation replacing the original land cover changes dramatically the vertical and horizontal water dynamics of the new cover. Vertically, the stand dynamics that are altered the most in the established plantation are: interception, throughfall, evaporation, transpiration and water use partitioning (Dunisch et al. 2003, Forrester 2014b, Massonnet et al. 2008, Zhou et al. 2004). Water partitioning (i.e., plants accessing water from different soil layers or water sources at a given time (Campoe et al. 2012, Hunt and Beadle 1998) is modified when trees of similar root characteristics and water requirements access intensively the same water resources. Horizontally, movement of soil water, nutrient transportation, evaporation, and transpiration distribution are the most affected stand dynamics (Binkley et al. 2013, Forrester 2014b), of the newly established plantation. Horizontal changes in evapotranspiration patterns are the result of low variability of transpiration rates throughout the plantation, which in turn reduces water and nutrient movement in the soil.

The extent to which the land cover change affects water use dynamics is also governed by the location of the site, the evaporative demand of the environment and the potential evapotranspiration of both the replaced and the introduced land covers. Research in eucalyptus plantations in Southeast Australia demonstrated that water use is related to stand age. Their results indicate a range from 0.4 mm day^{-1} to 1.9 mm day^{-1} in stands of 2 and 6-7 year-old (**YO**) trees, respectively (Forrester et al. 2010a). Hubbard et al (2010) found a range in daily water use from 2.6-3 mm d^{-1} (based on total water use per year) in eucalyptus plantations of 8 YO in Southeast Brazil. Studies of water use in 12 YO poplar plantations have found water use ranges from 2.2-6.7 mm d^{-1} in Germany (Petzold et al. 2011). However, since no reference water use rate of the replaced ecosystem is provided, it is hard however, to assess the impact these plantations had on the water balance.

Our scientific understanding of water use dynamics in plantations, and its implications to the ecosystem) has increase significantly in the last decade, and has also covered subjects such as carbon fixation and nutrient uptake, among others (Binkley 2004, Forrester 2014a, Forrester et al. 2006, Forrester et al. 2004, Forrester et al. 2012, Forrester et al. 2010b, Stape et al. 2008, Stape et al. 2010, Tricker et al. 2009). However, although many soil-plant-atmosphere processes (e.g., photoinhibition, water uptake, etc.) are well understood, there are still few studies that have dealt with the potential ecohydrological impacts of bioenergy production in plantations (e.g. (Wilske et al. 2009)). Further, log-term plans for bioenergy production, do not fully address issues regarding water quality and quantity in bioenergy plantations, and are often regarded as mere "potential negative effects" (BETO 2013, BRDB 2011).

Higher productivity of plantations of aspen and eucalyptus oriented for bioenergy purposes has shown to increase water use rates and result in hydrologic stress at both the plant and the stand scale, (Berndes 2008). The timing at which maximum water use occurs, however, depends largely on stand dynamics and characteristics of the species. Several studies have analyzed water use dynamics in eucalyptus (Forrester et al. 2010a, Hubbard et al. 2010, Morris et al. 2004), poplars (Jassal et al. 2013, Kim et al. 2008, Tricker et al. 2009, Xiao et al. 2013), and studied their respective biomass accumulation dynamics (Forrester 2013, Forrester et al. 2004, Kauter et al. 2003, Tullus et al. 2009), which at this stage are well documented and understood. However, only a few studies have linked the water use dynamics, biomass accumulation and their respective impacts at the stand and watershed level that result from the production of WBC for bioenergy, and how these impacts develop over time as plantations age (Forrester et al. 2010a, Hunt and Beadle 1998, Jassal et al. 2013, Morris et al. 2004).

If the amount of biomass accumulated is compared to the amount of water used during the same period, it is usually agreed that plants require vast amounts of water for their metabolic

needs (Hillel 2004). Based on preliminary results from our measurements in eucalyptus trees, trees can transpire in a day the amount of water equivalent to their dry weight. This excessive water use can often decrease significantly the water content in the surrounding soil. Based on our current understanding of water-carbon exchange dynamics, we can argue that at the ecosystem level, plant water uptake is a bidirectional process, in the sense that it can both regulate and maintain a balance between water inputs (precipitation, snowfall, etc.) and water outflows (runoff, deep percolation, etc.), but these regulation varies depending on the type of forest (natural vs. artificial/plantation).

Using eddy covariance techniques, research conducted in Canada on hybrid poplar plantations observed that plantations are able to shift from carbon sources to carbon sinks. According to Jassal et al. (2013), a newly established plantation can go from a carbon source (1.5 Mg C ha^{-1} y^{-1}) in its first year, to a carbon sink (0.8 Mg C ha^{-1} y^{-1}) by the third year of establishment. Their data also indicates that during high water demand periods, transpiration exeeded precipitation. These results provide evidence that even at an early age, hybrid poplar plantations can store large quantities of carbon, however, in the process, large quantities of water are lost through transpiration (272 and 321mm, 2010 and 2011, respectively). However, a recently published large-scale review of several ecosystems ranging from forestlands to pastures, provided evidence that water use and carbon acumulation dynamics are strongly influenced by latitude and elevation. Their conclude that gross primary productivity and transpiration decline with increased elevation, which leads to a reduction in net primary productivity with increasing altitude Xiao et al. 2013).

Studies from around the world (Di Matteo et al. 2012, Dillen et al. 2013, Petzold et al. 2011, Tullus et al. 2009, Werner et al. 2012, Zalesny et al. 2012) have reported high carbon accumulation estimates, unfortunately several of these studies focus on carbon accumulation

alone, and no estimates of water use are provided, making it difficult to assess water-carbon tradeoffs. However, understanding the local productivity and the potential responses to environmental conditions, it is possible to identify management practices that best fit environmental conditions of interest.

Methods for water use monitoring in woody species

Estimating water use at the tree level presents various challenges, which are directly associated to the methods used. Generally speaking all methods can be classified into direct or indirect. Direct methods are those that measure the actual water use gravimetrically in potted trees or using lysimeters (McCulloh et al. 2007, Sperling et al. 2012). Indirect methods rely on the measurement of a secondary property, process or variable, to infer water use. Mechanistic methods[2], such as Penman-Monteith, Priestley-Taylor, are also indirect and are based on assumed or validated tree-level responses to environmental variables. Clear examples of indirect methods are those that use heat to trace sap movement within the sapwood (Burgess et al. 2001a, Cohen et al. 1981, Granier 1985). These methods are commonly referred to as "thermometric", and are themselves classified into those that use constant heat and those with pulsed heat, each with their own sub-classification (Vandegehuchte and Steppe 2013b).

Thermometric sap flow methods (**TSF**) are by far the most used to estimate water use at the plant level. Sap flow sensors following various methodologies have been used in a variety of crop (Bethenod et al. 2000, De Swaef and Steppe 2010, Gerdes et al. 1994, Senock and Ham 1995, Zhang and Kirkham 1995) and tree species (Allen et al. 1999, Bleby et al. 2004, Fernandez et al. 2006, Gebauer et al. 2008). TSF methods are considered an important tool for plant

[2] Those that describe phenomena in purely physical or deterministic terms

irrigation and understanding of plant water use requirements. However, almost all are empirical and rely on tree or species-specific calibration (Vandegehuchte and Steppe 2013b).

Within the TSF methods, the most common ones used on woody species, that were also used in my research are: the heat pulse method (HPM, Cohen et al. 1981), the heat dissipation method (HDM, Granier 1985), and a relatively recently developed variation of the HPM able to measure reverse flows the heat ratio method (HRM, Burgess et al. 2001b). Despite being commonly used, several studies have highlighted the weaknesses of both HRM and HDM (Lu et al. 2004). The advantages, main contributions and weaknesses of each method, can be easily understood considering their working principles.

The HPM consists of two probes, spaced 0.5 to 1.5 cm apart. The probes are inserted parallel to the direction of sap flow. The lower probe is a heating element and the upper probe a thermocouple (or set of thermocouples positioned at different sapwood depths). This method works by releasing a pulse of heat of known dimensions and its behavior is tracked within the wood matrix for a bout 100 seconds after the release of the pulse. To estimate sap velocity (cm h^{-1}) and sap flow (L h^{-1}), the method relies on the maximum increase in temperature (ΔTemp) observed in a thermocouple at a radial distance "r" from the heater, and the time it takes to reach this temperature (ΔTime) (Cohen et al. 1981, Marshall 1958). Identifying medium to high sap velocities is relatively easily, due to the distinctive sharp peaks when ΔTemp versus ΔTime are plotted. At low flows, however, distinguishing ΔTime at maximum ΔTemp becomes more ambiguous due to the shape of the curve (i.e., ΔTemp is distributed over a larger time frame).

The HDM consists of two probes, installed 10-15 cm apart, a heated probe and a temperature reference probe. Both probes contain a thermocouple, and the upper probe is kept at a constant temperature (~0.2 W m^{-1}) applying a constant current through the heating element made of constantan wire. This method has been simplified in a way that no actual temperature

measurements are needed, using a single constantan wire to connect both thermocouples (from the heating probe and reference temperature probe) from their negative ends, and considering the principles of the Seebeck effect, differential voltage in millivolts (mV) can be read across both positive ends (copper wire), yielding a mV reading equivalent to the difference in temperature between heated and reference thermocouples (Granier 1985). The differential voltage across the probes is monitored at short intervals (5-60 seconds), and then averaged over more manageable time frames (10-30 minutes). This voltage difference is then correlated to sap flux density (m^3 m^2 s^{-1}). While this method was not developed for a specific set of environmental conditions or specific range of sap velocities, research has shown it is more suitable for medium to high sap flux ranges and for tree species with ring pores.

The HRM consists of three parallel probes spaced 0.5 cm apart. The middle probe is a heating element and the lateral probes are thermocouples. The number of thermocouples varies depending on specific (often user-defined) configuration. A typical measurement starts with the measurement of temperature for 30 seconds, then a 2-4 second pulse heat (~210 W m^{-1}) is applied, and temperature is monitored for another 110 seconds. Heat pulse velocity (cm h^{-1}) and sap flow (L h^{-1}) are estimated based on equations that use the ratio of the average change in temperature above and below the heater (ΔTemp), estimated from 60 to 100 seconds after the heat pulse (Burgess et al. 2001b). HRM was developed for dry environments and scenarios where the movement of sap within the trunk is relatively slow. Recent publications have shown the method is more suitable for sap velocities ranging from 0 to 45 cm h^{-1} (Vandegehuchte and Steppe 2013a), with the ability to measure inverse flows within the same range.

Important contributions

All methods played a critical role in improving our understanding in the following five major areas of plant physiology: (a) the role of stomatal and boundary layer conductance on water use, (b) whole-tree hydraulic conductance, (c) vapor and liquid phase water transport, (d) moving of water to and from storage in sapwood and (e) vulnerability of whole-plant to water cavitation (Vandegehuchte and Steppe 2013a, Wullschleger et al. 1998a). All methods offer unique advantages to estimate water use at the plant level that would be technically difficult using alternative methods, such as weighing lysimeters (Bryla et al. 2010, Evett et al. 2009), radioactive isotopes (Liesche et al. 2015) or dyes (Burgess et al. 2000).

The HPM, was the first TSF method used to explore water use at the plant level. Prior to the development of this method, researchers were limited to studies using isotopic tracers or chemical dyes, which required to cut the stem to trace sap movement (Huber 1932, Marshall 1958), and often resulted in extremely high estimates. Using this methodology, it was observed that sap flow velocities or sap flux densities had marked and more conservative ranges of sap flow rates based on the anatomy of the conducting tissue (i.e., ring porous, diffuse porous and non-porous). A comprehensive list of early estimates and a comparison with various methods used at the time can be found in early studies (Hinckley et al. 1978). However, Swanson (1994) who acknowledged that Marshall's (1958) work placed sap flow research on a strong theoretical base, and today the importance of the method remains unquestioned in the field.

The HDM has been an invaluable tool that simplified the methodology to estimate water use in a wide range of species including Scots pine (Oliveras and Llorens 2001), grapevines (Braun and Schmid 1999), Douglas Fir pine (Phillips et al. 2002), cashews trees (Oguntunde et al. 2004), coffee trees (Pimentel et al. 2010), and more recently palms (Sperling et al. 2012). By simplifying sap flow measurements, Granier (1987) showed that if the spatial variability is

considered during measurements, stand water use can be estimated, something that was considered technically challenging or impossible. More recently, studies using HDM have shown that stand and tree-level water use can be inferred and modeled from the relationship between environmental variables and sap flow (Lambs and Muller 2002, Lundblad and Lindroth 2002).

HRM, an improvement to the HPM developed by Burgess et al. (2001b) has allowed researchers to measure low and reverse flows. These improvements have provided new insights on the dynamics of water use. For example, using this method, Burgess et al. (2004) observed that Sequoia sempervirens are able to reverse the plant-atmosphere continuum via foliar uptake. Previously, using the same methodology, Burgess et al. (2000) provided evidence that upon water uptake, Banksia prionotes, an Australian phreatophyte, is able to redistribute water within the root system in a process known as "inverse hydraulic lift". Other relevant finding related to measurement precision, is the measurement of nocturnal transpiration (Buckley et al. 2011), which we now know in some species can be greater than 10% (Forster 2014), but was previously assumed to be zero. And last the measurement of sap flow in individual petioles, which was previously possible only via gas exchange measurements due to its low magnitude (flows lower than 5 g h^{-1}) (Clearwater et al. 2009).

Weaknesses

The original work on the HPM by Marshall (1958) was based on the heat convection-conduction theory for a infinitely large, isotropic and homogeneous medium where an infinitely small source of heat could release instantaneous heat pulses, taking point measurements around the heat source. In reality, these assumptions are uncommon, resulting in over-estimation of sap velocity. Considering sap flow based on wood anatomy properties, specifically the arrangement of the conducting tissue (e.g., tracheids or pores), point measurements tend to miss the

conductive area, especially in ring porous species (e.g., quercus, fraxinus), leading to underestimation of sap flow. While the original assumptions of HPM have been addressed (Cohen et al. 1981, Kluitenberg and Ham 2004, Vandegehuchte and Steppe 2012), the method still faces challenges with ring porous species. Further, to estimate the variability of the radial profile, more than one measurement point is needed, increasing the instrumentation, data storage and data processing requirements, and installation costs, which can range from 5 to 10 thousand dollars (estimated in 2014), per single sap flow station, depending on the sampling detail and method or methods used.

Since the HDM requires constant heat, the user relies heavily on custom-made current regulators, which, given the fixed resistance of the heating elements, provide an exact and constant temperature. A common error is to apply the wrong current for a given resistance, which results in a higher or lower wattage (or heater temperature) than the 0.2 W recommended by the method (Granier 1985). A common uncertainty with HDM is the potential effect of the wattage applied to the heater on sap flow measurements. Operators often use the original equations to estimate sap flux, but modify the characteristics of the sensors to fit requirements of the species being studied (Lu et al. 2004). Since the original parameters and equations were developed for specific sensor characteristics (e.g., length, resistance of heater, materials, etc.), the user can potentially under, or overestimates sap flow rates. HDM requires the precise measurement of the maximum temperature observed between the heated and the reference probe (ΔTMax), which occurs in the absence of sap flow, particularly at predawn. However, ΔTMax is highly influenced by natural temperature gradients (NTG) in the environment (Lu et al. 2004, Regalado and Ritter 2007).

The HRM works as expected within a range of sap velocities from 0 to 45cm h^{-1} (Vandegehuchte and Steppe 2013b) and after this range, the linearity between TSF and

gravimetric sap flow (**GSF**) breaks down. In cases where sap velocities are significantly high (>70 cm h^{-1}), this relationship disappears altogether. Part of this problem comes from the way the method described by Burgess (2001b) works. After the release of the pulse, the ratio is estimated from the data collected from temperatures from 40-100 seconds. At this point, based on sap velocity speed and NTG's, deltas for lower thermocouples can be close to zero, resulting in fictitious and extremely high ratios, positive and negative. It is possible however, to implement new algorithms to process the data and correct for the effect of NTG's (Vandegehuchte et al. 2015), and potentially increase the range of velocities the measurable with HRM.

In technical terms power consumption is a key disadvantage of HDM over HPM and HRM. Due to its constant-power requirements, a single HDM probe requires more power per unit of time than a HRM. While a single pulse (2-4 seconds) of HRM delivers ~210 J s^{-1} (compared to only ~20 J s^{-1} of HDM), total consumption over time is much lower than HDM. It takes only about 10 seconds for a single HDM sensor to use the power consumed by a single pulse of HPM and HRM.

Calibration experiments

The best way to address all these potential sources of error in sap flow studies is through the use of calibration or validation experiments, where TSF estimates are compared to GSF. Validation experiments are technically challenging, especially if the goal is to validate sap flow methodologies for large trees (e.g., (McCulloh et al. 2007, Sperling et al. 2012)). Nonetheless, validation experiments are regularly used in laboratory setups (Bush et al. 2010, Clearwater et al. 1999, Hubbard et al. 2010, Steppe et al. 2010, Sun et al. 2012). However, these are often criticized for simplifying and/or omitting environmental (e.g. temperature, solar radiation, etc.)

and physiological factors difficult to replicate and predict in laboratory setups, such as variability of water use within the tree crown.

Another common technique for validation of sap flow sensors is severing the stems of small trees (diameter < 15 cm), put them on water reservoirs, and monitor water use gravimetrically, allowing a direct comparison between TSF and GSF. These method, often referred to as the "cut-tree method", has been performed in a variety of species such as *Pinus patula* (Alvarado-Barrientos et al. 2013), *Eucalyptus regnans* (Dunn and Connor 1993), Aspen (*Populus tremuloides*) and Birch (*Betula papyrifera*) (Uddling et al. 2009), Sweetgum (*Liquidambar styraciflua* L.), Eastern Cottonwood (*Populus deltoids* Bart.), White Oak (Quercus alba L.), American elm (*Ulmus americana* L.), Shortleaf pine (*Pinus echinata* Mill.), Loblolly Pine (*Pinus taeda* L.) (Sun et al. 2012), Olive (*Olea europaea*), Plum (*Prunus domestica* L.), Orange (*Citrus sinensis* L.) (Fernandez et al. 2006). The reported variation between TSF and GSF observed in these studies (up to five fold in some cases (Hubbard et al. 2010)), together with the diversity of species in which validation studies have shown discrepancies (between TSF and GSF), confirms the long-standing assumption that sap flow studies require species and site specific validations, as long as these are feasible.

Mechanistic methods to estimate water use in non-woody species

Measurement of water use in non-woody species, particularly grasses and grasslands is inherently difficult due to their small stem sizes, and the variety of species to consider per unit of area (in the case of grasslands). However, several methods have been developed to estimate evapotranspiration rates (**ET**) in small species, particularly in crops. Similar to woody species, the methods can be classified into direct and indirect, where direct methods measure water use gravimetrically (Abedinpour 2015, Ruiz-Peñalver et al. 2015, Weaver 1941), and indirect

methods measure a secondary property, process or variable (Senock and Ham 1995, Zhang and Kirkham 1995), related to water use. However, there is a group of methods, often referred to as mechanistic (i.e., those that describe phenomena in purely physical or deterministic terms) that rely primarily on environmental factors and species-specific parameters used to estimate large-scale ET rates. Some of these methods include Penman-Monteith (Allen et al. 1998), the Presley-Taylor (Priestley and Taylor 1972), Bowen Ratio (Angus and Watts 1984), and Eddy Covariance (Twine et al. 2000), among others.

TSF methods have been successfully used to estimate water use and ET rates at the plant level. Senock and Ham (1995) tested the heat balance method on individual stems of tall grasses big bluestem (*Andropogon gerardii* Vitman) and indiangrass (*Sorghastrum nutans* L. Nash), and found a 10% error between TSF and GSF, which for a water use of less than 4 g h^{-1}, is a high precision measurement. Zhang and Kirkham (1995) conducted a similar comparison between TSF and GSF in sunflower (*Helianthus annuus* L. 'Hgsun 354') and sorghum (Sorghum bicolor (L.) Moench, Funk's hybrid G-522DR), and found good correlation at relatively high sap flow rates (>60 g h^{-1}). They concluded that sap flow rate was the main indicator for sensor accuracy, in other words, the lower the sap flow rate, the higher the estimation error. Ramirez et al. (2006) compared infrared gas analyzer, porometer and TSF (heat balance) with GSF in esparto grass (*Stipa tenacissima* (L.) Kunth), and found overestimations of +125%, +77% and +92%, respectively, compared to GSF. They concluded that overestimation scaling up from instantaneous transpiration measurements at the leaf level might be in part due to a higher concentration of chlorophyll in younger leaves (and thus higher photosynthetic capacity rates). Only when the shape of the plant and senescence distribution was considered, indirect water use estimated matched GSF by less than 5%. More recently, Clearwater et al. (2009) tested a modified version of the HRM on four species kiwi (*Actinidia spp.*), dwarf schefflera (*Schefflera*

arboricola), karo (*Pittosporum crassifolium*), and European beech (Fagus sylvatica) to estimate sap flow in individual pedicles. They found a linear relationship between TSF and GSF, within a sap flow range from as low as 0.025 g h^{-1}, to 1.8 g h^{-1}.

In natural ecosystems, however, especially grasslands, species and anatomical diversity makes difficult to implement intensive TSF measurements (i.e., multiple sensors on various species) to cover the natural variability. To overcome this challenge, a common methodology is to estimate water loss gravimetrically using weighing lysimeters. Young et al. (1996) estimated water use in bermudagrass (*Cynodon dactylon* x *transvaalensis* var. Tifway), and observed that deep-root water use can significantly reduce deep percolation. Evett et al. (2009) applied the same methodology on sweet corn Zea mays L., variety Merit, to develop crop coefficients in the Jordan Valley, in Jordan. Besides the successful implementation of the methodology, an important outcome from this study was the high cost (>60,000 USD/unit) associated with the design and installation of weighing lysimeters. Smaller and more economical versions (phytometers) such as the ones used by Weaver (1941) in Indian grass (Sorghastrum nutas) and big blustem (Andropogon scoparius), Hinds (1973) in dropping brome (Bromus tectorum), are considered now limited due to their inability to perform automated measurements. Recently, Ruiz-Peñalver et al. (2015) taking advantage of several technological advancements (i.e., automated measurements, data storage, and multiplexing capabilities) developed a relatively low-cost weighing lysimeter with the potential to be used in multiple species. Large-scale and ecosystem-level measurements, however, are still a limitation for both TSF and gravimetrically-estimated water use.

Mechanistic methods (e.g., Penman-Monteith, Priestley-Taylor) address some of these challenges describing evapotranspiration in purely physical or deterministic ways (Consoli 2011). The FAO's adopted standard Penman-Monteith (PM) (Allen et al. 1998) method, uses a

combination of energy balance and aerodynamics to estimate reference ET (mm d^{-1}). When using the PM method, it is recommended to collect the required variables above a grass or alfalfa reference. Irmak and Odhiambo, (2009) estimated reference ET from measurements above a grassland and a crop (Zea mays), and found that where a reference ET does not exist, it is possible to use an alternative crop, such as corn to estimate ET. Goulden and Field (1994), compared PM, TSF, and whole-canopy (i.e., chambers that covered entire trees) gas exchange measurements in oak trees (Quercus agrifolia, Quercus durat), and concluded that gas exchange measurements matched those observed mechanistically with PM, which also matched corrected TSF. In grassland and pasture, the results have varied. Sumner and Jacobs (2005) used PM, Priestley-Taylor (PT), reference evapotranspiration, and pan evaporation methods to estimate evapotranspiration in bahia grass (Paspalum notatum Flugge) and rotating agricultural fields of strawberries (Fragaria sp.) and brown top millet (Panicum ramosum). In their study, PT, coupled with green leaf area index (LAI) and solar radiation, provided better estimates of actual ET, compared to PM. They also concluded that PM and PT showed better ET estimates than the reference ET or the pan evaporation methods.

Given that these mechanistic methods were developed for homogeneous land covers, one of their weaknesses is their assumed low accuracy to estimate ET in "patchy" conditions, where land cover and species distribution is not homogeneous. Moran et al. (1996), tested the applicability of remotely-sensed measurements of surface reflectance and temperature, to allow the application of PM to estimate ET in heterogeneous grasslands when there is no prior knowledge of their percent cover or canopy resistance. They concluded that the approach was reasonable, and that sources of error are multiple for this approach, and their impacts on estimated ET need to be considered. Similar studies have been conducted in forest lands (Boegh

et al. 2009), citrus trees (Dzikiti et al. 2011) and crops (*Zea mays*) for bioenergy production (Wu et al. 2012).

Summary

This literature review covered areas that deal with the development of the bioenergy field, and targeted particularly the potential ecohydrological impacts of woody biomass production. I discussed the national trends, major research advancements, and showed that based on national-level documents published by the Bioenergy Technologies Office, and the U.S. Department of Energy, the ecohydrological impacts of bioenergy production are often regarded as "possible impacts", and are not fully addressed in long-term program plans. I described and explained advancements and weaknesses of the methods used in my research to estimate water use at the tree, and stand level, with a strong emphasis on thermometric methods. I also discussed key research advancements regarding the production of bioenergy and biomass in general, such as the dynamics and relevance of water and nutrients in plantations, where it has been shown that lack of nutrients slows down biomass accumulation, but lack of water halts is altogether. Another important finding discussed is that stand-level water use in eucalyptus, and possible aspen plantations reduces with stand age, as a result of the adaptation to a reduced growing space and consequent lower total leaf area per tree. I also discussed the tradeoffs between biomass accumulation and hydrological services, and highlighted the gaps related to water-carbon tradeoffs in both eucalyptus and aspen plantations, which based on the evidence gathered, it is strongly focused on biomass accumulation alone.

Figures

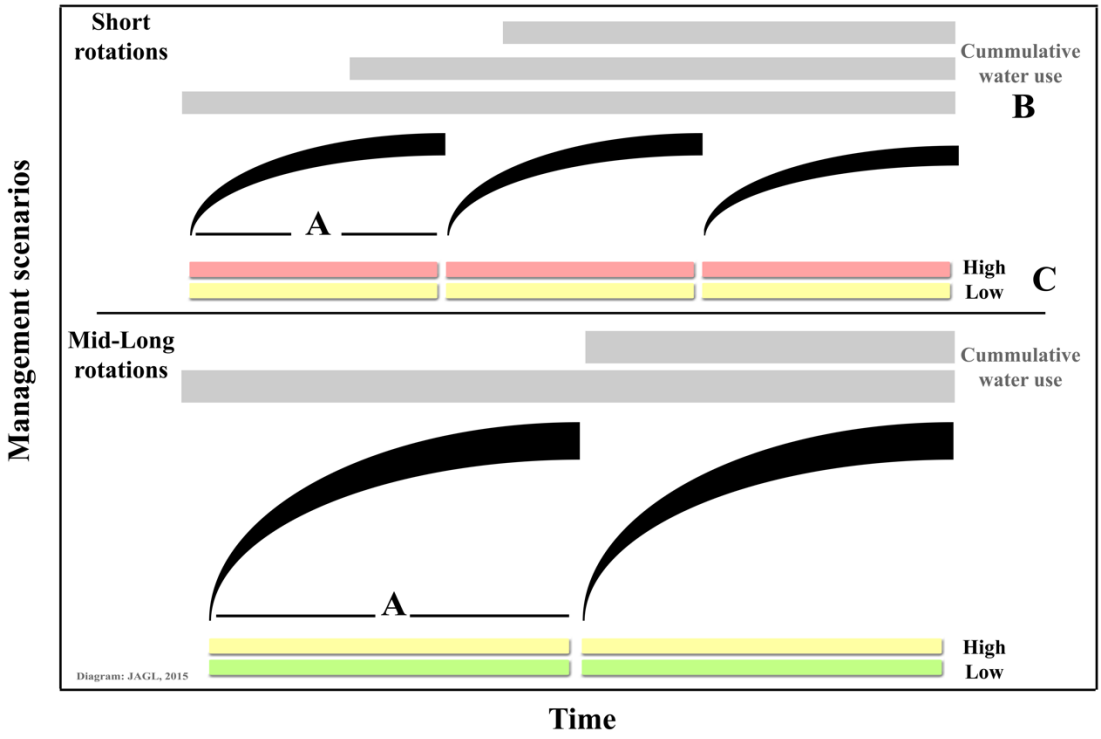

Figure I-1 Effects of rotation length of cumulative water use

This diagram shows the projected water use under two rotation scenarios: multiple short rotations (top panel), and few rotations (bottom panel). The top panel represents a species where multiple short rotations result in higher cumulative water use than the same species under longer rotations (bottom panel).

In this diagram: A) the rotation length, B) the cumulative water use, and C) the expected stress due to reductions in soil water availability. The black curves represent biomass accumulation. This diagram was not designed to represent a specific species or ecosystem. The long-term goal of this study, is to explore the possibility to elaborate such forecast scenarios, in order to manage plantations to achieve a desired outcome, considering the age response over time of the species studied.

Cited literature

Abbas, D., D. Current, M. Phillips, et al. 2011. Guidelines for harvesting forest biomass for energy: A synthesis of environmental considerations. Biomass & Bioenergy **35**:4538-4546.

Abedinpour, M. 2015. Evaluation of Growth-Stage-Specific Crop Coefficients of Maize Using Weighing Lysimeter. Soil and Water Research **10**:99-104.

Allen, R. G., L. S. Pereira, D. Raes, and M. Smith. 1998. Crop evapotranspiration: guidelines for computing crop water requiriments. Irrigation and drainage paper **56**.

Allen, S. J., R. L. Hall, and P. T. W. Rosier. 1999. Transpiration by two poplar varieties grown as coppice for biomass production. Tree Physiology **19**:493-501.

Almeida, A. C., J. V. Soares, J. J. Landsberg, and G. D. Rezende. 2007. Growth and water balance of Eucalyptus grandis hybrid plantations in Brazil during a rotation for pulp production. Forest Ecology and Management **251**:10-21.

Alvarado-Barrientos, M. S., V. Hernandez-Santana, and H. Asbjornsen. 2013. Variability of the radial profile of sap velocity in Pinus patula from contrasting stands within the seasonal cloud forest zone of Veracruz, Mexico. Agricultural and Forest Meteorology **168**:108-119.

Angus, D. E., and P. J. Watts. 1984. Evapotranspiration — How good is the Bowen ratio method? Agricultural Water Management **8**:133-150.

Babel, M. S., B. Shrestha, and S. R. Perret. 2011. Hydrological impact of biofuel production: A case study of the Khlong Phlo Watershed in Thailand. Agricultural Water Management **101**:8-26.

Balasus, A., W. A. Bischoff, A. Schwarz, et al. 2012. Nitrogen fluxes during the initial stage of willows and poplars in short-rotation coppices. Journal of Plant Nutrition and Soil Science **175**:729-738.

Baum, C., K. U. Eckhardt, J. Hahn, et al. 2013. Impact of poplar on soil organic matter quality and microbial communities in arable soils. Plant Soil and Environment **59**:95-100.

Berndes, G. 2008. Water demand for global bioenergy production: trends, risks and opportunities German Advisory Council on Global Change (WBGU), Berlin

Bethenod, O., N. Katerji, R. Goujet, et al. 2000. Determination and validation of corn crop transpiration by sap flow measurement under field conditions. Theoretical and Applied Climatology **67**:153-160.

BETO. 2013. Multi-year program plan. Government Document. Bioenergy Technologies Office. DOE/EE-0915

Binkley, D. 2004. A hypothesis about the interaction of tree dominance and stand production through stand development. Forest Ecology and Management **190**:265-271.

Binkley, D., O. C. Campoe, M. Gspaltl, and D. I. Forrester. 2013. Light absorption and use efficiency in forests: Why patterns differ for trees and stands. Forest Ecology and Management **288**:5-13.

Blanken, P. D., T. A. Black, P. C. Yang, et al. 1997. Energy balance and canopy conductance of a boreal aspen forest: Partitioning overstory and understory components. Journal of Geophysical Research-Atmospheres **102**:28915-28927.

Bleby, T. M., S. S. O. Burgess, and M. A. Adams. 2004. A validation, comparison and error analysis of two heat-pulse methods for measuring sap flow in Eucalyptus marginata saplings. Functional Plant Biology **31**:645-658.

Boegh, E., R. N. Poulsen, M. Butts, et al. 2009. Remote sensing based evapotranspiration and runoff modeling of agricultural, forest and urban flux sites in Denmark: From field to macro-scale. Journal of Hydrology **377**:300-316.

Braun, P., and J. Schmid. 1999. Sap flow measurements in grapevines (Vitis vinifera L.) - 2. Granier measurements. Plant and Soil **215**:47-55.

BRDB. 2011. Bioenergy feedstock best management practices: summary and research needs. Government Document. Feedstock production interagency working group.

Bryla, D. R., T. J. Trout, and J. E. Ayars. 2010. Weighing lysimeters for developing crop coefficients and efficient irrigation practices for vegetable crops. Hortscience **45**:1597-1604.

Buckley, T. N., T. L. Turnbull, S. Pfautsch, and M. A. Adams. 2011. Nocturnal water loss in mature subalpine Eucalyptus delegatensis tall open forests and adjacent E. pauciflora woodlands. Ecology and Evolution **1**:435-450.

Bungart, R., H. Grunewald, and R. F. Huttl. 2001. Productivity and water budget of two poplar clones on a mine spoil in the Lusatian Lignite Mining Region. Forstwissenschaftliches Centralblatt **120**:125-138.

Burgess, S. S. O., M. Adams, N. C. Turner, et al. 2001a. An improved heat pulse method to measure low and reverse rates of sap flow in woody plants (vol 21, pg 589, 2001). Tree Physiology **21**:1157-1157.

Burgess, S. S. O., M. A. Adams, N. C. Turner, et al. 2001b. An improved heat pulse method to measure low and reverse rates of sap flow in woody plants. Tree Physiology **21**:589-598.

Burgess, S. S. O., and T. E. Dawson. 2004. The contribution of fog to the water relations of Sequoia sempervirens (D. Don): foliar uptake and prevention of dehydration. Plant Cell and Environment **27**:1023-1034.

Burgess, S. S. O., J. S. Pate, M. A. Adams, and T. E. Dawson. 2000. Seasonal water acquisition and redistribution in the Australian woody phreatophyte, Banksia prionotes. Annals of Botany **85**:215-224.

Bush, S. E., K. R. Hultine, J. S. Sperry, and J. R. Ehleringer. 2010. Calibration of thermal dissipation sap flow probes for ring- and diffuse-porous trees. Tree Physiology **30**:1545-1554.

Campoe, O. C., J. L. Stape, J. P. Laclau, et al. 2012. Stand-level patterns of carbon fluxes and partitioning in a Eucalyptus grandis plantation across a gradient of productivity, in Sao Paulo State, Brazil. Tree Physiology **32**:696-706.

Cartisano, R., W. Mattioli, P. Corona, et al. 2013. Assessing and mapping biomass potential productivity from poplar-dominated riparian forests: A case study. Biomass & Bioenergy **54**:293-302.

Christersson, L. 2010. Wood production potential in poplar plantations in Sweden. Biomass & Bioenergy **34**:1289-1299.

Clearwater, M. J., Z. W. Luo, M. Mazzeo, and B. Dichio. 2009. An external heat pulse method for measurement of sap flow through fruit pedicels, leaf petioles and other small-diameter stems. Plant Cell and Environment **32**:1652-1663.

Clearwater, M. J., F. C. Meinzer, J. L. Andrade, et al. 1999. Potential errors in measurement of nonuniform sap flow using heat dissipation probes. Tree Physiology **19**:681-687.

Cohen, Y., M. Fuchs, and G. C. Green. 1981. Improvement of the heat pulse method for determining sap flow in trees. Plant Cell and Environment **4**:391-397.

Consoli, S. 2011. Evapotranspiration estimation using micrometeorological techniques, in G. Gerosa. Ed. Evapotranspiration - from measurements to agricultural and environmental applications. Catania, Italy.

Davis, S. C., M. Dietze, E. DeLucia, et al. 2012. Harvesting Carbon from Eastern US Forests: Opportunities and Impacts of an Expanding Bioenergy Industry. Forests **3**:370-397.

De Swaef, T., and K. Steppe. 2010. Linking stem diameter variations to sap flow, turgor and water potential in tomato. Functional Plant Biology **37**:429-438.

Di Matteo, G., G. Sperandio, and S. Verani. 2012. Field performance of poplar for bioenergy in southern Europe after two coppicing rotations: effects of clone and planting density. Iforest-Biogeosciences and Forestry **5**:224-229.

Dillen, S. Y., S. N. Djomo, N. Al Afas, et al. 2013. Biomass yield and energy balance of a short-rotation poplar coppice with multiple clones on degraded land during 16 years. Biomass & Bioenergy **56**:157-165.

Dougherty, D., and J. Wright. 2012. Silviculture and Economic Evaluation of Eucalypt Plantations in the Southern Us. Bioresources **7**:1994-2001.

Dunisch, O., M. Erbreich, and T. Eilers. 2003. Water balance and water potentials of a monoculture and an enrichment plantation of Carapa guianensis Aubl. in the Central Amazon. Forest Ecology and Management **172**:355-367.

Dunn, G. M., and D. J. Connor. 1993. An Analysis of Sap Flow in Mountain Ash (Eucalyptus-Regnans) Forests of Different Age. Tree Physiology **13**:321-336.

Dzikiti, S., S. J. Verreynne, J. Stuckens, et al. 2011. Seasonal variation in canopy reflectance and its application to determine the water status and water use by citrus trees in the Western Cape, South Africa. Agricultural and Forest Meteorology **151**:1035-1044.

El Kasmioui, O., and R. Ceulemans. 2013. Financial Analysis of the Cultivation of Short Rotation Woody Crops for Bioenergy in Belgium: Barriers and Opportunities. Bioenergy Research **6**:336-350.

Evans, J. M., R. J. Fletcher, and J. Alavalapati. 2010. Using species distribution models to identify suitable areas for biofuel feedstock production. Global Change Biology Bioenergy **2**:63-78.

Evett, S. R., N. T. Mazahrih, M. A. Jitan, et al. 2009. A Weighing Lysimeter for Crop Water Use Determination in the Jordan Valley, Jordan. Transactions of the Asabe **52**:155-169.

Ewers, B. E., R. Oren, H. S. Kim, et al. 2007. Effects of hydraulic architecture and spatial variation in light on mean stomatal conductance of tree branches and crowns. Plant Cell and Environment **30**:483-496.

Fernandez, J. E., P. J. Duran, M. J. Palomo, et al. 2006. Calibration of sap flow estimated by the compensation heat pulse method in olive, plum and orange trees: relationships with xylem anatomy. Tree Physiology **26**:719-728.

Fernández, M. E., and J. Gyenge. 2009. Testing Binkley's hypothesis about the interaction of individual tree water use efficiency and growth efficiency with dominance patterns in open and close canopy stands. Forest Ecology and Management **257**:1859-1865.

Forrester, D. I. 2013. Growth responses to thinning, pruning and fertiliser application in Eucalyptus plantations: A review of their production ecology and interactions. Forest Ecology and Management **310**:336-347.

Forrester, D. I. 2014a. The spatial and temporal dynamics of species interactions in mixed-species forests: From pattern to process. Forest Ecology and Management **312**:282-292.

Forrester, D. I. 2014b. A stand-level light interception model for horizontally and vertically heterogeneous canopies. Ecological Modelling **276**:14-22.

Forrester, D. I., J. Bauhus, A. L. Cowie, and J. K. Vanclay. 2006. Mixed-species plantations of Eucalyptus with nitrogen-fixing trees: A review. Forest Ecology and Management **233**:211-230.

Forrester, D. I., J. Bauhus, and P. K. Khanna. 2004. Growth dynamics in a mixed-species plantation of Eucalyptus globulus and Acacia mearnsii. Forest Ecology and Management **193**:81-95.

Forrester, D. I., J. J. Collopy, C. L. Beadle, et al. 2012. Effect of thinning, pruning and nitrogen fertiliser application on transpiration, photosynthesis and water-use efficiency in a young Eucalyptus nitens plantation. Forest Ecology and Management **266**:286-300.

Forrester, D. I., J. J. Collopy, and J. D. Morris. 2010a. Transpiration along an age series of Eucalyptus globulus plantations in southeastern Australia. Forest Ecology and Management **259**:1754-1760.

Forrester, D. I., S. Theiveyanathan, J. J. Collopy, and N. E. Marcar. 2010b. Enhanced water use efficiency in a mixed Eucalyptus globulus and Acacia mearnsii plantation. Forest Ecology and Management **259**:1761-1770.

Forster, M. A. 2014. How significant is nocturnal sap flow? Tree Physiology **34**:757-765.

Gebauer, T., V. Horna, and C. Leuschner. 2008. Variability in radial sap flux density patterns and sapwood area among seven co-occurring temperate broad-leaved tree species. Tree Physiology **28**:1821-1830.

Gerdes, G., B. E. Allison, and L. S. Pereira. 1994. Overestimation of Soybean Crop Transpiration by Sap Flow Measurements under Field Conditions in Central Portugal. Irrigation Science **14**:135-139.

Gochis, D. J., and R. H. Cuenca. 2000. Plant water use and crop curves for hybrid poplars. Journal of Irrigation and Drainage Engineering-Asce **126**:206-214.

Goulden, M. L., and C. B. Field. 1994. 3 Methods for Monitoring the Gas-Exchange of Individual Tree Canopies - Ventilated-Chamber, Sap-Flow and Penman-Monteith Measurements on Evergreen Oaks. Functional Ecology **8**:125-135.

Granier, A. 1985. Une nouvelle méthode pour la mesure du flux de sève brute dans le tronc des arbres. Annals of Forest Science **42**:193-200.

Granier, A. 1987. Evaluation of transpiration in a Douglas-Fir stand by means of sap flow measurements. Tree Physiology **3**:309-319.

Hamilton, L. S., N. Dudley, G. Greminger, et al. 2008. Forest and water. Forestry Department, Rome, Italy.

Hansen, A., A. Meyer-Aurich, and A. Prochnow. 2013. Greenhouse gas mitigation potential of a second generation energy production system from short rotation poplar in Eastern Germany and its accompanied uncertainties. Biomass & Bioenergy **56**:104-115.

Headlee, W. L., R. S. Zalesny, D. M. Donner, and R. B. Hall. 2013. Using a Process-Based Model (3-PG) to Predict and Map Hybrid Poplar Biomass Productivity in Minnesota and Wisconsin, USA. Bioenergy Research **6**:196-210.

Herrick, S., J. Kovach, E. Padley, et al. 2009. Wisconsin's Forestland Woody Biomass Harvesting Guidelines. Government Document. Division of Forestry and Wisconsin Council on Forestry. UB-FR-435-2009. Madison, Wisconsin

Hillel, D. 2004. Introduction to environmental soil physics. Elsevier Academic Press, Amsterdam ; Boston.494 pp.

Hinckley, T. M., J. P. Lassoie, and S. W. Running. 1978. Temporal and spatial variations in the water status of forest trees. Forest Science **24**:a0001-z0001.

Hinds, W. T. 1973. Small lysimeters for measurement of water use and herbage yield. Journal of Range Management **26**:304-306.

Hubbard, R. M., J. Stape, M. G. Ryan, et al. 2010. Effects of irrigation on water use and water use efficiency in two fast growing Eucalyptus plantations. Forest Ecology and Management **259**:1714-1721.

Huber, B. 1932. Beobachtung und Messung pflanzlicher Saftstrome. Berichte der Deutschen Botanischen Gesellschaft **50**:89-109.

Hunt, M. A., and C. L. Beadle. 1998. Whole-tree transpiration and water-use partitioning between Eucalyptus nitens and Acacia dealbata weeds in a short-rotation plantation in northeastern Tasmania. Tree Physiology **18**:557-563.

IDNR. 2007. Woody biomass feedstock for the bioenergy and bioproducts industries. Government Document. Indiana Department of Natural Resources. Forestry Division

Irmak, S., and L. O. Odhiambo. 2009. Impact of microclimatic data measured above maize and grass canopies on Penman-Monteith reference evapotranspiration calculations. Transactions of the Asabe **52**:1155-1169.

Jackson, S. 2007. Virginia biomass/bioenergy overview. Fact sheet 2.15, in Ed. Sustainable Forestry for Bioenergy and Bio-based Products: trainers curriculum Notebook. Southern Forest Research Partnership, Inc. Athens, GA. 99-102

Jassal, R. S., T. A. Black, C. Arevalo, et al. 2013. Carbon sequestration and water use of a young hybrid poplar plantation in north-central Alberta. Biomass & Bioenergy **56**:323-333.

Kauter, D., I. Lewandowski, and W. Claupein. 2003. Quantity and quality of harvestable biomass from Populus short rotation coppice for solid fuel use - a review of the physiological basis and management influences. Biomass & Bioenergy **24**:411-427.

Kim, H. S., R. Oren, and T. M. Hinckley. 2008. Actual and potential transpiration and carbon assimilation in an irrigated poplar plantation. Tree Physiology **28**:559-577.

Kluitenberg, G. J., and J. M. Ham. 2004. Improved theory for calculating sap flow with the heat pulse method. Agricultural and Forest Meteorology **126**:169-173.

Kozlowski, T. T., P. J. Kramer, and S. G. Pallardy. 1991. The physiological ecology of woody plants. Academic Press, San Diego.657 pp

Kull, O., and I. Tulva. 2000. Modelling canopy growth and steady-state leaf area index in an aspen stand. Annals of Forest Science **57**:611-621.

Lambs, L., and E. Muller. 2002. Sap flow and water transfer in the Garonne River riparian woodland, France: first results on poplar and willow. Annals of Forest Science **59**:301-315.

Lasch, P., C. Kollas, J. Rock, and F. Suckow. 2010. Potentials and impacts of short-rotation coppice plantation with aspen in Eastern Germany under conditions of climate change. Regional Environmental Change **10**:83-94.

Li, H., M. C. Li, J. Luo, et al. 2012. N-fertilization has different effects on the growth, carbon and nitrogen physiology, and wood properties of slow- and fast-growing Populus species. Journal of Experimental Botany **63**:6173-6185.

Liesche, J., C. Windt, T. Bohr, et al. 2015. Slower phloem transport in gymnosperm trees can be attributed to higher sieve element resistance. Tree Physiology **35**:376-386.

Lu, P., L. Urban, and P. Zhao. 2004. Granier's thermal dissipation probe (TDP) method for measuring sap flow in trees: Theory and practice. Acta Botanica Sinica **46**:631-646.

Lundblad, M., and A. Lindroth. 2002. Stand transpiration and sapflow density in relation to weather, soil moisture and stand characteristics. Basic and Applied Ecology **3**:229-243.

Man, H. M., R. Boriel, R. El-Khatib, and E. G. Kirby. 2005. Characterization of transgenic poplar with ectopic expression of pine cytosolic glutamine synthetase under conditions of varying nitrogen availability. New Phytologist **167**:31-39.

Marshall, D. C. 1958. Measurement of Sap Flow in Conifers by Heat Transport. Plant Physiology **33**:385-396.

Massonnet, C., J. L. Regnard, P. E. Lauri, et al. 2008. Contributions of foliage distribution and leaf functions to light interception, transpiration and photosynthetic capacities in two apple cultivars at branch and tree scales. Tree Physiology **28**:665-678.

McCulloh, K. A., K. Winter, F. C. Meinzer, et al. 2007. A comparison of daily water use estimates derived from constant-heat sap-flow probe values and gravimetric measurements in pot-grown saplings. Tree Physiology **27**:1355-1360.

Mizrachi, E., S. D. Mansfield, and A. A. Myburg. 2012. Cellulose factories: advancing bioenergy production from forest trees. New Phytologist **194**:54-62.

Molony, T. 2011. Bioenergy policies in Africa: mainstreaming gender amid an increasing focus on biofuels. Biofuels Bioproducts & Biorefining-Biofpr **5**:330-341.

Moran, M. S., A. F. Rahman, J. C. Washburne, et al. 1996. Combining the Penman-Monteith equation with measurements of surface temperature and reflectance to estimate evaporation rates of semiarid grassland. Agricultural and Forest Meteorology **80**:87-109.

Moreno-Cortes, A., T. Hernandez-Verdeja, P. Sanchez-Jimenez, et al. 2012. CsRAV1 induces sylleptic branching in hybrid poplar. New Phytologist **194**:83-90.

Morris, J., N. N. Zhang, Z. J. Yang, et al. 2004. Water use by fast-growing Eucalyptus urophylla plantations in southern China. Tree Physiology **24**:1035-1044.

Muller, E., and L. Lambs. 2009. Daily Variations of Water Use with Vapor Pressure Deficit in a Plantation of I214 Poplars. Water **1**:32-42.

Myburg, A. A., D. Grattapaglia, G. A. Tuskan, et al. 2014. The genome of Eucalyptus grandis. Nature **510**:356-+.

Nelson, A. S., M. R. Saunders, R. G. Wagner, and A. R. Weiskittel. 2012. Early stand production of hybrid poplar and white spruce in mixed and monospecific plantations in eastern Maine. New Forests **43**:519-534.

Nguyen, N. T., K. Nakabayashi, P. K. Mohapatra, et al. 2003. Effect of nitrogen deficiency on biomass production, photosynthesis, carbon partitioning, and nitrogen nutrition status of Melaleuca and Eucalyptus species. Soil Science and Plant Nutrition **49**:99-109.

Oguntunde, P. G. 2007. Water use pattern and canopy processes of cashew trees during a drying period in West Africa. International Journal of Plant Production **1**:81-94.

Oguntunde, P. G., N. C. van de Giesen, P. L. G. Vlek, and H. Eggers. 2004. Water Flux in a Cashew Orchard during a Wet-to-Dry Transition Period: Analysis of Sap Flow and Eddy Correlation Measurements. Earth Interactions **8**.

Oliveras, I., and P. Llorens. 2001. Medium-term sap flux monitoring in a Scots pine stand: analysis of the operability of the heat dissipation method for hydrological purposes. Tree Physiology **21**:473-480.

Pallardy, S. G., and T. T. Kozlowski. 1979. Stomatal Response of Populus Clones to Light-Intensity and Vapor-Pressure Deficit. Plant Physiology **64**:112-114.

Peltola, H. 1996. Swaying of trees in response to wind and thinning in a stand of Scots pine. Boundary-Layer Meteorology **77**:285-304.

Perlack, R. D., L. L. Wright, A. F. Turhollow, et al. 2005. Biomass as feedstock for a bioenergy and bioproducts industry: the technical feasibility of a billion-ton annual supply. Technical Report, Oak Ridge National Laboratory, Oak Ridge, Tennessee.

Perry, M. 2009. Food production vs. biomass export vs. land-use change: a CGE analysis for Argengina. Center for environmental policy. Imperial College, London.

Petzold, R., K. Schwarzel, and K. H. Feger. 2011. Transpiration of a hybrid poplar plantation in Saxony (Germany) in response to climate and soil conditions. European Journal of Forest Research **130**:695-706.

Phillips, N., B. J. Bond, N. G. McDowell, and M. G. Ryan. 2002. Canopy and hydraulic conductance in young, mature and old Douglas-fir trees. Tree Physiology **22**:205-211.

Pilate, G., A. Dejardin, and J. C. Leple. 2012. Field Trials with Lignin-Modified Transgenic Trees. Lignins: Biosynthesis, Biodegradation and Bioengineering **61**:1-36.

Pimentel, J. D., T. J. A. Silva, J. C. F. Borges, et al. 2010. Estimation of transpiration in coffee crop using heat dissipation sensors. Revista Brasileira De Engenharia Agricola E Ambiental **14**:187-195.

Priestley, C. H. B., and R. J. Taylor. 1972. On the Assessment of Surface Heat Flux and Evaporation Using Large-Scale Parameters. Monthly Weather Review **100**:81-92.

Radloff, G., X. Du, P. Porter, and T. Runge. 2012. Wisconsin strategic bioenergy feedstock assessment. Wisconsin Energy Institute, Madison, WI

Ramirez, D. A., F. Valladares, A. Blasco, and J. Bellot. 2006. Assessing transpiration in the tussock grass Stipa tenacissima L.: the crucial role of the interplay between morphology and physiology. Acta Oecologica-International Journal of Ecology **30**:386-398.

Regalado, C. M., and A. Ritter. 2007. An alternative method to estimate zero flow temperature differences for Granier's thermal dissipation technique. Tree Physiology **27**:1093-1102.

Rowe, R. L., N. R. Street, and G. Taylor. 2009. Identifying potential environmental impacts of large-scale deployment of dedicated bioenergy crops in the UK. Renewable & Sustainable Energy Reviews **13**:271-290.

Ruiz-Peñalver, L., J. A. Vera-Repullo, M. Jimenez-Buendia, et al. 2015. Development of an innovative low cost weighing lysimeter for potted plants: Application in lysimetric stations. Agricultural Water Management **151**:103-113.

Salisbury, F. B., and C. W. Ross. 1992. Plant physiology. 4th edition. Wadsworth Pub. Co., Belmont, Calif.xviii, 682 p.

Sandanandan, E. K. N., and A. G. Brown. 1997. Management of soil, nutrition and water in tropical plantation forests. Australian Centre for International Agricultural Research, Canberra.

SCFC. 2012. Forest biomass harvesting recommendations for Suth Carolina. A suplement fo South Carolina's best management practices for forestry. Government Document. South Carolina Forestry Commisions. Columbia, SC

Sellier, D., and T. Fourcaud. 2009. Crown structure and wood properties: influence on tree sway and response to high winds. American Journal of Botany **96**:885-896.

Senock, R. S., and J. M. Ham. 1995. Measurements of Water-Use by Prairie Grasses with Heat-Balance Sap Flow Gauges. Journal of Range Management **48**:150-158.

Sochacki, S. J., R. J. Harper, and K. R. J. Smettem. 2007. Estimation of woody biomass production from a short-rotation bio-energy system in semi-arid Australia. Biomass & Bioenergy **31**:608-616.

Sperling, O., O. Shapira, S. Cohen, et al. 2012. Estimating sap flux densities in date palm trees using the heat dissipation method and weighing lysimeters. Tree Physiology **32**:1171-1178.

Stape, J. L., D. Binkley, and M. G. Ryan. 2008. Production and carbon allocation in a clonal Eucalyptus plantation with water and nutrient manipulations. Forest Ecology and Management **255**:920-930.

Stape, J. L., D. Binkley, M. G. Ryan, et al. 2010. The Brazil Eucalyptus Potential Productivity Project: Influence of water, nutrients and stand uniformity on wood production. Forest Ecology and Management **259**:1684-1694.

Stenberg, P., T. Kuuluvainen, S. Kellomäki, et al. 1994. Crown Structure, Light Interception and Productivity of Pine Trees and Stands. Ecological Bulletins:20-34.

Steppe, K., D. J. W. De Pauw, T. M. Doody, and R. O. Teskey. 2010. A comparison of sap flux density using thermal dissipation, heat pulse velocity and heat field deformation methods. Agricultural and Forest Meteorology **150**:1046-1056.

Sumner, D. M., and J. M. Jacobs. 2005. Utility of Penman-Monteith, Priestley-Taylor, reference evapotranspiration, and pan evaporation methods to estimate pasture evapotranspiration. Journal of Hydrology **308**:81-104.

Sun, H. Z., D. P. Aubrey, and R. O. Teskey. 2012. A simple calibration improved the accuracy of the thermal dissipation technique for sap flow measurements in juvenile trees of six species. Trees-Structure and Function **26**:631-640.

Swanson, R. H. 1994. Significant Historical Developments in Thermal Methods for Measuring Sap Flow in Trees. Agricultural and Forest Meteorology **72**:113-132.

Taiz, L., and E. Zeiger. 2002. Plant physiology. 3rd edition. Sinauer Associates, Sunderland, Mass.xxvi, 690 p.

Tharakan, P. J., T. A. Volk, L. P. Abrahamson, and E. H. White. 2003. Energy feedstock characteristics of willow and hybrid poplar clones at harvest age. Biomass & Bioenergy **25**:571-580.

Toillon, J., B. Rollin, E. Dalle, et al. 2013. Variability and plasticity of productivity, water-use efficiency, and nitrogen exportation rate in Salix short rotation coppice. Biomass & Bioenergy **56**:392-404.

Tricker, P. J., M. Pecchiari, S. M. Bunn, et al. 2009. Water use of a bioenergy plantation increases in a future high CO2 world. Biomass & Bioenergy **33**:200-208.

Tullus, A., H. Tullus, T. Soo, and L. Parn. 2009. Above-ground biomass characteristics of young hybrid aspen (Populus tremula L. x P. tremuloides Michx.) plantations on former agricultural land in Estonia. Biomass & Bioenergy **33**:1617-1625.

Tuskan, G. A., S. DiFazio, S. Jansson, et al. 2006. The genome of black cottonwood, Populus trichocarpa (Torr. & Gray). Science **313**:1596-1604.

Twine, T. E., W. P. Kustas, J. M. Norman, et al. 2000. Correcting eddy-covariance flux underestimates over a grassland. Agricultural and Forest Meteorology **103**:279-300.

Uddling, J., R. M. Teclaw, K. S. Pregitzer, and D. S. Ellsworth. 2009. Leaf and canopy conductance in aspen and aspen-birch forests under free-air enrichment of carbon dioxide and ozone. Tree Physiology **29**:1367-1380.

van Dam, J., A. P. C. Faaij, J. Hilbert, et al. 2009. Large-scale bioenergy production from soybeans and switchgrass in Argentina: Part A: Potential and economic feasibility for national and international markets. Renewable and Sustainable Energy Reviews **13**:1710-1733.

Vandegehuchte, M. W., S. S. O. Burgess, A. Downey, and K. Steppe. 2015. Influence of stem temperature changes on heat pulse sap flux density measurements. Tree Physiology **35**:346-353.

Vandegehuchte, M. W., and K. Steppe. 2012. Sapflow+: a four-needle heat-pulse sap flow sensor enabling nonempirical sap flux density and water content measurements. New Phytologist **196**:306-317.

Vandegehuchte, M. W., and K. Steppe. 2013a. Sap-flux density measurement methods: working principles and applicability. Functional Plant Biology **40**:213-223.

Vandegehuchte, M. W., and K. Steppe. 2013b. Sap-flux density measurement methods: working principles and applicability. Functional Plant Biology **40**:213-223.

Verlinden, M. S., L. S. Broeckx, H. Wei, and R. Ceulemans. 2013. Soil CO2 efflux in a bioenergy plantation with fast-growing Populus trees - influence of former land use, inter-row spacing and genotype. Plant and Soil **369**:631-644.

Wang, J. H., S. Andersson-Gunneras, I. Gaboreanu, et al. 2011. Reduced Expression of the SHORT-ROOT Gene Increases the Rates of Growth and Development in Hybrid Poplar and Arabidopsis. Plos One **6**.

Weaver, R. J. 1941. Water usage of certain native grasses in prairie and pasture. Ecology **22**:175-192.

Werner, C., E. Haas, R. Grote, et al. 2012. Biomass production potential from Populus short rotation systems in Romania. Global Change Biology Bioenergy **4**:642-653.

White, E. H. 2010. Woody biomass for bioenergy and biofuels in the United States - A briefing paper. Government Document. Forest Service, Pacific Northwest Research Station. PNW-GTR-825.

Wilske, B., N. Lu, L. Wei, et al. 2009. Poplar plantation has the potential to alter the water balance in semiarid Inner Mongolia. Journal of Environmental Management **90**:2762-2770.

Wu, M., Y. Chiu, and Y. Demissie. 2012. Quantifying the regional water footprint of biofuel production by incorporating hydrologic modeling. Water Resources Research **48**.

Wu, Y. P., S. G. Liu, T. L. Sohl, and C. J. Young. 2013. Projecting the land cover change and its environmental impacts in the Cedar River Basin in the Midwestern United States. Environmental Research Letters **8**.

Wullschleger, S. D., F. C. Meinzer, and R. A. Vertessy. 1998a. A review of whole water use studies in trees. Tree Physiology.

Wullschleger, S. D., F. C. Meinzer, and R. A. Vertessy. 1998b. A review of whole-plant water use studies in trees. Tree Physiology **18**:499-512.

Xiao, J. F., G. Sun, J. Q. Chen, et al. 2013. Carbon fluxes, evapotranspiration, and water use efficiency of terrestrial ecosystems in China. Agricultural and Forest Meteorology **182**:76-90.

Young, M. H., P. J. Wierenga, and C. F. Mancino. 1996. Large weighing lysimeters for water use and deep percolation studies. Soil Science **161**:491-501.

Zalesny, R. S., D. M. Donner, D. R. Coyle, and W. L. Headlee. 2012. An approach for siting poplar energy production systems to increase productivity and associated ecosystem services. Forest Ecology and Management **284**:45-58.

Zamora, D. S., G. J. Wyatt, K. G. Apostol, and U. Tschirner. 2013. Biomass yield, energy values, and chemical composition of hybrid poplars in short rotation woody crop production and native perennial grasses in Minnesota, USA. Biomass & Bioenergy **49**:222-230.

Zhang, J. X., and M. B. Kirkham. 1995. Sap flow in a dicotyledon (sunflower) and a monocotyledon (sorghum) by the heat-balance method. Agronomy Journal **87**:1106-1114.

Zhou, G. Y., G. C. Yin, J. Morris, et al. 2004. Measured sap flow and estimated evapotranspiration of tropical Eucalyptus urophylla plantations in south China. Acta Botanica Sinica **46**:202-210.

CHAPTER II

MAXIMUM HEAT RATIO: NEW METHOD TO MEASURE HIGH SAP FLUX DENSITIES

Abstract

There is a wide variety of methods to monitor sap flow in conductive tissue of various plant types. However, because of the working principles of each method, in general terms most methods seem to perform better at either high or low sap flux densities ($\boldsymbol{F_d}$, $cm^3\ cm^{-2}\ h^{-1}$). A bi-directional method capable of measuring both high and low F_d with high accuracy can be of great value for the new areas of study where sap flow sensors are deployed in extreme environments to monitor the soil-plant-atmosphere continuum and where disentangling sap flow from transpiration is as important as it is challenging due the presence of freeze/thaw-induced sap flow. We assessed the performance of a new ratio-based algorithm, the maximum heat ratio (**MHR**), and the heat ratio (**HR**) methods under two controlled experiments: (a) a tree cut method with eight one-year-old *Eucalyptus grandis* trees and (b) an *Acer saccharum* trunk subjected to freeze/thaw cycles, and in the field we tested the performance of both methods on two contrasting environments with varying ranges of F_d: (c) three *E. grandis* plantations (one-, four-, and ten-years old), (d) *Escallonia myrtilloides* trees growing at 3800 m.a.s.l. Our results indicate that MHR and HR had a strong (R^2=0.90) linear relationship within a sap flux density (F_d, $cm^3\ cm^{-2}\ h^{-1}$) range of 0-40, above this threshold the linearity disappeared mainly due to the noise and fictitious estimates of HR. Using the MHR method, we were able to significantly extend the measuring range of HR. With the MHR algorithm, we estimated a maximum F_d range of 0-120 ($cm^3\ cm^{-2}\ h^{-1}$), compared to the maximum of 45 with HR alone. We observed that HR had an overestimation memory effect, especially on trees with F_d higher than 50, which was not observed with MHR. With MHR we measured a maximum F_d range of *E. grandis* plantations of

0-105 (one-year-old), 0-60 (four-year-old) and 0-35 (ten-year-old). On *E. myrtilloides*, we estimated a maximum F_d range of 0-10 with both methods, and MHR had noisier estimates within these low F_d range. In our freeze/thaw experiment, we estimated a F_d range from -16 to +38, and both methods had very similar estimates during thawing. Conversely, during freezing, HR consistently underestimated F_d (up to 10 cm^3 cm^{-2} h^{-1}), with respect to MHR. Since we were not able to regulate the flow within different annuli of the sapwood, our validation is based on the correlation between estimated flow and the measured gravimetric water use. With this study we show that a simple modification to the HR method, can significantly increase the measuring F_d range of the traditional HR method, which can be applied to already collected raw data, where HR did not perform satisfactorily. Additionally, we highlight the importance of raw-data collection in sap flow measurements. Finally, a low-power method capable of measuring high, low and inverse F_d that can be easily corrected for zero flow, can be of great value for studies required to capture this entire range with high precision.

Keywords: maximum heat ratio, heat ratio, sap flux, tree-cut experiment

Introduction

Research studies spanning different ecosystems and growing conditions often rely of various sap flow methods to make comparison, making the comparisons difficult or unreliable. Two of the most commonly used thermometric sap flow methods are the heat dissipation (**HD)** (Clearwater et al. 1999, Granier 1985) and the heat pulse (**HP**) methods (Cohen et al. 1981, Marshall 1958). Two of the common variations within the **HP** method include the **Tmax** (Cohen et al. 1981) and the heat ratio (**HR**) (Burgess et al. 2001a). Both the **Tmax** and **HR** methods are improvements from the original sensor designed to measure different ranges of sap flux density

($\boldsymbol{F_d}$, $cm^3\ cm^{-2}\ h^{-1}$) with high accuracy (Tmax for high, and HR for low and reverse). Due to their different performance ranges, the selection of HP sap flow methods is often based on method complexity, cost, power use, and more importantly, the expected ranges of F_d to be measured. Despite the latest improvements on HP sensors, no single easy-to-use method validated under field conditions or using whole trees is capable of measuring low, high and reverse flows with high accuracy.

Sap flow methods have become a fundamental part of studies seeking to understand responses of individual plants to whole stands and ecosystems to abiotic and biotic drivers (Alvarado-Barrientos et al. 2013, Eller et al. 2015, Kagawa et al. 2009, Kukowski et al. 2013, Lundblad and Lindroth 2002, Meinzer et al. 2004, Steppe et al. 2006, Vergeynst et al. 2014, Zalesny et al. 2006), In physiological studies, sap flow measurements can provide a means of identifying underlying mechanisms that explain changes in water movement along the soil-plant-atmosphere continuum at the individual plant scale. In ecological studies, sap flow measurements help examine the responses of ecosystem processes and functions related to water use and cycling to environmental change (e.g., disturbance, drought, nutrient amendments, etc.). In both ecological and physiological studies, HP methods capable of measuring extremely low and reverse flows (i.e., HR) have received less attention, partially because most studies focus primarily on transpiration-induced sap flow, where the vast majority of the flow is unidirectional (from the roots to the leaves). Only studies interested in hydraulic redistribution in roots (Burgess et al. 2000), foliar uptake, or studies focused on non-transpiration sap flow (e.g., freeze/thaw-induced sap flow for studies interested in syrup production) appear to benefit from sap flow methods capable of measuring reverse flows. Further, sap flow resulting from freeze/thaw cycles (or solid-liquid sap phase change) has not been reported in the scientific literature. Currently, we can identify two major fields of study where freeze/thaw-driven sap

flow studies can be of great relevance: (a) physiological studies where freeze/thaw sap flow in deciduous or evergreen species is the main objective (i.e., syrup production, sap transport and relocation of non-structural carbohydrates, etc.) and (b) studies where heat waves or sudden changes in temperature might trigger transpiration of evergreen species during winter months when sap is commonly frozen. Additionally, studies looking to understand the effects of climate change on winter-time transpiration on evergreen species, where there is a strong combination of high freeze/thaw-induced sap flow combined with pulses of transpiration-induced sap flow, can significantly benefit from ratio-based methods capable of measuring bi-directional flows.

Most sap flow methods are prone to technical complications and rely on calibrations (Swanson 1994, Vandegehuchte and Steppe 2013). For example, HD methods (e.g., Granier 1985) can result in significant underestimations of F_d (up to 60%) (Cabibel et al. 1991, Lu and Chacko 1998, Lundblad et al. 2001, Steppe et al. 2010, Sun et al. 2012). When calibrated, HD methods perform equally, or better than HP methods, specially at high F_d ranges (Gutiérrez Lopez et al. 2018). This documented underestimation, combined with their high-power requirements, often leads researchers to select HP method (e.g. **Tmax**, **HR**), over a HD method, which leads back to the limited measuring range of HP methods previously mentioned.

Alternatives to the HD and HP methods (e.g., Tmax, HR) exist, such as the Sapflow+ method (Vandegehuchte and Steppe 2012b), or the dual method approach (DMA, Forster 2019). However, at this time their application is limited. The Sapflow+ method (Vandegehuchte and Steppe 2012b) uses four probes to estimate sap flux density. In ecological studies the number of probes per sensor is an important factor to consider in the selection of the method to increase the sample size and to reduce the effect of wunding. The DMA is a recently published algorithm that combines the Tmax and the HR methods. With this algorithm, F_d is determined using Tmax and HR methods simultaneously, and the selected F_d is the one that meets a well-defined range

criterion. On new sap flow studies, this ratio-based method might be a good alternative to extend the measuring range of HR, but the effects of switching from a ratio (HR) to a non-ratio method (Tmax) remains to be tested. Another alternative is the compensated heat pulse (CHP) method, which has been validated under field and laboratory conditions (Poblete-Echeverria et al. 2012, Vandegehuchte et al. 2015), however, this method performs poorly at high F_d ranges (Becker 1998, Burgess et al. 2000).

An important advantage of ratio-based methods with equidistant temperature probes from the heater (e.g., HR), is that in the absence of sap flow, the temperature difference between the temperature probes above and below the heater is nearly zero and the temperature ratios equals one. On smaller data sets, this correction can be easily accomplished with the equations provided by Burgess et al (2001b). In long-term monitoring studies with large data sets, automatizing data analyses to correct for zero flow or seasonal drift, might be easily accomplished using as reference vapor pressure deficit (***VPD*,** kPa) data within a given threshold (e.g., 0.2 kPa), or when the slope of F_d or the temperature ratios are close to zero for 2-3 consecutive hours. Thus, increasing the measuring range of HR (initially estimated to be from -55 to +55 $cm^3\ cm^{-2}\ h^{-1}$) is of great interest for ecological and physiological studies, which could eliminate the need to use various methods to make comparisons. To our knowledge, only one study (Vandegehuchte et al. 2015) has experimented with the data analysis algorithm of HR. According to their modeling, estimating the ratio at different time intervals after the heat pulse (compared to the standard 60-100 s after the pulse), increases the measuring range of F_d, but to this day no validations of any additional algorithms to extend the measuring range of HR have been published.

In this study, we tested and validated a new data analysis algorithm that uses the same data as the traditional HR method, the maximum heat ratio (**MHR**) algorithm. The MHR algorithm is an alternative to extend the measuring range of HR, based on a similar algorithm commonly used

on HR. Both HR and MHR raw temperature data from thermocouples or thermistors can run simultaneously, be processed *in situ* (using the data logger's memory) and stored as a single value per measurement with limited programing. Additionally, if no data memory restrictions exist, all raw data can be stored and both HR and MHR algorithms can be run for comparison purposes a *posteriori*. Considering that sap flow methods are being deployed in extreme environments, we conducted a validation in two controlled experiments, (a) a tree-cut experiment using eight one-year-old *Eucalyptus grandis* Hill ex Maiden trees and (b) a freeze-thaw experiment. Additionally, we tested the performance of MHR and HR on two scenarios of expected low and high F_d (i.e., trees growing at high elevations and cold temperatures, and three *E. grandis* plantations of one, four and ten-years-old). The overarching goal of this study was to validate the new MHR algorithm and test its performance on different species and environmental conditions. Our specific objectives were to (a) validate the accuracy and precision of two HP data analysis algorithms (HR and MHR), (b) establish the maximum F_d range measurable with the traditional HR algorithm under controlled conditions, and (c) test the potential for the MHR algorithm to extend this range. To our knowledge, no previous studies have assessed and validated whether the same data commonly used for HR can be used to estimate high F_d, similar to those commonly estimated with HD sensors. In sap flow research a low-power ratio-based method capable of measuring high and low F_d at high precision and accuracy, is highly desirable, but thus far, no method seems to perform satisfactorily under contrasting F_d ranges. Additionally, studies that have previously collected raw data to estimate F_d using the HR method, might benefit from the extended measuring range of MHR algorithm, if HR was unable to estimate high flows.

Materials and methods

Tree-cut experiment set up

We used a total of 8 trees ranging from 3-6 cm in diameter (See Table II-1), harvested at the installations of the National Agricultural Technologies Institute (INTA) in Concordia, Argentina. For comparison purposes, all trees were instrumented with both heat dissipation (**HD**) and HP sensors. All HD sensors had an extra reference sensor (without a heater) installed below them to account for natural temperature gradients. To measure gravimetric water use, we used a modified tree-cut experiment, where a small water reservoir was attached to each tree with a tire tube which was connected to a 20 L bucket (Figure **II-1**). All buckets were weighed manually every 15 min using a single electronic balance with a 1 g resolution for four consecutive days (for further details, see: Gutiérrez Lopez et al. 2018). All tree stems were covered with a reflective insulation wrap (ISOLANT 5 mm), and sensors were installed in different cardinal directions across the individual trees (two replicates per cardinal direction).

Equipment set up and data collection

A data logger (CR1000, Campbell Scientific Inc., Logan, UT, USA) and two multiplexors (AM1632, Campbell Scientific Inc.) (one for HP and one for HD sensors) were used to read and store data during a six-day period (DOY 123-128, 2015). Air temperature and relative humidity were monitored with a HMP50 sensor (Campbell Scientific Inc.). Both HD and HP sensors were connected using low voltage double-shielded cables (75985K63-Mcmaster), and thermocouple cables (TFCC-005-100-Omega) were used as extensions of thermocouples in HP sensors. The heaters of the HP sensors had a resistance of ~19 Ω ±0.2 and were connected in parallel and controlled with a custom-designed solid-state relay circuit with a maximum current limit of 4 amperes. The entire station was powered with a 12V 105Ah lead-acid battery.

Temperature (T, ºC) of each of the six thermocouples per sensor was recorded at a scan rate of ~1.5 seconds for 143 consecutive seconds, at 15-minute intervals (94 temperature data points per interval). The full measurement period of HP sensors consisted of consecutive measurements of initial temperature (0-30 s), followed by a heat pulse (30-33 s), and ending with consecutive measurements of temperatures following the heat-pulse (34-143 sec).

Gravimetric water use (**GWU**, mL) was measured with an electronic balance by manually weighing the 20 L buckets at 15-minute intervals from 6 AM to 8 PM for four consecutive days (DOY 123-126, 2015). The electronic balance had a resolution of 1 g, and all data were recorded as mass of water loss per time interval (15 min), assuming that 1 g = 1 mL. We measured GWU for all trees simultaneously every 15 minutes.

Data processing and analysis

All our data were processed with custom-designed scripts developed for JMP Pro 14 (SAS Institute, Inc. Cary, NC, USA) and R Studio 1.1.423 (R Studio, Inc) that allowed us to estimate F_d and Q for both methods. First, we performed a filtering process of GWU, removing data that were collected when the balance malfunctioned, water leaks occurred, or measurements were not taken at exact 15 min intervals. To process the data temperature data from the sap flow sensors, we first estimated a three-point running average on the raw data for all data series (i.e., 143 s of temperature data before and after the heat pulse) from the six thermocouples per sensor (see Figure **II-1**-H). We then estimated the average of the first 30 s ($\mathbf{T_0}$) of each data series and subtracted this average to estimate increments of temperature before and after the pulse. For HR, average temperature was estimated from 60-100 s ($\mathbf{T_{60\text{-}100}}$) after the pulse for all thermocouples, and heat ratios were calculated by dividing $T_{60\text{-}100}$ of corresponding thermocouples (i.e., upper over lower for each monitoring depth). For the MHR algorithm, ratios were estimated using the

maximum temperature observed after the pulse (**$T_{33\text{-}110}$**). Next, heat pulse velocity (v_h, cm h^{-1}), and v_h corrected for wounding ($\boldsymbol{v_c}$, cm h^{-1}) were estimated for HR and MHR, according to Burgess et al. (2001a) using the following equations:

$$V_h = \frac{\mathrm{k}}{x} ln \frac{v_1}{v_2} 3600 \qquad \text{Eq. 1}$$

$$V_c = bV_h + cV_h^2 + dbV_h^3 \qquad \text{Eq. 2}$$

Where k is the thermal conductivity and x the distance between probes, and v1/v2, the temperature ratio.

v_c was converted to F_d according to Vandegehuchte and Steppe (2013) using:

$$F_d = \frac{\rho_d}{\rho_s}\left(MC + \frac{C_{dw}}{C_s}\right) V_c \qquad \text{Eq. 3}$$

Where ρ_d is the density of the sapwood, ρ_s the density of water, MC the volumetric water content of the sapwood, C_{dw} the thermal conductivity of dry wood, and C_s the thermal conductivity of water.

To estimate whole tree water use (Q, mL per measurement), we multiplied the estimated F_d obtained from each method (MHR ad HR) by the corresponding sapwood area. During the installation of the sensors of Tree 7 and 8, we inadvertently affected the pulse intensity of some trees, which resulted in underestimations of F_d, especially on DOY 124 and part of DOY 125.

This issue was addressed at midday on DOY 125, and was considered at the time we estimated measuring ranges for MHR and HR and during the entire study.

Validation process

To validate F_d estimates from MHR and HR, we focused on the differences between estimated Q for each algorithm and GWU. A direct comparison between measured and estimated F_d was not feasible because we cannot regulate the sap flow within different annuli of the sapwood. Additionally, our comparison between F_d estimated from both HR and MHR and HD sensors is for reference purposes only, because HD sensors measure one point inside the sapwood, and our HP sensor design measures three depths (See Figure **II-1**-H).

Performance MHR on different environmental conditions

We tested the performance of both HR and MHR algorithms on scenarios o varying ranges of ambient temperature, that would result in contrasting F_d ranges: (a) one 17 cm diameter *Acer saccharum* log subjected to artificial freeze-thaw cycles (25 to -15ºC) in Durham, New Hampshire, USA (b) one, four and ten-year-old *E. grandis* plantations in Ubajay, Entre Rios, Argentina, growing under temperature fluctuations between 8 to 36ºC, and (c) *Escallonia myrtilloides* trees, growing at 3800 m.a.s.l., in Cuenca, Azuay, Ecuador subjected to temperature fluctuations between 4 to 12ºC. The freeze/thaw cycles applied to the *A. saccharum* log, were done using a commercial freezer that was kept at -16 ºC. Every night, the log was placed inside the freezer, and it was removed from it the following morning and placed at room temperature (26ºC). We also collected data when the log was continuously at lower than -10ºC or more than 20ºC for more than 24 hours, but we show mainly periods with fast freeze/thaw cycles. GWU was not available for any of these study sites because these are ongoing research projects and

destructive means for validation was not allowed. Data from *A. saccharum* was collected in January 2018, data for *E. grandis* plantations in May, 2015, and *E. myrtilloides* trees in April, 2018.

Results

Gravimetric water use

With exception of Trees 6 and 8, all other trees showed relatively stable GWU rates ranging from 0.050 to 0.350 L per 15-min measurement interval. Trees 6 and 8 showed a rapid decline in water use in the first day of the experiment, did not recover on the second day, and their water use was significantly lower (Tukey-Kramer test: $p = <0.0001$: Table II-2). As a result, trees 6 and 8 were not used in the validation study. Similarly, GWU measurements that were not measured at 15-minute intervals were filtered out from the analysis (e.g., Figure II-2: Tree 7, DOY 124). Based on night-time gravimetric water use (data not shown), none of the trees reached zero night-time transpiration values (Figure II-2).

Measurable F_d range of HR and MHR algorithms

Using data from our tree cut experiment, we were able to measure a F_d range from 0-45 ($cm^3\ cm^{-2}\ h^{-1}$) using the HR algorithm, and a range of 0-130 ($cm^3\ cm^{-2}\ h^{-1}$) using MHR on one-year-old *E. grandis* trees ranging from 3 to 6 cm in diameter. We did not observe significant under or overestimations of Q for each algorithm within these ranges when the instrumentation was functioning correctly (equipment malfunction resulted in underestimated Q on some trees on DOY 124-125; see discussion for further details). The maximum measurable F_d ranges estimated by with MHR varied by tree, for example, on Tree 1 we observed a maximum F_d value of 90, and on Tree 5 a maximum of 130 (panels B, Figure II-3). We observed a rapid decline in F_d from

the first to the second day of our experiment on almost all trees. This reduction was in some cases higher than 100%, for example Tree 1, reduced from 90 (cm^3 cm^{-2} h^{-1}, estimated with MHR) to less than 40 from DOY 123 to DOY 124. Our analysis suggest that such reduction was not associated with changes in *VPD*. The highest F_d reduction occurred when *VPD* was lowest and when the total daily rate change was minimum (Figure II-3, panel A).

Comparison between MHR and HR algorithms

An initial comparison between HR and MHR showed that temperature ratios estimated with HR were noisier and had a higher number of aberrant positive and negative values (i.e., values with a difference higher than four standard deviations), especially at high transpiration rates. Conversely MHR ratios appeared more stable and we did not observe extremely high or negative values, especially when the full F_d range was higher than 40 (cm^3 cm^{-2} h^{-1}). Averaging all data (six days) from Tree 2 (middle thermocouple, which had F_d values as high as 120 (cm^3 cm^{-2} h^{-1}) F_d estimates derived from MHR and HR algorithms were similar within a range of 0-40 cm^3 cm^{-2} h^{-1} (R^2=0.90, linear regression: HR = 0.56+1.063*MHR). Above this threshold, the F_d estimates differed significantly, mainly due to the abnormally high estimates of HR (Figure II-4, DOY 123-128). The correlation between HR and MHR varied significantly within each day and seemed to be driven by the daily variations in VPD. For example, the total rate of change in *VPD* on DOY 127 was less than 0.8 kPa, on this day HR and MHR (Tree 2, middle thermocouple) had a high correlation within a range of 0-65 cm^3 cm^{-2} h^{-1} (R^2=0.97: HR = -0.339+1.219*MHR; Figure II-4, DOY 127). Conversely, when the *VPD* total rate change was higher (e.g., 1 kPa on DOY 124-126), the range for the relationship between HR and MHR was lower (approximately 0-40 cm^3 cm^{-2} h^{-1}). At high F_d the linearity between HR and MHR was broken mainly due to fictitious high flows estimated with HR. This indicates that the maximum measurable range of

HR is not only dependent on the maximum F_d of a given tree, but also on the magnitude of the increments in F_d. In other words, if F_d increases rapidly, the measuring range of HR might be reduced, compared to the range observed if F_d increases more slowly (Figure II-4).

Differences between MHR and HR were also dependent on the time of the day. From 0 to 12 h, the correlation between HR and MHR when F_d was lower than 40 $cm^3\ cm^{-2}\ h^{-1}$ was stronger (HR=-0.1303+1.074*MHR, R^2=0.96) than between 13-24 h (HR=2.192+1.02*MHR, R^2 = 0.79). Additionally, the HR algorithm showed an overestimation memory effect (average: 5 $cm^3\ cm^{-2}\ h^{-1}$) with respect to MHR on the second half of the day (13-24 h) in trees that had F_d greater than ~50 $cm^3\ cm^{-2}\ h^{-1}$. This memory effect was characterized by a continuous overestimation, even after F_d estimates were again lower than 50 $cm^3\ cm^{-2}\ h^{-1}$ (e.g. Figure II-5, top panel). Nonetheless, no overestimation was observed when F_d was lower than 50, which suggests that this overestimation occurs only when F_d falls outside the measuring range of HR.

Water use (Q) estimates

Patterns of whole tree water use estimates (Q, L per 15 min measurement interval) from HR and MHR algorithms had similar patterns to those of F_d, particularly at low water use rates. However, since Q is integrated from different annuli within the sapwood, and some annuli had F_d outside the measurable range of HR, the underestimation observed using HR was the result of missing values, caused by the limited F_d measurement range of this algorithm. Comparing average water use (DOY 123-126, Figure II-6) estimated with each method (HR, MHR) with their respective GWU, MHR had a higher correlation (R^2=0.82) than HR (R^2=0.46). Despite neither HR nor MHR being calibrated, both were more accurate than HD in one-year-old *E. grandis* trees. The main error of HD sensors was associated with the parameters (a and b) used to

estimate F_d from the flux coefficient (K) (For details see: Gutierrez Lopez et al. 2018). Once the parameters were adjusted, no difference was observed between HD and both HP algorithms.

Performance of HR and MHR in contrasting environmental conditions

In one-year-old *E. grandis* plantation we estimated F_d values within a range of 0-105 (cm^3 cm^{-2} h^{-1}) (Figure II-7-A). F_d in this site was often higher than 60 (cm^3 cm^{-2} h^{-1}), which is already outside of the upper F_d range for HR that we validated with gravimetric measurements in similar trees using a tree-cut experiment. In the four and ten -year-old trees with diameters ranging from 15 to 30 cm in diameter, we observed maximum F_d values of approximately 50 cm^3 cm^{-2} h^{-1} for four-year-old and 30 cm^3 cm^{-2} h^{-1} for ten-year-old trees (Figure II-7-B, C). HR and MHR F_d estimates followed the same patterns as those observed in our validation experiment, i.e., HR overestimated F_d higher than ~50 cm^3 cm^{-2} h^{-1}, were noisier than MHR at high F_d, and had an overestimation memory effect on the second half of the day when F_d was higher than 50 cm^3 cm^{-2} h^{-1}.

On *E. myrtilloides* trees, the average range of F_d was 0-5 cm^3 cm^{-2} h^{-1}. At these low F_d, MHR estimates were noisier and occasionally were higher than HR F_d estimates (Figure II-7-E). On a day with relatively high flows, F_d estimated with HR was 9 cm^3 cm^{-2} h^{-1}, and on the same day, MHR estimated a maximum F_d of 12 cm^3 cm^{-2} h^{-1}. This period was characterized by an increment in *VPD* and air temperature, as shown in panel E in Figure II-7. Consistent with previous observations, when air temperature and *VPD* increased rapidly, the linearity between HR and MHR disappeared. At low F_d, MHR seemed to be more responsive to changes in *VPD*, than HR. When *VPD* decreased and increased rapidly, HR detected a smaller or no F_d change, with respect to MHR. Fitting a locally estimated smoothing function (Cleveland 1979, Cleveland 1981) to MHR and HR, produced nearly identical F_d estimates.

On *A. saccharum* log which we subjected to freeze/thaw cycles, we observed a total F_d range from -20 to 40 ($cm^3\ cm^{-2}\ h^{-1}$). Under these contracting conditions, HR and MHR had nearly identical F_d estimates during thawing, however, during freezing HR underestimated F_d, compared with MHR (up to 10 $cm^3\ cm^{-2}\ h^{-1}$) (Figure II-7-D). While it was not always the case, most of the negative F_d were observed during freezing. Both positive and negative flows seemed to be more pronounced when the log temperature was kept at lower (e.g., < 10ºC) temperature range. When the log temperature was higher than approximately 20 ºC, a freeze cycle did not result in high F_d (data now shown). When the log was left for more than 24 outside the freezer at room temperature (26ºC), all sap flow ceased and both HR and MHR registered F_d insignificantly different from zero. A similar pattern was observed when the log was left continuously under -10ºC inside the freezer.

Discussion

Measurable range of F_d, and expansion using alternative algorithms

Using the same wood properties (e.g., moisture content, density, etc.) and the same heat pulse velocity, F_d estimated with Eq. 4 is similar to v_s estimated following Burgess et al. (2001a). Thus, we consider it appropriate to compare our results with other studies that have focused on v_s as a unit of flow. On average, the HR method resulted in a strong correlation between Q and GWU within F_d ranges of 0-45 ($cm^3\ cm^{-2}\ h^{-1}$), with variability among trees, some showing a range up to 0-60 on (Tree 2). The MHR algorithm allowed for a wider range of F_d. On the first day of our experiment, we estimated F_d up to 130 on Tree 5 (and up to 120 on DOY 126), which is considerably higher than the measured range achievable with HR. This range (0-130 cm h^{-1}) is higher than the maximum v_s observed in other studies and tree species: 83 cm h^{-1} in *E. regnans* (Vertessy et al. 1997), 33 cm h^{-1} in *P. patula* (Alvarado-Barrientos et al. 2013), ~75 in *L.*

tulipifera (Wullschleger and King 2000)], and even the maximum v_s reported for *E. grandis*: 60 cm h^{-1} in 4-year old plantations (Benyon 1999), and 60 cm h^{-1} in ~26 year-old plantations (Kallarackal 2010). On grapevines, where the LAI to sapwood area ratios are extremely high, studies have measured maximum v_s (cm h^{-1}) of 110 using the Tmax method (Intrigliolo et al. 2009), which is still within the range of F_d measured with MHR.

The ability to measure high F_d is of great importance in ecological and physiological research. Studies often require to comparing the same species at different developmental stages, which often results in significantly different ranges of F_d. For example, Forrester et al (2010) observed higher F_d in two-year-old *Eucalyptus globulus* trees, compared to eight-year-old trees (average of 13 to 6 cm h^{-1}). According to their results these changes in F_d were strongly associated with changes with age of the ratio between LAI and sapwood area (**LAI/As**). Other studies using various sap flow sensors have reported similar patterns of high F_d when the LAI/As ratios are high (Alsheimer et al. 1998, Delzon and Loustau 2005, Dye et al. 1996, Forrester et al. 2010, Kostner et al. 2002). Nonetheless, studies reporting high F_d (>100 cm^3 cm^{-2} h^{-1}) on whole rooted trees are rare, which we consider it can be associated, in part, due to the difficulty in measuring it. Conversely, in artificial setups commonly used in sensor validation experiments, high F_d are often observed. For example, Vandegehuchte and Steppe (2012b) using the Sapflow+ method, estimated v_h close 150 cm h^{-1} on artificial columns filled with sawdust. Similarly, in our tree cut experiment, the F_d estimated from our sensors were significantly higher than those on trees of the same characteristics. We consider that this difference is the result of the removal of the root systems, which eliminates the resistance to water flow. This can additionally help explain the higher F_d values observed in our study on the first days on the experiment. Vertessy et al. (1997) observed a similar pattern, i.e., higher F_d in the first day of a tree cut experiment, compared to consecutive days, which was also attributed to the removal of the root system.

While vessel clogging or the formation of tyloses or callus tissue around the where the stems were cut might explain the reduction over time, as can be seen in Figure II-1, the main reduction was from the first to the second day of our experiment. On additional days, the reduction was observed in only some trees, but not all. As observed in Figure II-5, estimated average Q and F_d for all trees, did not show a significant reduction after the second day of our experiment. Additionally, the formation of tylosys is an unlikely explanation of such reduction under short periods of time, because tylosys takes longer to form (Kitin et al. 2010, McElrone et al. 2010). Clogging of the conductive tissue due to impurities in the water can definitely result in a reduction in F_d during our entire study, but it does not explain the reductions from one day to the next without changes in consecutive days.

Performance of MHR on different environmental conditions

Similar to the results from other studies (Dunn and Connor 1993, Forrester et al. 2010, Forster 2017), we observed a reduction in F_d of *E. grandis* trees as age increased (Figure II-7, A, B, C). We measured F_d up to a 105 ($cm^3\ cm^{-2}\ h^{-1}$) in one-year-old, 60 on four-year-old, and a maximum of 40 on ten-year-old trees. Consistent with our result, MHR and HR showed a strong linear relationship within a F_d range of 0-55, and HR was noisier, especially closer to the upper range. We collected data on these three plantations for several months during the growing season and did not observed F_d values higher than 110 but were often higher than the measuring range of HR, especially in the one-year-old trees. In this particular study, the MHR algorithm allowed us to compare contrasting ranges of F_d, and detect pulses of increased transpiration following precipitation events, that were higher than the measuring range of HR. Such comparison would not have been possible using HR alone. While there is a practical lower limit on the diameter size that HP sensors of a given probe size can measure, the ability to use the same method to make

comparisons among and between species can be of great interest in sites with an expected high F_d variability. In studies with a high variability of species and tree diameters, a combination of HD and HP sensors is often needed before changing the design of the sensors, or selecting a different method such as the heat balance (Trcala and Cermak 2012, Vellame et al. 2010, Zhang and Kirkham 1995), to be able to account for transpiration of trees of relatively small sizes in the com

Despite the ecological importance of transpiration at high elevations (Gale 2004, Smith and Geller 1979), studies reporting transpiration based on sap flow measurements are rare. Under these conditions, fluctuations in ambient temperature and solar radiation results in sap flow patterns that are not well understood. Difficult access to many of these sites renders high-power-use sap flow methods difficult to implement due to the need of solar panels. Our results on *E. myrtilloides* trees (we show data for only one) growing at 3800 m.a.s.l. show that MHR had noisier estimates and occasional higher or lower F_d estimates, compared to HR (Figure II-7, E). Given that HR was originally designed for low and inverse flows, the cleaner estimates observed within this F_d range were expected. At low F_d ranges, the relationship between MHR and HR was as good from 0-8 $cm^3\ cm^{-2}\ h^{-1}$ ($R^2 = 0.82$). While this might indicate that HR is superior than MHR under these conditions, when we applied a locally weighted regression (Cleveland and Loader 1994) to both methods, F_d estimates were identical.

As sap flow research becomes more prevalent in extreme environments (Chan and Bowling 2017), understanding the role of freeze/thaw-driven sap flow and non-traditional water-loss pathways such as stem water loss or water loss from leafless branches becomes highly relevant. For example, Höltä et al. (2018) studied sap pressurization in birch (*Betula pendula* Roth.), and discussed that HD sensors, while accurate within the growing season, they might overestimate sap flow during the winter because of the various factors affecting the measuring

principle of the method (i.e., the differences in temperature). This has also been highlighted by Chan and Bowling (2017) where they subjected HD sensors to conditions similar to those expected in very cold climates. In their laboratory experiments, sap flow stopped when the temperature of the stem was below the freezing point, which confirmed that HD sensors can estimate very small or zero flows, despite sudden changes in temperature. However, in both studies, the ability of the HD method to estimate F_d from differences in temperature (an important characteristic of the method), becomes a strong limitation under the extreme temperature changes observed during winter. Additionally, the unidirectional measuring nature of this method, limits the study of freeze/thaw-driven sap flow, which is often bidirectional, and often on opposite directions at different depths of the sapwood simultaneously. While not the goal of this study, we have observed in both field and Laboratory experiments, that the direction of flow at a given sapwood depth, results from the complex interaction between: a) the source of the nucleation point during freezing, b) the intensity, frequency and duration of the changes in temperature, and c) the mass of the stem and the conducting tissue. When these factors interact in specific ways, different sections of the sapwood might be frozen at different times, resulting in flow in opposite directions. In our freeze/thaw experiment using both HR and MHR algorithms to estimate F_d, we observed that sections inside the sapwood 1.5 cm apart can, under specific conditions, have flows in opposite directions (Figure II-7, D). Under such conditions, a single measurement point, which is typical of the traditional HD method, might miss some relevant patterns that can help explain redistribution of sap for cavitation repair, or redistribution of non-structural carbohydrates during the winter months (Hartmann and Trumbore 2016, Hölttä et al. 2018, Quentin et al. 2015). While most of our F_d estimates with both HR and MHR on *A. saccharum* were under the measuring range of HR, on other ongoing research studies on maple syrup production, we are aware of F_d as high as 60 cm^3 cm^{-2} h^{-1} in living tapped trees.

Thermal conductivity of green wood and water changes with temperature (Steinhagen 1977, Vandegehuchte and Steppe 2012a). Additionally, the conditions under which ice crystals form, also affect its thermal conductivity (Bonales et al. 2017). The review on thermal conductivity changes with temperature and volumetric water contents provided by Steinhagen (1977), indicates that some of the F_d measured at low temperatures might be the result of changes in thermal diffusivity at low temperatures. However, according to our results, once sapwood temperature in the *A. saccharum* log was lower than -5 ºC, both HR and MHR registered near zero F_d values. According to Bonales et al. (2017) and Steinhagen (1977), thermal diffusivity should continue to change below -5 ºC. Then if the F_d we measured as a result of freeze/thaw cycles is heavily influenced by changes in thermal diffusivity, such influence should also be present at lower temperatures, which as just mentioned is not the case in our laboratory experiment. Recently, we observed the same pattern on pine (*Pinus silvestris*) and spruce (*Picea abies*) trees in an ongoing study on transpiration of boreal forests in Northern Sweden: on nearly all monitored trees, once sapwood temperature and sap was below -5 ºC, no F_d was measured with either HR nor MHR, eve when sapwood temperature fluctuated between -5 ºC and -13ºC for several days. Finally, we have tested MHR with both Type-T thermocouples and with thermistors, and the only difference we have observed so far, is the higher measurement stability of thermistors. At this moment, we are not aware of how HD sensors can truly monitor F_d during winter time, considering that the heated probe is maintained at approximately 40ºC, which we are certain it results in a bubble of liquid sap around the heating element, which might affect F_d measurements during critical times during the winter.

Conclusions

The alterative MHR method allowed us to significantly increase the measuring range of HR to F_d values up to 130 cm^3 cm^{-2} h^{-1}, which is greater than the range reported for most tree species. In general MHR and HR were well correlated within -45 to 45 in all the species we studied, but HR had an overestimation memory effect only when F_d was outside the measuring range of HR. At very low F_d (<5) HR resulted in more stable estimates and less noise than MHR, however, there was a high correlation between them, and when a smoothing function was applied to both, no significant differences were observed. In this study, which is based on field measurements and laboratory experiments, we show that MHR is a viable alternative that can be easily implemented in three-probe HP sensors to monitor inverse, low and high flux densities. Additionally, it can also be applied on previously collected raw data, if HR was unable to predict F_d values higher than 60 cm^3 cm^{-2} h^{-1}. However, further research and experiments under controlled conditions on different species and wood anatomies are needed to understand how thermal diffusivity and thermal conductivity at low temperatures affect sap flow estimates.

Figures and tables

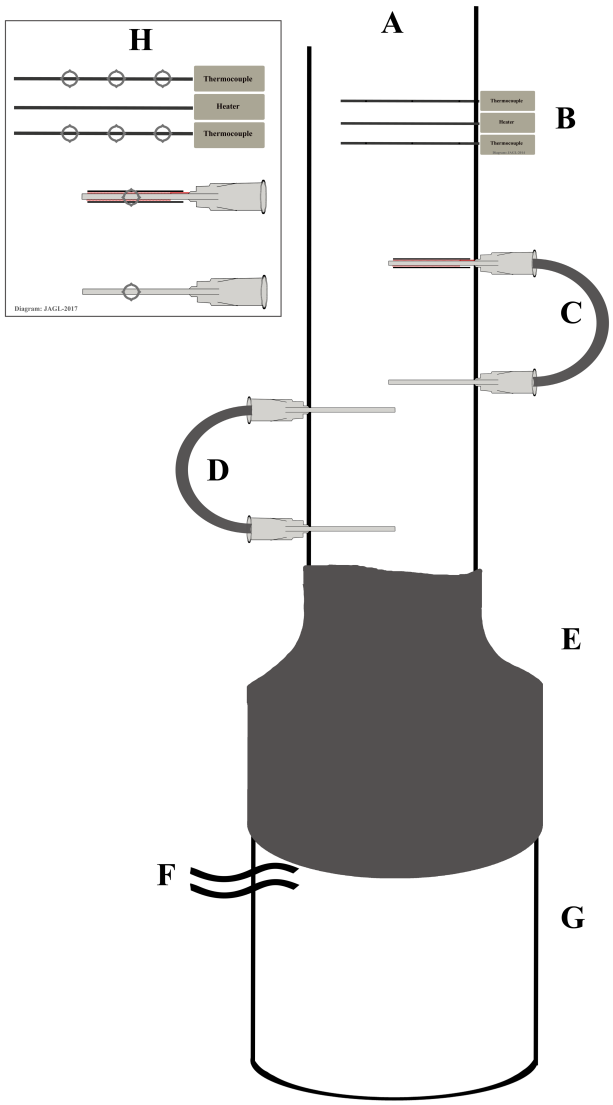

Figure II-1 Diagram of the sensor installation set up. A = the stem, B = heat pulse sensor, C = heat dissipation sensor, D = natural temperature gradient sensor E = tire tube, F = tubing connected to 20 L bucket, G = fixed-volume reservoir and H = position of thermocouples in each sensor

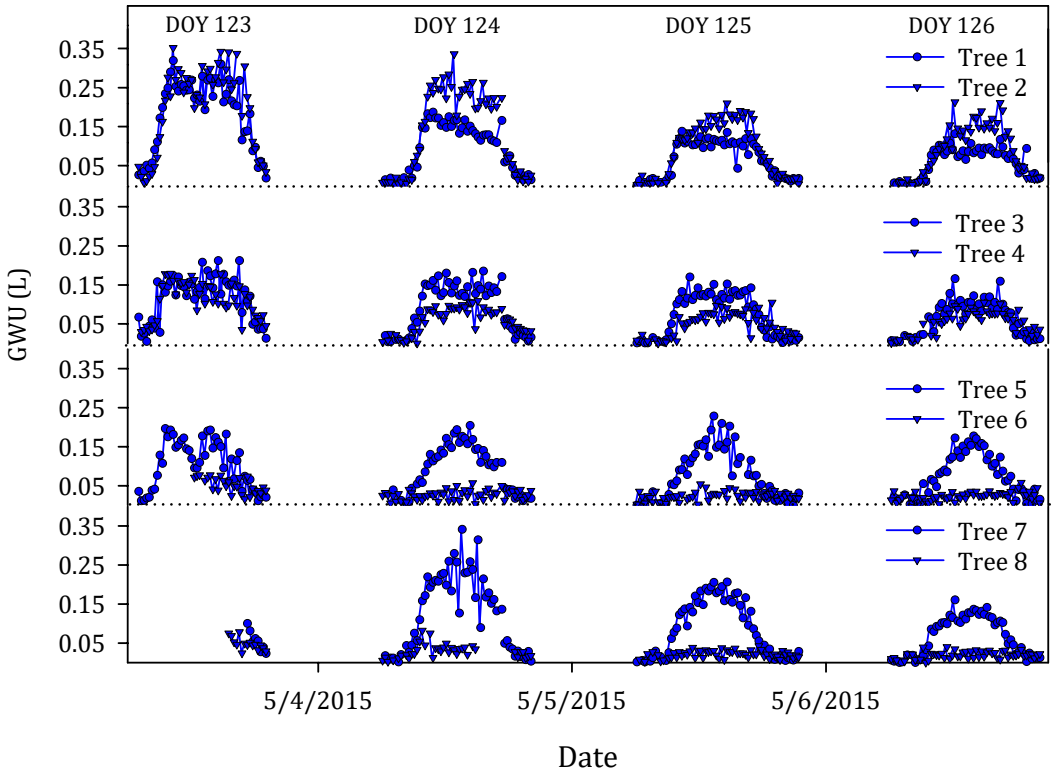

Figure II-2 Gravimetric water use for all trees during the four days of our experiment, collected at 15-minute intervals.

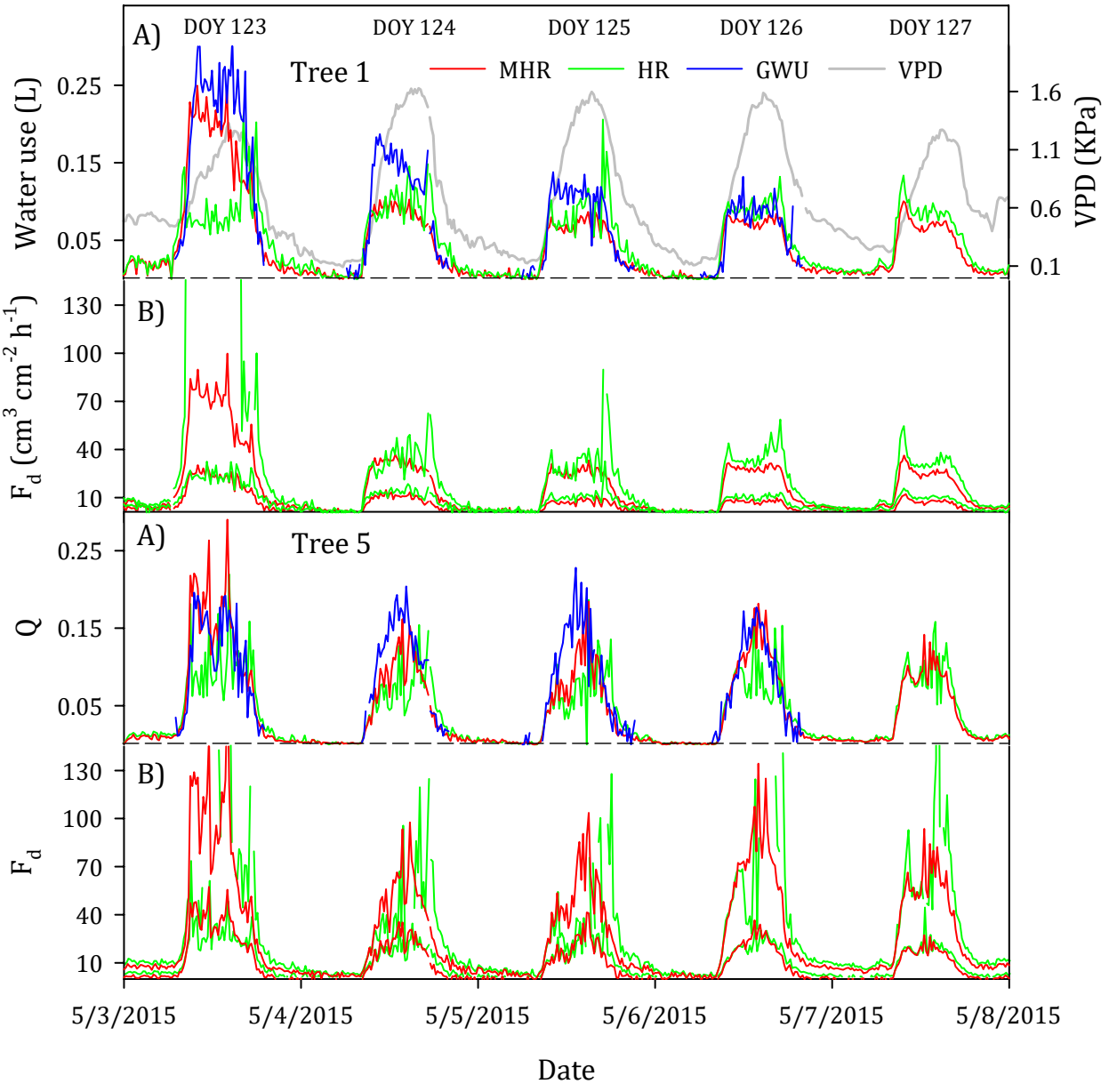

Figure II-3 Sap flux density estimated with HR and MHR in trees 1 and 2. In this graph we compare Q (A), and one measuring point with the highest F_d range (B) estimated obtained with both algorithms, for trees 1 and 5. Only two of three F_d measurement points are shown per tree.

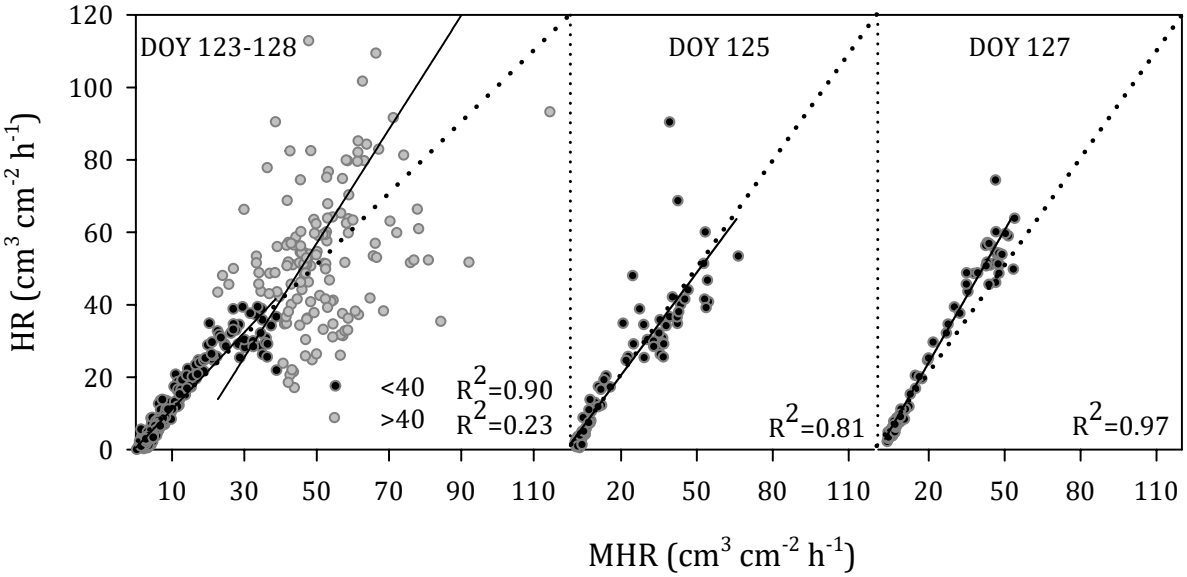

Figure II-4 Correlation of F_d estimates between MHR and HR algorithms for the middle thermocouple of tree 2. In this figure we compare the linearity between MHR and HR. We used data from Tree 2 middle thermocouple only. On average both algorithms showed a strong linear correlation within a range of 0-40. On DOY 127, this range was from 0-70, but HR F_d estimates were slightly higher than MHR

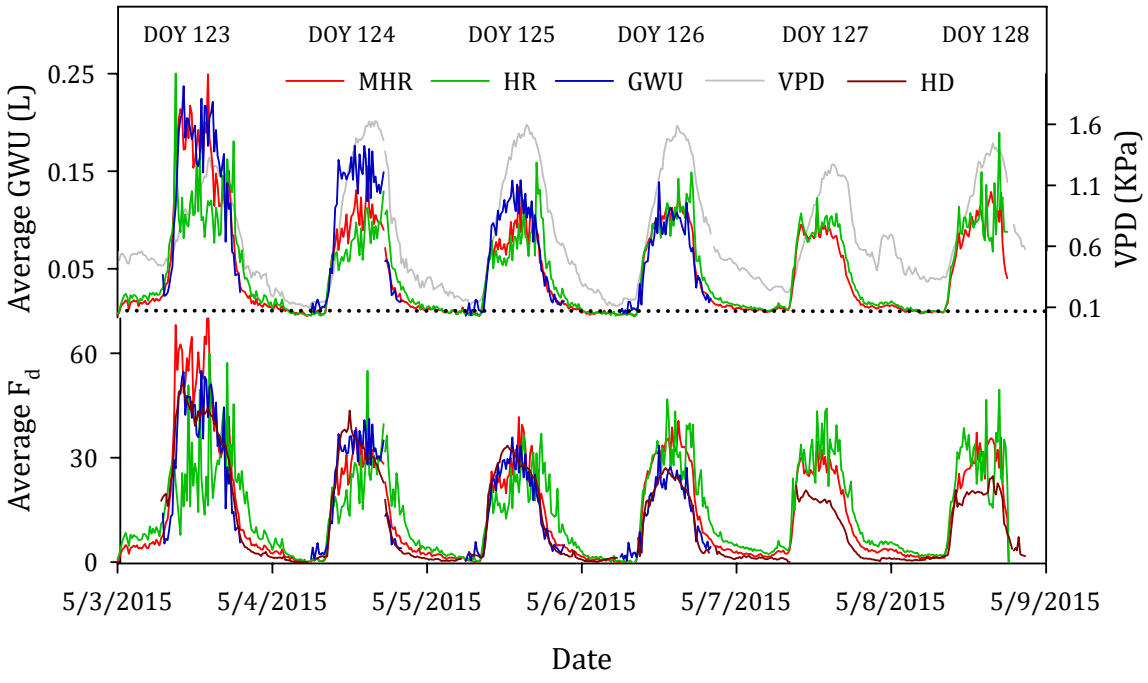

Figure II-5 Average water use (top panel) and average F_d (bottom panel) measured directly using a scale (GWU) or using an algorithm. In this graph we compare average GWU, with average Q for each algorithm, and average F_d for HR, MHR, and our previously calibrated HD F_d estimates for reference purposes. F_d estimates for MHR and HR were not calibrated. We can see that only HR showed an overestimation memory effect on the second half of the day for both F_d and Q

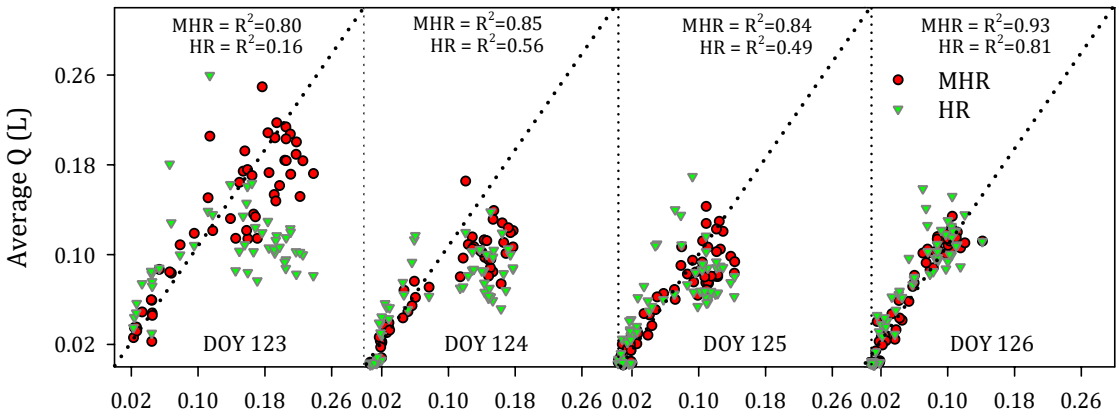

Figure II-6 The relationship between GWU and the MHR and HR algorithms. Here we compare average estimated Q for each algorithm, with average GWU. We used all data from Trees 1, 2, 3, 5, 7 and 8 including the time intervals when F_d was underestimated. All data (Q and GWU) corresponds to 15-minute intervals

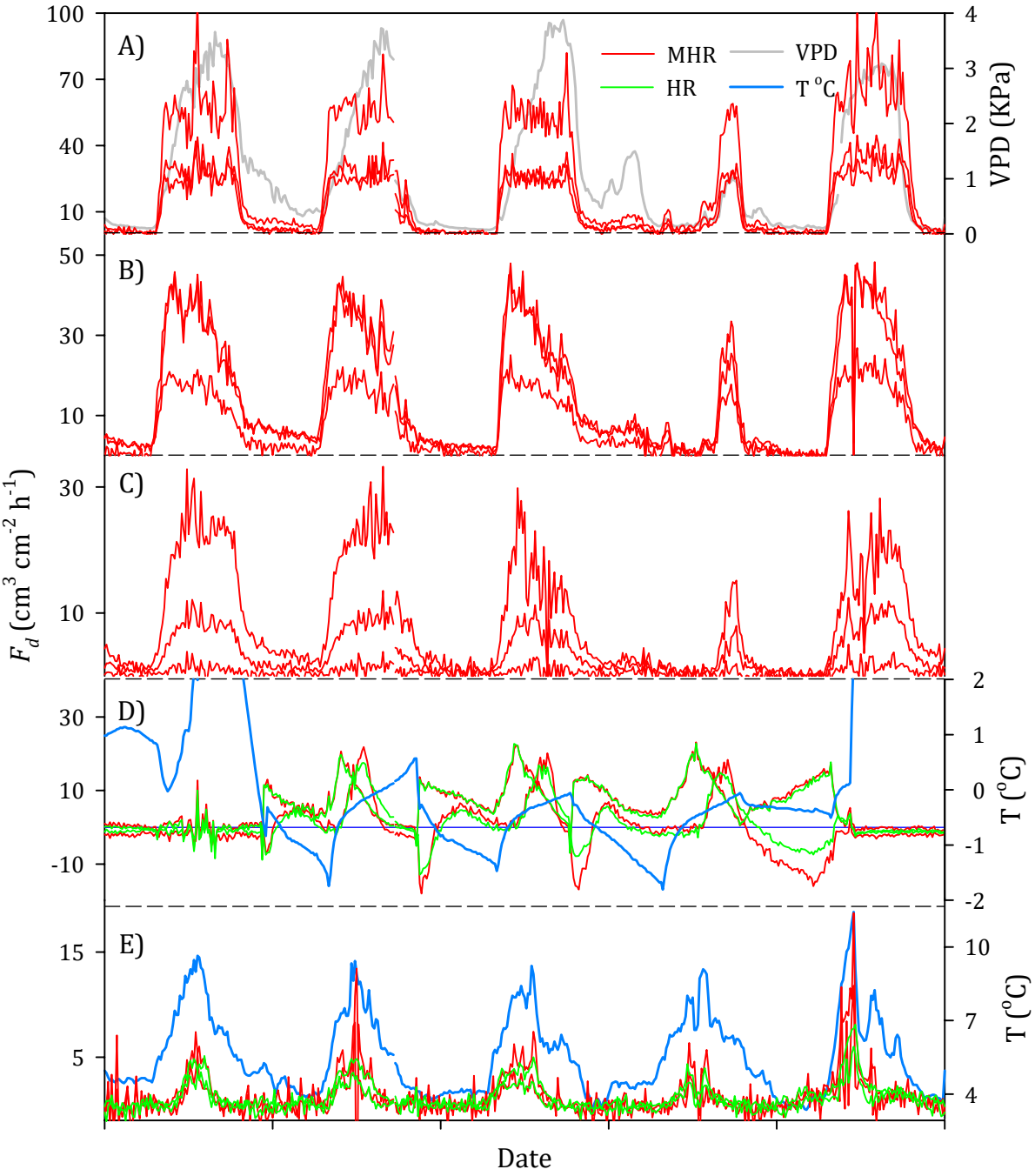

Figure II-7 Ranges of F_d measured with MHR and HR on different species and environmental conditions. A) 1 YO, B) 4 YO, and C) 10 YO *E. grandis* trees, growing in plantations. D) *A. saccharum* log subjected to freeze/thaw cycles, and E) *E. myrtilloides* tree. Each line for MHR and HR is a position inside the sapwood, we show three in *E. grandis* trees, and two in *A. saccharum* and *E. myrtilloides* tree. All measurements were collected at 15-minute intervals.

Table II-1 Summary of the tree harvesting protocol and sap flow methods installed in each tree

Tree	Diameter	Harvest date/time
1	5.3	May 1, ~8:00
2	6.1	May 1, ~8:00
3	3.9	May 1, ~9:00
4	6.1	May 1, ~12:00
5	4.3	May 1, ~12:00
6	6.1	May 3, ~13:00
7	5.6	May 3, ~13:00
8	5	May 3, ~15:00

HPM = heat pulse method
HDM = heat dissipation method

Table II-2 Comparison of means of gravimetric water use measured in all trees

Tree	Anova DOY 153-156	Anova DOY 154-156	Welch Anova DOY 153-156	Welch Anova DOY 154-156
1 average = 394	F = 53.61 p = <0.0001	F = 8.68 p = 0.0003	F =35.91 p = <0.0001	F =7.70 p = 0.0008
2 average = 518	F = 53.61 p = <0.0001	F = 6.75 p = 0.0015	F = 18.87 p = <0.0001	F = 5.00 p = 0.0084
3 average = 347	F = 14.82 p = <0.0001	F = 4.25 p = 0.0158	F = 17.49 p = <0.0001	F = 4.26 p = 0.0166
4 average = 268	F = 53.53 p = <0.0001	F = 2.96 p = 0.054	F = 38.4 p = <0.0001	F = 2.79 p = 0.0723
5 average = 250	F = 3.81 p = 0.01	F = 1.55 p = 0.21	F = 3.97 p = 0.0099	F = 1.56 p = 0.2150
6 average = 112	F = 118.02 p = <0.0001	F = 6.02 p = 0.003	F = 37.68 p = <0.0001	F = 7.59 p = 0.0008
7 average = 397	F = 9.54 p = <0.0001	F = 11.43 p = <0.0001	F = 10.21 p = <0.0001	F = 10.88 p = <0.0001
8 average = 114	F = 135.77 p = <0.0001	F = 15.91 p = <0.0001	F = 43.05 p = <0.0001	F =11.43 p = <0.0001

References

Alvarado-Barrientos, M. S., V. Hernandez-Santana, and H. Asbjornsen. 2013. Variability of the radial profile of sap velocity in Pinus patula from contrasting stands within the seasonal cloud forest zone of Veracruz, Mexico. Agricultural and Forest Meteorology **168**:108-119.

Becker, P. 1998. Limitations of a compensation heat pulse velocity system at low sap flow: implications for measurements at night and in shaded trees. Tree Physiology **18**:177-184.

Benyon, R. G. 1999. Nighttime water use in an irrigated Eucalyptus grandis plantation. Tree Physiology **19**:853-859.

Burgess, S. S. O., M. Adams, N. C. Turner, et al. 2001. An improved heat pulse method to measure low and reverse rates of sap flow in woody plants (vol 21, pg 589, 2001). Tree Physiology **21**:1157-1157.

Burgess, S. S. O., M. A. Adams, and T. M. Bleby. 2000. Measurement of sap flow in roots of woody plants: a commentary. Tree Physiology **20**:909-913.

Burgess, S. S. O., and T. E. Dawson. 2004. The contribution of fog to the water relations of Sequoia sempervirens (D. Don): foliar uptake and prevention of dehydration. Plant Cell and Environment **27**:1023-1034.

Clearwater, M. J., F. C. Meinzer, J. L. Andrade, et al. 1999. Potential errors in measurement of nonuniform sap flow using heat dissipation probes. Tree Physiology **19**:681-687.

Cohen, Y., M. Fuchs, and G. C. Green. 1981. Improvement of the heat pulse method for determining sap flow in trees. Plant Cell and Environment **4**:391-397.

Dunn, G. M., and D. J. Connor. 1993. An Analysis of Sap Flow in Mountain Ash (Eucalyptus-Regnans) Forests of Different Age. Tree Physiology **13**:321-336.

Eller, C. B., S. S. O. Burgess, and R. S. Oliveira. 2015. Environmental controls in the water use patterns of a tropical cloud forest tree species, Drimys brasiliensis (Winteraceae). Tree Physiology **35**:387-399.

Forrester, D. I., J. J. Collopy, and J. D. Morris. 2010. Transpiration along an age series of Eucalyptus globulus plantations in southeastern Australia. Forest Ecology and Management **259**:1754-1760.

Forster, M. 2017. How Reliable Are Heat Pulse Velocity Methods for Estimating Tree Transpiration? Forests **8**:350.

Granier, A. 1985. Une nouvelle méthode pour la mesure du flux de sève brute dans le tronc des arbres. Annals of Forest Science **42**:193-200.

Gutiérrez Lopez, J. A., J. Licata, T. Pypker, and H. Asbjomsen. 2018. Analysis of changes in the current supplied to heat dissipation sensors using an improved tree-cut experiment on young Eucalyptus grandis trees. Tree Physiology.

Intrigliolo, D. S., A. N. Lakso, and R. M. Piccioni. 2009. Grapevine cv. 'Riesling' water use in the northeastern United States. Irrigation Science **27**:253-262.

Kagawa, A., L. Sack, K. Duarte, and S. James. 2009. Hawaiian native forest conserves water relative to timber plantation: Species and stand traits influence water use. Ecological Applications **19**:1429-1443.

Kallarackal, J. 2010. Water use by Eucalyptus grandis plantations in comparison with grasslands located in the downhill areas of Mannavan Shola in the Western Ghats of Kerala. Thrissur, Kerala, India.

Kukowski, K. R., S. Schwinning, and B. F. Schwartz. 2013. Hydraulic responses to extreme drought conditions in three co-dominant tree species in shallow soil over bedrock. Oecologia **171**:819-830.

Lundblad, M., and A. Lindroth. 2002. Stand transpiration and sapflow density in relation to weather, soil moisture and stand characteristics. Basic and Applied Ecology **3**:229-243.

Marshall, D. C. 1958. Measurement of Sap Flow in Conifers by Heat Transport. Plant Physiology **33**:385-396.

Meinzer, F. C., S. A. James, and G. Goldstein. 2004. Dynamics of transpiration, sap flow and use of stored water in tropical forest canopy trees. Tree Physiology **24**:901-909.

Poblete-Echeverria, C., S. Ortega-Farias, M. Zuniga, and S. Fuentes. 2012. Evaluation of compensated heat-pulse velocity method to determine vine transpiration using combined measurements of eddy covariance system and microlysimeters. Agricultural Water Management **109**:11-19.

Steppe, K., D. J. W. De Pauw, R. Lemeur, and P. A. Vanrolleghem. 2006. A mathematical model linking tree sap flow dynamics to daily stem diameter fluctuations and radial stem growth. Tree Physiology **26**:257-273.

Steppe, K., M. W. Vandegehuchte, R. Tognetti, and M. Mencuccini. 2015. Sap flow as a key trait in the understanding of plant hydraulic functioning. Tree Physiology **35**:341-345.

Swanson, R. H. 1994. Significant Historical Developments in Thermal Methods for Measuring Sap Flow in Trees. Agricultural and Forest Meteorology **72**:113-132.

Vandegehuchte, M. W., S. S. O. Burgess, A. Downey, and K. Steppe. 2015. Influence of stem temperature changes on heat pulse sap flux density measurements. Tree Physiology **35**:346-353.

Vandegehuchte, M. W., and K. Steppe. 2012. Sapflow+: a four-needle heat-pulse sap flow sensor enabling nonempirical sap flux density and water content measurements. New Phytologist **196**:306-317.

Vandegehuchte, M. W., and K. Steppe. 2013. Sap-flux density measurement methods: working principles and applicability. Functional Plant Biology **40**:213-223.

Vergeynst, L. L., M. W. Vandegehuchte, M. A. McGuire, et al. 2014. Changes in stem water content influence sap flux density measurements with thermal dissipation probes. Trees-Structure and Function **28**:949-955.

Vertessy, R. A., T. J. Hatton, P. Reece, et al. 1997. Estimating stand water use of large mountain ash trees and validation of the sap flow measurement technique. Tree Physiology **17**:747-756.

Wullschleger, S. D., and A. W. King. 2000. Radial variation in sap velocity as a function of stem diameter and sapwood thickness in yellow-poplar trees. Tree Physiology **20**:511-518.

Zalesny, R. S., A. H. Wiese, E. O. Bauer, and D. E. Riemenschneider. 2006. Sapflow of hybrid poplar (Populus nigra L. x P-maximowiczii A. Henry 'NM6') during phytoremediation of landfill leachate. Biomass & Bioenergy **30**:784-793.

CHAPTER III

WATER BALANCE AND ECOHYDROLOGICAL IMPACTS OF BIOENERGY PRODUCTION IN ASPEN STANDS

Abstract

Demand for timber and biomass from poplars, specially from short rotation woody crops (**SRWC**) is increasing in the East North Central region in the USA. With an increase in the total area managed to meet these needs, understanding how stand level transpiration (***T***, mm d^{-1}) changes during the average rotation length can help improve model parameterization and prediction capabilities to estimate *T* using stand age as a main predictor variable. However, a major challenge for this approach is to address site-specific differences that can significantly override the age affect. In this study, we monitored three aspen-dominated (*Populus tremuloides* Michx.) natural stands located in Oneida County, Wisconsin, USA: a 34-year-old (Mature) reference mature forest, and two coppice-managed plantations (24 and 10-year-old, Mid-aged, Young, respectively). Our objectives were to: a) determine whether site age is correlated to stand *T*, and b) assess the role of soil saturation (***S***, unitless) in driving *T* and explaining inter-site variability. Sap flow sensors were used to estimate average sap flux density ($\boldsymbol{F_d}$, $cm^3\ cm^{-2}\ h^{-1}$) at each site, and whole-tree water use (***Q***, L d^{-1}) and *T* were estimated by multiplying F_d by predicted sapwood area ($\boldsymbol{A_S}$ **,** m^2) from allometric equations fitted for each site. To test the effects of site-specific differences in *T* estimates, we adjusted a two-dimensional *S* model for each site, and predicted *S* under two scenarios: limited and non-limited *S*. Modeled *S* was used to model stand transpiration ($\boldsymbol{T_{mod}}$, mm d^{-1}) for each site and determine whether under similar *S* conditions, age and *T* are correlated. According to our statistical analysis, estimated Mature stand *T* had a maximum of 5.5 m d^{-1} early in the growing season (seasonal average 2.7) and was higher than the Mid-aged and Young sites, which both had a maximum early-growing season *T* of 2.5 mm (seasonal average 1

and 0.3 mm, respectively). T_{mod} under an *S*-limiting scenario reduced average transpiration rates by ~10% across sites, but these reductions were not significantly different from estimated *T*. T_{mod} under non-limiting *S* conditions resulted in significantly higher transpiration rates in the Young (+170%), but not in the Mid-aged (+34%) or Mature (+5%) sites. While not significantly different between the Mid-aged and Young sites, annual average *T* was positively correlated with stand age, and this relationship was maintained under both *S* scenarios. Dominant trees accounted for 76% of stand *T* in the Mature site, and 58% and 51% in Mid-aged and Young sites, respectively. These results match previous studies in mature aspen forests, and also highlight the important role of small-diameter trees in sites where they are present in large numbers. Our results indicate that site-specific differences in soil properties and their associated moisture availability, can have an overriding effect on age, nonetheless, this effect can be accounted for by modeling the effects of *S* on stand *T* under potentially different *S* scenarios. Once this approach was applied, stand age was related to average stand *T*. Our results documenting the relationship between stand age and water use, combined with our modeling approach to account for site-specific differences, provide valuable baseline information for predicting impacts of aspen-dominated SRWC on site water balance under different management scenarios.

Keywords: ecohydrology, sap flow, aspen, transpiration, modeling

Introduction

Despite increasing scientific interest and research initiatives on bioenergy-water relationships, there is a strong focus on industrial water use associated with biomass feedstock processing (Berndes 2008, Chiu and Wu 2013, IDNR 2007, Perlack et al. 2005, Rupesh et al. 2016, White 2010, Yeh et al. 2011), and less attention has been given to water use (transpiration,

T, mm d^{-1}) associated with plant growth (Hinchee et al. 2009, Jassal et al. 2013, Mueller et al. 2012, Popp et al. 2014, Powers et al. 2011, Watkins et al. 2015). Consequently, the potential ecohydrological impacts of the production of bioenergy might be underestimated. Further, at the regional scale, the lack of studies on stand-level *T* and its impacts on the water cycle, are reflected in the absence of strategies to address these issues in long-term bioenergy development plans (BETO 2013, Perlack et al. 2005).

In the East North Central region of the USA short rotation woody crops (**SRWC**) are commonly used to produce wood pellets, timber, and whole tree biomass for bioenergy (Davis et al. 2012, Hinchee et al. 2009, Perlack et al. 2005, Zamora et al. 2013), with common rotation cycles varying depending on the end use (under three years if it is used for feedstock biomass, or up to 15 if trees are sold for timber). At the national scale, about 27% of the renewable energy consumed is derived from SRWC, and it is expected to increase from 2% of total energy consumed nationally, to 9% by 2030 (White 2010). The rapidly growing demand for alternative renewable bioenergy sources will likely result in the expansion of SRWCs and the conversion of mature forests into bioenergy plantations.

Understanding how stand management (e.g., rotation, thinning, etc.) impacts *T* dynamics is fundamental in order to foresee potential negative impacts under future environmental conditions, and to improve current management systems or adjust rotation lengths in ways that balance both biomass productivity with *T* rates (Berndes 2010, Berndes et al. 2010). In most cases, such as with SRWC, the primary goal is to maximize timber and biomass production per unit land area (Forrester 2013, Nelson et al. 2012, Tullus et al. 2009). However, since plant productivity and biomass accumulation are directly related to water use (Dillen et al. 2013, Kanowski 1997, White 2010, Zamora et al. 2013), management practices aimed at increasing biomass productivity are likely to result in higher *T* rates.

Previous research on SRWC in poplars and willows has provided evidence on the potential impacts to hydrologic services under current and future climate change conditions (Dimitriou and Mola-Yudego 2017a, b, Lasch et al. 2010, Oliver et al. 2015), potential nitrogen and CO_2 fluxes and greenhouse gas mitigations associated to their production (Balasus et al. 2012, Hansen et al. 2013, Verlinden et al. 2013), the impacts of their production to water quality, soil organic matter and microbial communities (Baum et al. 2013), and the quality and quantity of the biomass that can be harvested (Kauter et al. 2003). However, despite the current state of knowledge on SRWC, there are several questions that remain unanswered regarding *T* patterns and potential impacts on hydrologic services. For example, the rotation cycle for most short rotations of hybrid poplars for biomass feedstock production are under 5 years (Nikiema et al. 2012, Zamora et al. 2013), while the rotation length is commonly increased to more than 10 for timber or wood pellet production (Christersson 2010, Karacic et al. 2003, Liesebach et al. 1999), especially for *Populus tremuloides* Michx. However, rotation cycles for feedstock biomass or timber production do not take into consideration potential changes in *T* over time, which could be very helpful in the creation of modelling scenarios using stand age as a main predictor variable. In other fast-growing species plantations studies have found a trend in water use strongly associated with age. For example, in *E. grandis* plantations, *T* increases from the moment of the establishment and reaches maximum rates at canopy closure (3-6 years of age), followed by decreases in *T* until transpiration rates are similar to those observed the first year of establishment. The subsequent reduction in *T* has been linked to canopy closure; the faster canopy closure occurs, the steeper the post-canopy closure decline in *T* (Almeida et al. 2007, Du Toit 2008, Forrester et al. 2010, Ryan et al. 2008). While a decline in stand *T* as pronounced as what has been observed in *E. grandis* plantations is not expected in *P. tremuloides* SRWC plantations, primarily due to the relatively slower growth rates. Nonetheless, information about

the relationship between *T* and plantation age can help land managers incorporate stand *T* in their management strategies and define rotation scenarios that take into consideration both biomass accumulation and water use at the tree and stand levels. Unlike other fast-growing species (e.g., eucalyptus spp.), there is a lack of studies for many SRWCs, including aspen, that address changes in *T* in rotation lengths greater than 10 years, and most studies focused on rotations under 5YO (e.g., Bloemen et al. 2017, Gochis and Cuenca 2000, Jassal et al. 2013, Pataki et al. 2011, Petzold et al. 2011). However, the available studies have observed similar trends to those observed in eucalyptus and other fast-growing species. For example, Gochis and Cuenca (2000) observed an increment in stand *T* from 1 to 3 year-old (**YO**) poplar hybrids (*P. trichocarpa* x *P. deltoids*) plantations, similar to the results by Wilske et al. (2009) in 3 and 6YO poplars. Angstmann et al. (2012) estimated stand *T* using sap flow sensors in longer rotations (10, 43 and 77 YO) in sites where *P. tremuloides* was not a dominant species, and observed an inverse relationship with age for aspen trees. When all species were considered, they observed an increment from 18 to 43 and a reduction afterwards from 43 to 77 YO. A similar study by Ewers et al. (2005) found that average *T* reduced from 12 to 20YO in sites where *P. tremuloides* were present, and an increment from 20 to 37YO. However, in these sites, *P. tremuloides* abundance was different among sites, which might explain their results. Considering all species in their sites, stand *T* increased with age from 12 to 37YO, similar to the results by Angstmann et al. (2012). These results highlight that at the stand level, *T* is related to stand age, and this relationship can only be observed at the stand level in mixed species.

Deterministic models are commonly used for various species to estimate and model stand *T* under different environmental conditions. Most of these models estimate *T* using a combination of tree or plant-level measurements scaled to the site level, soil water content data, water and carbon fluxes measured with eddy covariance, or with energy balance equations (Barella-Ortiz et

al. 2013, Bloemen et al. 2017, Domec et al. 2012, Fischer et al. 2013, Jones et al. 2017, Kim et al. 2008, Muller and Lambs 2009, Valipour 2015, Wilske et al. 2009, Zhao et al. 2013). However, a key limitation of these methods is the need for validation. Studies that rely on energy balance equations or eddy covariance measurements (Arneth et al. 1999, Poblete-Echeverria et al. 2012, Schume et al. 2005) often validate the measurements against watershed-level discharges, which have a strong lag effect on daily *T* estimates, or plant-based references (i.e., sap flux measurements) which can be limited by small sample size (Kume et al. 2010, Peters et al. 2018, Smith and Allen 1996). Another limitation is the difficulty in monitoring tree-level *T* for extended periods of time, at time intervals relevant to derive water use estimates for entire rotation cycles. On SRWC, most studies cover time frames within one to five years (Allen et al. 1999, Bloemen et al. 2017, Jassal et al. 2013, Jones et al. 2017, Kim et al. 2008, Perry et al. 2001, Uddling et al. 2008), primarily due to the limitations previously mentioned. An alternative to estimating water use based on continuous measurements over time for plantations managed under different rotation lengths, is to study plantations of the same species at different ages in chronosequence studies (e.g., Delzon and Loustau 2005, Grau et al. 1997, Naranjo et al. 2011, Petrone et al. 2015, Walker et al. 2010, Zewdie et al. 2009). Following this approach, it is possible to make inferences about the development of the species/ecosystem of interest over time, assuming that site characteristics such as soil type, topography, or nutrients are accounted for, and the site has low diversity and is not subjected to extreme disturbances.

To test whether stand age and average stand-level *T* relationships can be established for SRWC of *P. tremuloides*, the objectives of this study were to: a) estimate seasonal and daily *T* of three (Young, Mid-aged, and Mature, see next section for details) coppice plantations dominated by *P. tremuloides* and b) determine how variability in site conditions can influence the age effect on stand *T*. **Our first hypothesis** was that at the tree level, whole tree water use (Q L d^{-1}) would

be highest in the Mature site, compared to the other two sites. Conversely, we expected that the rate of water uptake per unit sapwood area (i.e., sap flux density; F_d) would be greatest in the Young site, and lowest at the Mature site, due to the overall lower leaf area to sapwood area ratios. **Our second hypothesis** was that stand *T* will increase with stand age, primarily as a result of greater total leaf area and leaf area index (**LAI**, unitless) and overall larger individual tree sizes. Specifically, we expected stand *T* to be correlated with stand age. Finally, we were also interested in understanding how variability among sites can override age effects on stand *T*, and if through modeling approaches, it is possible to account for these differences and elucidate the underlying relationship between age and stand *T*.

The expected increase in the demand for biomass feedstock and timber from SRWCs will likely result in an expansion of poplar-dominated forests and plantations in the Midwestern U.S. A. Understanding how age and site effects interact to influence stand *T* can be of great value for the development of models to better predict potential ecohydrological impacts of the expansion of SRWC on water yield and, hence, improve management strategies for maintaining diverse benefits to society.

Methodology

Description of the study sites

This study was conducted in three naturally-regenerated aspen (*Populus tremuloides* Michx.) stands located in Oneida County, Wisconsin, USA: a 34-year-old (**YO**) reference mature forest (45°48’24.43”N-89°39’59.18”W), a 24-YO coppiced-managed plantation (45°37’14.52”N- 89°35’35.63”W) and a 10-YO a coppice-managed plantation (45°42’47.06”N-89°47’30.31”W) (henceforth, **Mature**, **Mid-aged** and **Young** sites).

The area is dominated by glacial moraines and outwash plains that create a set of deep sand, sandy-loam soils ranging from moderately well-drained to excessively drained. The dominant soil types at each site were: Mature (Padus-Pence sandy loams – well drained sandy loam and gravelly sandy loam), Mid-aged (Padus-Goodman complex – well drained sandy loam and gravelly sandy loam), Young (Sayner loamy sand – excessively drained loamy sand) (Hartemink et al. 2012). Soil bulk density, percent sand and clay content, and porosity were estimated at each site from 0-60 cm in 15 cm increments (Table III-1) (Cisz-Brill et al, in prep).

Data collection

The data collected at each site included: whole-tree (***Q***, L d^{-1}) and stand-level water use (***T***, mm d^{-1}), solar radiation (CNR2, watts m^{-2}), relative humidity (HMP45, **RH**, %), and air temperature (HMP45, **AirT**, %), precipitation, vapor pressure deficit (***VPD*** , kPa) throughfall, stemflow, volumetric water content (EC5, **VWC**, cm^3 cm^{-3}) and stand characteristics (e.g., density, composition, basal and sapwood area). All environmental data were collected at a weather station installed near the Mature site. All environmental sensors were read and stored every 15 minutes using a CR1000 datalogger (Campbell Scientific. Inc. Utah, USA) from June 10 to October 5, 2013 (DOY: 167-280). A second set of environmental variables including RH, *AirT* and wind speed (***u***, m s^{-1}) were downloaded from the MesoWest weather station (ID = KRHI). Stemflow and throughfall were measured after precipitation events of varying magnitudes using 10 collectors for stemflow installed in trees of various diameters and 20 collectors randomly distributed in each site for throughfall. However, due to constant overflow, we were unable to use our stemflow data. Throughfall data were averaged per collection period, and we subtracted the precipitation registered for the same time intervals to estimate precipitation interception for each site. A linear equation was fitted between precipitation and

percent precipitation interception to compare precipitation interception at each site. VWC was measured in the first 100 cm of soil at 20, 40 and 100 cm, with two replicates per site, and converted to soil saturation (***S***, unitless) according to van Genuchten (1980):

$$S = \frac{\theta - \theta_r}{\theta_s - \theta_r} \qquad \text{Eq. III-1}$$

Where S is the saturation, θ the volumetric water content (averaged for the entire 100 cm), θ_r the residual water content (0.05 % for sandy soils, according to (Zhang 2011)), and θ_s the volumetric water content at saturation. θ_s was estimated as the average porosity from 0-60 cm for each site. Once S was estimated, a new class variable was created to identify five S ranges (***SR***, unitless) based on the absolute saturation value: 0.03-0.16, 0.16-0-18, 0.18-0.19, 0.19-0.22, 0.22-0.38. Additionally, we estimated S for the top 40 cm of soil ($\boldsymbol{S_{40}}$) for modeling purposes and to assess whether soil moisture in the top soil had a higher influence on transpiration rates than the entire 100 cm soil profile.

Stand characteristics

As part of a different study on biodiversity of pollinators Jarvi et al. (2018) ten 100 m^2 plots were randomly established at the Mature and Mid-aged sites, and 50 m^2 due to higher tree density in the Young site. At each plot, measurements were taken of diameter at breast height (**DBH**) of trees greater than 1 cm in DBH. We used these data to determine species composition, stand density and average height (Table IV-3). Using the data from all plots, we determined the diameter distribution of *P. tremuloides* trees for each site in diameter categories in increments of 1 cm. The diameter distribution estimated for each site was later used in the scaling procedure (see "Scaling process" below).

For comparison purposes, total above-ground biomass for *P. tremuloides* trees was estimated according to Jenkins et al. (2003) using the following formula:

$$bm = Exp(\beta_0 + \beta_1 \ln(DBH)) \qquad \text{Eq. III-2}$$

Where *bm* is the total aerial biomass in kg, β_0 and β_1 the predictor parameters (-2.2094, and 2.3867, respectively). Biomass was estimated for all trees in each of the 10 plots per site, and scaled up to 1 ha to estimate total dry biomass per ha (**TDB**, t ha-1). For other species present at each site, we estimated TDB using Eq. III-2 selecting their respective β_0, and β_1 parameters for each species, as indicated by Jenkins et al. (2003).

Measurement of sapwood area

Populus tremuloides is a heartwood species characterized by the presence of diffuse pores evenly distributed across the sapwood (Hart et al. 2013); consequently, there is no clear boundary to differentiate sapwood from heartwood. While the sapwood is whiter than the heartwood, and heartwood is white/light brown or creamy, they are often indistinguishable, making it difficult to create allometric equations to predict sapwood area ($\boldsymbol{A_S}$, m^2) (Mackes and Lynch 2001). To address this issue and ensure accurate measurements, a subset of samples from each site were dyed using the following dyes and concentrations: Fuschine (1 and 0.1%), ferric chloride (10%), methyl orange (0.1%), bromocresol green (1%) and soaking the samples in ethyl alcohol and acetone, following the protocol by Wengert (1976). All dyes were applied on a recently sanded sample and monitored over a 48-hour period. The ethyl alcohol was applied directly to the samples and monitored while the sample remained wet. A flashlight (Maglite Led Pro®) was used to enhance the visibility of sapwood in all samples, referred to here as the light diffusion method, whereby light is diffused where the sapwood absorbs the applied chemical.

Methyl orange yielded favorable results after approximately 10 minutes of application and remained effective for another 20, approximately. However, ethyl alcohol yielded instantaneous results, similar to the methyl orange dye, but remained active only while the sample was wet. Based on these results, sapwood depth was estimated by combining ethyl alcohol treatment with the light diffusion method.

A total of 74 tree cores were collected (Mature: 24, Mid-aged: 18, Young: 32). Sapwood depth and tree diameter were used to estimate $\boldsymbol{A_S}$, m^2 following the light diffusion method described above. All the samples were taken at the end of the growing season (October 6th, 2013) approximately 10 cm below the area where the sensors were installed. One sample was taken in the direction of the sap flow sensors and the other one at approximately a 90º angle to cover the radial variability of sapwood/heartwood. We sampled the entire width of every stem. All samples were shipped to the Ecohydrology Laboratory at the University of New Hampshire and oven-dried over a 24-hour period. Once A_S was estimated we fitted the following equation for each site to predict A_S (in m^2) from diameter (in cm, with bark):

$$A_S = Exp(\beta_0 + \beta_1 \ln(DBH)) \qquad \text{Eq. III-3}$$

Where A_S is the sapwood area, and β_0 and β_1 the predictor parameters. We estimated parameters (β_0 and β_1) for each site (see Table III-3), but given the relatively low number of trees sampled in the Mid-aged site, the R^2 between predicted and observed A_S was low. To increase the predictability of the allometric equation for this site, we merged Mid-aged and Mature into a single category and generated β_0 and β_1 parameters. Ultimately, A_S was estimated for the Young site using the parameters derived from that site, and for the Mid-aged and Mature sites using the parameters derived from the merged data.

Tree-level water use

To estimate average tree-level water use, we used sap flow sensors following the heat ratio (**HR**) method (Burgess et al. 2001b). We selected a total of eight trees per site, based on physical characteristics (e.g., diameter, crown size, overall visual health), to cover as much as possible the variability at each site. We installed one sap flow sensor per tree at breast height, and sensors were installed in all four cardinal positions (North, East, South, West) at each site. All sensors were designed and built by JGL at the Ecohydrology Laboratory at the University of New Hampshire. Due to the high wildlife (deer) traffic in the area, the sensors were designed to include a 4-pin connector that allowed the communication cables to detach from the sensors when pulled, to avoid unnecessary damage to our equipment. According to the third law of thermocouples, a third metal can be added to the thermocouple without affecting the voltage generated at the junction of interest. We tested in the Laboratory sensors with and without the 4-pin connector at different temperatures and saw no difference in the measured voltages . Each sensor set consisted of two probes with three type-T thermocouples and one probe with coiled 20 Ω nichrome wire heater. The thermocouples were positioned at 0.5, 1.75 and 3 cm from the base of the sensor. During the installation of the sensors, we did not remove the bark from the trees, but for some large trees, we used a spatula to create an even surface to facilitate thermocouple alignment. After installation, all sensors were covered with 1 m (height) reflective insulation (Reflectix ®) to protect the sensors against sudden changes in ambient temperature or sunflecks. We estimated heat pulse velocity (V_h, cm h^{-1}) and wound-corrected heat pulse velocity (V_c, cm h^{-1}) according to Burgess et al. (2001a) using:

$$V_h = \frac{\mathrm{k}}{x} ln \frac{v_1}{v_2} 3600 \qquad \text{Eq. III-4}$$

$$V_c = bV_h + cV_h^2 + dbV_h^3 \qquad \text{Eq. III-5}$$

Where V_h is the heat pulse velocity, k is the thermal conductivity and x the distance between probes, and v1/v2, the temperature ratio. b, c, and d, are the parameters used to correct V_h for wounding effects. V_c was converted to sap flux density (***F_d***, $cm^3\ cm^{-2}\ h^{-1}$**)** according to Vandegehuchte and Steppe (2013) with the following equation:

$$F_d = \frac{\rho_d}{\rho_s}\left(MC + \frac{C_{dw}}{C_s}\right)V_c \qquad \text{Eq. III-6}$$

Where ρ_d is the density of the sapwood, ρ_s the density of water, MC the volumetric water content of the sapwood, C_{dw} the thermal conductivity of dry wood, and C_s the thermal conductivity of water.

Upscaling of plant transpiration

To scale whole-tree level measurements Q ($L\ d^{-1}$) to stand-level transpiration (***T***, $mm\ d^{-1}$), first we averaged F_d (estimated using Eq. III-6) for each site using all the measurement points (approximately 24 points per site). F_d data with constant noise (likely the result of sensor, or equipment malfunction) were filtered out and not used to estimate site-average F_d. Next, we predicted A_S of all trees within each of the diameter categories derived from each site (see "Stand characteristics" above) using Eq. III-3. We estimated sap flow (***Q***, $L\ h^{-1}$) for all trees of each diameter category multiplying site-average F_d by the predicted A_S of each tree. Daily Q ($L\ d^{-1}$) was estimated first integrating all hourly estimates for each tree, and then averaging the integrating measurements for all trees of each site. For each site, T was estimated using the following formula:

$$\sum_{d=i}^{d=n} \frac{(F_d \,.\, A_s)}{A} D \qquad \text{Eq. III-7}$$

Where d_i-d_n are the first to last diameter categories, F_d the average flux density (converted to L m^{-2} d^{-1}) , A_S the predicted sapwood area (in m^2), A the total area (in m^2) of the subplots (Young = 500 m^2; Mid-aged & Mature = 1000 m^2), D the ratio (unitless) of aspen trees, with respect to other species to correct for the abundance ratio of aspen trees (Table IV-3).

Cross-site comparison

To perform a cross-site comparison and assess the influence of soil water availability on our *T* estimates, we first estimated ET_0 using the Penman-Monteith equation (Allen et al. 1998), then adjusted a soil water balance model (the bucket model) (Guswa et al. 2002, Rodriguez-Iturbe et al. 1999) to predict different scenarios of *S* ($\boldsymbol{S_{mod}}$) (see below for details). We then fitted a linear mixed model (Littell et al. 2006, West et al. 2007) to predict site *T*, using ET_0, *S* and other environmental variables (see below for details). Once the model was fit, we replaced *S* in the mixed model with S_{mod} from the bucket model and estimated stand *T* at similar *S* (based om the seasonal *S* average). Finally, we performed a series of statistical analyses on both the initial *T* and the modeled *T* ($\boldsymbol{T_{mod}}$) to test whether different sites responded similarly to *S*.

Reference evapotranspiration was estimated using:

$$ET_0 = \frac{0.408\Delta(R_\mathrm{n} - G) + \gamma \frac{900}{T + 273} u_2 (e_\mathrm{s} - e_\mathrm{a})}{\Delta + \gamma(1 + 0.34u_2)} \qquad \text{Eq. III-8}$$

Where ET_0 (mm d^{-1}) is the reference evapotranspiration, Δ the slope of the vapor pressure curve (kPa $^oC^{-1}$), R_n the net radiation (MJ m^{-2} d^{-1}), G the soil heat flux density (MJ m^{-2} d^{-1}), γ the

psychometric constant (kPa $^{o}C^{-1}$), T the mean air temperature (^{o}C), u_2 the wind speed (m s^{-1}), e_s the saturation vapor pressure (kPa), and e_a the actual vapor pressure (kPa).

The bucket model was fit for each site to estimate a general saturation-based water balance using the following formula:

$$nZ_r \frac{dS}{dt} = I(S,t) - L(S) - T(S) - E(S) \qquad \text{Eq. III-9}$$

Where n is the porosity of the soil, Z_r soil depth, $I(S,t)$ infiltration rate, $L(S)$ leakage, $T(S)$ transpiration, and $E(S)$ the evaporation from the soil. A full description of the parameters used for this model is shown in Table III-4, and additional details for the estimation of each parameter are shown in Appendix III-II. To reduce the error due to unknown changes in saturated conductivity ($\boldsymbol{K_{sat}}$) at different soil depths, we limited the modeling to the first 40 cm of soil ($\boldsymbol{S_{40}}$). Once the model was fit for each site (see

Appendix III-IV for regression between observed vs. predicted S), we artificially increased or decreased every precipitation event in the Young and Mature sites to generate S_{mod} that resulted in seasonal S averages for two scenarios: a) where S is a limiting factor (seasonal S average of 0.09) and b) where S is not a limiting factor (seasonal S average of 0.2). To minimize the artificial changes (increments or reductions) to every precipitation event to produce the S scenario of interest, S and precipitation data from the Young site was used to generate the S-limited scenario and the data from the Mature site to generate the S-non-limited scenario. These

sites were chosen due to their low and high *S* (Young and Mature, respectively), which were close to our targeted scenarios.

The linear mixed model was fit for each site to predict *T*, using the following general equation:

$$T_{mod} = X\beta + Z\gamma + \varepsilon \qquad \text{Eq. III-10}$$

Where $\boldsymbol{T_{mod}}$ is the modeled (or predicted) site transpiration, *X* is the series of fixed variables (ET_0, S_{40}, *SR*, *VPD*, *RH*, *AirT*, *pp*, *NetRad*), *Z* the random effects (DOY), β and γ are the slopes of *X* and *Z*, and ε the error of the model. We tested three configurations of fixed variables and selected the model with the lowest corrected Akaike and Bayesian Index criterion (Table III-5). Initially, the model was fit using *S* from the top 40 cm of soil, and once the model was fit, *S* was replaced by estimated S_{mod} corresponding to the non-limiting and limiting *S* scenarios.

Statistical analysis

All statistical analyses, including model fitting, and analyses of variance, were performed in JMP Pro 13 (SAS Institute Inc. Cary, North Carolina, USA). To assess the impact of various environmental variables on stand *T*, as part of our second hypothesis (i.e., higher stand *T* in young stands), first we fitted a Standard Least Squares model, where stand *T* was the response variable, and average *AirT*, *RH*, NetRad, *VPD*, daily precipitation, and S_{40} the model effects. Additionally, this analysis was done at different time intervals to detect seasonal effects. These time intervals were selected based on five major *S* recharge periods: July 10 – July25, July 26 – August 6, August 7 – August 27, August 28 – September 9, September 10 – October 8.

A similar analysis was conducted on T_{mod} where we replaced S for S_{mod} corresponding to the S limited and non-limited scenarios, to: a) determine how stand T varied across sites under similar water contents, and b) test how changes in water content affects stand T, potentially overriding the age effect. We used ANOVA's to assess the effects of individual variables on Q or T, or to compare their differences by month or at times of interest. Finally, we averaged F_d from 11AM-3PM (considered the F_d daily peaks) and performed a similar analysis as with Q and T, adding both S and S_{40}, to test if F_d was influenced by changes in top (40 cm) soil water content.

Results

Meteorological variables

According to the local weather station in Rhinelander, WI (MESOWEST Station ID: KRHI), the study area received 420 mm of precipitation from June 16 to October 5th, 2013. Precipitation data collected at each site agreed with the overall pattern but varied in the magnitude of each event and in total precipitation. For the same period, we measured a total of 320 mm. According to the precipitation data, there were two short periods with precipitation under 1mm: a 10-day (DOY: 191-202) and a 20-day period (DOY: 118-238). The maximum solar radiation observed on clear days varied from approximately 700 to 1050 W m^{-2}, the temperature ranged from 1ºC to 32ºC, and relative humidity from 25 to 100%.

General patterns of observed and predicted soil saturation

Soil saturation within the first 100 cm varied by site (annual average 0.14, 0.16 and 0.24, Young, Mid-aged, and Mature, respectively) and these differences were significantly different

(P= <0.0001, F=51220). As shown in Figure III-1, *S* was equally sensitive to precipitation inputs at all three sites, which resulted in a similar *S* seasonal profile.

The bucket model satisfactorily predicted the general trends of *S*. As seen in

Appendix III-IV, combining data from all sites resulted in an R^2 between observed and predicted *S* of 0.86 (RMSE = 0.01). The R^2 at the Young site between predicted and observed was 0.5 (RMSE = 0.01), 0.54 in the Mid-aged site (RMSE = 0.01), and 0.74 in the Mature site (RMSE = 0.01). The largest estimation error was observed in the Young site (Figure III-1), particularly on the driest day (DOY: 237) and at the end of the growing season (DOY: 275). Predicted *S* was lower in the Young and Mature sites at the end of the growing season, but this reduction was likely associated to the fact that the bucket model assumes constant *T* during the entire monitoring period, which results in a reduced modeled *S*.

Stand characteristics and allometric relationships

Analysis of the stand data showed that density was higher in the Young and Mid-aged sites (6680 and 6690 trees ha^{-1}, respectively), compared to the Mature site (4620 trees ha^{-1}), and that the percent of dead trees increased with age from 2 to 15% (Table IV-3). Estimated basal areas of *P. tremuloides* trees were 7.2, 9.2 and 19.4 m^2 ha^{-1} (for Young, Mid-aged, and Mature stands, respectively). Total above ground biomass estimates were 145, 101, and 18 tons of dry biomass per hectare (**TDB** h^{-1}) (Mature, Mid-aged and Young sites, respectively), assuming pure aspen sites. Considering all species combined, the total biomass estimates were slightly higher: 159, 114 and 18 (Mature, Mid-aged, and Young, respectively). Diameter and A_S were more

strongly correlated in the Young and Mature sites (R^2, 0.98 and 0.92, respectively. Table III-3), compared to the Mid-aged site (R^2, 0.45). Combining all sites, diameter and A_S were strongly correlated (Figure III-2), but the A_S of the Young sites was overestimated (Appendix III-I). Conversely, T (L d^{-1}) was poorly correlated with A_S or basal area by site. R^2 between daily water use and diameter was 0.0, 0.09, and 0.08 in the Young, Mid-aged and Mature sites, respectively. Combining all sites, the correlation between daily water use and diameter improved (R^2 = 0.38), but the regression varied during different times of the year (e.g., R^2 = 0.6 from DOY 213-236). The linear equations fitted for each site between average precipitation and percent interception were nearly identical among sites (

Appendix III-IV). Based on the precipitation events we sampled, interception was 100% of precipitation when the total precipitation was 1.6, 2.2 and 1.6 mm in the Mature, Mid-aged and Young sites, respectively. However, based on the intercept of the linear equations, the Mature site had higher overall interception rates, and the Mid-aged and Young sites were 4 and 6% lower, respectively.

Sap flux density patterns

Averaging all trees per site, and three sapwood depths measured per tree, our results indicate that F_d (in cm^3 cm^{-2} h^{-1}) was significantly different among sites (F=1890, p=<0.0001). The Mature site showed the highest F_d average (37 ±12), followed by the Mid-aged (26 ±7) and Young sites (24 ±7.6). F_d averages were generally stable throughout the measurement period in the Mature and Mid-aged sites; however, as shown in Figure III-3, the Young site showed a significant reduction after DOY 180 to an average F_d of 5 at the end of the growing season.

The response of F_d to *VPD* was different at each site. In the Mature site F_d was linearly related to *VPD* within a range from 0-0.8 kPa, and this response remained similar from June to

September, and declined significantly in October (Figure III-4). Our statistical analysis considering the entire monitoring period indicated that peak F_d in the Mature site was significantly influenced by *VPD* (F-ratio = 391, p=<0.0001, Table III-6), and a similar response was observed in the analysis by *SR* except during the second *SR* period (Table III-7). The F_d response to *VPD* in the Mid-aged site showed an inflection point in July and August after approximately 0.8 kPa, but was relatively stable throughout the monitoring period (Figure III-4). Similar to the Mature site, F_d was influenced by *VPD* considering the entire monitoring period (F-ratio = 6, p=<0.01. Table III-6), and similar results were observed in the analysis by *SR*, except during the second *SR* period (Table III-7). In the Young site F_d responded similarly to *VPD* as the Mid-aged site in June and July, but it was significantly lower than the other two sites the remainder of the growing season. Similar to the other sites, F_d in the Young site continued after *VPD* values were higher than 1.5 kPa, but at much lower rates (< 5 cm^3 cm^{-2} h^{-1}) (Figure III-4). In the Young site, the statistical analyses showed that *VPD* was a strong driver of F_d when the entire monitoring period was considered, and a similar response was observed when analyzed by time interval (Table III-6 and Table III-7).

In general, combining all the data, *S* and S_{40} had a strong influence on F_d for all sites (p=<0.0011, Table III-6). As seen in Figure III-5, the shape of the response curve between F_d and *VPD* was influenced by differences in *SR*. At lower *SR* ($S < 0.18$), F_d showed an inflection point at high *VPD* values (greater than approximately 1.2 kPa); conversely at high *S*, no inflection points in F_d were observed at high *VPD*, and in the Mature site F_d and *VPD* were nearly linearly correlated. Analyzed by time interval, *S* had no detectable effects on maximum F_d in the Young site in the first interval (time interval 1, F-ratio=0.3, p=0.57), but became a significant driver of max F_d in consecutive intervals (Table III-7). Conversely, *S* had a significant (p=<0.0001) influence on maximum F_d rates of both Mature and Mid-aged sites, during the first

three intervals. During the interval 4, the interval with the highest precipitation and highest *S*, maximum F_d was not significantly influenced by *S* in these sites (Mature: F-ratio=0.6, p-value=0.43; Mid-aged: F-ratio=0.1, p-value=0.81).

Average whole-tree daily water use (Q) trends

Averaging all estimated *Q* data per site (321, 156, and 126 trees. Young, Mid-aged, and Mature, respectively), the Mature site showed the highest *Q* (Figure III-6). The maximum average *Q* at this site was 11.6 L d^{-1}, and this site showed a 45% (6.3 L d^{-1}) decrease in *Q* at end of the monitoring period. Average *Q* in the Mid-aged site was 7.4 L d^{-1} at the beginning of the growing season and declined by 54% towards the end of the growing season (2 L d^{-1}). Similar to the Mature site, the Mid-aged site continued to actively transpire until leaf abscission at the end of the growing season. The Young site had an average *Q* of 9.4 L d^{-1} early in the growing season but had a reduction of more than 95% starting on DOY 180 (the first period with reduce precipitation), that continued declining until the end of the growing season when *Q* was 0.3 L d^{-1}.

Site-level transpiration (T)

Stand-level transpiration (*T*, mm d^{-1}) varied significantly among sites (Figure III-7, p=<0.0001, F=456) and throughout the growing season. The estimated *T* in the Mature site was 5 mm d^{-1} early in the growing season and declined to 2.7 by the end of the growing season. The Mid-aged site had a similar pattern to the Mature site, with a daily *T* of 2.5 at the beginning of the growing season and maximum of 1.2 towards the end. By contrast, the Young had a higher *T* (2.8 mm) than the Mid-aged (2.5 mm) site early in the growing season, but decreased rapidly after DOY 180, which was the first extended period with no precipitation in the middle of the growing season (Figure III-7).

According to our statistical analyses combining all the data by site, *RH* , *NetRad* and *S* significantly influenced *T* in all sites (Table III-8). *AirT* and S_{40} had a significant influence only on the Mature and Mid-aged sites. Conversely, only the Young site seemed to be significantly (p=<0.0001*) influenced by VPD and not by *AirT* or S_{40}. Finally, *pp* was the only variable that did not seem to influence *T* in any site.

Splitting the analysis by time interval, in the interval 1, *NetRad* and S_{40} significantly influenced *T* at all sites (Table III-9). Only during this first period did *pp* have a significant (p=<0.0185) influence on *T* in the Mature site; no other significant effects of *pp* on *T* were observed during the remainder of the growing season on any of the three sites. As the growing season progressed no variable seemed to affect *T* during periods 2 and 3, only the Young site was influenced by *NetRad* (p=<0.0111). In period 4, *T* in the Young site was significantly (p= 0.0200) influenced by S_{40}, and at the end of the monitoring period *NetRad* was the only variable with a significant influence on *T* in both the Mid-aged and the Young sites.

Modeled stand transpiration and effects of soil saturation

Modeled stand-level transpiration (T_{mod}) was strongly correlated with stand *T* (measured) (Figure III-8). R^2 between *T* and T_{mod} was 0.92 at all sites (RMSE=0.11, 0.12 and 0.33, Young, Mid-aged and Mature, respectively). T_{mod} was estimated after DOY 187 due to the lack of measured *S* prior to this day. Replacing measured *S* with modeled *S* for a water-limiting scenario (average *S*=0.09) and a non-limiting scenario (average *S*=0.2) affected each site differently. First, T_{mod} for the *S*-limiting scenario resulted in general lower T_{mod} at all sites: a reduction of -9% (with respect to estimated average *T*) at the Mature site, -10% at the Mid-aged site, and 11% at the Young site (Figure III-9). Conversely, T_{mod} in a *S* non-limiting scenario (average *S* = 0.2) resulted in significantly larger changes in T_{mod} in the Mid-aged and Young sites (+34 and +170%

increment, respectively) (Figure III-10). The Mature site was the least influenced by high *S*, and T_{mod} was +5% higher than measured *T*. A one-way Anova between observed *T* and T_{mod} under the two saturation scenarios showed no difference in the Mature site (Table III-10. p=0.30, F-ratio=1.2), and significant differences in both Mid-aged and Young sites (p=<0.001).

Discussion

Average stand sap flux density and its relationship with whole-tree water use (Q L d^{-1})

Average site-level F_d is commonly used to estimate stand *T* (Hogg and Hurdle 1997, Uddling et al. 2008). Unlike ***Q***, which requires total A_S to be calculated, F_d is independent of tree size, and in general terms is the result of the interaction of several factors, such as atmospheric conditions of (e.g., *VPD*, *NetRad*), wood anatomical traits (e.g., ring vs diffuse pores), plant water use requirements, and the LA/A_S area ratio. Consequently, once the variability (between species, within diameter ranges of the same species, or within the sapwood profile) has been addressed, F_d can provide near real-time responses of trees to their environment, whether derived from heat pulse (Burgess et al. 2001b) or heat dissipation (Granier 1987) sap flow sensors. In the absence of strong mid-day depressions in F_d (Lu et al. 2004), maximum F_d represents the integrated effects of atmospheric demand, plant physiological traits, and soil water availability. Consequently, average stand F_d is a good indicator of mean *Q*, which can be used to estimate or model site *T* (mm d^{-1}).

According to our first hypothesis, *Q* would increase with site age, and F_d was expected to show an opposite pattern. We observed increases in F_d with site age from a maximum average of 22 in Mid-aged and Young plantations to a maximum average of 46 in the Mature reference forest. Hogg et al. (1997) measured a maximum sap velocity of 65 (in mm h^{-1}) in 70 YO aspen trees, consistent with our trend for aspen-dominated forests. They observed seasonal differences

in F_d that were insensitive to changes in *VPD*. Conversely, we found that *VPD* was a strong driver of F_d, and a strong linear relationship was maintained at low *VPD* (*VPD* < 0.8 kPa), which we attributed to low stomatal control at low evaporative atmospheric demand, which has been previously observed in various species, including poplars and *P. tremuloides* trees (Hogg et al. 1997, Hogg and Hurdle 1997, Oren et al. 1999). Past this *VPD* threshold, the F_d-*VPD* relationship was no longer linear and occasionally an inflection point was observed. This inflection point resulted in a reduction of F_d of up to 40%, before *VPD* reached maximum values. Further exploration of the F_d-*VPD* relationship showed that it was not driven by *VPD* or *NetRad* alone. For example, the average for July (Figure III-4) showed a non-linear response in both the Mid-aged and Young sites, but not in the Mature sites, suggesting an age or a site interaction. While the age effect has been documented for F_d and *T* (Angstmann et al. 2012, Gochis and Cuenca 2000), it is also a plausible explanation, in our study, curve relationships with significant reductions in F_d, observed when high *VPD* and low *S* occurred simultaneously (*SR*: 0.16-0.18, Figure III-5), regardless of the site age. These results can explain why one study reported a correlation between F_d and *VPD*, but limited prediction of stand *T* in European beech-dominated sites (Renner et al. 2016). On *P. tremuloides* trees, Ewers et al. (2005) observed a similar linear relationship at low *VPD*, but a relationship that approximated an exponential curve when considering all the monitoring period. According to their results, the F_d-*VPD* relationship was also related to site age, with the oldest 37YO stand having a steeper slope compared to the younger 20 or 12YO stands, which is similar to the patterns observed in our study.

The development of LAI over time, and its impacts on the LAI/A_S ratio, can also have a strong impact on stand average F_d across stands of different ages. In natural aspen forests, where initial tree density is not controlled, studies have measured canopy covers up to 100% and LAI up to 3.8 within 10-15 years (Frouz et al. 2015, Huang et al. 2013). In young sites with high

densities the LA/A_S ratio per tree can be higher than a site with the same age but lower tree density, which may explain the similarly high maximum F_d observed in between our Young and Mid-aged site (see Figure III-3). Management operations, such as thinning (Rytter and Stener 2005) and self-thinning resulting from competition (Huang et al. 2013, Trugman et al. 2016) reduce the number of stems and sapwood area and increases growth rates of remaining tees, thereby increasing the LA/A_S ratio. Thus, in aspen coppice plantations, an initial prediction would be that LA/A_S increases over time due to more rapid increases in total leaf area relative to A_S, compared to an undisturbed stand. This should result in increasing rates of F_d with age, which matches our findings on average F_d changes with age. Although we were unable to obtain LAI data for our study, the positive relationship between A_S and stand age observed in our study (Table IV-3: average A_S 8.5 to 24 cm^2 $tree^{-1}$, Young and Mid-aged, respectively), was likely related to increasing F_d and the LAI/A_S ratio over time. Although LAI would initially decline after thinning, Petrone et al. (2015) found that reductions in T and potentially the LA/A_S ratio resulting from partial harvesting, can recover to pre-harvest conditions within two years. Further research is needed into this specific topic under different growing densities at different ages can help better predict annual water budgets (Gochis and Cuenca 2000, Kim et al. 2008, Muller and Lambs 2009, Wilske et al. 2009).

Finally, according to our results, Q was on average lower in both young sites, compared to the mature site (Figure III-6; p=<0.001, difference: 3.8 for both), but not between the Young and the Mid-aged sites (p=0.9, difference: 0.009). While on average tree diameter was directly related to site age (Table IV-3), seasonal changes in mean Q were more complex and did not follow a clear trend with age throughout the growing season. Before DOY 185, we observed a similar Q between the Young and Mature sites, both of which were higher than the Mid-aged site. After DOY 185, Q decreased in the Young site and was lower than the Mid-aged and

Mature sites. Consequently, our results only partially support our hypothesis, when the entire average for the monitoring period is considered. These temporal trends may relate to changes in WUE in response to stand development and environmental drivers. For example, at leaf level, studies have found increments in water use efficiency (**WUE**) with tree age (Vickers et al. 2012, We et al. 2018, Weiwei et al. 2018). In poplar hybrids (*Populus deltoides* x *Populus petrowskyana*) plantations, Jones et al. (2017) observed an increase in WUE from 1 to 3YO of plantations establishment, that plateaued after the third and fifth years. The higher tree *T* rates observed early in the growing season, might be the result of lower WUE of *P. tremuloides* trees, and the significant reduction, which coincided to low *S*, might be explained by the well documented sensitivity of young *P. tremuloides* trees to seasonal drought, compared to older trees (Greer et al. 2018, Vickers et al. 2012).

Relationship between stand age and T

Our second hypothesis was that that stand *T* would increase with stand age, due to the larger tree size and higher LA and LAI in older stands. Both LA and LAI, as well as tree size, are known to be directly related to stand *T.* Studies on poplar hybrids have estimated stand *T* rates from 5 to 8 mm d^{-1} in young poplar plantations (ages between 1-3 YO) (Gochis and Cuenca 2000, Kim et al. 2008, Wilske et al. 2009), and their high transpiration rates are often associated with high stand densities. Angstmann et al. (2012) estimated significantly higher transpiration rates on stands dominated by 18YO *P. tremuloides* trees, compared to 43 and 77YO trees. Considering these observations, our second hypothesis was that at the stand level the Young site will have higher transpiration rates resulting from higher transpiration, growth and stand densities, than the Mature forest (Angstmann et al. 2012, Bloemen et al. 2017, Jones et al. 2017, Oliver et al. 2015, Peterson and Peterson. 1999). However, our results did not support this

hypothesis, and contrary to our initial prediction, we observed a trend of increasing *T* with stand age. Similar to the tree-level results, Mature stand T was significantly greater compared to both Mid-aged and Young sites but no clear difference was observed between the Mid-aged and Young sites (Figure 1-7). Despite the high density (6690 trees h^{-1}), high F_d (Figure III-3) and high tree *T* before DOY 185, stand *T* in the Young site was higher than Mid-age site only before DOY 180, but lower than the Mature site. While these results agree with the study by Perry et al. (2001), where modeled *T* was similar between 8-9 and 24-34 YO stands, the observed trend at the tree level contradicts the reduction with age reported for *P. tremuloides* by Angstmann et al. (2012).

A recent study by Berry et al. (2018), highlighted the importance of tree size distribution, and its influence on estimates of stand *T*. They observed based on modeling and tree level measurements, that large trees can contribute significantly more to stand *T* than smaller trees. Similar studies in montane tropical forests, have found that dominant trees (13% of stand tree density) can contribute to nearly 80% of the stand transpiration (Aparecido et al. 2016). In our sites, the upper 25 percentile (considered dominant trees) of the diameter distribution per site accounted for 76%, 58% and 51% (Mature, Mid-aged and Young, respectively) of total stand *T*. These results support previous studies (Aparecido et al. 2016, Berry et al. 2018), particularly our Mature site. However, the Young and Mid-aged sites had similar densities (~6600 trees h^{-1}) and smaller trees accounted for nearly 50% (40% Mid-aged, 50% Young) of total stand *T*. Thus, in these sites, the relative contribution of smaller trees, is significantly higher than in old/mature sites, which highlights the importance of site density and the relative abundance of a large number of smaller trees in younger stands when tree-level measurements are scaled up to the stand level.

The importance of site factors in explaining water use patterns

Our statistical analysis showed that *S* was significantly different across sites. In order to further elucidate the role of *S* in controlling water use patters, we modeled *T* ($\boldsymbol{T_{mod}}$) under two scenarios: a limiting and a non-limiting *S* (average 0.09, and 0.2). Studies have documented that *P. tremuloides* trees and poplars in general, are sensitive to changes in soil moisture (or soil saturation: *S*). Pataki et al. (2000) studied sap flow in various dominant species in the Rocky Mountains, USA (*Pinus contorta*, *Abies lasiocarpa*, *Pinus flexilis*, and *P. tremuloides*). In their study, aspen trees were the least sensitive to changes in soil moisture. However, Larcheveque et al. (2011) observed that different poplar clones have different responses to *S*, but in general most poplar clones are sensitive to changes in soil water content. On irrigated sites, Kim et al. (2008) observed that reductions in irrigation of hybrid poplars can reduce growth by about 18%. In *P. tremuloides* in particular, soil water availability has been identified as the main driver of growth and *T* (Peterson and Peterson. 1999). Moreover, several studies have concluded that site selection is an important factor when establishing new poplar SRWC, to guarantee maximum growth rates (Angstmann et al. 2012, Petzold et al. 2011).

In our sites, percent sand content was higher in the Young (0-60 cm soil profile mean: 86%) site than the Mid-aged and Mature sites (Table III-1). We consider that soil type is perhaps the major factor defining differences among sites, that could only be overwritten by slope, which was not an issue in our sites. In general, soil structure in combination with other factors such as precipitation and evapotranspiration, have been identified by various studies as the drivers for soil moisture dynamics (D'odorico et al. 2000, Guswa et al. 2002, Isham et al. 2005, Puma et al. 2005, Puma et al. 2007). Specifically, sand percent content has a strong control on infiltration and retention curves (Kosugi et al. 2002, Yang et al. 2004, Zhang 2011), which ultimately define *S*, water available for plant uptake and thus stand *T* rates. *S* was on average lower in the Young

site, but it was not related to sand percent content by site (Figure III-1). Sand content was in fact lower in the Mid-aged site (73%), but *S* was higher in this site, compared to the Young site, which had a higher percent sand content (86%).

In this study, T_{mod} in a *S*-limiting scenario resulted in similar transpiration rates across sites with an average reduction of -10% (with respect to observed *T*) across sites (Figure III-9). Conversely, T_{mod} under a *S* non-limiting scenario, increased significantly (with respect to T_{mod} estimated under a *S*-limiting scenario) in both Mid-aged and Young sites (+34 and +170% increment, respectively. Figure III-10). Estimated *T* and T_{mod} were significantly different among scenarios in the Mid-age (F-ratio = 15.28, p=<0.0001) and Young (F-ratio = 7.96, p=0.0058) sites. The Mature site had a 5% increment but was not significantly different than estimated *T* (F-ratio = 1.71, p=0.193). As shown in Figure III-11, while not significantly different between the Mid-age and the Young sites (especially early in the growing season; see Figure III-9 and Figure III-10), *T* increased with stand age from 10 to 34YO. Thus, since a general trend was maintained between average T_{mod} and site age under limiting and non-limiting *S* conditions, we conclude that under similar site conditions, stand age can be used to estimate average *T*. Gochis and Cuenca (2000) observed a similar trend (increment in *T* with age) in an irrigation study but in shorter (1-3YO) rotations. However, unlike our sites, they reported no stress or growth limitations due to low *S*. The trend observed in our study, was opposite to the study by Ansgtmann et al. (2012) considering *P. tremuloides* trees alone, their results showed a reduction in *T* with age for *P. tremuloides* (18 to 77 YO), which could be explained due to the lower contribution of *P. tremuloides* to total stand *T*. Considering all the species in their study, stand *T* increased from 10 to 43YO, consistent with our study, and later decreased after that from 43 to 77YO. Similar increments from the time of plantation establishment, and reductions after canopy closure have been observed in fast growing species. Almeida et al. (2007) and Forrester et al. (2010),

observed these trends in stand T and F_d within the common rotation cycles of Eucalyptus *spp*. trees. Site density has shown to control the peaks and reductions in T, when initial plantation density is high, studies on *Eucalyptus grandis* have found a peak in T (and subsequent decline) within the first three years of establishment (Almeida et al. 2007, Du Toit 2008, Ryan et al. 2008). Unlike most Eucalyptus plantations, in SRWC the stand density changes over time as a result of natural die-offs and pre and commercial thinning. While changes in T are expected as a result of thinning, Petrone et al. (2015) observed that *P. tremuloides* stands in particular, can return to pre-thinning T rates within two years. Then in long-rotation studies of expected T rates, the effects of thinning on T estimates can be relatively easily accounted for.

Limitations of our study and recommendations for future studies

Soil moisture has been considered a strong factor regulating T and growth rates in poplars and *P. tremuloides* trees (Bloemen et al. 2017, Chen et al. 2014, Larcheveque et al. 2011). While we were able to monitor soil moisture to a depth of 100 cm in all sites, our modeling makes two strong assumptions. First that S in the first 40 cm of soil has the strongest influence on T. While in fast growing plantations most of the fine roots are located in the top 50 cm of soil (Bouillet et al. 2002, Laclau et al. 2001), deep roots may still be able to access water from deeper soil profiles (Toillon et al. 2013, Xi et al. 2013). The second assumption in our model is that changes in S is linearly related to stand T and F_d. According to Larcheveque et al. (2011), this relationship might be true within a volumetric water content range of 5-20%, but the slopes may change as water content decreases. In modeling scenarios, the effects of T on soil moisture are expressed as a curve (extraction curve) (Guswa et al. 2002, Rodriguez-Iturbe et al. 2006, Rodriguez-Iturbe et al. 2001), with different slopes depending on the expected extraction rates (Rodriguez-Iturbe et al. 2001). At the Young and Mid-aged sites, S varied significantly and we are confident on the

slopes estimated for these two sites, however, in the Mature site, it was never lower than 0.14, and consequently, the slope estimated by our model in this particular site, might underestimate the effects of *S* on stand *T*.

Two common limitations in sap flow studies are the sample size and the proper determination of stand-level A_S (Berry et al. 2018). Sample size is directly linked to equipment cost, and the spatial distribution of the species of interest. With wired sap flow stations, most studies limit the cable length between 10 and 15 m, to reduce to signal to noise ratio. This creates a radius around the sap flow station for the selection of the trees to be monitored, which can leave diametric categories or species of interest outside this radius. In single-species stands, Kume et al. (2012) recommended an optimal sample size of 15 measuring points to capture most of the tree-to-tree F_d variability. However, this recommendation was developed for heat dissipation sensors with only one measuring point per sensor. As described in our methods section, we monitored a total of 24 measuring points distributed across 8 different trees; despite the relatively small sample size, we captured the entire radial profile of all trees monitored. Proper determination of A_S and the F_d radial profile in large trees is difficult, and can lead to major under or overestimations of tree and stand *T* (Alvarado-Barrientos et al. 2013, Ford et al. 2004, Gebauer et al. 2008, Kubota et al. 2005, Poyatos et al. 2007). To address sapwood depth radial variability, we collected two cores per tree to estimate A_S, and measured sapwood depth on four points per tree. Additionally, we installed trees in all four cardinal directions to cover the potential radial variations in F_d, and in all our trees the entire F_d radial profile was monitored. Finally, studies on *P. tremuloides* trees have reported diameters of 24 cm in 150 YO trees (Bond-Lamberty et al. 2002, 2014), thus we extended our sampling range for A_S to include trees up to 25 cm in diameter, and adjusted allometric equations for each site and predicted A_S with site-specific equations (see Table III-3). Species-specific allometric equations are of great value to

scale up plant-to-stand level processes (Bond-Lamberty et al. 2002, Jenkins et al. 2003, Perala 1993), but adjusting equations for a specific site can reduce the error associated with the estimation of A_S.

Based on our experience, we make the following recommendations to future studies looking to estimate stand-level annual water balances or interested in modeling stand-level *T*. First, establish a weather station (with all the variables needed to estimate ET_0: air temperature, relative humidity, incoming short-waver radiation, outgoing long-wave radiation, wind speed) and additionally monitor soil moisture, precipitation, photosynthetically active radiation prior to the deployment of sap flow sensors. This weather station can be deployed months in advanced, to parameterize models from using sap flow data (when it becomes available) to estimate stand transpiration. Next, track the development of LAI, and in evergreen species, we recommend measuring it two or three times during the growing season, to address potential variability due to crown development. Monitor both throughfall and stemflow, considering that in *P. tremuloides* trees 15 cm in diameter, precipitation events under 30 mm (over two or three days) overfilled our containers, which were designed to fit 10 L. For throughfall, a minimum of thirty collectors per site are recommended, which should also be designed to fit the precipitation expected for a monitoring period. Next, we recommend establishing replicates under different site conditions, and developing a site profile (i.e., soil characteristics, stand density, allometric equations, etc.) for each. If sap flow sensors are used to estimate F_d, under budgetary constraints, the design of the sensors can be modified to allow them to detach from the communication cables, so that the heat source and temperature probes remain in the trees. This way, the same data logger and multiplexor (approx. 70% of the cost of a sap flow station) can be moved between sites (where sensors of the same design will be installed in the trees) at intervals of 10-15 days. With the site and environmental variables monitored at each site, it is possible to estimate stand-level

transpiration for the periods where no F_d was not monitored at each site, using various gap-filling procedures (i.e., a linear mixed model) similar to the one used in our sites. If runoff is difficult to monitor, a model can be adjusted to the soil saturation of each site, and based in soil properties to estimate potential runoff and infiltration.

Conclusions

In this study we estimated tree and site-level transpiration of three aspen-dominated sites (10, 24 and to 34 YO). Our overarching goal was to determine the relationship between site age and stand transpiration. Establishing such relationship can be of great value for the bioenergy industry, to elaborate scenarios of potential hydrological impacts associated with the production of whole biomass or timber in short rotation woody crops (SRWC). Considering the transpiration rates observed in previous studies, we hypothesized that the Mature site will have higher transpiration rates (mm d^{-1}) because of higher LAI and overall larger tree size. Our results did not fully support this hypothesis.

In general, we observed an increment in stand *T* with age (season average: 0.57, 1.12, and 2.7 mm d^{-1} for Young, Mid-aged and Mature sites, respectively), which varied seasonally. However, our statistical results showed that site characteristics, specifically *S* resulting from differences in soil type, had a strong effect on the estimated stand *T*. *S* followed the trend observed for *T*, and according to our statistical analyses, was a strong driver of the response to F_d to *VPD*. When high *VPD* and low *S* occurred simultaneously, the *VPD*–F_d response changed from linear to a curve, that reduced F_d at high *VPD*. Finally, site effects could override age effects, but addressing such site effects allowed us to establish a trend between *T* and stand age.

To address site effects in estimated *T* rates, we modeled transpiration under two contrasting *S* conditions, a limited and a non-limited scenario (seasonal average 0.09, and 0.2). Under our

limited scenario, *T* rates decreased by about 10%, with insignificant differences from observed *T*. Conversely, in the non-limiting scenario, the modeled *T* increased significantly (160%) with respect to observed *T*. Modeled *T* in the Mid-aged and Mature sites increase by 34% and 5%, but was only statistically greater in the Mid-aged site. Since both in observed and modeled *T* increase with age, we conclude that there is evidence to indicate that stand age can be used in modeling scenarios to elaborate scenarios of whole biomass and timber in SRWC of aspen-dominated sites.

Figures and tables

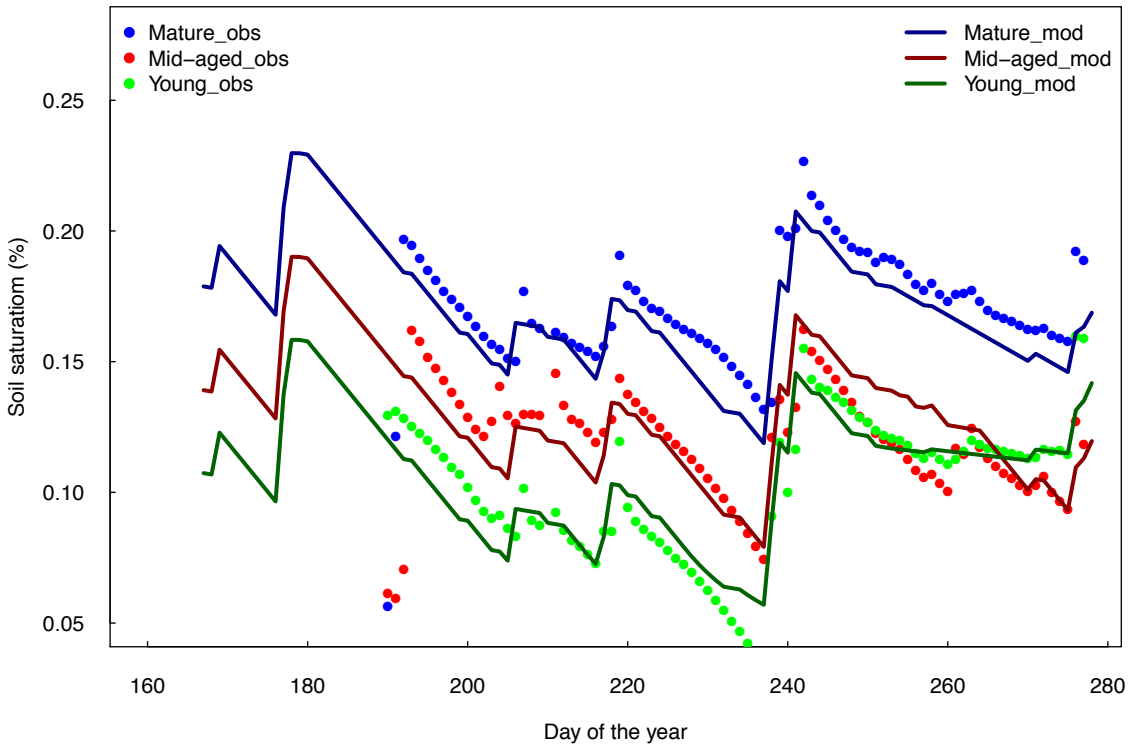

Figure III-1 Predicted vs. observed soil saturation (*S*) in the first 40 cm of soil throughout the growing season. *S* was predicted with the bucket model assuming a depth of interception of 2 mm, and a maximum initial *T* of 2.37 for the Mature site, and 2.15 for the Mid-aged and Young sites. Further details can be found in Table III-4.

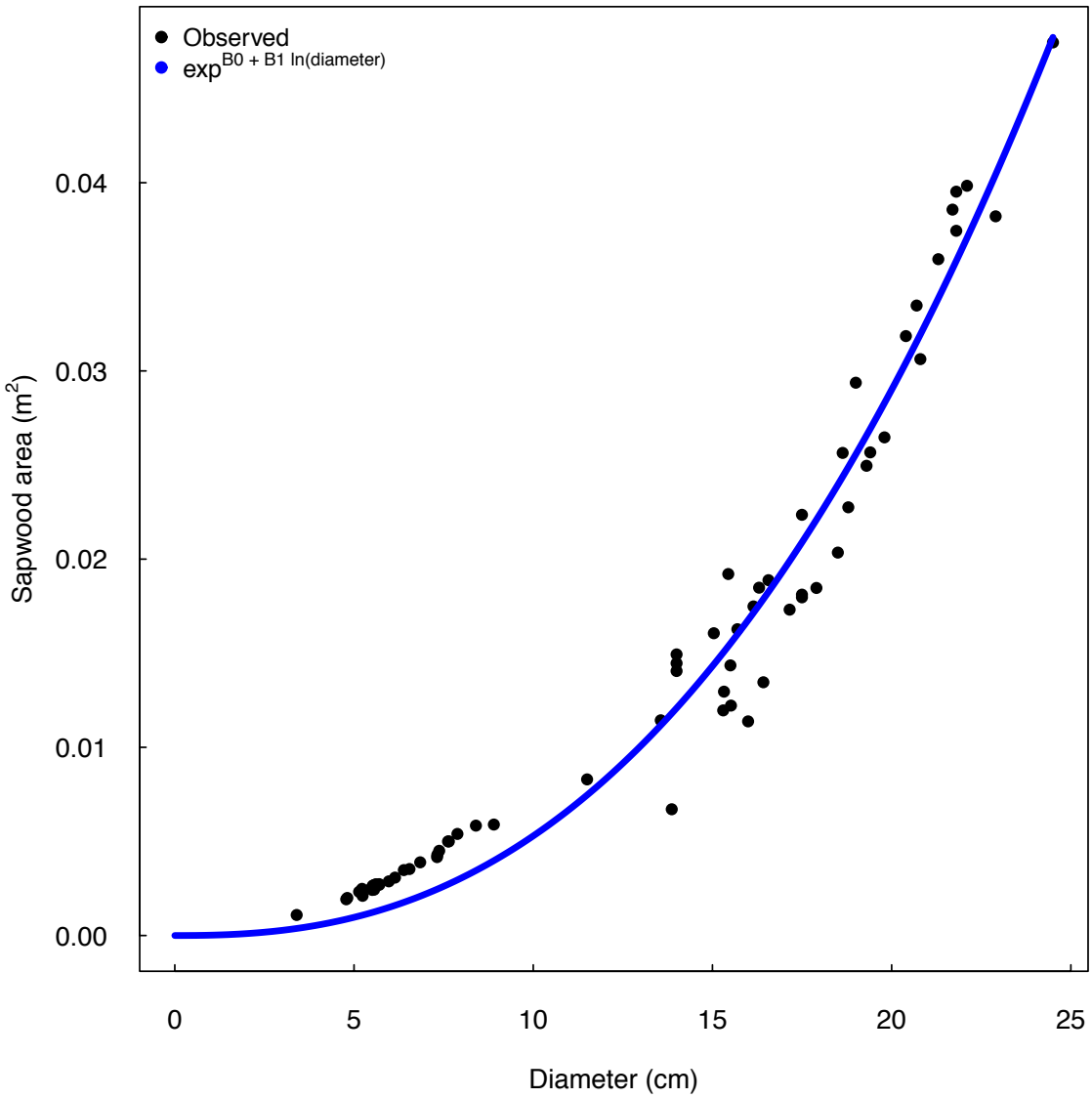

Figure III-2 Estimated regression between sapwood area (A_S) and basal area (m^2). The blue line is the equation fitted using all data. A_S was predicted at each site using site-specific allometric equations. β0 and β1 parameters estimated for each site, and regression coefficients can be found in Table III-3.

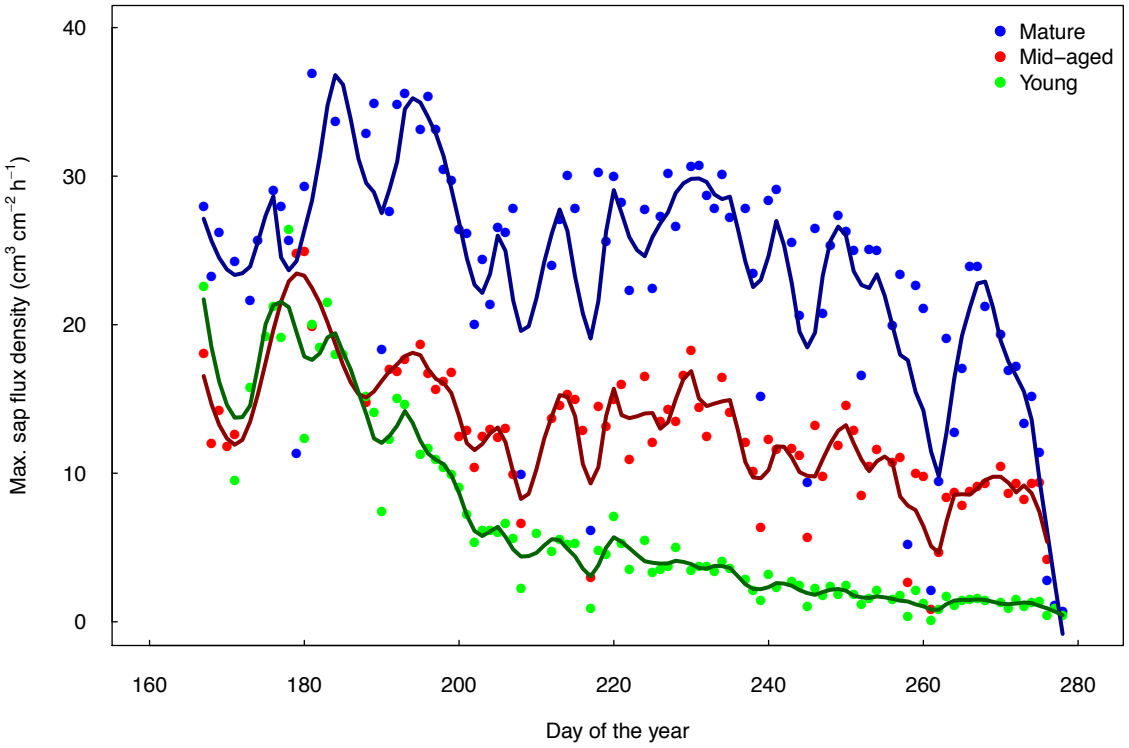

Figure III-3 Maximum sap flux density (F_d, $cm^3\ cm^{-2}\ h^{-1}$) by site during the entire monitoring period. The solids dots are the F_d and the lines a locally weighted scatterplot smoothing (LOWESS) function fitted with an alpha = 0.1

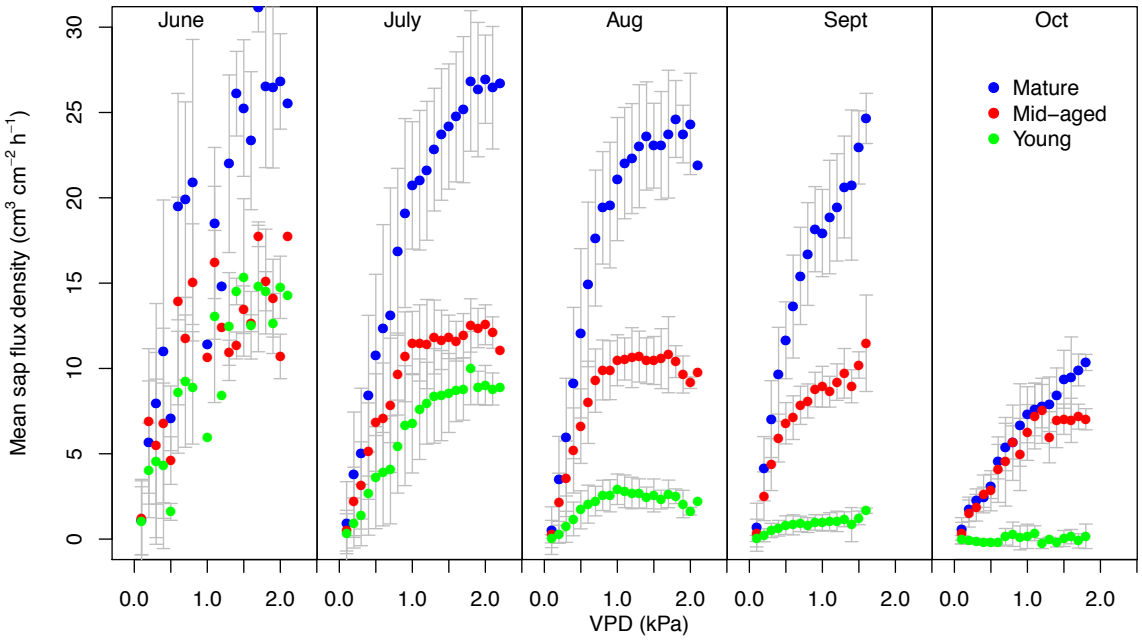

Figure III-4 Response of F_d to VPD at different times of the year. For visualization purposes, we first binned F_d into *VPD* increments of 0.1. The error bars represent one standard deviation from the mean, and were estimated from binned data

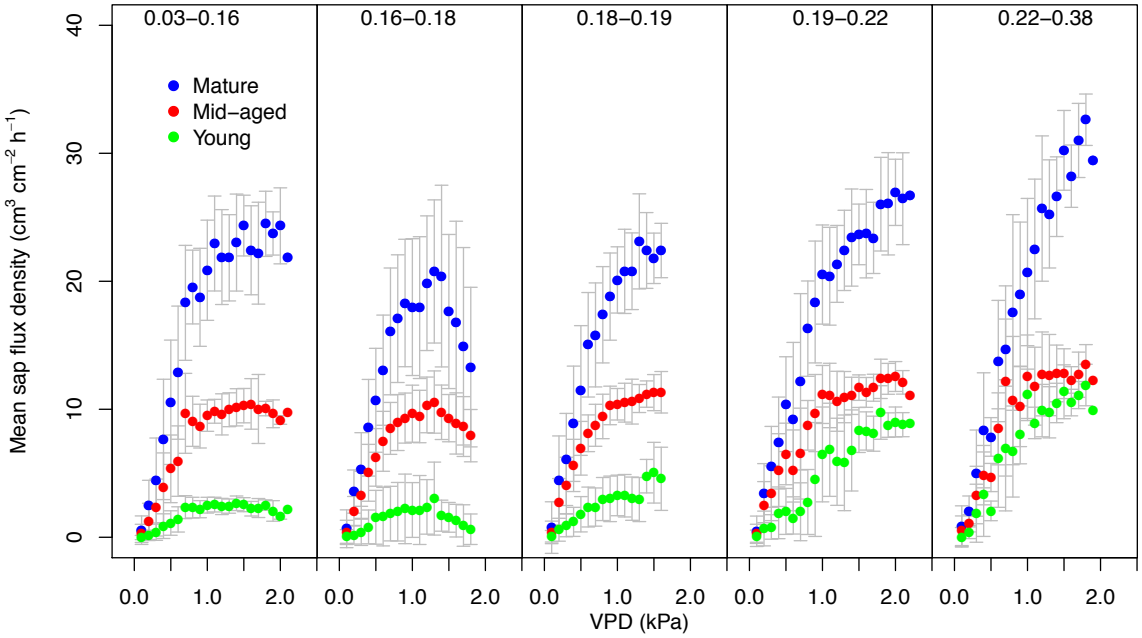

Figure III-5 Response of F_d to VPD at different soil saturations. Saturation ranges are shown at the top of each panel. F_d was binned by *VPD* increments of 0.1. The error bars for each data point represent one standard deviation, and were estimated from binned data. Soil saturation ranges shown at the top of each panel was estimated from the soil saturation average estimated from all the sites

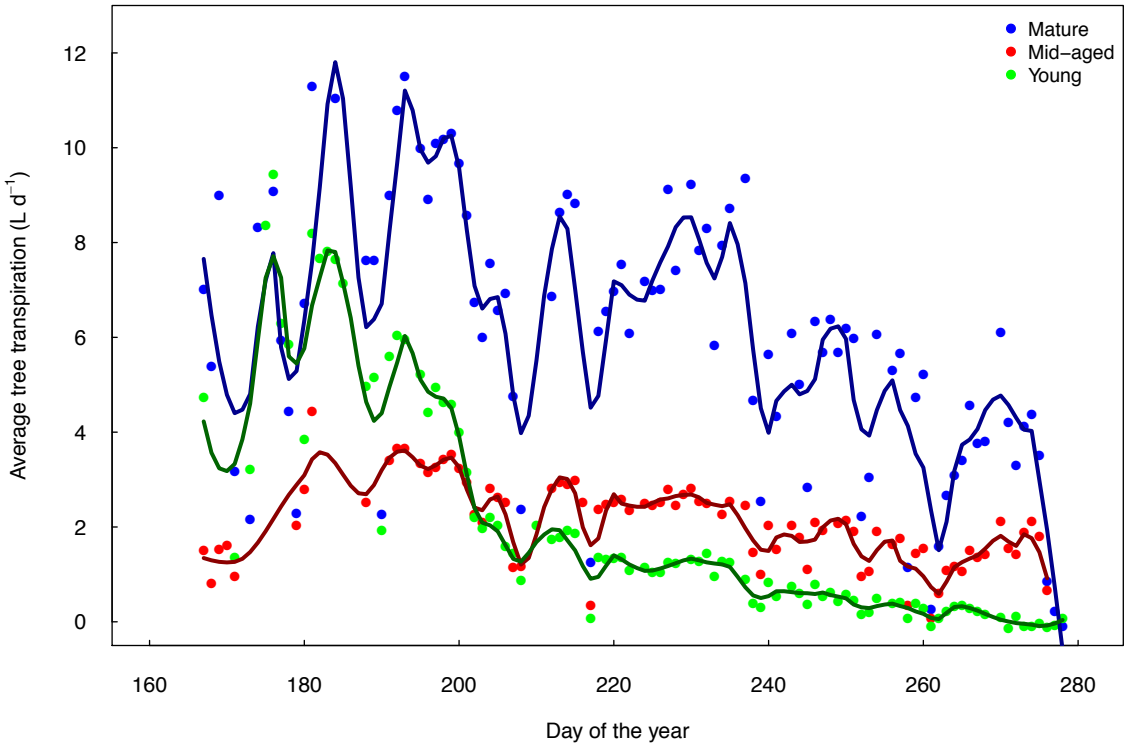

Figure III-6 Tree-level average transpiration (L d^{-1}) during the monitoring period. Average tree T (L d^{-1}) is the average from 126, 156, ad 321 trees (Mature, Mid-aged and Young, respectively) for which water use was predicted multiplying average F_d vs. the estimated A_S of each tree. The solids lines are a locally weighted scatterplot smoothing (LOWESS) function fitted with an alpha = 0.1.

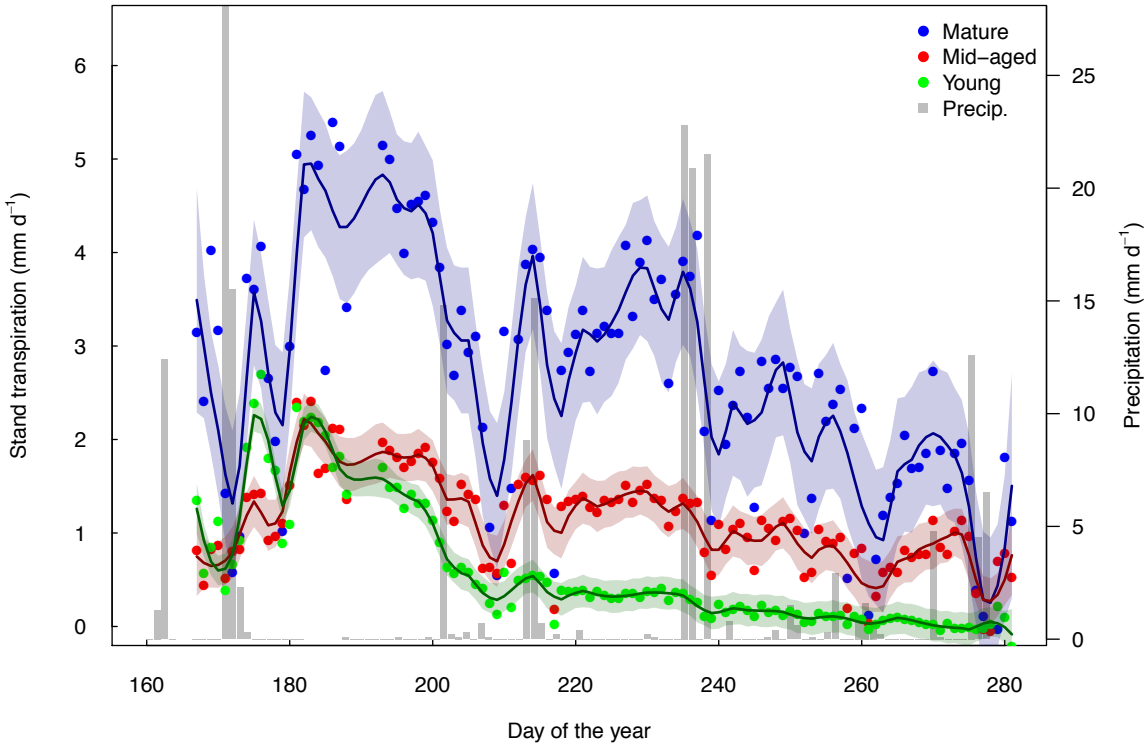

Figure III-7 Estimated stand transpiration (T, mm d^{-1}) for each site. Solids lines are a locally weighted scatterplot smoothing (LOWESS) function fitted to the observations per site, with an alpha = 0.1. Shaded lines represent one standard deviation from the mean, estimated for the LOWESS function.

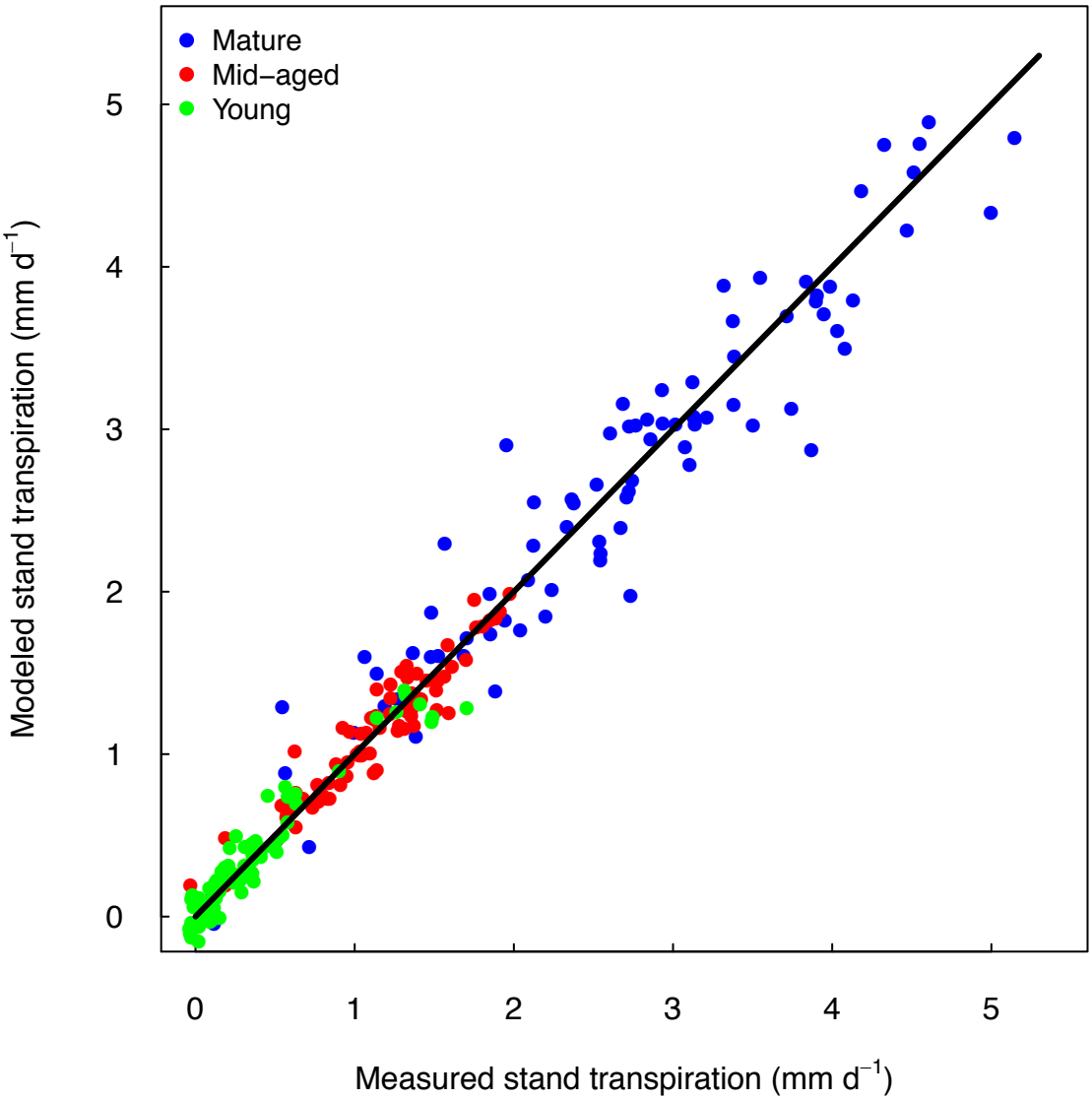

Figure III-8 Linear regression between predicted and scaled up transpiration by site. The solid line is the fitted linear equation using data from all sites (y= 0.0 + 1.0*X ,F=911, p-value=<0.0001, Adjusted R^2 = 0.91).

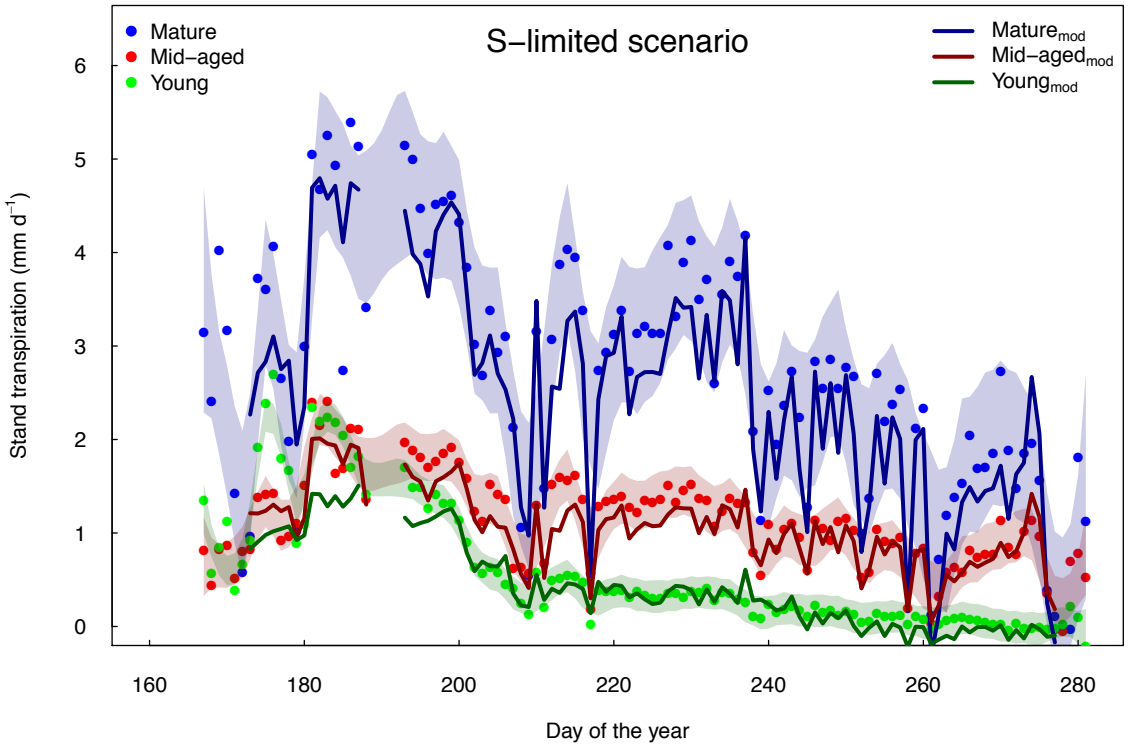

Figure III-9 Observed (dots) vs. modeled transpiration (T_{mod}) (solid lines) in a saturation-limiting scenario. Soil saturation = 0.09, was estimated with the bucket model (Further details and parameters used to estimate *S*, can be found in Table III-4.). Shaded lines represent one standard deviation from the mean, estimated for the observed *T* values.

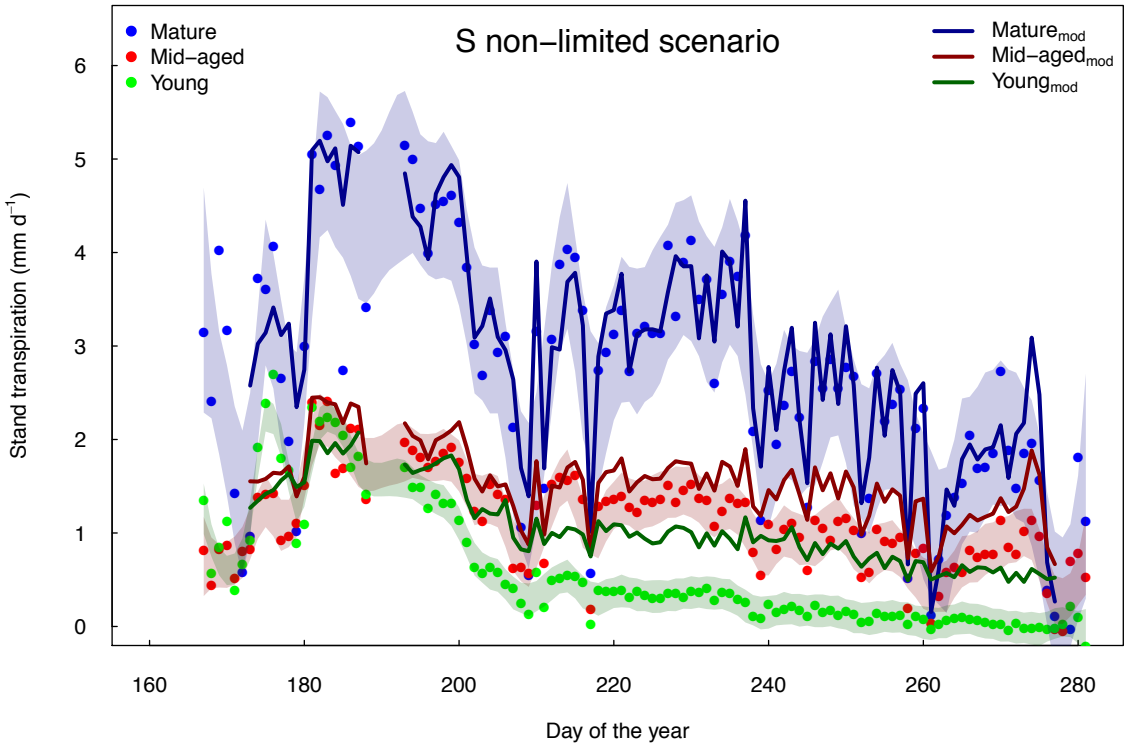

Figure III-10 Observed (dots) vs. modeled transpiration (T_{mod}) (solid lines) in a saturation non-limiting scenario. Soil saturation = 0.2, was estimated with the bucket model (Further details and parameters used to estimate S, can be found in Table III-4.). Shaded lines represent one standard deviation from the mean, estimated for the observed T values.

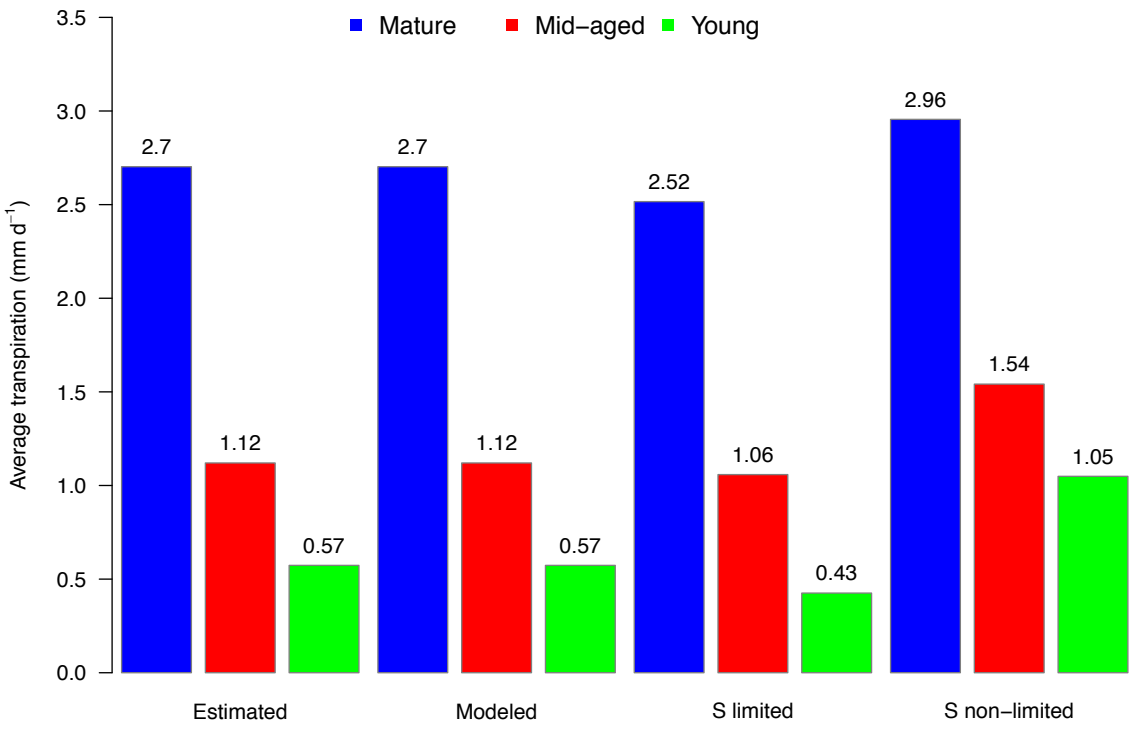

Figure III-11 Comparison of seasonal average transpiration by site. Modeled = estimated with linear mixed model (see Table III-5 for details and AICc/BAI indeces), S-limited = estimated with average *S* of 0.09, S non-limited = average *S* of 0.2

Table III-1. Soil characteristics per site (From Cisz-Brill et al in Prep)

Site	Depth (cm)	Bulk density (g cm^3)	Sand (%)	Clay (%)	Porosity (%)
Young	0-15	0.81	81	3	69.28
	15-30	1.15	85	3	56.78
	30-45	1.29	88	2	51.15
	45-60	1.33	91	3	49.85
Mid-aged	0-15	0.55	73	3	79.09
	15-30	1.03	73	4	61.05
	30-45	1.22	69	6	54.13
	45-60	1.57	75	5	40.71
Mature	0-15	0.79	78	4	70.20
	15-30	1.09	74	5	59.05
	30-45	1.29	79	5	51.22
	45-60	1.27	90	4	52.20

Table III-2 Stand characteristics

Site	**Density (trees ha^{-1})**	**Density - aspen only**	**Mortality rate (%)**	**Average diameter (cm)**	**Average sapwood area* (m^2)**	**Average height (m)**	**Subsample N**
Young	6680	6420	2%	3.72 (± 0.98)	0.000849 (±0. 0.000429)	7	321
Mid-aged	6690	1560	10%	8.45 (± 4.13)	0.00239 (±0.00366)	16	156
Mature	4620	1260	15%	12.8 (± 4.41)	0. 00604 (±0.00584)	16.4	126
All	5996		9%	6.85 (± 4.73)	0.00203 (±0.00383)		

*Average sapwood area per tree, using N trees of the subsample

Table III-3 Parameters for allometric equations to predict sapwood area from diameter

Site	**β_0**	**β_1**	**StErr - β_0**	**StErr - β_1**	**RMSE**	***R^2**
Young	-9.4313	1.7609	0.0999	0.0515	0.0015	0.98
Mid-aged	-10.9021	2.2130	1.5476	0.5553	0.0257	0.45
Mature	-12.5719	2.8180	0.5938	0.1953	0.0227	0.92
Mid-aged + Mature	-12.5498	2.8093	0.4367	0.1456	0.0241	0.91
All	-11.8421	2.5744	0.3360	0.1124	0.0208	0.95

*Linear relationship between predicted and observed sapwood area

Table III-4 Vegetation and soil parameters used to fit the bucket model

Vegetation parameters	Young	Mid-aged	Mature
Depth of Interception	2	2	2
Maximum *E* (mm d^{-1})	0.5	0.5	0.5
Maximum *T* (mm d^{-1})	2.15	2.15	2.37
Saturation at stomatal closure	0.08	0.08	0.08
Saturation at wilting point	0.04	0.04	0.04
Root depth (cm)	40	40	40
Soil parameters			
Porosity (n)	0.63	0.71	0.64
Saturated Conductivity *E* (mm d^{-1})	300	300	300
Hygroscopic saturation	0.02	0.02	0.02
Field Capacity	0.3	0.3	0.3
Drainage Curve Parameter	5	5	5

Table III-5 Corrected Akaike and Bayesian information criterion for each of the models tested by site.

Site	Fixed effects	- 2 log likelihood	AICc	BIC
Young	*AirT*, *RH*, *NetRad*, *VPD*, ET_0, *WindS*, *pp*, S_{40}	-80.29	-52.08	-26.70
	RH, *VPD*, S_{40}, *SR*	-66.18	-52.79	-36.75
	ET_0, S_{40}, *SR*	-55.55	-42.52	-28.61
Mid-aged	*AirT*, *RH*, *NetRad*, *VPD*, ET_0, *WindS*, *pp*, S_{40}, *SR*	-88.29	-60.01	-34.84
	RH, *VPD*, S_{40}, *SR*	-25.38	-9.96	5.84
	ET_0, S_{40}, *SR*	-45.65	-32.29	-18.92
Mature	*AirT*, *RH*, *NetRad*, *VPD*, ET_0, *WindS*, *pp*, S_{40}, *SR*	60.6	97.4	127.4
	RH, *VPD*, S_{40}, *SR*	153.28	168.67	184.70
	ET_0, S_{40}, *SR*	101.47	114.50	128.33

Table III-6 Mixed-model result for maximum F_d by site (full monitoring period)

	Mature		**Mid-aged**		**Young**	
Source	**F Ratio**	**Prob > F**	**F Ratio**	**Prob > F**	**F Ratio**	**Prob > F**
AirT	315	<.0001*	699	<.0001*	63	<.0001*
RH	586	<.0001*	1807	<.0001*	371	<.0001*
NetRad	37	<.0001*	2	0.1232	18	<.0001*
ET_0	196	<.0001*	40	<.0001*	95	<.0001*
VPD	391	<.0001*	6	0.0150*	1063	<.0001*
S	21	<.0001*	156	<.0001*	171	<.0001*
S - 40 cm	16	<.0001*	99	<.0001*	112	<.0001*

Table III-7 Mixed-model result for maximum F_d by site (analysis split by time interval)

Time interval	Source	Mature		Mid-aged		Young	
		F Ratio	Prob > F	F Ratio	Prob > F	F Ratio	Prob > F
1	*AirT*	28.0	<.0001*	13.8	0.0002*	8.7	0.0034*
	RH	74.5	<.0001*	17.1	<.0001*	42.4	<.0001*
	NetRad	2.7	0.0998	0.0	0.9982	8.4	0.0039*
	ET_0	4.0	0.0462*	34.5	<.0001*	14.2	0.0002*
	VPD	20.6	<.0001*	5.9	0.0153*	16.7	<.0001*
	S	35.7	<.0001*	63.6	<.0001*	0.3	0.5766
	S - 40 cm	16.3	<.0001*	77.1	<.0001*	0.0	0.8238
2	*AirT*	27.7	<.0001*	77.1	<.0001*	83.0	<.0001*
	RH	9.6	0.0022*	4.9	0.0285*	163.2	<.0001*
	NetRad	10.1	0.0019*	2.2	0.141	9.3	0.0026*
	ET_0	10.9	0.0012*	2.6	0.109	11.9	0.0007*
	VPD	1.4	0.2299	0.0	0.9752	124.8	<.0001*
	S	25.4	<.0001*	62.8	<.0001*	14.3	0.0002*
	S - 40 cm	20.8	<.0001*	59.3	<.0001*	12.2	0.0006*
3	*AirT*	99.6	<.0001*	70.2	<.0001*	51.3	<.0001*
	RH	123.7	<.0001*	108.9	<.0001*	81.7	<.0001*
	NetRad	3.9	0.0481*	1.4	0.2455	8.5	0.0037*
	ET_0	6.0	0.0148*	1.9	0.1673	16.0	<.0001*
	VPD	48.2	<.0001*	74.4	<.0001*	78.6	<.0001*
	S	70.0	<.0001*	74.5	<.0001*	199.4	<.0001*
	S - 40 cm	89.4	<.0001*	109.7	<.0001*	208.3	<.0001*
4	*AirT*	31.2	<.0001*	90.9	<.0001*	3.8	0.0531
	RH	47.1	<.0001*	177.8	<.0001*	29.5	<.0001*
	NetRad	1.0	0.3153	0.5	0.4646	12.4	0.0005*
	ET_0	0.0	0.8315	0.0	0.8392	24.8	<.0001*
	VPD	10.2	0.0015*	23.8	<.0001*	20.8	<.0001*
	S	0.6	0.4358	0.1	0.8152	33.7	<.0001*
	S - 40 cm	2.8	0.0929	0.0	0.847	17.1	<.0001*
5	*AirT*	23.5	<.0001*	50.8	<.0001*	0.0	0.8285
	RH	32.7	<.0001*	166.0	<.0001*	12.4	0.0005*
	NetRad	1.7	0.1986	8.8	0.0033*	0.0	0.9662
	ET_0	5.7	0.0180*	19.7	<.0001*	3.7	0.0551
	VPD	5.8	0.0170*	71.5	<.0001*	18.3	<.0001*
	S	19.8	<.0001*	4.6	0.0326*	7.2	0.0076*
	S - 40 cm	20.0	<.0001*	6.5	0.0112*	7.9	0.0052*

Table III-8 Standard Least Squares results on the effects of site-level transpiration

Source	Mature		Mid-aged		Young	
	F Ratio	**Prob > F**	**F Ratio**	**Prob > F**	**F Ratio**	**Prob > F**
AirT	15.85	0.0002*	21.66	<.0001*	0.10	0.86
RH	5.93	0.0173*	26.01	<.0001*	0.0002*	0.0486*
NetRad	70.33	<.0001*	29.89	<.0001*	0.0173*	0.0212*
VPD	0.27	0.60	2.62	0.11	<.0001*	0.0039*
precip	0.47	0.50	0.12	0.73	0.60	0.80
S_{40}	13.48	0.0004*	10.43	0.0018*	0.50	0.11
S	10.65	0.0016*	24.17	<.0001*	0.0004*	0.00

Table III-9 Standard Least Squares results on the effects of site-level transpiration by saturation range

Time interval	Variable	Mature		Mid-aged		Young	
		F Ratio	Prob > F	F Ratio	Prob > F	F Ratio	Prob > F
1	*AirT*	0.06	0.81	1.01	0.35	0.56	0.48
	RH	1.87	0.21	0.35	0.57	0.21	0.66
	NetRad	15.57	0.0056*	13.08	0.0085*	5.94	0.0450*
	VPD	0.02	0.88	5.01	0.06	2.87	0.13
	pp	9.32	0.0185*	5.10	0.06	0.00	0.96
	S_{40}	35.13	0.0006*	20.45	0.0027*	186.74	<.0001*
2	*AirT*	0.45	0.55	0.02	0.90	7.43	0.05
	RH	0.00	0.99	0.03	0.88	2.93	0.16
	NetRad	0.16	0.71	0.33	0.62	1.27	0.32
	VPD	0.14	0.73	0.33	0.62	0.06	0.82
	pp	0.04	0.85	0.03	0.87	0.59	0.48
	S_{40}	0.11	0.76	7.30	0.11	6.98	0.06
3	*AirT*	0.07	0.80	0.04	0.85	0.08	0.78
	RH	0.03	0.87	0.08	0.79	0.77	0.40
	NetRad	0.15	0.70	0.00	0.96	8.74	0.0111*
	VPD	0.59	0.46	0.15	0.71	0.00	0.99
	pp	0.05	0.83	0.48	0.50	0.02	0.88
	S_{40}	0.50	0.49	0.74	0.41	0.39	0.54
4	*AirT*	2.85	0.11	5.29	0.0353*	0.16	0.70
	RH	4.79	0.0439*	3.20	0.09	0.06	0.81
	NetRad	2.70	0.12	0.82	0.38	0.14	0.72
	VPD	2.28	0.15	0.73	0.40	3.63	0.07
	pp	0.43	0.52	0.00	0.97	4.16	0.06
	S_{40}	0.00	0.97	1.65	0.22	6.67	0.0200*
5	*AirT*	0.01	0.93	1.21	0.30	0.45	0.52
	RH	1.41	0.26	0.00	1.00	1.53	0.24
	NetRad	3.95	0.08	11.03	0.0077*	13.17	0.0046*
	VPD	2.02	0.19	0.43	0.53	3.38	0.10
	pp	0.27	0.62	0.11	0.74	2.10	0.18
	S_{40}	0.18	0.68	0.01	0.94	0.32	0.58

Table III-10 Summary of modeled stand transpiration

Site	Measured *T*		T_{mod} *S*-limited		T_{mod} Non *S*-limited		F-ratio P-value
	Average	StDev	Average	StDev	Average	StDev	R^2
Mature	2.58	0.11	2.34 (-9%)	0.12	2.79 (+8%)	0.12	1.20 0.3020 0.0
Mid-aged	1.08	0.04	0.97 (-10%)	0.04	1.47 (+45%)	0.04	12.78 <0.0001 0.07
Young	0.341	0.67	0.29 (-10%)	0.50	0.93 (+160%)	0.48	1.70 <0.0001 0.06

Appendices

Appendix III-I Linear regression between predicted and observed sapwood area

A different equation was fir for each site, and the blue line represents the linear regression observed for all sites.

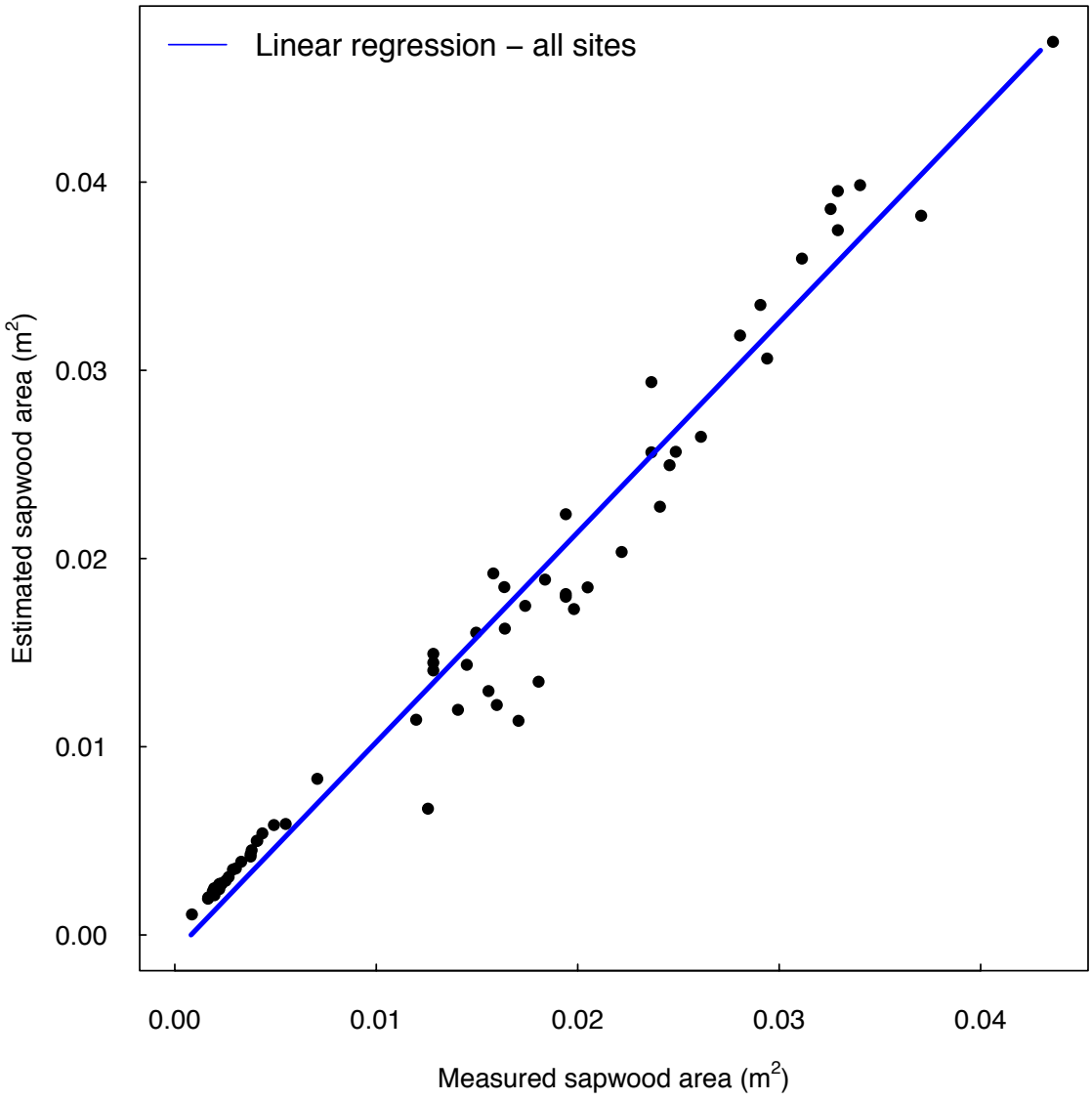

Appendix III-II Steps to estimate bucket model components

The first parameter in the bucket model is infiltration, which is calculated based on the current *S*, and the depth of precipitation as:

$$I'(S(t_{\bar{i}}), t_i) = \min\left[P(t_i), nZr(1 - S(t_{\bar{i}}))\right] \qquad \text{Eq. III-11}$$

Where $I'(S(t_i), t_i)$ is the infiltration at t_i, at a saturation $t_{i^\wedge}$, *min* the minimum value between [,], $P(t_i)$ depth of net precipitation, *nZr* soil depth of porosity *n*, and $S(t_{i^\wedge})$ the saturation before $t_{i^\wedge}$

When saturation is higher than field capacity (S_{fc}), in the absence of soil evaporation or any additional precipitation is converted to leakage using:

$$L(S) = K_{sat}\frac{e^{\beta(S - S_{fcs})} - 1}{e^{\beta(1 - S_{fcs})} - 1} \qquad \text{Eq. III-12}$$

Where $L(s)$ leakage at a saturation *S*, K_{sat} saturated conductivity, β is an infiltration soil parameter and S_{fc} saturation at field capacity

A nominal value was used for $E(S)$ (see Table III-4), and was adjusted to different *S*, using:

$$E(S) = \begin{cases} 0 & S < S_h \\ \dfrac{S - S_h}{S^* - S_h}E & S_h < S < S^* \\ E & S \geq S^* \end{cases} \qquad \text{Eq. III-13}$$

Where S_h is the hygroscopic saturation, S^* the saturation at stomatal closure, *E* the maximum evaporation from the soil

The maximum transpiration estimated early in the monitoring period was used for $T(S)$. Similarly to $E(S)$, *T* was adjusted to different *S*, considering that *T* is directly influenced by water availability.

$$T(S) = \begin{cases} 0 & S < S_w \\ \dfrac{S - S_w}{S^* - S_w}T & S_w < S < S^* \\ T & S \geq S^* \end{cases} \qquad \text{Eq. III-14}$$

Where $T(s)$ is the transpiration at saturation S, S_w the saturation at wilting point, S^* the saturation at stomatal closure, and T the maximum transpiration per site.

Appendix III-III Adjusted equations for throughfall data

In this graph, we show the average precipitation estimated for the time interval when the throughfall was measured. Each point is the average of 20 collectors installed per tree. Dashed lines represent the linear functions fitted for each site.
Linear equations fitted for each site: Mature: y=101.2-7121*x (R^2=0.93), Mid-aged: y=95.66-7127*x (R^2=0.76), Young: y=93.3-7116*x (R^2=0.96)

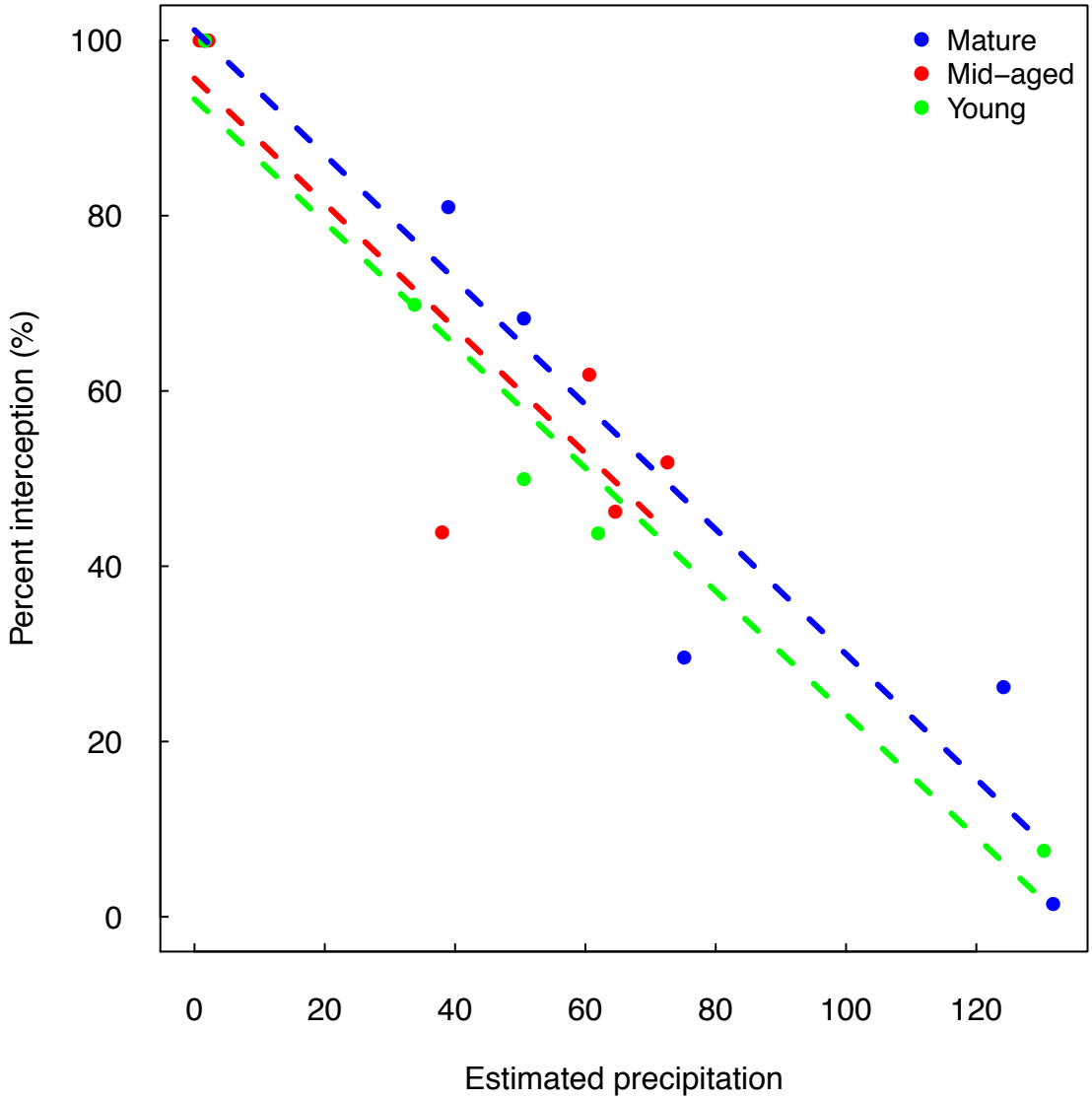

Appendix III-IV Regression between observed and predicted soil parameters
Predicted and observed values correspond to *S* for the first 40 cm of soil.

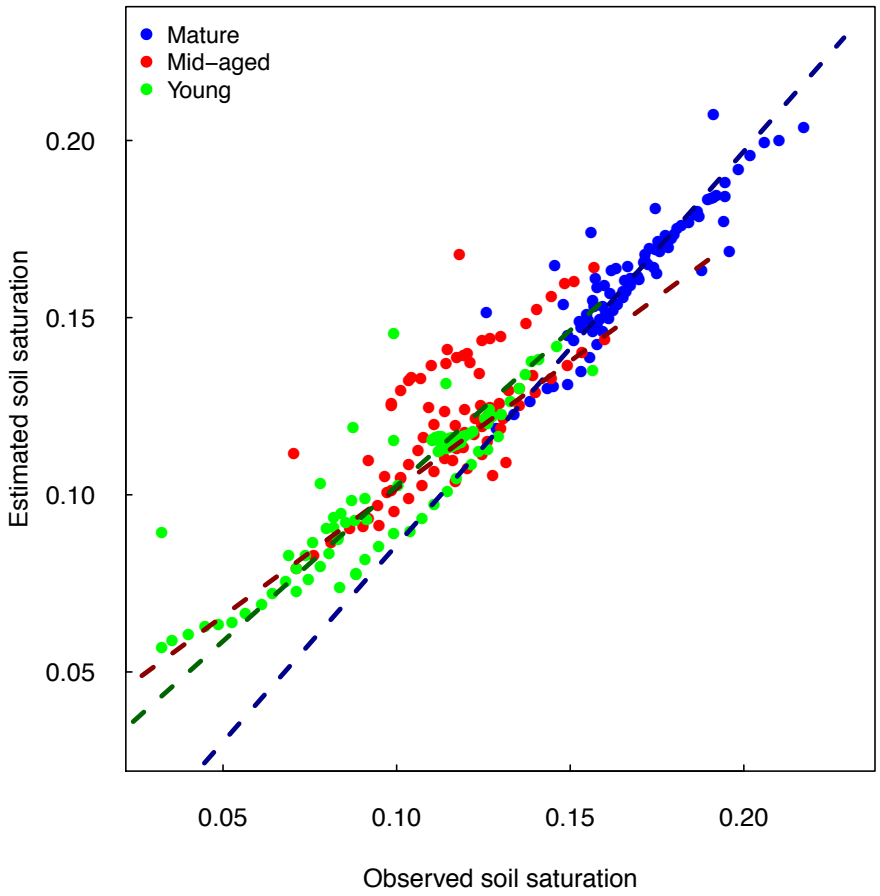

Cited literature

Allen, R. G., L. S. Pereira, D. Raes, and M. Smith. 1998. Crop evapotranspiration: guidelines for computing crop water requiriments. Irrigation and drainage paper **56**.

Allen, S. J., R. L. Hall, and P. T. W. Rosier. 1999. Transpiration by two poplar varieties grown as coppice for biomass production. Tree Physiology **19**:493-501.

Almeida, A. C., J. V. Soares, J. J. Landsberg, and G. D. Rezende. 2007. Growth and water balance of Eucalyptus grandis hybrid plantations in Brazil during a rotation for pulp production. Forest Ecology and Management **251**:10-21.

Alvarado-Barrientos, M. S., V. Hernandez-Santana, and H. Asbjornsen. 2013. Variability of the radial profile of sap velocity in Pinus patula from contrasting stands within the seasonal cloud forest zone of Veracruz, Mexico. Agricultural and Forest Meteorology **168**:108-119.

Angstmann, J. L., B. E. Ewers, and H. Kwon. 2012. Size-mediated tree transpiration along soil drainage gradients in a boreal black spruce forest wildfire chronosequence. Tree Physiology **32**:599-611.

Aparecido, L. M. T., G. R. Miller, A. T. Cahill, and G. W. Moore. 2016. Comparison of tree transpiration under wet and dry canopy conditions in a Costa Rican premontane tropical forest. Hydrological Processes **30**:5000-5011.

Arneth, A., F. M. Kelliher, T. M. McSeveny, and A. N. Byers. 1999. Assessment of annual carbon exchange in a water-stressed Pinus radiata plantation: An analysis based on eddy covariance measurements and an integrated biophysical model. Global Change Biology **5**:531-545.

Balasus, A., W. A. Bischoff, A. Schwarz, et al. 2012. Nitrogen fluxes during the initial stage of willows and poplars in short-rotation coppices. Journal of Plant Nutrition and Soil Science **175**:729-738.

Barella-Ortiz, A., J. Polcher, A. Tuzet, and K. Laval. 2013. Potential evaporation estimation through an unstressed surface-energy balance and its sensitivity to climate change. Hydrology and Earth System Sciences **17**:4625-4639.

Baum, C., K. U. Eckhardt, J. Hahn, et al. 2013. Impact of poplar on soil organic matter quality and microbial communities in arable soils. Plant Soil and Environment **59**:95-100.

Berndes, G. 2008. Water demand for global bioenergy production: trends, risks and opportunities German Advisory Council on Global Change (WBGU), Berlin

Berndes, G. 2010. Bioenergy and water: risks and opportunities. Biofuels Bioproducts & Biorefining-Biofpr **4**:473-474.

Berndes, G., N. Bird, and A. Cowie. 2010. Bioenergy, land use change and climate change mitigation. Chalmers University of Technology, Sweden.

Berry, Z. C., N. Looker, F. Holwerda, et al. 2018. Why size matters: the interactive influences of tree diameter distribution and sap flow parameters on upscaled transpiration. Tree Physiology **38**:263-275.

BETO. 2013. Multi-year program plan. Government Document. Bioenergy Technologies Office. DOE/EE-0915

Bloemen, J., R. Fichot, J. A. Horemans, et al. 2017. Water use of a multigenotype poplar short-rotation coppice from tree to stand scale. Global Change Biology Bioenergy **9**:370-384.

Bond-Lamberty, B., C. Wang, and S. T. Gower. 2002. Aboveground and belowground biomass and sapwood area allometric equations for six boreal tree species of northern Manitoba. Canadian Journal of Forest Research-Revue Canadienne De Recherche Forestiere **32**:1441-1450.

Bond-Lamberty, B., C. Wang, and S. T. Gower. 2014. Aboveground and belowground biomass and sapwood area allometric equations for six boreal tree species of northern Manitoba (vol 32, pg 1441, 2002). Canadian Journal of Forest Research-Revue Canadienne De Recherche Forestiere **44**:389-389.

Bouillet, J.-P., J.-P. Laclau, M. Arnaud, et al. 2002. Changes with age in the spatial distribution of roots of Eucalyptus clone in Congo: Impact on water and nutrient uptake. Forest Ecology and Management **171**:43-57.

Burgess, S. S. O., M. Adams, N. C. Turner, et al. 2001a. An improved heat pulse method to measure low and reverse rates of sap flow in woody plants (vol 21, pg 589, 2001). Tree Physiology **21**:1157-1157.

Burgess, S. S. O., M. A. Adams, N. C. Turner, et al. 2001b. An improved heat pulse method to measure low and reverse rates of sap flow in woody plants. Tree Physiology **21**:589-598.

Chen, L. X., Z. Q. Zhang, T. G. Zha, et al. 2014. Soil water affects transpiration response to rainfall and vapor pressure deficit in poplar plantation. New Forests **45**:235-250.

Chiu, Y. W., and M. Wu. 2013. The water footprint of biofuel produced from forest wood residue via a mixed alcohol gasification process. Environmental Research Letters **8**.

Christersson, L. 2010. Wood production potential in poplar plantations in Sweden. Biomass & Bioenergy **34**:1289-1299.

D'odorico, P., L. Ridolfi, A. Porporato, and I. Rodriguez-Iturbe. 2000. Preferential states of seasonal soil moisture: The impact of climate fluctuations. Water Resources Research **36**:2209-2219.

Davis, S. C., M. Dietze, E. DeLucia, et al. 2012. Harvesting Carbon from Eastern US Forests: Opportunities and Impacts of an Expanding Bioenergy Industry. Forests **3**:370-397.

Delzon, S., and D. Loustau. 2005. Age-related decline in stand water use: sap flow and transpiration in a pine forest chronosequence. Agricultural and Forest Meteorology **129**:105-119.

Dillen, S. Y., S. N. Djomo, N. Al Afas, et al. 2013. Biomass yield and energy balance of a short-rotation poplar coppice with multiple clones on degraded land during 16 years. Biomass & Bioenergy **56**:157-165.

Dimitriou, I., and B. Mola-Yudego. 2017a. Impact of Populus Plantations on Water and Soil Quality. Bioenergy Research **10**:750-759.

Dimitriou, I., and B. Mola-Yudego. 2017b. Poplar and willow plantations on agricultural land in Sweden: Area, yield, groundwater quality and soil organic carbon. Forest Ecology and Management **383**:99-107.

Domec, J. C., G. Sun, A. Noormets, et al. 2012. A Comparison of Three Methods to Estimate Evapotranspiration in Two Contrasting Lob lolly Pine Plantations: Age-Related Changes in Water Use and Drought Sensitivity of Evapotranspiration Components. Forest Science **58**:497-512.

Du Toit, B. 2008. Effects of site management on growth, biomass partitioning and light use efficiency in a young stand of Eucalyptus grandis in South Africa. Forest Ecology and Management **255**:2324-2336.

Ewers, B. E., S. T. Gower, B. Bond-Lamberty, and C. K. Wang. 2005. Effects of stand age and tree species on canopy transpiration and average stomatal conductance of boreal forests. Plant Cell and Environment **28**:660-678.

Fischer, M., M. Trnka, J. Kucera, et al. 2013. Evapotranspiration of a high-density poplar stand in comparison with a reference grass cover in the Czech-Moravian Highlands. Agricultural and Forest Meteorology **181**:43-60.

Ford, C. R., M. A. McGuire, R. J. Mitchell, and R. O. Teskey. 2004. Assessing variation in the radial profile of sap flux density in Pinus species and its effect on daily water use. Tree Physiology **24**:241-249.

Forrester, D. I. 2013. Growth responses to thinning, pruning and fertiliser application in Eucalyptus plantations: A review of their production ecology and interactions. Forest Ecology and Management **310**:336-347.

Forrester, D. I., J. J. Collopy, and J. D. Morris. 2010. Transpiration along an age series of Eucalyptus globulus plantations in southeastern Australia. Forest Ecology and Management **259**:1754-1760.

Frouz, J., P. Dvorscik, A. Vavrova, et al. 2015. Development of canopy cover and woody vegetation biomass on reclaimed and unreclaimed post-mining sites. Ecological Engineering **84**:233-239.

Gebauer, T., V. Horna, and C. Leuschner. 2008. Variability in radial sap flux density patterns and sapwood area among seven co-occurring temperate broad-leaved tree species. Tree Physiology **28**:1821-1830.

Gochis, D. J., and R. H. Cuenca. 2000. Plant water use and crop curves for hybrid poplars. Journal of Irrigation and Drainage Engineering-Asce **126**:206-214.

Granier, A. 1987. Evaluation of transpiration in a Douglas-Fir stand by means of sap flow measurements. Tree Physiology **3**:309-319.

Grau, H. R., M. F. Arturi, A. D. Brown, and P. G. Aceñolaza. 1997. Floristic and structural patterns along a chronosequence of secondary forest succession in Argentinean subtropical montane forests. Forest Ecology and Management **95**:161-171.

Greer, B. T., C. Still, G. L. Cullinan, et al. 2018. Polyploidy influences plant-environment interactions in quaking aspen (Populus tremuloides Michx.). Tree Physiology **38**:630-640.

Guswa, A. J., M. A. Celia, and I. Rodriguez-Iturbe. 2002. Models of soil moisture dynamics in ecohydrology: A comparative study. Water Resources Research **38**.

Hansen, A., A. Meyer-Aurich, and A. Prochnow. 2013. Greenhouse gas mitigation potential of a second generation energy production system from short rotation poplar in Eastern Germany and its accompanied uncertainties. Biomass & Bioenergy **56**:104-115.

Hart, J. F., F. de Araujo, B. R. Thomas, and S. D. Mansfield. 2013. Wood Quality and Growth Characterization across Intra- and Inter-Specific Hybrid Aspen Clones. Forests **4**:786-807.

Hartemink, A. E., B. Lowery, and C. Wacker. 2012. Soil maps of Wisconsin. Geoderma **189**:451-461.

Hinchee, M., W. Rottmann, L. Mullinax, et al. 2009. Short-rotation woody crops for bioenergy and biofuels applications. In Vitro Cellular & Developmental Biology-Plant **45**:619-629.

Hogg, E. H., T. A. Black, G. den Hartog, et al. 1997. A comparison of sap flow and eddy fluxes of water vapor from a boreal deciduous forest. Journal of Geophysical Research-Atmospheres **102**:28929-28937.

Hogg, E. H., and P. A. Hurdle. 1997. Sap flow in trembling aspen: implications for stomatal responses to vapor pressure deficit. Tree Physiology **17**:501-509.

Huang, J. G., K. J. Stadt, A. Dawson, and P. G. Comeau. 2013. Modelling Growth-Competition Relationships in Trembling Aspen and White Spruce Mixed Boreal Forests of Western Canada. Plos One **8**.

IDNR. 2007. Woody biomass feedstock for the bioenergy and bioproducts industries. Government Document. Indiana Department of Natural Resources. Forestry Division

Isham, V., D. R. Cox, I. Rodriguez-Iturbe, et al. 2005. Representation of space-time variability of soil moisture. Proceedings of the Royal Society a-Mathematical Physical and Engineering Sciences **461**:4035-4055.

Jarvi, G. M., J. L. Knowlton, C. C. Phifer, et al. 2018. Avian Community Response to Short-rotation Aspen Forest Management. SPIE.11

Jassal, R. S., T. A. Black, C. Arevalo, et al. 2013. Carbon sequestration and water use of a young hybrid poplar plantation in north-central Alberta. Biomass & Bioenergy **56**:323-333.

Jenkins, J. C., D. C. Chojnacky, L. S. Heath, and R. A. Birdsey. 2003. National-scale biomass estimators for United States tree species. Forest Science **49**:12-35.

Jones, H., T. A. Black, R. S. Jassal, et al. 2017. Water balance, surface conductance and water use efficiency of two young hybrid-poplar plantations in Canada's aspen parkland. Agricultural and Forest Meteorology **246**:256-271.

Kanowski, P. J. 1997. Afforestation and plantation forestry: plantation forestry for the 21st century, in Ed. Preceedings of the XI World Forestry Congress, Antalya, October 1997. UN Food and Agriculture Organization. Rome. 23-34

Karacic, A., T. Verwijst, and M. Weih. 2003. Above-ground woody biomass production of short-rotation populus plantations on agricultural land in Sweden. Scandinavian Journal of Forest Research **18**:427-437.

Kauter, D., I. Lewandowski, and W. Claupein. 2003. Quantity and quality of harvestable biomass from Populus short rotation coppice for solid fuel use - a review of the physiological basis and management influences. Biomass & Bioenergy **24**:411-427.

Kim, H. S., R. Oren, and T. M. Hinckley. 2008. Actual and potential transpiration and carbon assimilation in an irrigated poplar plantation. Tree Physiology **28**:559-577.

Kosugi, K., J. W. Hopmans, and J. H. Dane. 2002. Water Retention and Storage - Parametric Models, in Ed. Soil Science Society of America Book Series. 739-758

Kubota, M., J. Tenhunen, R. Zimmermann, et al. 2005. Influences of environmental factors on the radial profile of sap flux density in Fagus crenata growing at different elevations in the Naeba Mountains, Japan. Tree Physiology **25**:545-556.

Kume, T., K. Otsuki, S. Du, et al. 2012. Spatial variation in sap flow velocity in semiarid region trees: its impact on stand-scale transpiration estimates. Hydrological Processes **26**:1161-1168.

Kume, T., K. Tsuruta, H. Komatsu, et al. 2010. Effects of sample size on sap flux-based stand-scale transpiration estimates. Tree Physiology **30**:129-138.

Laclau, J. P., J. P. Arnaud M Fau - Bouillet, J. Bouillet Jp Fau - Ranger, and J. Ranger. 2001. Spatial distribution of Eucalyptus roots in a deep sandy soil in the Congo: relationships with the ability of the stand to take up water and nutrients.

Larcheveque, M., M. Maurel, A. Desrochers, and G. R. Larocque. 2011. How does drought tolerance compare between two improved hybrids of balsam poplar and an unimproved native species? Tree Physiology **31**:240-249.

Lasch, P., C. Kollas, J. Rock, and F. Suckow. 2010. Potentials and impacts of short-rotation coppice plantation with aspen in Eastern Germany under conditions of climate change. Regional Environmental Change **10**:83-94.

Liesebach, M., G. von Wuehlisch, and H. J. Muhs. 1999. Aspen for short-rotation coppice plantations on agricultural sites in Germany: Effects of spacing and rotation time on growth and biomass production of aspen progenies. Forest Ecology and Management **121**:25-39.

Littell, R. C., G. A. Milliken, W. W. Stroup, et al. 2006. SAS for mixed models. Second Edition edition. SAS Institute Inc., Cary, NC, USA.814

Lu, P., L. Urban, and P. Zhao. 2004. Granier's thermal dissipation probe (TDP) method for measuring sap flow in trees: Theory and practice. Acta Botanica Sinica **46**:631-646.

Mackes, K. H., and D. L. Lynch. 2001. The effect of aspen wood characteristics and properties and utilization. USDA Forest Service Proceedings **RMRS**.

Mueller, A., V. Horna, C. Zhang, and C. Leuschner. 2012. Different growth strategies determine the carbon gain and productivity of aspen collectives to be used in short-rotation plantations. Biomass & Bioenergy **46**:242-250.

Muller, E., and L. Lambs. 2009. Daily Variations of Water Use with Vapor Pressure Deficit in a Plantation of I214 Poplars. Water **1**:32-42.

Naranjo, J. A. B., M. Weiler, and K. Stahl. 2011. Sensitivity of a data-driven soil water balance model to estimate summer evapotranspiration along a forest chronosequence. Hydrology and Earth System Sciences **15**:3461-3473.

Nelson, A. S., M. R. Saunders, R. G. Wagner, and A. R. Weiskittel. 2012. Early stand production of hybrid poplar and white spruce in mixed and monospecific plantations in eastern Maine. New Forests **43**:519-534.

Nikiema, P., D. E. Rothstein, and R. O. Miller. 2012. Initial greenhouse gas emissions and nitrogen leaching losses associated with converting pastureland to short-rotation woody bioenergy crops in northern Michigan, USA. Biomass & Bioenergy **39**:413-426.

Oliver, R. J., E. Blyth, G. Taylor, and J. W. Finch. 2015. Water use and yield of bioenergy poplar in future climates: modelling the interactive effects of elevated atmospheric CO2 and climate on productivity and water use. Global Change Biology Bioenergy **7**:958-973.

Oren, R., J. S. Sperry, G. G. Katul, et al. 1999. Survey and synthesis of intra- and interspecific variation in stomatal sensitivity to vapour pressure deficit. Plant Cell and Environment **22**:1515-1526.

Pataki, D. E., C. G. Boone, T. S. Hogue, et al. 2011. Ecohydrology Bearings-Invited Commentary Socio-ecohydrology and the urban water challenge. Ecohydrology **4**:341-347.

Pataki, D. E., R. Oren, and W. K. Smith. 2000. Sap flux of co-occurring species in a western subalpine forest during seasonal soil drought. Ecology **81**:2557-2566.

Perala, D. A. 1993. Allometric Biomass Estimators for Aspen-Dominated Ecosystems in the Upper Great-Lakes. Usda Forest Service North Central Forest Experiment Station Research Paper:1-&.

Perlack, R. D., L. L. Wright, A. F. Turhollow, et al. 2005. Biomass as feedstock for a bioenergy and bioproducts industry: the technical feasibility of a billion-ton annual supply. Technical Report, Oak Ridge National Laboratory, Oak Ridge, Tennessee.

Perry, C. H., R. C. Miller, and K. N. Brooks. 2001. Impacts of short-rotation hybrid poplar plantations on regional water yield. Forest Ecology and Management **143**:143-151.

Peters, R. L., F. Patrick, F. D. C., et al. 2018. Quantification of uncertainties in conifer sap flow measured with the thermal dissipation method. New Phytologist **219**:1283-1299.

Peterson, E. B., and N. M. Peterson. 1999. Ecology, management, and use of aspen and balsam poplar in the prairie provinces, Canada. Edmonton, AB, Canada.

Petrone, R. M., L. Chasmer, C. Hopkinson, et al. 2015. Effects of harvesting and drought on CO2 and H2O fluxes in an aspen-dominated western boreal plain forest: early chronosequence recovery. Canadian Journal of Forest Research **45**:87-100.

Petzold, R., K. Schwarzel, and K. H. Feger. 2011. Transpiration of a hybrid poplar plantation in Saxony (Germany) in response to climate and soil conditions. European Journal of Forest Research **130**:695-706.

Poblete-Echeverria, C., S. Ortega-Farias, M. Zuniga, and S. Fuentes. 2012. Evaluation of compensated heat-pulse velocity method to determine vine transpiration using combined measurements of eddy covariance system and microlysimeters. Agricultural Water Management **109**:11-19.

Popp, J., Z. Lakner, M. Harangi-Rakos, and M. Fari. 2014. The effect of bioenergy expansion: Food, energy, and environment. Renewable & Sustainable Energy Reviews **32**:559-578.

Powers, S. E., J. C. Ascough, R. G. Nelson, and G. R. Larocque. 2011. Modeling water and soil quality environmental impacts associated with bioenergy crop production and biomass removal in the Midwest USA. Ecological Modelling **222**:2430-2447.

Poyatos, R., J. Cermak, and P. Llorens. 2007. Variation in the radial patterns of sap flux density in pubescent oak (Quercus pubescens) and its implications for tree and stand transpiration measurements. Tree Physiology **27**:537-548.

Puma, M. J., M. A. Celia, I. Rodriguez-Iturbe, and A. J. Guswa. 2005. Functional relationship to describe temporal statistics of soil moisture averaged over different depths. Advances in Water Resources **28**:553-566.

Puma, M. J., I. Rodriguez-Iturbe, M. A. Celia, and A. J. Guswa. 2007. Implications of rainfall temporal resolution for soil-moisture and transpiration modeling. Transport in Porous Media **68**:37-67.

Renner, M., S. K. Hassler, T. Blume, et al. 2016. Dominant controls of transpiration along a hillslope transect inferred from ecohydrological measurements and thermodynamic limits. Hydrology and Earth System Sciences **20**:2063-2083.

Rodriguez-Iturbe, I., V. Isham, D. R. Cox, et al. 2006. Space-time modeling of soil moisture: Stochastic rainfall forcing with heterogeneous vegetation. Water Resources Research **42**.

Rodriguez-Iturbe, I., A. Porporato, F. Laio, and L. Ridolfi. 2001. Intensive or extensive use of soil moisture: plant strategies to cope with stochastic water availability. Geophysical Research Letters **28**:4495-4497.

Rodriguez-Iturbe, I., A. Porporato, L. Ridolfi, et al. 1999. Probabilistic modelling of water balance at a point: the role of climate, soil and vegetation. Proceedings of the Royal Society a-Mathematical Physical and Engineering Sciences **455**:3789-3805.

Rupesh, S., C. Muraleedharan, and P. Arun. 2016. ASPEN plus modelling of air–steam gasification of biomass with sorbent enabled CO2 capture. Resource-Efficient Technologies **2**:94-103.

Ryan, M. G., D. Binkley, and J. L. Stape. 2008. Why don't our stands grow even faster? Control of production and carbon cycling in eucalypt plantations. Southern Forests **70**:99-104.

Rytter, L., and L. G. Stener. 2005. Productivity and thinning effects in hybrid aspen (Populus tremula L. x P-tremuloides Michx.) stands in southern Sweden. Forestry **78**:285-295.

Schume, H., H. Hager, and G. Jost. 2005. Water and energy exchange above a mixed European Beech - Norway Spruce forest canopy: a comparison of eddy covariance against soil water depletion measurement. Theoretical and Applied Climatology **81**:87-100.

Smith, D. M., and S. J. Allen. 1996. Measurement of sap flow in plant stems. Journal of Experimental Botany **47**:1833-1844.

Toillon, J., B. Rollin, E. Dalle, et al. 2013. Variability and plasticity of productivity, water-use efficiency, and nitrogen exportation rate in Salix short rotation coppice. Biomass & Bioenergy **56**:392-404.

Trugman, A. T., N. J. Fenton, Y. Bergeron, et al. 2016. Climate, soil organic layer, and nitrogen jointly drive forest development after fire in the North American boreal zone. Journal of Advances in Modeling Earth Systems **8**:1180-1209.

Tullus, A., H. Tullus, T. Soo, and L. Parn. 2009. Above-ground biomass characteristics of young hybrid aspen (Populus tremula L. x P. tremuloides Michx.) plantations on former agricultural land in Estonia. Biomass & Bioenergy **33**:1617-1625.

Uddling, J., R. M. Teclaw, M. E. Kubiske, et al. 2008. Sap flux in pure aspen and mixed aspen-birch forests exposed to elevated concentrations of carbon dioxide and ozone. Tree Physiology **28**:1231-1243.

Valipour, M. 2015. Comparative Evaluation of Radiation-Based Methods for Estimation of Potential Evapotranspiration. Journal of Hydrologic Engineering **20**.

Vandegehuchte, M. W., and K. Steppe. 2013. Sap-flux density measurement methods: working principles and applicability. Functional Plant Biology **40**:213-223.

Vangenuchten, M. T. 1980. A closed-form equation for predicting the hydraulic conductivity of unsaturated soils. Soil Science Society of America Journal **44**:892-898.

Verlinden, M. S., L. S. Broeckx, H. Wei, and R. Ceulemans. 2013. Soil CO2 efflux in a bioenergy plantation with fast-growing Populus trees - influence of former land use, inter-row spacing and genotype. Plant and Soil **369**:631-644.

Vickers, D., C. K. Thomas, C. Pettijohn, et al. 2012. Five years of carbon fluxes and inherent water-use efficiency at two semi-arid pine forests with different disturbance histories. Tellus Series B-Chemical and Physical Meteorology **64**.

Walker, L. R., D. A. Wardle, R. D. Bardgett, and B. D. Clarkson. 2010. The use of chronosequences in studies of ecological succession and soil development. Journal of Ecology **98**:725-736.

Watkins, D., Jr., M. G. A. de Moraes, H. Asbjornsen, et al. 2015. Bioenergy Development Policy and Practice Must Recognize Potential Hydrologic Impacts: Lessons from the Americas. Environmental Management:1-20.

We, G. J., X. H. Liu, S. C. Kang, et al. 2018. Age-dependent impacts of climate change and intrinsic water-use efficiency on the growth of Schrenk spruce (Picea schrenkiana) in the western Tianshan Mountains, China. Forest Ecology and Management **414**:1-14.

Weiwei, L. U., Y. U. Xinxiao, J. I. A. Guodong, et al. 2018. Responses of Intrinsic Water-use Efficiency and Tree Growth to Climate Change in Semi-Arid Areas of North China. Scientific Reports **8**.

Wengert, E. M. 1976. Quick Method to Distinguish Aspen Heartwood and Sapwood. Wood and Fiber **8**:114-115.

West, B. T., K. B. Welch, A. T. Gatechi, and B. W. Gillespie. 2007. Linear mixed models. A practical guide using statistical software. Taylor & Hall(CRC, Boca Raton, FL, USA

White, E. H. 2010. Woody biomass for bioenergy and biofuels in the United States - A briefing paper. Government Document. Forest Service, Pacific Northwest Research Station. PNW-GTR-825.

Wilske, B., N. Lu, L. Wei, et al. 2009. Poplar plantation has the potential to alter the water balance in semiarid Inner Mongolia. Journal of Environmental Management **90**:2762-2770.

Xi, B. Y., Y. Wang, L. M. Jia, et al. 2013. Characteristics of fine root system and water uptake in a triploid Populus tomentosa plantation in the North China Plain: Implications for irrigation water management. Agricultural Water Management **117**:83-92.

Yang, H., H. Rahardjo, E. C. Leong, and D. G. Fredlund. 2004. Factors affecting drying and wetting soil-water characteristic curves of sandy soils. Canadian Geotechnical Journal **41**:908-920.

Yeh, S., G. Berndes, G. S. Mishra, et al. 2011. Evaluation of water use for bioenergy at different scales. Biofuels Bioproducts & Biorefining-Biofpr **5**.

Zamora, D. S., G. J. Wyatt, K. G. Apostol, and U. Tschirner. 2013. Biomass yield, energy values, and chemical composition of hybrid poplars in short rotation woody crop production and native perennial grasses in Minnesota, USA. Biomass & Bioenergy **49**:222-230.

Zewdie, M., M. Olsson, and T. Verwijst. 2009. Above-ground biomass production and allometric relations of Eucalyptus globulus Labill. coppice plantations along a chronosequence in the central highlands of Ethiopia. Biomass & Bioenergy **33**:421-428.

Zhang, Z. F. 2011. Soil Water Retention and Relative Permeability for Conditions from Oven-Dry to Full Saturation. Vadose Zone Journal **10**:1299-1308.

Zhao, L. L., J. Xia, C. Y. Xu, et al. 2013. Evapotranspiration estimation methods in hydrological models. Journal of Geographical Sciences **23**:359-369.

CHAPTER IV

WATER USE PATTERNS OF EUCALYPTUS GRANDIS PLANTATIONS

Abstract

Demand for timber from fast growing species is increasing in Argentina. Current management alternatives such as rotation cycles are strongly focused on biomass and timber accumulation, and little attention has been given to changes in tree and stand water use within a rotation cycle. Incorporating age-related changes in water use into management plans can help land managers mitigate potential negative effects associated with high water use rates of fast-growing species. In this study we measured stand transpiration (***T***, mm d^{-1}) in four *Eucalyptus grandis* W. Hill ex Maiden plantations near Ubajay, Entre Rios, Argentina having three different ages, 10, 4 and 1 years old (YO), at regular density, and one 1YO plantation with high (double) density (1YOHD). Reference potential evapotranspiration (***ET₀***) (Penman-Monteith) and crop evapotranspiration (***ETₖ***) estimated for a fallow site with minimal pasture cover (Pasture) provided reference conditions for comparative purposes. We analyzed inflection points of sap flux density (***Fd***, cm^3 cm^{-2} h^{-1}) for *VPD* (***IP$_{VPD}$***) and PAR (***IP$_{PAR}$***) by fitting a local polynomial regression (LOESS) surface to the relationship between F_d and *AirT*, *VPD* or PAR and hysteresis curves (***H$_{VPD}$*** and ***H$_{PAR}$***, *VPD* and PAR respectively) to assess the effects of stand age and density on tree response to environmental stress. F_d was measured using the maximum heat ratio method (**MHR**) and scaled up to estimate stand transpiration based on allometric relationships with sapwood area. Our results indicate that *T* in *E. grandis* increased with age from 1 to 4 years and decreased significantly at 10 years. During the peak of the growing season *T* was 5.2, 3 and 2.2 mm d^{-1} (4YO, 10YO, and 1YO, respectively) in the regular density sites, and up to 3.4 mm d^{-1} in the high-density 1YO site. During the same period ET_k was 3.3 and ET_0 4.2 mm d^{-1}. During the peak of the 2015 dry season, *T* in the 10YO and 4YO stands were similar and did not differ

significantly from ET_k, while the 1YO and the 1YOHD stands had significantly lower *T* rates and were very similar with each other. Comparing across the four treatments, the 1YOHD was more responsive to precipitation events than the other sites. Inflection points generated at varying soil moisture conditions, were more pronounced at lower *VPD* when soil moisture was low, suggesting that both soil moisture and *VPD* are important in controlling stomatal response to moisture stress. Comparing across treatments, the 10YO maintained relatively stable inflection points across a wide soil moisture range, while the 1YOHD showed the greatest variability, indicating more opportunistic water use behavior, increasing their water use rates when soil moisture was abundant, but reducing to similar rates of other sites of the same age when soil moisture is limiting. Analysis of hysteresis curves, indicated that H_{VPD} were larger at lower soil moistures, despite the reduced F_d rates. A significant reduction and inversion of the F_d -VPD rate change before *VPD* reached maximum values, followed by a rapid decline during *VPD* reduction in the second part of the day, resulted in the commonly-observed *butterfly* curves for H_{PAR}. *Butterfly* hysteresis curves, which are associated with reversals in F_d -*VPD* change rates, resulting from hydrologic stress, were observed in all sites except the 10YO. In general, our results indicate that mature (10YO) *E. grandis* plantations, are more capable of regulating transpiration rates under high *VPD* and low soil moisture, reducing their risk for hydraulic failure, compared to younger sites.

Introduction

Demand for timber products, especially of fast growing species like *Eucalyptus grandis* W. Hill ex Maiden, is increasing globally (Berndes 2008, Perez-Cruzado et al. 2011, Stape et al. 2010) and in Argentina (Braier et al. 2004). At the same time, climate change forecasts predict an increase in climate variability, including greater frequency and severity of extreme weather

events such as drought and strong precipitation events (Burke et al. 2006), which may exert new constraints on the potential for sustainable production of timber and bioenergy feedstocks. Understanding water use patterns (transpiration, $\boldsymbol{T}$ mm d^{-1}) in woody plantations is an important step to implement appropriate management alternatives designed to promote resilience of plantations to climate variability and extreme weather events.

Highly productive timber and bioenergy plantations are known for their high-water requirements (Dunn and Connor 1993, Jassal et al. 2013), which can result in undesirable hydrological consequences. In particular, fast growing species such as *E. grandis* have the potential to use large amounts of water, altering stand-level water balance and reducing water yield at the watershed scale (Almeida et al. 2007a, Wilske et al. 2009). Additionally, in areas where intensive grazing or agricultural production have reduced the infiltration capacity of the soil, even moderate precipitation events can lead to high overland flows, soil erosion and flooding (Adler and Morales 1999, Bouza et al. 2016). Some of these negative environmental impacts of land use can be partially mitigated by establishing woody plantations, through their potential to enhance soil hydraulic properties such as infiltration capacity and hydraulic conductivity.

Compared to most other tree species commonly used for fast growing plantations, studies on eucalyptus trees have reported exceptionally strong stomatal control on *T* rates during both soil and atmospheric moisture stress (Almeida et al. 2007a, Hubbard et al. 2010, Myers et al. 1996). Native to Eastern Australia, *E. grandis* trees have adaptive strategies that allow them to respond quickly to changes in precipitation patterns and soil water availability due to its strong seasonal changes in soil water availability (Boland et al. 2006). However, when they are established as plantations on sites where soil moisture is not limiting, they are capable of significantly increasing their water use and biomass accumulation (Almeida et al. 2007a, Stape et

al. 2004, Stape et al. 2010). This strong self-regulation suggests that *E. grandis* trees can adjust their transpiration to optimize the use of various resources under a range of environmental conductions, such as low soil moisture, high vapor pressure deficit (***VPD***, kPa), and high photosynthetic active radiation (**PAR**, mmol m^{-2} s^{-1}), while also avoiding excessive physiological stress or damage to tissues when soil moisture is limiting. However, it is not clear whether these self-regulation mechanisms are equally present in old and young *E. grandis* plantations.

The common management practices used in eucalyptus plantations to maximize productivity, such as short rotations or increased planting density, significantly influence both *T* rates and biomass accumulation. Aboveground, increasing stand densities or pruning (when higher timber quality is desired) changes processes of canopy foliage development and the timing of maximum leaf area index (**LAI,** m^2 m^{-2}), which is directly related to stand water use (Forrester et al. 2010). Additionally, research has shown that in fast growing species, LAI patterns can peak and decline within the first six years of the common rotation cycles (0-15 years) (Almeida et al. 2007a, Forrester et al. 2010). In *E. grandis* in particular, this increase and reduction in LAI can occur within the first 3 years (Almeida et al. 2007b, Du Toit 2008, Ryan et al. 2008), often resulting from punning or thinning, which is done to increase timber quality and direct carbon allocation (Forrester 2013, Forrester et al. 2012). When pruning is not part of a management strategy, reductions in LAI over time have also been associated to low photosynthetic rates in lower branches and their subsequent die off when leaves are unable to maintain a positive carbon balance (Kozlowski et al. 1991). Additionally, in both woody trees and palms, height has been associated to reductions in stomatal conductance, resulting from an increase in the energy needed to transport water from the roots to the leaves, which can limit transpiration and potentially reduce LAI (Renninger et al. 2009, Schafer et al. 2000, Williams et al. 2001).

Belowground, studies have shown that preferential carbon allocation commonly observed in young eucalyptus plantations to stems and leaves results in shallower roots (Bouillet et al. 2002, Laclau et al. 2001). While shallow rooting may be a disadvantage in terms of water uptake from deep soil profiles, it can also be a desirable trait to promote surface soil infiltration and reduce runoff. Young *E. grandis* trees with underdeveloped root systems might be more likely to suffer from hydrologic stress when soil water content in the upper soil horizon is low (Bouillet et al. 2002), and the atmospheric demand is high (high *VPD*). In contrast, older trees with well-established root systems have the ability to access deeper water sources throughout the growing season (Brando 2018, Engel et al. 2005, Fan et al. 2017, Giardina et al. 2018, Xi et al. 2018), when water in the top soil is limiting. Recent studies have shown that larger trees are more resilient to drought in general, and that their photosynthetic rates respond differently to changes in soil moisture, compared to younger and smaller trees (Brienen et al. 2017).

Hysteresis, which refers to the lag response between two variables, can also be understood as the rate change over time between two variables. In soils and other artificial porous media, the observed hysteresis between water content and water tension has been attributed to various factors, including the contact angles between water and the pore spaces, and the structure of the macro and micropores (Haines 1930, Staple 1965). However, in general terms it is known that in porous media, these factors point towards the different forces or energies required to refill, or empty the pores at different volumetric water contents, and the energy loss during the process, which makes the process inherently irreversible with zero energy loss (Haines 1930, Pavlakis and Barden 1972, Staple 1965). Early studies of water flow in porous media offered simplified analogies to understand the presence of inflection points (Haines 1930, Staple 1965). First, direct comparison of water flow through a common porous medium and sapwood are not appropriate, because of the fundamental differences in the arrangement of

the matrix (i.e., tightly packed spheres vs. a collection of small conduits for soil and sapwood, respectively). However, the cases which arise as result of flow through porous media, and that have received extensive attention (Haines 1930, Pavlakis and Barden 1972, Staple 1965), are of great value in understanding hysteresis areas, inflection points, and more importantly how they are related to tree hydraulics and their value in synthesizing the general stress in the soil-plant-atmosphere continuum. First, the ***pendular*** case which refers to the minimum amount of water that conductive tissue can have, where there is only a small film of water trapped in spaces where the contact angles of two walls are too small, and where the force holding the water is higher than the force that was needed to empty the pore spaces. At higher water contents, there can be two clear distinctions, the ***funicular*** case, and the ***capillary*** case. In the *funicular* case, several pores are filled with water, and there is an uneven and irregular distribution of the filled pores and empty pores. In this case, there is a virtual network of connectivity between the filled pores that surround the empty pores. In the *capillary* case, all pores are filled and there is a continuous and air-free connectivity of the water filling the pores. Models with glass and ceramic beads have shown that changes in water content within the *pendular* case are reversible and symmetrical with respect to the force applied during emptying or refilling. During the *funicular* and *capillary* cases, in an open system such as cut stem, and in the absence of stomates, the equilibrium of water potential and water content resulting from evaporation from the other end (or transpiration if stomates are present), can only be accomplished through transmission of water tension inside the conductive tissue, or through the flow of water. The tortuous water network created in the *funicular* case, increases the contact area between water and air, which increases the resistance to water flow and equilibrium. Such increases in surface area, together with the increase in resistance to equilibrium at low water contents, results in a delayed response between water flow and equilibrium to evaporative potential i.e., *VPD*.

Hysteresis areas created by the relationship between sap flux density ($\boldsymbol{F_d}$, $cm^3\ cm^{-2}\ h^{-1}$) and *VPD* ($\boldsymbol{H_{VPD}}$) or PAR ($\boldsymbol{H_{PAR}}$) are commonly reported in the literature (Brum et al. 2018, Zeppel et al. 2004), and various studies have explained their observed patterns (Zeng et al. 2016, Zhang et al. 2014). The diel patterns commonly observed: clock, anticlockwise or butterfly-like patterns, where scanning lines are present in the hysteresis curves, allow us to make inferences about the drivers and limiting factors of F_d and daily transpiration, much of which comes from early studies on flow through porous media (Haines 1930, Pavlakis and Barden 1972, Zeng et al. 2016). In simple terms, hysteresis curves show which variables (e.g., soil moisture, *VPD*, PAR) if any, result in increased resistance to water movement through the sapwood. In plant studies, extensive research that has been dedicated to similar curves known as "cavitation curves" in the field of tree hydraulics to understand the relationships between pore structure and adaptation to hydraulic stress (Cochard et al. 2009, Meinzer et al. 2009, Pfautsch 2016, Tyree 2003).

Adding inflection curves between F_d and *VPD* ($\boldsymbol{IP_{VPD}}$) and PAR ($\boldsymbol{IP_{PAR}}$), to the study of hysteresis areas, can further help us understand which variables exert the strongest controls on F_d and T rates. While in three hydraulics, there is no clear boundary at which water content in the sapwood changes from *funicular* to *capillary* state, the point where the rate change between conductivity and pressure changes significantly, indicates the points when sufficient air has entered the sapwood to increase its resistance to water flow, decreasing its conductivity. This point is termed air-entry pressure and it seems to vary significantly depending on the characteristics of the species and even the method used (Martin-StPaul et al. 2014, Meinzer et al. 2009). However, at the plant level, stomatal closure is an earlier response mechanism whereby swelling of the guard cells, cause by inhibition of the activity of proton pumps and the delivery of abscisic acid into the guard cells, results in stomatal closure (Daszkowska-Golec and Szarejko 2013, Tallman 2004). The process of stomatal regulation occurs much earlier and at much lower

pressure deficits than those needed for air entry. And similar to the response between resistance to water flow and pressure deficits (e.g., *VPD*) in sapwood, an inflection point can be identified between the rate change between water flow (i.e., F_d) and *VPD*. As a result, this inflection point can integrate the stress response from the soil to the atmosphere and be a great indicator of the environmental conditions or combination of them (e.g., soil saturation, *VPD*, PAR) at which stomatal closure is triggered. Additionally, it has been well documented that in soils and conductive tissues in plants, conductivity increases directly with water content (Staple 1965, Vergeynst et al. 2014). In the case of F_d in plants, its rate change with respect to *VPD* or PAR, and the hysteresis resulting therein, not only depends on the physical characteristics of the conductive tissue such as vessel diameter and sapwood area. It is also driven by the water content of the sapwood, and other regulatory mechanisms within the plant, such as stomatal control, or root access to water, which are directly associated to hydraulic stress.

While they are not commonly the focus of research studies, IP_{VPD} and IP_{PAR} are often observed and attributed generally to stomatal regulation. At the leaf level, four major factors that have been studied extensively can help better establish the link between inflection points stomatal regulation and the resilience of different plants to various environmental stressors. First, water stress triggers the production of abscisic acid (**ABA**), which can close already opened stomates, or prevent closed stomates from opening (Daszkowska-Golec and Szarejko 2013, Tallman 2004). Additionally, high sucrose concentrations in the apoplast in the midday, resulting from lower water content during dry conditions, have been shown to inhibit midday stomatal apertures (Lu et al. 1997, Lu et al. 1995), through the exceeding capacity of guard cells to catabolize ABA internalized from the apoplast. Such excess of non-degraded ABA, as previously mentioned, can trigger stomatal closure, but also result in the inhibition of the stomatal aperture next day. Third, during the daytime, guard cells are capable of catabolizing both endogenously-

produced and some of the ABA absorbed from the apoplast, but the osmotica (Niu et al. 1997) used for stomatal opening seem to change during the day; ions early in the day and sucrose replaces ions later in the day (Talbott and Zeiger 1996). The last one is the well documented age-related changes in leaf morphology and leaf anatomy commonly observed in eucalyptus trees. Increase presence of cuticular waxes and xeromorphic traits have been observed as *E. regnans* and *E. grandis* trees age (Battie-Laclau et al. 2014, England and Attiwill 2005), which allow them to resist drought and limit their exposure to sunlight, which in turn increases their resilience to severe weather.

Previous studies have quantified how *T* water use varies with plantation ages of different eucalyptus species (Almeida et al. 2007b, Forrester et al. 2010, Hubbard et al. 2010, Liu et al. 2017, Morris et al. 2004, Salama et al. 1994). However, most were based on modeled reference potential evapotranspiration (***ET_0***) assuming no soil moisture limitation or were estimated from daily changes in water table depth. Only a few studies are based on tree-level (sap flow) measurements (e.g., Engel et al. 2005, Forrester et al. 2010), yet we are not aware of any studies conducted in *E. grandis,* or that included different plantation ages as well as both regular and high-density stand conditions. Further, water use models based on ET_0, which are commonly used to elaborate large-scale *T* studies, often disregard the well documented peaks and declines in LAI with age, and the differences in response and its effects on stand *T*. Thus, understanding how different plantation ages respond to changes in environmental conditions such as soil water content, *VPD* or PAR is important in order to design the best management practices to maximize site productivity (e.g., biomass accumulation) while minimizing potential hydrological and physiological risks. Additionally, due to the growing interest in Argentina for timber wood from *E. grandis* (Sanchez Acosta 2012), studying the physiological responses to *VPD* or PAR at

different growing stages can significantly improve management practices through our understanding of resilience of *E. grandis* at different growing stages.

Our goal for this study was to estimate whole tree (***Q***, L d^{-1}) and stand-level *T* in *Eucalyptus grandis* plantations of three different ages, 10, 4 and 1 years-old (**YO**) at regular density (henceforth; **10YO**, **4YO**, **1YO**), one one-year-old at a high (double) density (**1YOHD**), and reference crop evapotranspiration ($\boldsymbol{ET_k}$) in an adjacent fallow pasture site (common during rotation cycles). Our two main objectives were: (a) understand the relationship between plantation age, density, and tree and stand-level transpiration rates, and (b) assess the response of different plantations ages to variations in atmospheric and soil moisture stress, to understand resilience of eucalyptus plantations at different growing stages. **Our first hypothesis** is that, similar to previous studies, stand *T* will increase from 1 to 4 YO, and decrease after that resulting in lower *T* in the 10YO site. **Our second hypothesis** is that older (4 an 10YO) plantations, will be less susceptible to environmental changes (*VPD* and soil moisture), which will be reflected in smaller hysteresis areas for *VPD* and PAR at low *S*, and in inflection points at higher *VPD* rates when soil moisture is limiting. These results can help managers to better understand how transpiration in *E. grandis* plantations changes over time and develop planting designs and rotation cycles that optimize both hydrological and biomass production.

Materials and methods

Study sites

Our study was conducted in three *Eucalyptus grandis* Hill ex Maiden plantations located near Ubajay, Entre Rios, Argentina of ten (31°49'02.8"S 58°14'28.1"W), four (31°48'06.5"S 58°15'10.6"W), and one- (31°48'05.7"S 58°15'07.4"W) -year-old (**YO**) at regular density, and one one-YO plantation at high density (henceforth: **10YO**, **4YO**, **1YO**, and **1YOHD**). All sites

were a year older by the end of our study, but for simplification purposes we will refer to each site by the initial age. For comparison purposes, we also monitored an adjacent fallow land with sparse pasture cover (**Pasture**), due to its recent establishment. This site represents the conditions when no vegetation cover is established. The soils in the region belong to the order of Mollisols, subgroup fluventic hapludolls, with sandy loam texture in the top-soil and sandy clay loam in the subsurface. The topographic symbol reported is MJFv-2. They are cataloged as low-productivity soils and characterized by deficient drainage. They are also considered highly susceptible to erosion, although current erosion rates are considered moderate (Alberto Tasi 2009, INTA 2014). Soil density, porosity, and structure for each site are shown in Table IV-1 (from Cisz-Brill et al.). The four-year average precipitation derived from a weather station located at El Palmar National Reserve is 1262 mm y^{-1}. Annual temperature ranges from an average minimum of 5ºC to an average maximum of 32ºC (SIGA 2015).

Data collection

Tree and site level transpiration

Water use was estimated at the tree-level using heat pulse methods following the maximum heat ratio (**MHR**) method (Gutiérrez Lopez et al. In Prep.), and one heat dissipation (**HD**) method (Granier 1985). Details for HD sensor construction and calibration, including current regulators can be found online (Gutiérrez López 2015, Gutiérrez Lopez et al. 2018). Each MHR sensor set consisted of two probes with three type-T thermocouples and one probe with coiled nichrome wire heater of 20 Ω. The thermocouples were positioned at 0.5, 1.75 and 3 cm from the base of the sensor. Sensors were designed and built by JGL at the installations of the National Agricultural Technologies Institute (INTA) in Concordia, Argentina, and at the Ecohydrology Laboratory at the University of New Hampshire in Durham, NH, USA. We

selected a total of twelve trees that represented the stem diameter distribution and other physical characteristics (e.g., crown size, overall visual health) within each site. All sap flow and environmental data were stored every 15 minutes using CR1000 (Campbell Scientific Inc., Logan Utah, USA) data loggers, and AM16/32 multiplexers (Campbell Scientific Inc.). Our equipment was programed to use one multiplexor per sap flow method (i.e., heat pulse, and heat dissipation sensors). MHR and HD sensors were installed at breast height (1.2 m), and positioned across all four cardinal directions (North, East, South, West) to account for radial variability among trees. To avoid affecting the thermal properties of the trees, and to avoid unwanted reductions of sapwood conductivity, or production of excessive scar tissue, we did not remove the bark of any trees. Instead we conducted an initial sampling to determine the average bark depth (cm) of all sites at breast height and modified the sensor design to make sure the thermocouples were in contact with the sapwood without having to remove the bark. By not removing the bark, we observe that some trees had pushed out the MHR sensors during growth, thus self-adjusting the position of the thermocouples inside the sapwood during the monitoring period. This process was not observed in HD sensors, perhaps as a result of the smaller epoxy resin in contact with the tree. Due to site accessibility caused by road blockages and field logistics that impeded regular access to the sites, the sap flow stations were turned on and off intermittently, and we adjusted a linear mixed model (see below for details) to fill gaps during periods without sap flow measurements.

Environmental variables

Volumetric water content (**EC5**, $cm^3\ cm^{-3}$) at three depths (20, 40 and 100 cm), air temperature (***AirT***, HMP45, ºC), and relative humidity (***RH***, HMP50, %) were measured at each site. No soil moisture data was collected in 2014 for 1YO and Pasture. Additionally, a weather

station was installed at the pasture site to monitor net radiation (CNR2, W m^{-2}), *RH* (%), *AirT* (HMP45, ºC), precipitation (ONSET, mm), photosynthetically active radiation (***PAR***) (LI-190R, mmol m^{-2} s^{-1}), and wind speed (03101, m s^{-1}) at 15-minute intervals.

Data from the weather station were used to estimate potential evapotranspiration ($\boldsymbol{ET_0}$) and crop evapotranspiration ($\boldsymbol{ET_k}$) in the Pasture site following the FAO Penman-Monteith (Allen et al. 1998, Allen et al. 1999) equations. We used factory-provided parameters to convert soil permittivity into volumetric water content. For comparisons across sites, and to perform statistical analysis without the influence of soil porosity, volumetric water content was converted to soil saturation (***S***) for two soil depth ranges, 0-100 cm and 0-40 cm of soil according to Vangenughten (1980) using the following equation:

$$S = \frac{\theta - \theta_r}{\theta_s - \theta_r} \qquad \text{Eq. IV-1}$$

Where *S* is the saturation, θ the volumetric water content (averaged for the entire 100 cm), θ_r the residual water content (0.05 % for sandy soils, according to (Zhang 2011)), and θ_s the volumetric water content at saturation. θ_s was estimated as the average porosity for the profile of interest for each site. Additionally, to compare across sites, and to estimate expected runoff and infiltration rates, we adjusted the Bucket model (Guswa et al. 2002a, Porporato et al. 2004) for each site, using the following formula:

$$nZ_r \frac{dS}{dt} = I(S,t) - L(S) - T(S) - E(S) \qquad \text{Eq. IV-2}$$

Where *n* is the porosity of the soil, Z_r soil depth, *I(S,t)* infiltration rate, *L(S)* leakage, *T(S)* transpiration, and *E(S)* the evaporation from the soil. A full description of the parameters used for this model is shown in Table III-4, and additional details for the estimation of each parameter are shown in Appendix III-II. Precipitation and transpiration needed in the model were estimated

at each site (see details below), and we used reference values of saturated conductivity for the soil type.

Stand characteristics

Considering that all sites were established at fixed spacings, (3 x 2.5 m, in regular density sites and 3 x 1.5 m in high density sites), site density, average diameter and height were estimated at each site following the line-to object approach (Ducey 2018, Lynch et al. 2018) (Table IV-3). Ten 10-m sections were randomly located at each site, at least 20 m from the edges, and we measured the diameters and heights of all trees within each 10-m section and counted the number of missing trees due to mortality. Diameters were binned for each site at 1 cm intervals, and a we estimated a diameter distribution charts for each site, which were later used in the scaling-up process (see below). To estimate sapwood area ($\boldsymbol{A_S}$, m^2) for each site, we injected a 0.05% safranin solution directly into the sapwood about 10 cm below the area where the sap flow sensors were installed and collected a sample 5 cm above the sensor using a Pressler Drill (Suunto, Vantaa, Finland) 48 hours after the application of the dye, and sapwood, total length and bark depth were measured immediately after the samples were collected. All tree cores were oven-dried over a 24-hour period to estimate volumetric water content and wood density. Once A_S was estimated for each tree, an allometric equation was adjusted for each site between diameter with bark and estimated A_S, using the following equation:

$$A_s = Exp(\beta_0 + \beta_1 \ln(D)) \qquad \text{Eq. IV-3}$$

Where A_S is the sapwood are in m^2, D the diameter, and β_0 and β_1 the predictor parameters. Additionally, to increase sample size and the prediction power of the allometric equations, we merged both 10YO and 4YO sites (considered Mature), and both 1YO sites (considered Young), and generated parameters for both Mature and Young categories,

additionally to the parameters by site, and a set of global parameters (all sites). The parameters, estimated errors and R^2 with respect to observed measurements are shown in Table IV-4.

Additionally, we monitored diameter increments in all sites (10YO, 4YO, 1YO, 1YO-HD), at intervals of approx. 2-3 weeks. Due to the lower growth rates, we collected only three measurements in the 10YO site. In 2014, diameter was initially measured at 40 cm from the ground surface in the 1YO sites, due to the smaller diameters at breast height. We fit a quadratic function only within the measured points, to account for changes in diameter in sapflow calculations (see below for details). Finally, total biomass for comparative purposes at each site was estimated following the adjusted model by Wink et al. (2015):

$$Ln(TB) = -a + b * \ln(DBH) + c * \ln(h) \qquad \text{Eq. IV-4}$$

Where TB the total aerial biomass, *a*, *b* and *c* are the adjusted parameters (3.32, 2.12, and 0.65, respectively), and *h* the tree height.

Data processing and analysis

All data were processed with custom-designed scripts developed for JMP Pro 13 (SAS Institute Inc., Cary, NC. USA), and R Studio (R Core Team, Vienna, Austria) that allowed us to estimate heat pulse velocity ($\boldsymbol{v_h}$), sap flux density ($\boldsymbol{F_d}$, $cm^3\ cm^{-2}\ h^{-1}$) and whole tree sap flow ($\boldsymbol{Q}$, $L\ d^{-1}$) for each tree. First we estimated the heat ratios following the maximum heat ratio method, which we previously validated for *E. grandis* trees (Gutiérrez Lopez et al. In Prep.). Heat pulse velocity (v_h $cm\ h^{-1}$), and v_h corrected for wounding ($\boldsymbol{v_c}$) were estimated according to Burgess et al. (2001) using the following equations:

$$V_h = \frac{\mathrm{k}}{x} ln \frac{v_1}{v_2} 3600 \qquad \text{Eq. IV-5}$$

$$V_c = bV_h + cV_h^2 + dbV_h^3 \qquad \text{Eq. IV-6}$$

Where V_h is the heat pulse velocity, k is the thermal conductivity and x the distance between probes, and v1/v2, the temperature ratios. b, c, and d, are the parameters used to correct V_h for wounding effects. V_c was converted to F_d according to Vandegehuchte and Steppe (2013) with the following equation:

$$F_d = \frac{\rho_d}{\rho_s}\left(MC + \frac{C_{dw}}{C_s}\right)V_c \qquad \text{Eq. IV-7}$$

Where ρ_d is the density of the sapwood, ρ_s the density of water, MC the volumetric water content of the sapwood, C_{dw} the thermal conductivity of dry wood, and C_s the thermal conductivity of water.

Scaling sap flux measurements to estimate stand T

To estimate tree ($\boldsymbol{Q}$, L d^{-1}) and stand-level T, first we averaged F_d (estimated using Eq. III-6) for each site using all the measurement points for MHR sensors (approximately 24 measuring points per site). Thermocouples that showed constant noise (likely the result of sensor, or equipment malfunction) were filtered out and not used to estimate site-average F_d. Next, we predicted A_S of all trees belonging to each diameter category for each site (see Stand characteristics above) using the allometric equation adjusted for each site (Eq. III-9), and estimated sap flow Q for all trees of each diameter category multiplying site-average F_d by their respective predicted A_S. Q was estimated integrating all measurements per day (96), and average Q was estimated averaging all trees in the subsample per site. Site transpiration ($\boldsymbol{T}$, mm d^{-1}) was estimated using the following formula:

$$\sum_{d=i}^{d=n} (F_d \,.\, A_s . n) \frac{D}{N} \qquad \text{Eq. IV-8}$$

Where d_i-d_n are the first to last diameter categories, F_d the average flux density (converted to L m^{-2} d^{-1}), A_S the predicted A_S (in m^2), n the total number of trees per each diameter category, D the number of trees per hectare, and N the number of trees in the subsample.

Gap filling

To fill gaps of T, we fitted the following linear mixed model by year (2014, 2015) in JMP PRO 13 for each site:

$$T_{mod} = X\beta + Z\gamma + \varepsilon \qquad \text{Eq. IV-9}$$

Where $\boldsymbol{T_{mod}}$ is the modeled (or predicted) site transpiration, X is the series of fixed variables (*AirT, RH, NetRad, VPD , ET_0*, *WindS*, *pp*, *S*), Z the random effects (DOY), β and γ are the slopes of X and Z, and ε the error of the model. We tested three configurations of fixed variables, first with all variables, then removing *S,* to be able to estimate T_{mod} for days when *S* data was missing. The third model was adjusted selecting the variables that had the overall highest influence on T_{mod} for all sites (ET_0, *PAR* and *NetRad*), and to address the potential redundancy of including variables with high correlation. In Table III-5 we show the corrected Akaike and Bayesian Index criterion for each model fitted including both years.

Hysteresis and inflection points of sap flux density

To test our second hypothesis, first we filtered out days with precipitation events or with forecasted conditions, and then generated hysteresis graphs for each site between average F_d -

VPD and F_d-PAR. All data, including F_d, PAR and *VPD*, were normalized with respect to the maximum values observed for each variable at each site. All data were split into four *S* ranges (0.2-0.55, 0.55-0.75, 0.75-0.9, 0.9-1.0), and we created a hysteresis graphs with normalized data for each of these *S* ranges. Finally, we used the *geometry* library in R-studio 1.1.423 and estimated the hysteresis area of *VPD* and *PAR* (***H_{VPD}*,** unitless; ***H_{PAR}*,** unitless, respectively).

To determine inflection points of F_d for both *VPD* and PAR, we estimated monthly averages of F_d for each site, binned in 15-minute intervals. A Locally Weighted Scatterplot Smoothing (LOESS) (Cleveland 1981) was fitted (span of 0.9, n= 1:1000) to each F_d-PAR and F_d-*VPD* response curves. Each LOESS predicted data was treated as a vector of size (*n*) 1:1000, and the inflection point was considered the value at which the difference: [(1+lag) : n] – n [1: (n-lag)] = inflection threshold, where: lag = 5% of *n*, and inflection threshold = 0.1. The inflection threshold value of 0.1 was selected to identify the point in the F_d -*VPD* or F_d -PAR response curves before the slope of the fitted LOESS line turned zero, and to identify inflection points that did not result in slopes =< 0, which occurred frequently in our data.

Statistical analysis

We selected F_d within 11AM-5PM, to capture the maximum F_d rates of each site and analyzed how maximum F_d was influenced by various environmental variables (*AirT, RH, NetRad, VPD , ET_0*, *WindS*, *pp*, *S*). We fitted a mixed linear model by site, where the environmental variables were the fixed effects and DOY, Month and Year the random effects (Table IV-7). A similar analysis was performed for stand *T* for each site, using a Standard Least Squares model with a Restricted Maximum Likelihood (REML) method in JMP Pro 13 (Table IV-6). We treated all environmental factors as fixed effects, and DOY of each year as a random variable. Each site was analyzed independently by year detect year-specific effects. Differences

among sites for periods of interest were done in JMP PRO 13 with ANOVA's and Tukey tests at alpha values of 0.05. Finally, hysteresis areas (H_{PAR}; H_{VPD}) were analyzed with a standard least squares model in JMP PRO 13, using H_{PAR} and H_{VPD} as response variables, and month, site and saturation range as model effects.

Results

Soil saturation

During the monitoring period, our sites received a total precipitation of ~650 mm, often concentrated in pulses of 5 and up to 12 days. Soil bulk density (g cm^{-3}) was significantly different between soil depths (F-ratio=7.86, p=0.0069), but no significant difference was observed by site (F-ratio=3.60, p=0.055), and since porosity was estimated as a function of bulk density, the results for density where similar (site: F-ratio=3.85, p=0.059; depth: F-ratio=8.06, p=0.006). Due to the high sand content across sites (Table IV-1), *S* increased and decreased rapidly after significant precipitation events, and in response to stand transpiration (see details below). In general, *S* was higher in 2014, than 2015 (Figure IV-1, Figure IV-2, panel A for both), as a result of higher precipitation. Considering the entire (100 cm) soil profile, the 4YO site had the lowest average *S*, and based on 2015 data, the Pasture site had the highest. In 2014, on two occasions after two precipitation events greater than 30 mm, most sites had a *S* close to 100%. Conversely, in 2015, soils were never fully saturated, even after significant precipitation events.

According to our *S* modeling in the upper 40 cm using the bucket model (Guswa et al. 2002b), *S* followed a similar trend as the *S* observed in the same soil profile (panel B, Figure IV-1, Figure IV-2). However, despite following a similar *S* trend, the coefficient of regression between modeled and predicted was in general low for all sites (R^2 = 0.41, 0.34, 0.53 and 0.27, for 10YO, 4YO, 1YO, and 1YOHD, respectively), except Pasture (R^2 = 0.91). While no data

were collected in January 2015, our *S* modeling indicates that the upper 40 cm of soil had *S* higher than 90% after an eight-day period with precipitation events greater than 10 mm.

Allometric relationships

Considering data from all sites, the A_S predicted with the exponential model (Eq. III-2) had a strong correlation (R^2=0.94, RMSE= 0.0012) with observed A_S (Appendix IV-III). As shown in Table IV-4, the correlation between observed and predicted A_S for each site was higher in both 1YO (R^2=1, RMSE= 0.0) and 1YOHD (R^2=0.98, RMSE= 0.003), primarily because most trees sampled were 100% sapwood. The coefficient of regression declined as the plantation age increased, primarily due to the presence of trees with relatively thin sapwood depths for their diameters. Combining the 4YO and 10YO sites into a Mature category, did not improve the coefficient of regression (R^2=0.86, RMSE= 0.0018) between observed and estimated A_S. Similarly, combining data from 1YO and 1YOHD into a "Young" category did not result in any improvement (R^2=0.96, RMSE= 0.0003); however, for both categories, merging the data significantly increased the diameter range, which increases the predictive power of the models we fitted.

Whole-tree water use

For whole tree water use (Q, L d^{-1}), at regular density sites we observed an increase in Q from 1YO to 4YO, and a reduction thereafter (between 4YO to 10YO). The high-density site (1YOHD) was on average lower than the 1YO regular density site and followed a similar trend as the other sites (Figure IV-3). Towards the end of the monitoring period, 4YO and 1YO sites had similar Q (4.94 ±0.24 and 4.86 ±0.11, respectively) and were significantly higher than 10YO

and 1YOHD (1.7, 2.1, respectively). Analyses of variance among sites by month indicates that *Q* was significantly different (p=<0.0001) among sites during all months except March (p=0.0561). In 2014 (November and December) the 4YO site had the highest *Q* (12.2 ±1.7 L d^{-1}) followed by 1YO (7.8 ±0.8 L d^{-1}), 10YO (5.4 ±0.6 L d^{-1}) and finally 1YOHD (7.3 ±0.9 L d^{-1}). In 2015 (February, March, April and May) the pattern was similar, with the 4YO site having the highest *Q* (8.5 ±0.64 L d^{-1}), followed by the 1YO (7.76 ±0.44 L d^{-1}), and similar *Q* for both the 10YO and 1YO-HD (4.6 and 5 L d^{-1}). During the driest period in 2015 (DOY 97-107), 4YO and 10YO had similar *Q* (approx. 4 L d^{-1}), and both 1YO and 1YOHD showed the lowest *Q* (approx. 3, and 1.7 L d^{-1}, respectively).

Stand-level water use

In 2014, the 4YO site had a maximum *T* (all in mm d^{-1}) of 5.2, followed by the 1YOHD (3.4), 10YO (3), and 1YO (2.2). For the same period, the maximum ET_k estimated for the Pasture site was 3.7 (Figure IV-4). In general, all sites increased transpiration after precipitation events, but there was a clear difference in the response observed in 2014 and 2015. In 2014, precipitation events resulted in significant increments in *T*, particularly at the 4YO and 1YOHD sites. For example, the 1YOHD site increased *T* by approximately 85% after the precipitation events on DOY 302-307. By contrast, *T* in the 10YO site increased by less than 5% after the same precipitation event. In 2015, there was a similar trend in *T* rates across sites, with 4YO and 1YOHD having a similar maximum *T* of 3 mm d^{-1}, followed by 10 YO and 1YO with a maximum of 2 mm d^{-1} (Figure IV-5). However, after DOY 63, at the onset of a 43-day rainless period, and also the period the with the lowest *S* (see: Figure IV-2), we observed clear differences by age group; both 4YO and 10YO had similar *T* (average 1.1) and greater than both 1YO and 1YOHD sites (average 0.5 mm d^{-1}). Considering both years, the 10YO and 1YO, had

the lowest variability in *T* (standard deviation: 0.55 and 0.50, respectively), and the 4YO the highest (standard deviation: 1.3), followed by the 1YOHD (0.92).

Estimated cumulative *T* for the entire monitoring period (220 days, Sept 2014-May 2014) followed a similar pattern as that observed for *Q* and *T*. In regular density sites, cumulative *T* was higher in the 4YO site (526 mm), followed by the 1YOHD (360), the 10YO (320), and the 1YO site had the lowest total water use (265 mm). For the same period, estimated ET_0 for the Pasture was 400 mm, and the total precipitation was 820 mm (Figure IV-6).

Considering all the data over the entire sampling period Nov 2014 – May 2015, *S* in the upper 40 cm had the strongest influence on daily *T* across all sites (Table IV-6). No other variable had a significant effect on all sites, however, *VPD* and *AirT* significantly influenced daily *T* at the 10YO, 4YO, and 1YOHD sites (p-value = <0.0001, 0.0112, and 0.0118, respectively). *PAR* and *NetRad* significantly affected *T* at the 10YO and 1YO sites (PAR p-value=<0.0001 and <0.001. *NetRad* p-value=0.0130 and 0.0042, respectively for 10YO and 1YO), but not at the 4YO and 1YOHD sites.

Inflection points of sap flux density and hysteresis

Within each site, F_d -*VPD* response curves changed significantly during the monitoring period, while annual patterns were generally similar across sites despite differences in magnitude. All sites showed a linear relationship between F_d and *VPD*, when *VPD* was under ca. 2 kPa (Figure IV-7). After this threshold, all sites had an inflection point between a *VPD* range of 1.5-2.4 kPa, but no inflection points were observed at *VPD* greater than 2.5 kPa. Comparing rates of F_d at different temperatures, all inflection points occurred between 26 and 30ºC (data not shown). Except for the 10YO site, the IP_{VPD} of all sites were influenced by precipitation and changes in *S*. In March, a 30 mm precipitation event that followed a 43-day rainless period

(DOY 63-106, 2015) resulted in increments in F_d, but no significant changes in the inflection points were observed in this month, partially because monthly averages include periods of high and low *S*. Analyzed by *S* ranges (0.2-0.55, 0.55-0.75, 0.75-0.9, 0.9-1.0), IP_{VPD} showed a clear increasing trend at higher *S* (Appendix IV-IV). The respective IP_{VPD} were 1.95, 2.01, 2.08, and 2.18 kPa, respectively for increasing *S* ranges. However, these differences were not statistically different (F-ratio=1.47, p=0.27) within the *S* ranges we selected. Testing more extreme *S* ranges resulted occasionally in significant differences (data not shown), but in general the trend of increased IP_{VPD} at high *S* remained.

Analyzed by site including all data from each site, inflection points were not statistically different (F-ratio=2.38, p=0.11). Removing the high-density site (1YOHD) from the analysis, which had the highest IP_{VPD} variability (average: 2.18 ±0.27 kPa) of all the sites, resulted in statistically different inflection points by site (F-ratio=7.67, p=0.01). Inflection points for regular-density sites were on average greatest for the 10YO (2.12 kPa), Intermediate for 1 YO (2 kPa), and lowest for the 4 YO (1.93 kPa) (Appendix IV-IV). F_d patterns after the observed inflection points (when present) showed different patterns for each site, with the least changes observed in the 10YO site. The other sites showed a stagnation or reduction in F_d rates at low *S*. The 1YO and 4YO sites showed reductions in F_d after the inflection points even at high *S*, and conversely, the 1YOHD site showed an opportunistic pattern, increasing inflection points at high *S*.

F_d -PAR response curves showed a negative exponential curve for most of the sampling period and increments in *PAR* did not result in sharp inflection points, in contrast to those observed for *VPD* (Figure IV-8). According to our analysis all inflection points occurred within a range of 1.5-2.2 mmol m^{-2} s^{-1}, and during periods of high *S* no inflection point was observed in the 10YO site in response to PAR. Changes in *S* resulted in changes in the shape of the F_d -PAR

response curve, but only towards the end of the growing season (April) the response curve was significantly negative after reaching the inflection point (average 0.9 mmol). Finally, while most sites had an inflection point greater than 1 mmol from November through March, the 10YO site had an inflection point in February at a much higher PAR (1.9 mmol), and no inflection point was observed for November, December, and March.

H_{VPD} showed a high rate-change (e.g., slope of the F_d -*VPD* line) in early morning, that plateaued when approaching maximum *VPD*. From maximum to minimum *VPD*, the reduction in the F_d -*VPD* rate was highest immediately following *VPD* declines, resulting in a clockwise H_{VPD} pattern (Figure IV-9). In general, we observed higher F_d ranges at high *S* (0.8-1.0), compared to low *S* (0.2-0.4); however, H_{VPD} followed an opposite pattern. First, despite the higher F_d rates at high *S*, H_{VPD} were in fact higher at lower *S* (Figure IV-9: first panel from left), resulting from an inversion in the F_d -*VPD* rate-change, i.e., F_d decreased while *VPD* was still increasing. Despite the trend observed of increasing H_{VPD} at lower *S*, when all sites were included, the changes were not statistically different for the *S* ranges analyzed (F-ratio=2.42, P-value= 0.13). We observed a clear relationship between plantation age and H_{VPD} (10YO, 1YOHD, 1YO, 4YO, increasing order), but this trend was not statistically significant (F-ratio=2.97, P-value= 0.09).

H_{PAR} showed a high rate of change that remained stable from minimum to maximum PAR. During PAR reduction, there was a sharp increment in the F_d -PAR rate-change at the onset of reducing PAR, which resulted in an anti-clockwise pattern (Figure IV-10). While no statistical differences were observed in PAR for the four *S* ranges tested, H_{PAR} increased significantly at higher *S* (F-ratio=34.62, P-value=<0.0001), and was strongly correlated with site (4YO, 1YOHD, 1YO, 10YO, increasing order) (F-ratio=24.3, P-value=0.0001). At low *S* the initial high F_d -PAR rate-change reduced significantly, and turned negative (i.e., F_d decreased

while PAR continued increasing) before PAR reached maximum values in 4YO, 1YO and 1YOHD sites. During PAR reduction, the significantly lower F_d -PAR rate-change resulted in a "butterfly" shape.

Statistical analysis of maximum daily F_d, showed that PAR had a significant influence on the 4YO only (F-ratio=18.1, P-value=<0.0001), which was also the site with the highest H_{PAR}, but no significant influence on the other sites (All, Table IV-7). Conversely, *VPD* hat a stronger influence on maximum F_d in all sites (p=<0.0001, for all), and the results were similar by *AirT* and *RH*. Removing *S* from the model source did not change the response patterns between maximum F_d and *VPD* for any of the sites. Based on this analysis, the only difference was that both 4YO and 1YOHD sites were significantly influenced by PAR (p=<0.0001, and 0.0046, respectively) (Table IV-7).

Discussion

Change in stand T with plantation age

Our first hypothesis, that stand *T* would increase from 1 to 4 YO, then decrease to a lower *T* in the 10YO site, was supported by our results, as daily whole-tree water use *Q* initially increased from 6.2 to 9.07 L d^{-1}, then sharply declined to 4.5 L d^{-1}. In fact, during most of the growing season, *Q* was higher in 1YO, compared to 10YO. Comparing the two 1YO sites, Q was consistently lower in 1YOHD, and during the wet season, Q was similar between the 10YO and 1YOHD sites. Similar reductions in tree-level water use with age have been extensively reported in the scientific literature in natural forests (Alsheimer et al. 1998, Kostner et al. 2002), and plantations (Delzon and Loustau 2005, Forrester et al. 2010), despite some studies suggesting an opposite pattern (Dye 1996, Naranjo et al. 2011).

Reductions in *Q* with stand age have been attributed to several factors, such as greater limitation on stomatal conductance resulting from increases in water potential when tree height increases (Brienen et al. 2017, Ewers et al. 2007, Han 2011, Schafer et al. 2000). In our sites, despite the average height increasing from 5.6 m in 1YO trees to 15 m in 4YO trees, *Q* increased within this age range, while the much smaller height increased from 4YO to 10YO (15 to 17 m) seems insufficient to account for the nearly 50% reduction in average *Q* observed. Further, in *E. grandis,* such reductions have been reported to start much earlier (i.e., 1.5 to 3 years) before reaching maximum tree height, and continued to decline even when tree heights remain stagnant (Almeida et al. 2007b, Du Toit 2008, Ryan et al. 2008). Other studies have attributed this reduction to nutrient deficiencies such as N or P (Ward et al. 2008), resulting from multiple intensive short rotations. Data available on soil fertility at our sites (top 60 cm) indicates that only P was on average low (0.013 Mg ha^{-1}) but sufficient for growth in the entire soil profile studied, with higher concentration sin the top 15 cm. In terms of nutrient depletion due to intensive rotations, there is not a clear trend in extractable P at different rotations (Brill et al, unpublished). Other studies have suggested that reductions in soil water availability might account for the decline in water use with age (Ainsworth and Rogers 2007, Oguntunde 2005); however, our *S* data clearly show (Figure IV-1) that even when soil water was plentiful, differences in *Q* remained.

Doubling stand density in 1YOHD, compared to 1YO, reduced *Q* by about 20% early in the growing season and increased Q by about 60% at the end of our study. Considering that these two sites were established under the same site characteristics (i.e., slope, soil type, etc.) and exposed to similar environmental conditions, an initial explanation for the reductions in whole tree water use observed between these two sites is the available growing space for individual trees, and reductions in LAI at the tree level. In general, reductions in *Q* with tree age observed

in this and similar reductions reported in other studies (Alsheimer et al. 1998, Delzon and Loustau 2005, Forrester et al. 2010, Kostner et al. 2002) are mostly due to a combination of the following factors: differences in management practices, the methods used to estimate tree water use rates, which may be limited to specific tree sizes (e.g., potted trees or weighing lysimeters), and primarily, the LAI stage and age of the stands. The development of LAI over time has been extensively studied in natural forests and plantations. In general, LAI increases from the time of establishment of the vegetation cover, and can remain constant after a slight reduction in mixed natural forests, or reduce significantly (40-60%) before stabilizing in fast growing species such as *E. grandis* (Almeida et al. 2007a, Du Toit 2008).

The development pattern of LAI seems to differ in forests and plantations (Allen et al. 1999, Blanken et al. 1997, Forrester et al. 2010), and consequently, its role as a main driver of both water use and primary productivity may also vary (Ares and Fownes 2000, Campoe et al. 2012, Jassal et al. 2013). Delzon and Loustau (2005) observed LAI (and tree water use) reductions in *Pinus pinaster* Ait. sites from 2.8 $m^2 m^{-2}$ in 10YO stands, to 1.9 in 54YO sites, followed by stable LAI in the 92YO stands. In a similar study, Alsheimer (1998) observed a 30% (visually estimated from their graphs) reduction in LAI of *Picea abies* natural forests from 40 to 140YO stands. Both *P. pinaster* and *P. abies* are relatively slow-growing species, and similar results have been observed for fast-growing species at sites that are also past the canopy closure stage. In *Eucalyptus regnans* mature forests of 50, 90, 150 and 230YO, Dunn and Connor (1993) observed that despite stable sap velocities (average of 11.4, 11.5, 9.9 and 11.8 mm h^{-1}, respectively), LAI decreased with age. In *E. globulus* plantations in southeastern Australia, Forrester et al. (2010) observed a decline in F_d and Q with increasing age in 2, 4, 5, 6, 7 and 8YO plantations. However, in this study, LAI peaked at around 6YO, which is consistent with plantations growing in drier environments. In *E. grandis* in particular, studies have observed

peaks in LAI and *Q* at 3YO (Almeida et al. 2007a) and 2YO (Du Toit 2008). These studies indicate that the more quickly canopy closure and LAI peaks occur with age, the steeper the decline afterwards (Almeida et al. 2007b, Du Toit 2008, Ryan et al. 2008). In our regular-density sites, *Q* declined by approximately 60% from 4YO to 10YO, consistent with previous studies conducted in *E. grandis* plantations (Almeida et al. 2007a).

At the stand level, *Q* was not a good indicator of the estimated *T*. On average the 4YO site had the highest *T*, followed by 1YOHD, 1YO and 10YO (whole season average: 0.98, 0.81, 0.62, 0.48 mm d^{-1}, respectively), and excluding the high-density site, average *T* was strongly correlated with stand density (R^2 = 0.91, RMSE=80.5). These findings indicate a strong age effect, with *T* increasing rapidly during the early years of stand development, from 1 to 4YO in our sites, followed by a sharp decline after reaching maximum *T* rates, estimated at four years since plantation establishment in this study. These results strongly align with previous studies on eucalyptus plantations at similar densities that, depending on the age range studied, have seen an increase in the first years, followed by a decline in stand *T* (Almeida et al. 2007a, Dunn and Connor 1993, Dye 1996, Engel et al. 2005, Forrester et al. 2010, Liu et al. 2017).

Sensitivity of eucalyptus plantations to environmental stress

Our second hypothesis stated that older plantations (>4YO) would be less susceptible to environmental changes and show a larger buffering capacity, as reflected in a lower hysteresis area for *VPD* and PAR (H_{VPD} and H_{PAR}), and inflection points of F_d ($\boldsymbol{IP_{VPD}}$) at higher *VPD* and PAR ($\boldsymbol{IP_{PAR}}$) at lower soil saturations (*S*), compared to younger sites (1YO, 1YOHD). In our study, we observed that the initial F_d -*VPD* rate change was linear at low *VPD* (approximately 1.8 kPa), which is consistent with findings from previous studies on diverse tree species (Kostner et al. 2002, Ma et al. 2017, Wang et al. 2005). According to our results, most inflection points

occurred after this linear relationship, between a *VPD* of approximately 1.5-2.4 kPa. IP_{VPD} were higher on average in the 1YOHD stand (2.18 kPa), followed by the 10YO, 1YO and 4YO stands (average: 2.12, 2.0, and 1.93 kPa, respectively). This pattern, however, may be attributed to a more opportunistic water use behavior of the 1YOHD site, which increased significantly its IP_{VPD} at high *S*, resulting in a higher overall average. While differences among sites were expected due to differences in LAI and rooting depth, inflection points among sites were very similar in November (1.85 kPa ± 0.11). This low variability in IP_{VPD} can be attributed to high precipitation registered in November, which resulted in similar *S* across sites (Figure IV-1). Considering that *VPD*, PAR, and *S* did not vary significantly across the study sites in November, these results strongly suggest that under similar environmental conditions, *E. grandis* trees of different sizes and ages exhibit similar threshold responses to *VPD*, regardless of their differences in F_d, which at times differed by up to 400% within sites. While our study was not designed to allow for analysis of inflection points by tree size, differences in hydraulic properties (i.e., P50: where 50 percent of the conductivity has been lost) by stem size have been observed for cavitation curves of various species including eucalyptus trees (Meinzer et al. 2009, Wheeler et al. 2013). The greatest difference in IP_{VPD} was observed in the months of March and April 2015, which was primarily the result of the differences observed among sites (10YO=2.35, 4YO=1.8, 1YO=1.67, and 1YODH=1.65 kPa), in particular, to the reduction of inflection points in the young stands, which seemed to respond most strongly to reductions in *S*. This response was reflected in our results for stand transpiration, where *S* in the top 40 cm was found to exert a significant control across all stands (Table IV-6).

Recent studies have observed that repetitive exposure to hydrologic stress induces a memory effect on the regulatory functions of guard cells (Virlouvet et al. 2018, Virlouvet and Fromm 2015), and that this effect remains active even after the stress is eliminated. These results

may can help explain the degree of variability in inflection points observed in this study, since younger trees, which presumably have not experienced as much hydrologic stress previously, may have a weaker memory system compared to older trees, potentially leading to greater increases in F_d rates when water was available. Conversely, the 10YO stand, which potentially had a better developed memory system due to its age and greater exposure to seasonal drought, did not increase F_d in response to water availability.

In our sites, low *S* reduced inflection points in all stands (Appendix IV-IV), and while these inflection points were not statistically different, there was a clear trend that supports what previous studies have found regarding the strong regulatory mechanisms for *E. grandis* hybrids (Soares and Almeida 2001). Overall, in mature *E. grandis* plantations, studies have found that daily maximum stomatal conductance decreases significantly when pre-dawn leaf water potential becomes more negative, supporting a strong stomatal regulation of mature *E. grandis* trees when soil water is limiting (Almeida and Soares 2003, Soares and Almeida 2001). However, comparisons of IP_{VPD} with other studies are difficult because they are not commonly reported in the literature.

Similar to what has been observed in other studies, PAR peaked before *VPD*, on average two hours earlier considering the entire dataset (data not shown). Compared to IP_{VPD}, IP_{PAR} did not result in significant stagnation or reductions in F_d. At the leaf level, increments in blue light trigger proton pumps in guard cells, which induce stomatal opening, however, while light saturation can be achieved in the early hours of the morning, light saturation primarily limits CO_2 uptake, and typically does not limit transpiration (Buckley 2005, Quinones et al. 1996, Zeiger 2000, Zhu et al. 1995). A cross-site comparison showed that the 10YO site was the least responsive to PAR and did not reveal any inflection points during most of the monitoring period (Figure IV-8). An initial explanation for this pattern could be rooting depth (Duursma et al. 2011,

Fan et al. 2017, Laclau et al. 2001) and access to soil water, which could limit stomatal closure if trees had access to a stable water source. However, considering that the 10YO stand was not the wettest (based on *S* in the first 100 cm. Figure IV-1, Figure IV-2), and that it showed relatively small IP_{VPD}, the observed patterns contradict the expected behavior for this stand (i.e., larger IP_{VPD} and IP_{PAR}). A more likely explanation are changes in leaf morphology and anatomy. England and Attiwill (2005) observed a significant reduction in leaf width and area in *E. regnans* associated with age. In their study, as trees aged, leaf area reduced, and a stronger expression of xeromorphic traits (e.g., increased presence of cuticular waxes) was observed. Battie-Laclau (2014) observed similar patterns in two-year-old *E. grandis* trees in a nutrient amendments study in Brazil. Such anatomical adaptations, specifically the reduction in leaf size, can significantly lower the total area exposed to incoming radiation, effectively lowering the need for transpiration as a cooling mechanism. Additionally, the patterns observed of whole-tree water use (see previous Discussion section), fully align with these changes in leaf morphology and anatomy.

Hysteresis areas for VPD and PAR

In our sites, the PAR-*VPD* rate-change was higher (i.e., PAR increased faster than *VPD*) early in the morning when *VPD* was increasing, and similar high rate-changes were observed during the period of declining *VPD* in the afternoon, which resulted in an anticlockwise hysteresis loop. This anticlockwise pattern is typically observed when a variable that has a delayed, but direct effect on another one (e.g., PAR and *VPD*) is plotted as a dependent variable (x axis) binned by time increments.

As shown in Figure IV-9, there was a clear difference in the H_{VPD} by site and by *S*. Considering that the area of the hysteresis curve reflects the degree of resistance between the dependent (F_d) and the independent variables (*VPD* or PAR) (Everett and Smith 1954, Haines

1930, Klomkliang et al. 2014, Pavlakis and Barden 1972), the overall lower hysteresis areas observed in the 10YO site indicates that this site was under lower stress, compared to the other sites. Additionally, the 10YO stand had the lowest overall variability of H_{VPD} area at different S, and the hysteresis area at low S was statistically smaller than for the other stands. These results suggest that the 10YO trees had adaptations or regulating mechanisms that allowed them to reduce resistance to F_d despite limited soil water availability, while maintaining constant F_d rates. Increased rooting depth providing access to deeper water sources is a known factor that can limit stomatal closure (Pereira et al. 1992), thereby reducing the stress to sap flow and reducing the hysteresis areas. However, as discussed in the previous section, the soil in the 10YO stand was at times drier than the other sites in the top 100 cm, and thus a higher hysteresis area would be expected. While access to deeper soil depths where soil moisture is higher is currently unaccounted for, because we only measured soil moisture within the first 100 cm of soil, this was not reflected in our measurements of whole-tree water use (Figure IV-3), where we observed that 10YO trees had a lower whole-tree water use, compared to trees in the younger stands. Additionally, it was observed that after precipitation events, younger stands showed an increment in transpiration rates and reductions in H_{VPD}, but the 10YO site only reduced its H_{VPD} without increasing F_d rates. In terms of water use efficiency between 10YO and other sites, our results are in accordance to what it was observed by Otto et al. (2014), where they observed that in terms of biomass productivity, mature trees had a higher water use efficiency, compared to young trees.

Considering that IP_{VPD} occurred at higher VPD in the 10YO stand than in the other stands, a simple stomatal closure mechanism to reduce resistance to F_d in mature trees seems to insufficiently explain the patterns observed. In this particular case, the memory effect of guard cells described in the previous section (Virlouvet et al. 2018, Virlouvet and Fromm 2015), which

involves a higher expression of ABA rate-limiting genes, seems to better explain both patterns of IP_{VPD} and $H_{VPD.}$ The presence of such a memory effect combined with documented changes in leaf anatomy and leaf morphology in *Eucalyptus* trees, can result in overall reductions in the resistance to sap flow, which in turn will result in stable H_{VPD} and H_{PAR} when reductions in S combined with high VPD occur.

Further exploration of our data showed that H_{PAR} had a butterfly pattern at low S (Figure IV-10). Hysteresis curves with a butterfly pattern have been observed in several studies (Brum et al. 2018, Ewers et al. 2002, Ma et al. 2017, Zeppel et al. 2004), which can be explained in part, by the shifting nature of the factors that drive stomatal closure. In studies of flow through porous medium and general studies of hysteresis, the lines resulting from the partial influence, or a shift or interruption in the variables driving the response of the curve, are known as "scanning curves" (Everett and Smith 1954, Haines 1930, Klomkliang et al. 2014, Pavlakis and Barden 1972, Staple 1965, Zeng et al. 2016), which are commonly created in studies of pore structure (Klomkliang et al. 2014, Zeng et al. 2016), by inverting or modifying the water or vapor content of the pores. The butterfly pattern observed for H_{PAR}, can be explained considering both the patterns of IP_{VPD} and H_{VPD}. First, as shown in Appendix IV-IV, inflection points for VPD resulted in significant reductions in F_d in all stands except the 10YO stand. This pattern is also evident in Figure IV-9, where we show that F_d inflection points occurred before VPD reached maximum values, with the exception of the 10YO stand, which did not show an inflection point and maintained a reduced H_{VPD}. This reduction in F_d resulting from an increase in the resistance to water flow through the sapwood due to limiting soil moisture, interrupted the expected H_{VPD} loop, and lowered the expected maximum point of the H_{VPD} loop. In the absence of environmental factors inducing inflection points, the hysteresis loop will follow the outer margins of a loop that defines that system. But when one variable experiences constraints and

releases, resulting in one or multiple scanning curves, hysteresis loops will present the *butterfly* pattern which can have more than one loop. Since soil moisture is unlikely to change significantly enough multiple times in one day to produce multiple scanning curves, solar radiation or PAR likely play the major driving force in creating these additional loops.

In conclusion for out second hypothesis, our results indicate that mature *E. grandis* trees develop regulatory mechanisms that allow them to reduce transpiration rates, that seems to be active not only when soil moisture is limiting, but also when soil water is plentiful. Our initial hypothesis was that sensitivity to environmental changes, such as high *VPD* and low *S*, would decline with plantation age, and while we expected both 4YO and 10YO to show such lower sensitivity, we only saw this pattern in 10YO trees. Considering these results and the current evidence, we conclude that there is partial evidence to support our hypothesis, and emphasize the need for more long-term monitoring to better understand the effect of plantation age on water use patterns in response to environmental change. At the same time, our results suggest that it takes more than four years for the regulatory mechanism to have measurable effects.

Implications for management

Approximately 70% of the total area planted with *E. grandis* in Argentina is located in the Province of Entre Rios (SAGPYA 2001), with a high concentration of plantations on the West side of the Uruguay River. However, the demand for whole biomass for bioenergy from this or other tree species is very low, compared with other biomass sources such as sugar cane, corn, and other grains (Goldstein and Gutman 2010, Rozenberg et al. 2009, van Dam et al. 2009). Most of timber production is currently used in industry for packing, particle boards and housing (e.g., flooring, frames, etc.) (Sanchez Acosta 2012). Consequently, intensive short (<2YO) rotations of *E. grandis* for biomass or bioenergy purposes are unlikely to occupy large

areas in the region. However, there is a strong potential to modify management practices to use eucalyptus plantations as providers for environmental services, specifically to help mitigate flooding or river overflows. In this study, increasing plantation density in 1YO plantations increased their cumulative stand level water use by 34% (~80 mm). Additionally, 1YO high-density plantations seem to be more responsive to precipitation inputs during both the wet and the dry season, reflected in their increased *T* after each precipitation event. This response pattern was also observed in the 1YO site, but the increase in *T* was higher in the high-density plantation (Figure IV-6).

The area of Entre Rios, is highly sensitive to flooding, in part due to its location (Ulla 2015), and many argue that flooding events in 2015 were primarily influenced by El Niño. Despite this, evidence suggests that planning and preparedness has not been efficiently implemented. As a result, on December 27, 2015 the government announced long-term plans to build two aqueducts in Concordia, Entre Rios. While it is known that trees have a limited control on major environmental events such as river overflows, or major rainfall events, they have a strong potential to increase soil infiltration and reduce runoff (Bronstert and Kundzewicz 2006, Calder and Aylward 2006). Engineering projects focused on flood control have a higher impact when they are accompanied by watershed and land-use management practices (Calder and Aylward 2006). Our analysis of *S* in the first 100 cm of soil indicates that there is a higher potential for infiltration under plantations, than in soils covered by pasture in both the wet and the dry seasons, and that this infiltration potential increases in high-density plantations (Figure IV-4, Figure IV-5).

We acknowledge that a simplistic afforestation program is not the only solution to reduce runoff or to reduce soil erosion risk during mild or moderate precipitation events. However, the current demand for *E. grandis* timber (and other species) (Bouza et al. 2016, Sanchez Acosta

2012, Winck et al. 2015) offers the opportunity to implement management alternatives aimed to produce timber in the long-term, while increasing the soil infiltration capacity in the short term. Due to the fast peaks in stand *T*, *E. grandis* plantations can be established at high densities, to promote soil infiltration in the first year or two. Since LAI and *T* are directly related, if high *T* rates are no longer desired in one site, thinning or pruning can directly reduce *T*, thus allowing more water to remain in the soil. Forrester et al. (2013) conducted a pruning/thinning experiment om *E. nitens* and found that while pruning removed 75% of the leaf area, biomass productivity decreased only 12%. Unlike *Pinus* trees, where a removal of only 20% of the leaf area can significantly reduce growth rates, *E. grandis* increase their light absorption efficiency (Forrester 2013). These observations are consistent with our results. As seen in Figure IV-8, unlike *VPD*, increments in PAR did not seem to result in significant reductions in tree *Q*. Further, the relationship between PAR and *Q* were nearly linear in the 10YO site, where LAI has been reduced through management, compared to other sites.

Conclusion

Our results indicate that sap flux density and stand-level *T* increased from 1 to 4YO, to later decrease from 4 and 10YO. Whole tree average daily water use rates were higher in at 4 years and significantly lower at 10 years, which coincides with previous studies on this species. Changes in water availability in the soil seem to influence strongly how F_d and *Q* responded to *VPD*, but not to PAR, and the 10YO site did not seem influenced significantly by *VPD*, PAR or changes in *S*, as reflected by both inflection points and hysteresis areas, suggesting that old trees have better mechanisms to cope with environmental stress, unlike young (1-4 year-old) plantations. Cumulative water use indicates that 1YO high-density plantations use 34% more

water plantations the same age at regular densities (146 mm y^{-1}), conversely, *T* in the 10YO was 25% lower than the 1YO site.

Figures and Tables

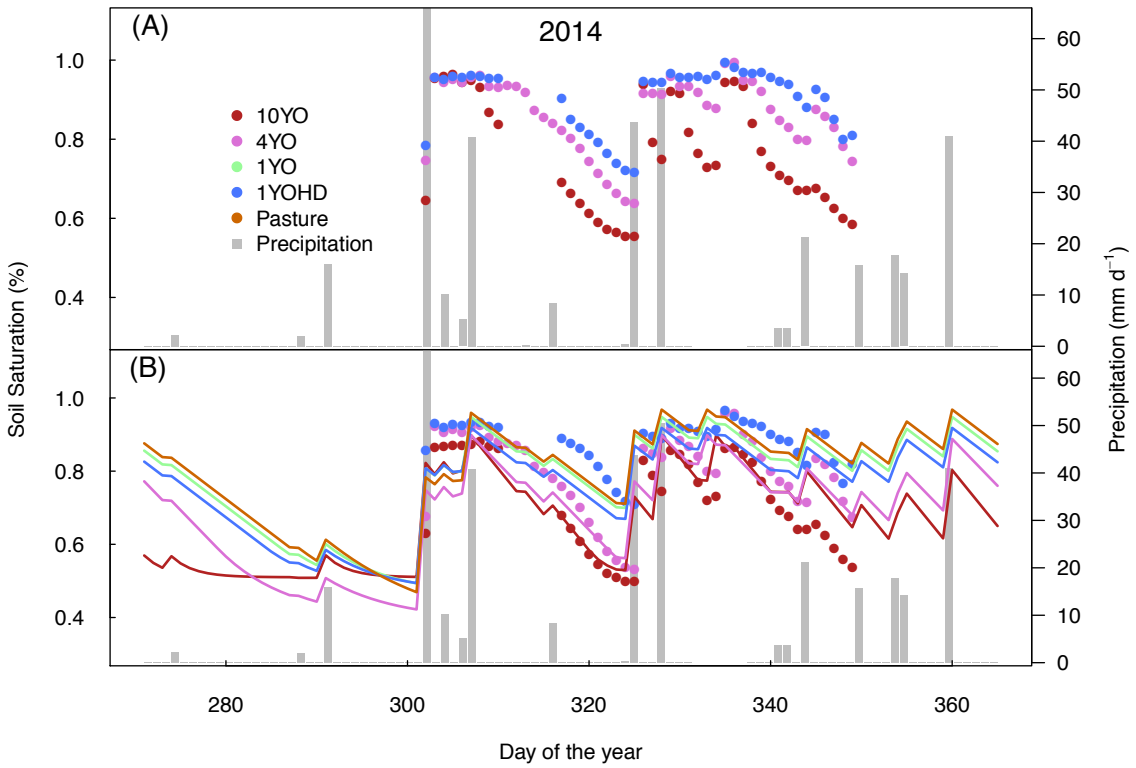

Figure IV-1 Soil saturation by site, 2014. A: soil saturation estimated for the first 100 cm of soil profile. B: Soil saturation estimated for the first 40 cm of soil. Solid lines represent the *S* estimated for each site using the bucket model

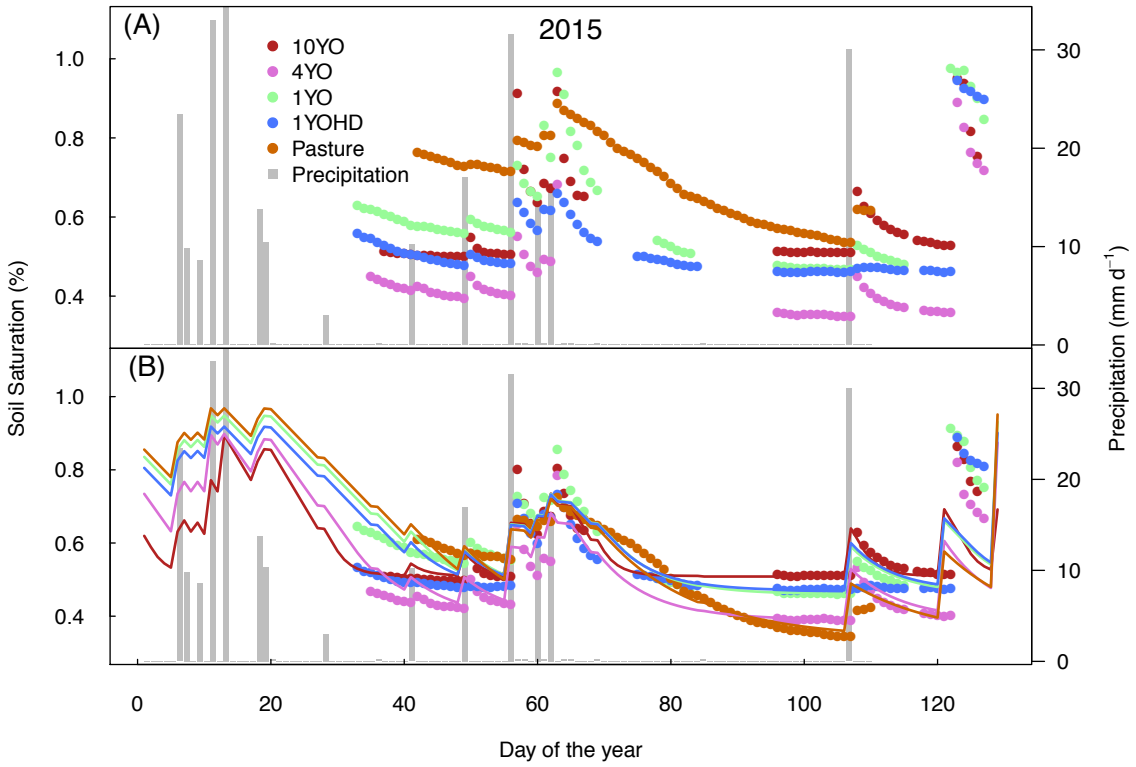

Figure IV-2 Soil saturation by site, 2015. A: soil saturation estimated for the first 100 cm of soil profile. B: Soil saturation estimated for the first 40 cm of soil. Solid lines represent the *S* estimated for each site using the bucket model. Pluviometers were uninstalled on DOY 120

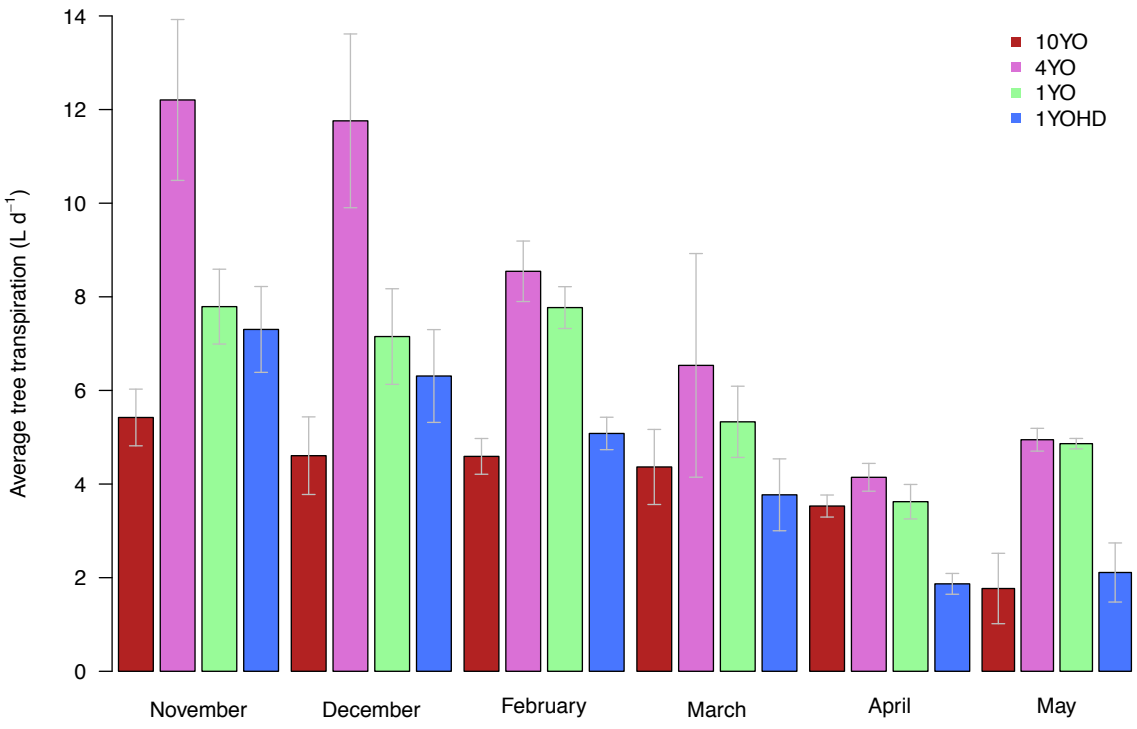

Figure IV-3 Average whole-tree water use by site and month of the year. Error bars = standard error of the mean

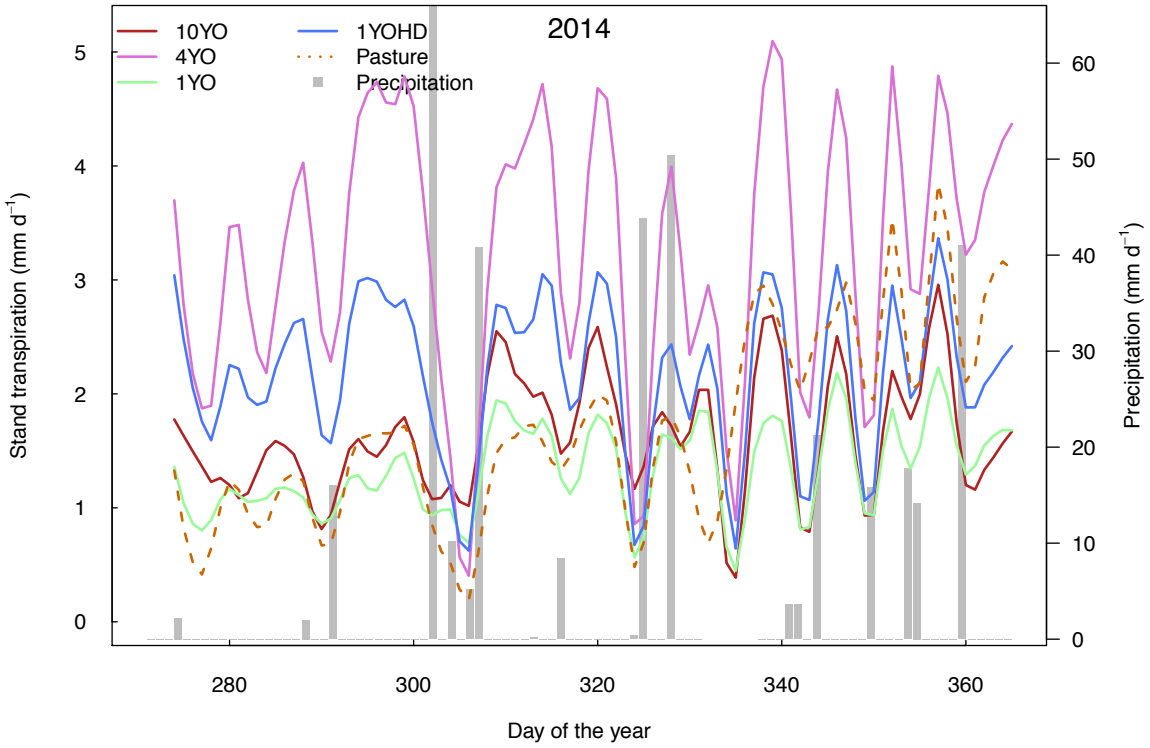

Figure IV-4 Stand transpiration during the wet season in four bioenergy plantations in Argentina
No precipitation data on DOY 334 due to equipment failure

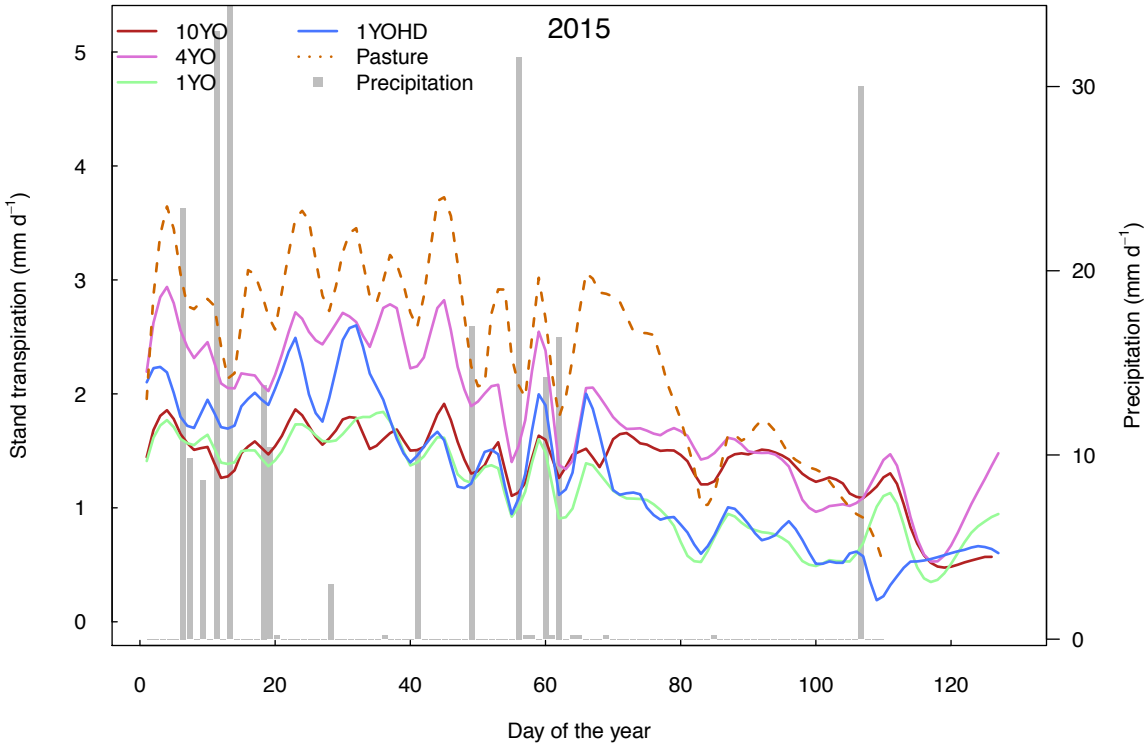

Figure IV-5 Stand transpiration during the dry season in four bioenergy plantations in Argentina

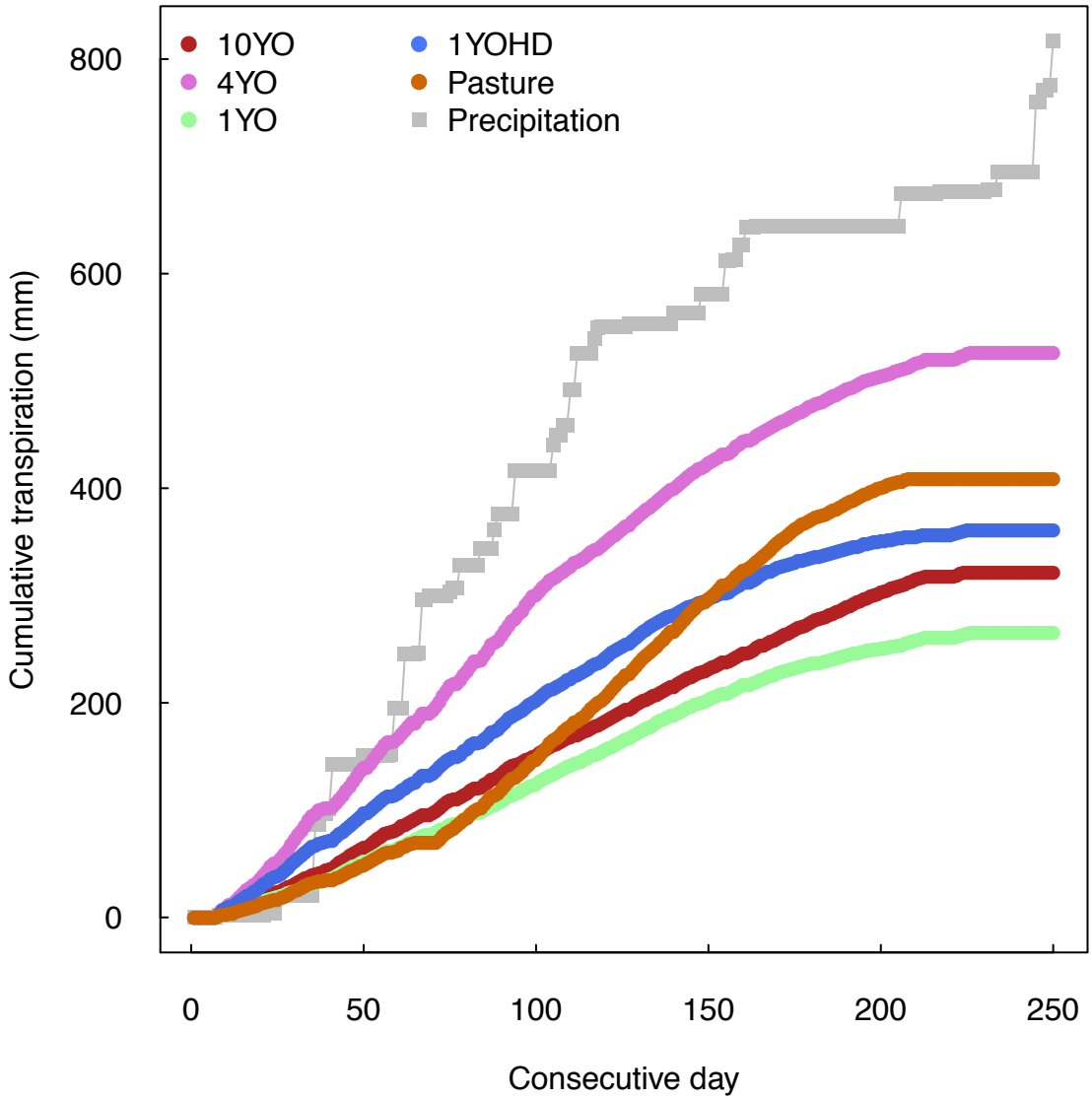

Figure IV-6 Estimated cumulative water use for the entire monitoring period (November 2014-May 2015).

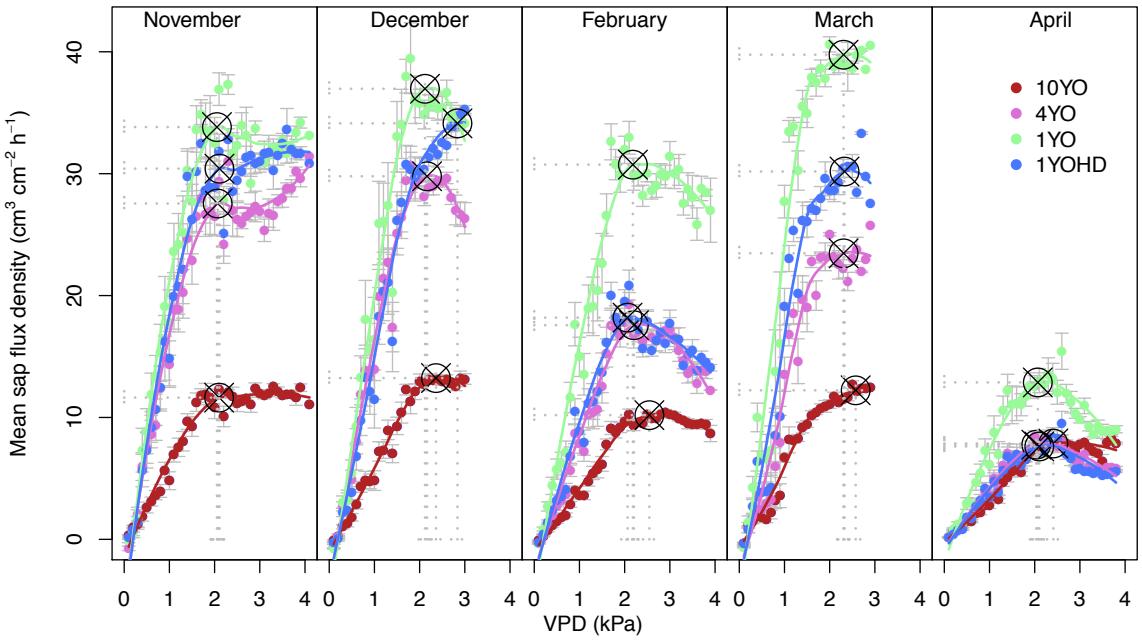

Figure IV-7 Response of average sap flux density per site to *VPD*, at different months of the year (shown at the top of each panel). A Locally Weighted Scatterplot Smoothing Model was fitted to each response curve, and inflection points were estimated along the fitted line before the slope = 0, to allow the detection of inflection points that did not result in F_d -*VPD* response curves with slopes <= 0. Dashed lines show the coordinates of the inflection point (if found), and crossed circle symbols represent the inflection point for each line.

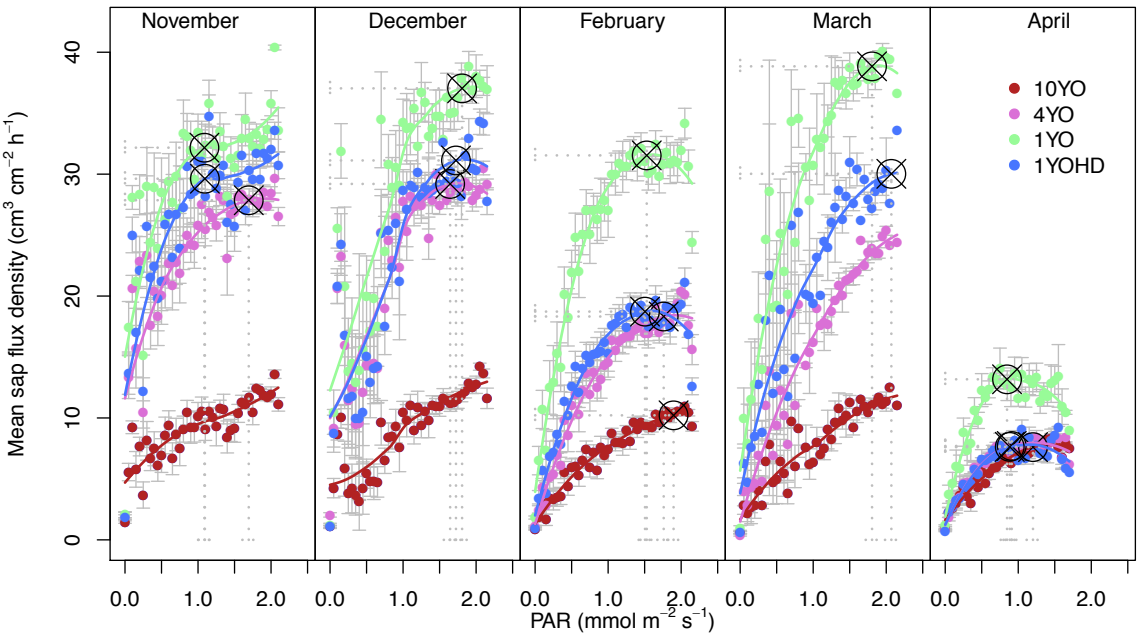

Figure IV-8 Response of average tree-level sap flux density per site, to PAR at different months of the year (shown at the top of each panel). A Locally Weighted Scatterplot Smoothing Model was fitted to each response curve, and inflection points were estimated along the fitted line before the slope = 0, to allow the detection of inflection points that did not result in F_d -*VPD* response curves with slopes <= 0. Dashed lines show the coordinates of the inflection point (if found), and crossed circle symbols represent the inflection point for each line.

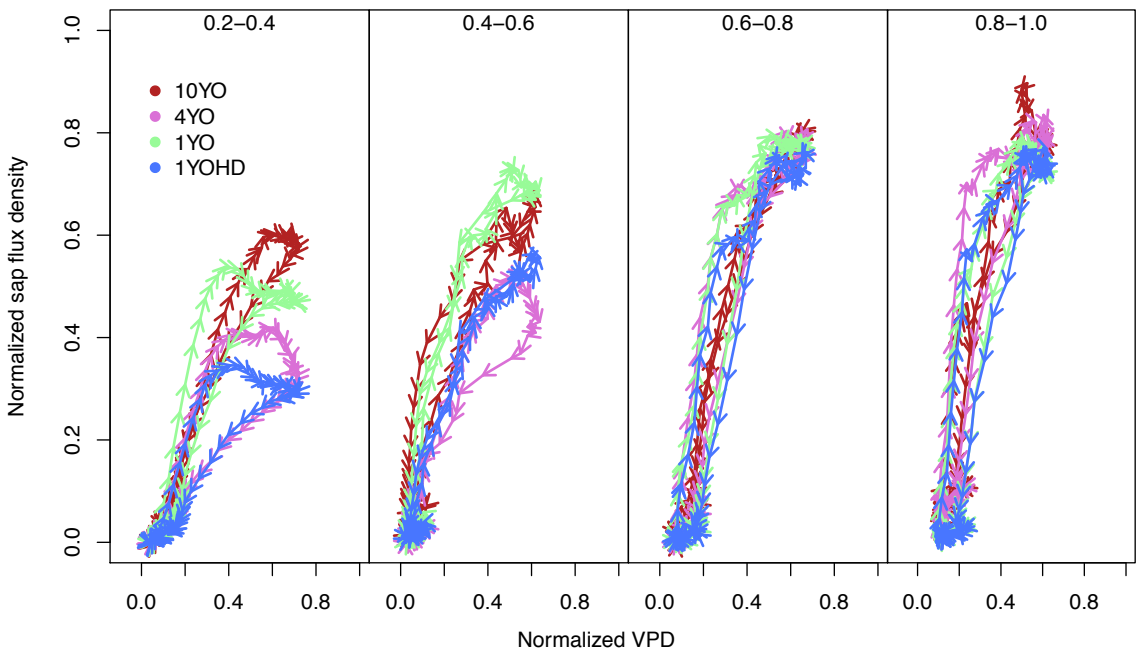

Figure IV-9 Hysteresis response between *VPD* and sap flux density, at different soil saturation ranges (shown at the top of each panel). *VPD* and F_d data were normalized by dividing the value of row *n*, over the maximum value of the corresponding column of *n*. Additionally, data corresponding to days with precipitation events, or with cloud cover were not used in this graph. Arrows represent the direction response of F_d to *VPD* (primarily clockwise).

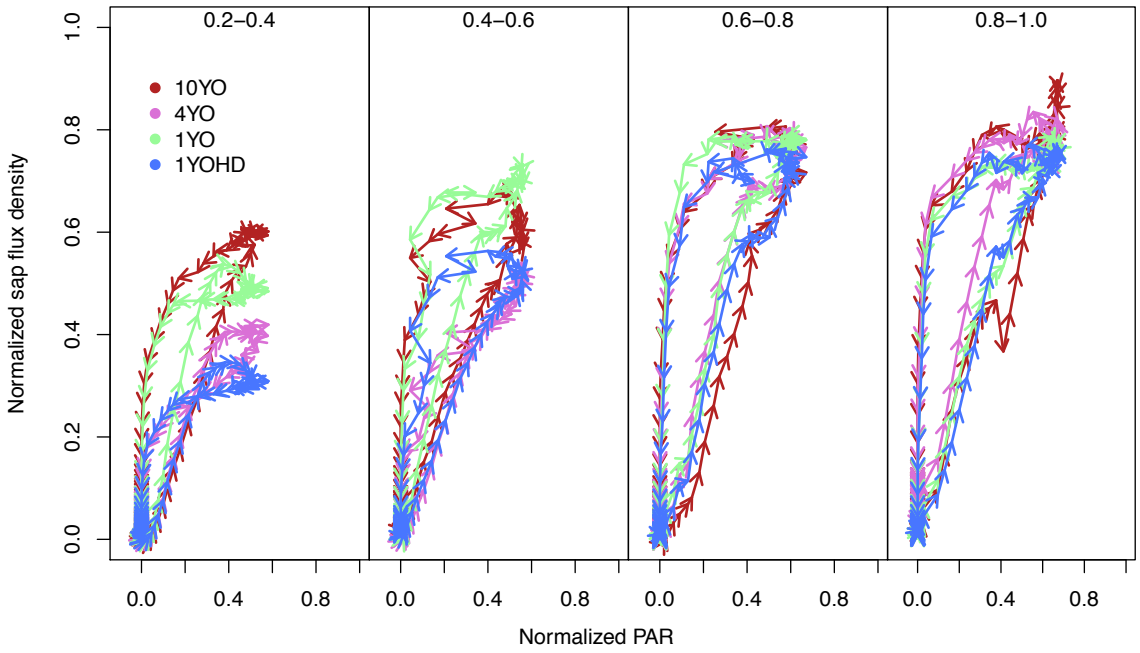

Figure IV-10 Hysteresis response between F_d and PAR, at different soil saturation ranges (shown at the top of each panel). PAR and F_d data were normalized by dividing the value of row n, over the maximum value of the corresponding column of n. Additionally, data corresponding to days with precipitation events, or with cloud cover were not used in this graph. Arrows represent the direction response of F_d to PAR (primarily anti-clockwise).

Table IV-1 Soil properties by site (from Cisz-Brill et al.)

Site	Depth (cm)	Bulk density (g cm^3)	Porosity (%)	Sand (%)	Clay (%)	Silt (%)
10YO	0-15	1.26	52.36	0.76	0.09	0.15
	15-30	1.53	42.29	0.76	0.09	0.15
	30-45	1.58	40.47	0.66	0.20	0.14
	45-60	1.63	38.51	0.66	0.20	0.14
4YO	0-15	1.43	45.93	0.80	0.08	0.13
	15-30	1.50	43.56	0.80	0.08	0.13
	30-45	1.56	41.02	0.71	0.17	0.12
	45-60	1.66	37.49	0.71	0.17	0.12
1YO	0-15	1.55	41.62	0.71	0.12	0.17
	15-30	1.63	38.34	0.71	0.12	0.17
	30-45	1.64	38.12	0.61	0.22	0.16
	45-60	1.65	37.76	0.61	0.22	0.16
1YOHD	0-15	1.55	41.62	0.71	0.12	0.17
	15-30	1.63	38.34	0.71	0.12	0.17
	30-45	1.64	38.12	0.61	0.22	0.16
	45-60	1.65	37.76	0.61	0.22	0.16

Table IV-2 Vegetation and soil parameters used to fit the bucket model

Vegetation parameters	10YO	4YO	1YO	1YOHD	Pasture
Depth of Interception	2	2	4	3	2
Maximum E (mm d^{-1})	2	2	2	2	2
Maximum T (mm d^{-1})	5	5	3.6	4	4
Saturation at stomatal closure	0.3	0.3	0.3	0.3	0.3
Saturation at wilting point	0.205	0.205	0.205	0.23	0.16
Root depth (cm)	40	40	40	40	40
Soil parameters					
Porosity (n)	0.45	0.4	0.45	0.45	0.45
Saturated Conductivity E (mm d^{-1})	200	200	200	200	200
Hygroscopic saturation	0.02	0.02	0.02	0.02	0.02
Field Capacity	0.3	0.3	0.3	0.3	0.3
Drainage Curve Parameter	9	9	9	9	9

Table IV-3 Stand characteristics

Site	**Actual density (trees ha^{-1})**	**Mortality rate (%)**	**Average diameter (cm)**	**Average sapwood area* (m^2)**	**Average basal area (m^2)**	**Average height (m)**	**Subsample N**
10YO	1118	7%	18.2	0.0127 (±0.0036)	0.0272 (±0.0123)	17.5	68
4YO	1386	40%	14.7	0.0099 (±0.0015)	0.0175 (±0.0070)	15	70
1YO	1380	25%	5.71	0.0027 (±0.0013)	0.0027 (±0.0013)	6.01	56
1YO-HD	3112	24%	4.35	0.0017 (±0.0010)	0.0017 (±0.0011)	5.29	91

*Average sapwood area per tree, using N trees of the subsample

Table IV-4 Parameters and allometric equations adjusted for each site to predict sapwood area with tree diameter

Site	β_0	β_1	StErr - β_0	StErr - β_1	RMSE	*R^2
10YO	-8.1033	1.2854	0.5570	0.1812	0.0021	0.88
4YO	-6.6478	0.7610	0.2763	0.1004	0.0006	0.92
1YO	-9.4789	2.0090	0.0233	0.0111	0.0000	1
1YOHD	-9.0174	1.7342	0.1902	0.0872	0.0003	0.98
Mature	-7.8337	1.1946	0.3638	0.1218	0.0018	0.86
Young	-8.9164	1.7143	0.1857	0.0871	0.0003	0.96
All	-7.8786	1.2104	0.1649	0.0570	0.0012	0.94

Table IV-5 Corrected Akaike and Bayesian information criterion for each of the models tested by site.

Site	Fixed effects	- 2 log likelihood	AICc	BIC
10YO	*AirT*, *RH*, *NetRad*, *VPD*, *ET_0*, *WindS*, *pp*, *S*	-6.4	21.1	38.6
	AirT, *RH*, *NetRad*, *VPD*, *ET_0*, *WindS*, *pp*	3.4	27.8	44.5
	ET_0, *PAR*, NetRad	7.3	20.9	32.0
4YO	*AirT*, *RH*, *NetRad*, *VPD*, *ET_0*, *WindS*, *pp*, *S*	112.7	139.8	158.4
	AirT, *RH*, *NetRad*, *VPD*, *ET_0*, *WindS*, *pp*	127.2	151.3	168.8
	ET_0, *PAR*, NetRad	130.3	143.8	155.2
1YO	*AirT*, *RH*, *NetRad*, *VPD*, *ET_0*, *WindS*, *pp*, *S*	22.2	50.4	158.4
	AirT, *RH*, *NetRad*, *VPD*, *ET_0*, *WindS*, *pp*	26.5	49.7	70.3
	ET0, PAR, NetRad	55.0	68.1	81.3
1YOHD	*AirT*, *RH*, *NetRad*, *VPD*, *ET_0*, *WindS*, *pp*, *S*	83.0	109.4	130.1
	AirT, *RH*, *NetRad*, *VPD*, *ET_0*, *WindS*, *pp*	107.1	130.5	150.4
	ET0, PAR, NetRad	110.3	123.5	136.3

Table IV-6 Summary of the fixed effects tests for the linear mixed model run for each site. For each site, the response variable was site *T*, the fixed effects the environmental variables (Source), and to account for changes overtime, DOY was considered the random variable

Source	10YO		4YO		1YO		1YOHD	
	F Ratio	Prob > F	F Ratio	Prob > F	F Ratio	Prob > F	F Ratio	Prob > F
ET_0	0.2	0.7	4.7	0.0316*	1.7	0.2	9.6	0.0023*
AirT	24.2	<.0001*	6.6	0.0112*	2.3	0.1	6.5	0.0118*
RH	2.7	0.1	15.4	0.0001*	0.2	0.7	26.3	<.0001*
PAR	68.2	<.0001*	0.1	0.7	43.8	<.0001*	0.6	0.5
VPD	0.2	0.7	10.6	0.0013*	3.4	0.1	20.8	<.0001*
pp	7.2	0.0082*	0.1	0.8	5.6	0.0192*	1.1	0.3
NetRad	6.3	0.0130*	0.8	0.4	8.4	0.0042*	0.6	0.4
S40	14.2	0.0002*	10.2	0.0017*	14.9	0.0002*	32.3	<.0001*

Table IV-7 Summary of the effects of environmental variables on daily maximum F_d (11AM-5PM)

	Source	10YO		4YO		1YO		1YOHD	
		F Ratio	Prob > F	F Ratio	Prob > F	F Ratio	Prob > F	F Ratio	Prob > F
All	*ET₀*	6.6	0.0102*	5.5	0.0187*	0.7	0.4	2.4	0.1
	AirT	167.2	<.0001*	288.0	<.0001*	102.9	<.0001*	240.5	<.0001*
	RH	370.0	<.0001*	349.6	<.0001*	130.4	<.0001*	303.3	<.0001*
	PAR	1.1	0.3	18.1	<.0001*	2.2	0.1	1.3	0.3
	VPD	222.9	<.0001*	335.5	<.0001*	172.4	<.0001*	269.5	<.0001*
	pp	2.9	0.1	0.1	0.8	3.0	0.1	0.2	0.7
	NetRad	7.3	0.0071*	0.8	0.4	1.8	0.2	4.3	0.0393*
	S	2.2	0.1	3.9	0.1	1.5	0.2	3.9	0.1
No S	*ET₀*	56.9	<.0001*	33.1	<.0001*	10.4	0.0013*	0.0	0.9
	AirT	327.2	<.0001*	484.0	<.0001*	649.9	<.0001*	441.8	<.0001*
	RH	643.3	<.0001*	638.0	<.0001*	1003.6	<.0001*	707.3	<.0001*
	PAR	0.0	0.9	91.2	<.0001*	0.6	0.4	8.0	0.0046*
	VPD	552.0	<.0001*	786.7	<.0001*	1066.4	<.0001*	765.5	<.0001*
	pp	6.6	0.0103*	0.9	0.4	0.1	0.8	1.5	0.2
	NetRad	54.9	<.0001*	7.1	0.0077*	15.4	<.0001*	1.0	0.3

Appendices

Appendix IV-I Steps to estimate bucket model components

The first parameter in the bucket model is infiltration, which is calculated based on the current *S*, and the depth of precipitation as:

$$I'(S(t_{\bar{i}}), t_i) = \min\left[P(t_i), nZr(1 - S(t_{\bar{i}}))\right] \qquad \text{Eq. IV-10}$$

Where $I'(S(t_i), t_i)$ is the infiltration at t_i, at a saturation $t_{i^\wedge}$, *min* the minimum value between [,], $P(t_i)$ depth of net precipitation, *nZr* soil depth of porosity *n*, and $S(t_{i^\wedge})$ the saturation before $t_{i^\wedge}$

When saturation is higher than field capacity (S_{fc}), in the absence of soil evaporation or any additional precipitation is converted to leakage using:

$$L(S) = K_{sat}\frac{e^{\beta(S - S_{fcs})-1}}{e^{\beta(1 - S_{fcs})-1}} \qquad \text{Eq. IV-11}$$

Where $L(s)$ leakage at a saturation *S*, K_{sat} saturated conductivity, β is an infiltration soil parameter and S_{fc} saturation at field capacity

A nominal value was used for $E(S)$ (see Table III-4), and was adjusted to different *S*, using:

$$E(S) = \begin{Bmatrix} 0 & S < S_h \\ \frac{S - S_h}{S^* - S_h}E & S_h < S < S^* \\ E & S \geq S^* \end{Bmatrix} \qquad \text{Eq. IV-12}$$

Where S_h is the hygroscopic saturation, S^* the saturation at stomatal closure, *E* the maximum evaporation from the soil

The maximum transpiration estimated early in the monitoring period was used for $T(S)$. Similarly to $E(S)$, *T* was adjusted to different *S*, considering that *T* is directly influenced by water availability.

$$T(S) = \begin{Bmatrix} 0 & S < S_w \\ \frac{S - S_w}{S^* - S_w}T & S_w < S < S^* \\ T & S \geq S^* \end{Bmatrix} \qquad \text{Eq. IV-13}$$

Where *T(s)* is the transpiration at saturation *S*, S_w the saturation at wilting point, S^* the saturation at stomatal closure, and *T* the maximum transpiration per site.

Appendix IV-II Linear regression between observed and estimated *T* for each site. The dashed line represents a 1:1 relationship, and the solid line the linear regression (R^2=94) combining observed and predicted for all sites. In Table III-5 we show the variables used in the linear mixed model, and the AICc and BIC corresponding to each model.

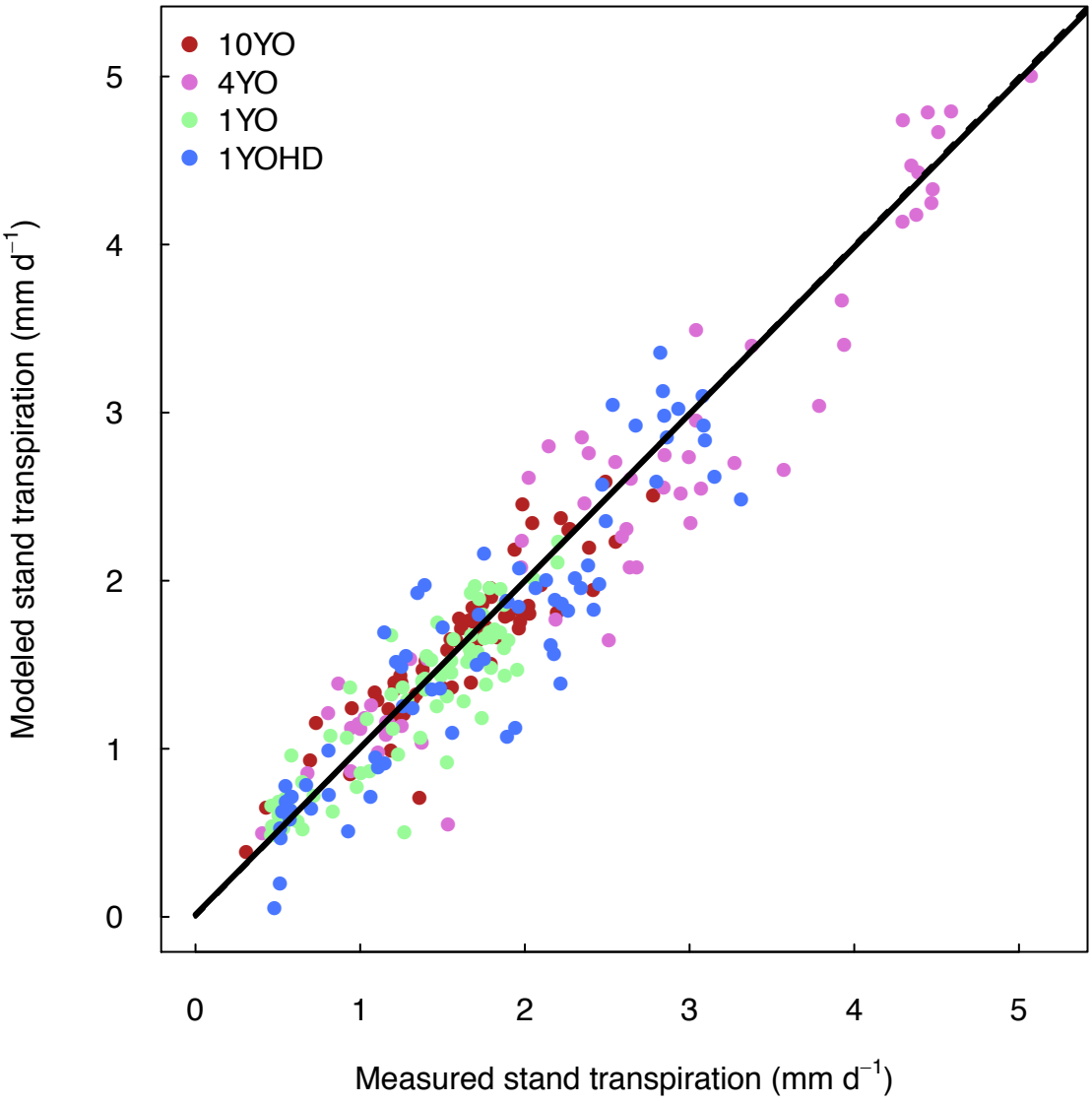

Appendix IV-III Relationship between diameter and estimated sapwood area (m^2). The grey line represents the equation fitted to all the data (R^2 = 0.94, RMSE = 0.0012). In Table IV-4, we show the parameters adjusted for each site. Additionally, we merged data from both one-year-old sites, and data from 4YO and 10YO, to increase the predictability of the model.

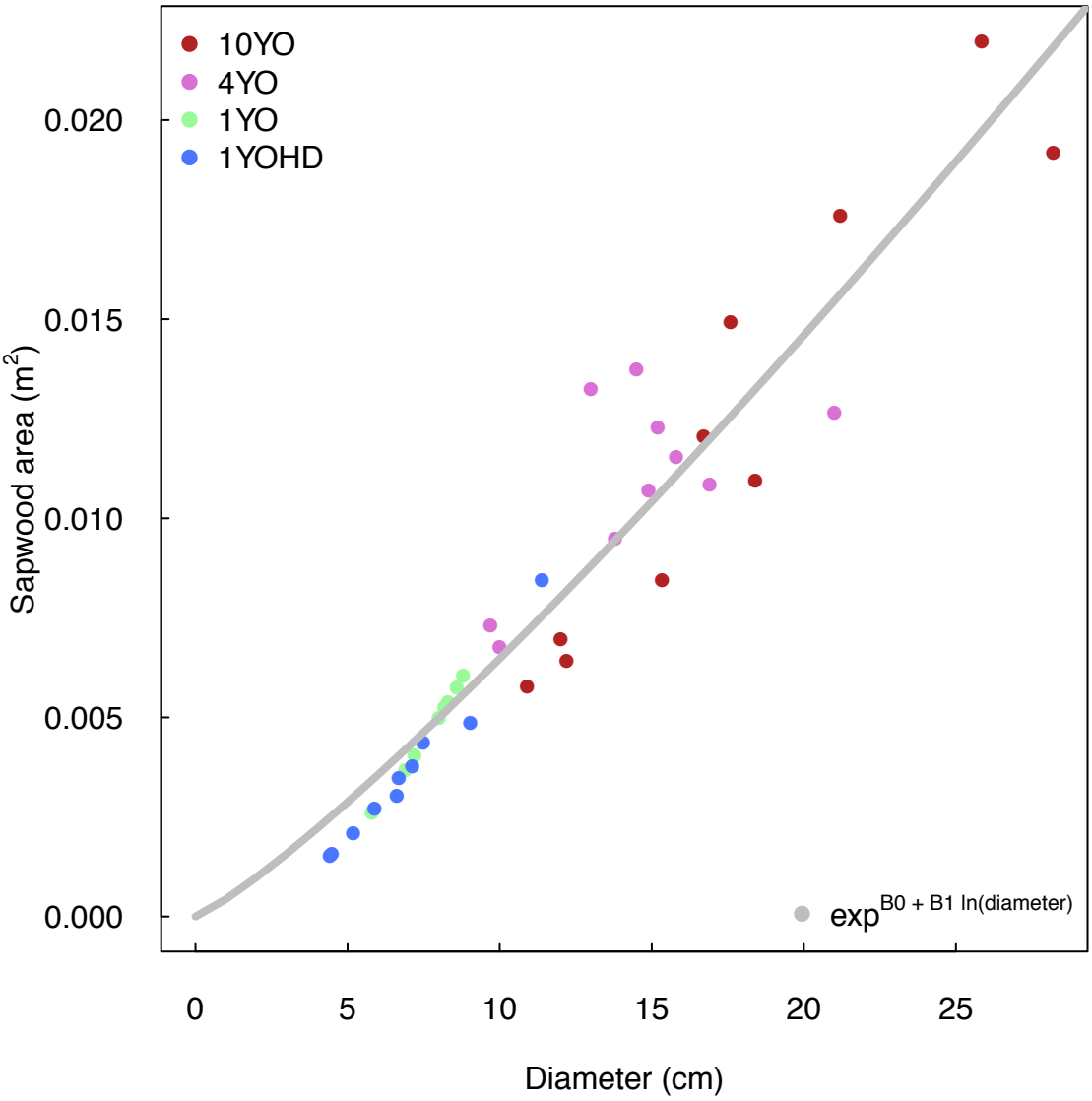

Appendix IV-IV Sap flux density response curves to *VPD* at different soil saturations (shown in the top of each panel). A Locally Weighted Scatterplot Smoothing Model was fitted to each response curve, and inflection points were estimated along the fitted line before the slope = 0, to allow the detection of inflection points that did not result in F_d -*VPD* response curves with slopes <= 0. Dashed lines show the coordinates of the inflection point (if found), and crossed circle symbols represent the inflection point for each line.

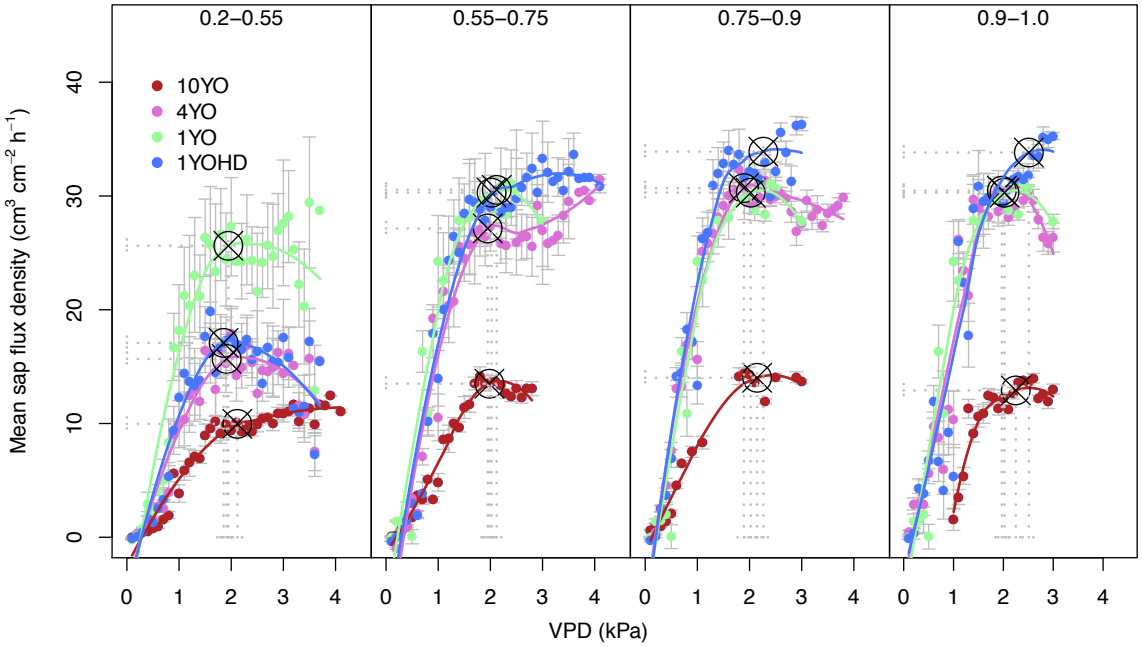

References

Adler, P. B., and J. M. Morales. 1999. Influence of environmental factors and sheep grazing on an Andean grassland. Journal of Range Management **52**:471-481.

Ainsworth, E. A., and A. Rogers. 2007. The response of photosynthesis and stomatal conductance to rising [CO2]: mechanisms and environmental interactions. Plant Cell and Environment **30**:258-270.

Alberto Tasi, H. A. 2009. Aplicación de las cartas de suelos de Entre Ríos, Argentina, para evaluar indices de productividad específicos para los principales cultivos agrícolas. Universidade da Coruña.

Allen, R. G., L. S. Pereira, D. Raes, and M. Smith. 1998. Crop evapotranspiration: guidelines for computing crop water requiriments. Irrigation and drainage paper **56**.

Allen, S. J., R. L. Hall, and P. T. W. Rosier. 1999. Transpiration by two poplar varieties grown as coppice for biomass production. Tree Physiology **19**:493-501.

Almeida, A. C., and J. V. Soares. 2003. Comparação entre uso de água em plantações de Eucalyptus grandis e floresta ombrófila densa (Mata Atlântica) na costa leste do Brasil. Árbore **27**:159-170.

Almeida, A. C., J. V. Soares, J. J. Landsberg, and G. D. Rezende. 2007a. Growth and water balance of Eucalyptus grandis hybrid plantations in Brazil during a rotation for pulp production. Forest Ecology and Management **251**:10-21.

Almeida, A. C., J. V. Soares, J. J. Landsberg, and G. D. Rezende. 2007b. Growth and water balance of Eucalyptus grandis hybrid plantations in Brazil during a rotation for pulp production. Forest Ecology and Management **251**:10-21.

Alsheimer, M., B. Kostner, E. Falge, and J. D. Tenhunen. 1998. Temporal and spatial variation in transpiration of Norway spruce stands within a forested catchment of the Fichtelgebirge, Germany. Annales Des Sciences Forestieres **55**:103-123.

Ares, A., and J. H. Fownes. 2000. Productivity, nutrient and water-use efficiency of Eucalyptus saligna and Toona ciliata in Hawaii. Forest Ecology and Management **139**:227-236.

Battie-Laclau, P., J. P. Laclau, J. C. Domec, et al. 2014. Effects of potassium and sodium supply on drought-adaptive mechanisms in Eucalyptus grandis plantations. New Phytologist **203**:401-413.

Berndes, G. 2008. Water demand for global bioenergy production: trends, risks and opportunities German Advisory Council on Global Change (WBGU), Berlin

Blanken, P. D., T. A. Black, P. C. Yang, et al. 1997. Energy balance and canopy conductance of a boreal aspen forest: Partitioning overstory and understory components. Journal of Geophysical Research-Atmospheres **102**:28915-28927.

Boland, D. J., M. I. H. Brooker, M. W. McDonald, and G. M. Chippendale. 2006. Forest Trees of Australia. CSIRO Publishing

Bouillet, J.-P., J.-P. Laclau, M. Arnaud, et al. 2002. Changes with age in the spatial distribution of roots of Eucalyptus clone in Congo: Impact on water and nutrient uptake. Forest Ecology and Management **171**:43-57.

Bouza, M. E., A. Aranda-Rickert, M. M. Brizuela, et al. 2016. Economics of Land Degradation in Argentina, in E. Nkonya, A. Mirzabaev, and J. von Braun. Ed. Economics of Land Degradation and Improvement – A Global Assessment for Sustainable Development. Springer International Publishing. Cham. 291-326

Braier, G., N. Esper, and L. Corinaldesi. 2004. Tendendias y perspectivas del sector forestal al año 2020. Government Document. Secretaría de ambiente y desarrollo sustentable. Buenos Aires, Argentina

Brando, P. 2018. Tree height matters. Nature Geoscience **11**:390-391.

Brienen, R. J. W., E. Gloor, S. Clerici, et al. 2017. Tree height strongly affects estimates of water-use efficiency responses to climate and CO2 using isotopes. Nature Communications **8**.

Bronstert, A., and Z. W. Kundzewicz. 2006. Discussion of the article: Calder, I. R. & Aylward, B. (2006) Forest and floods: Moving to an evidence-based approach to watershed and integrated flood management. Water international, 31(1) 87-99. Water International **31**:427-431.

Brum, M., J. Gutiérrez López, H. Asbjornsen, et al. 2018. ENSO effects on the transpiration of eastern Amazon trees. Philosophical Transactions of the Royal Society B: Biological Sciences **373**.

Buckley, T. N. 2005. The control of stomata by water balance. New Phytologist **168**:275-291.

Burgess, S. S. O., M. Adams, N. C. Turner, et al. 2001. An improved heat pulse method to measure low and reverse rates of sap flow in woody plants (vol 21, pg 589, 2001). Tree Physiology **21**:1157-1157.

Burke, E. J., S. J. Brown, and N. Christidis. 2006. Modeling the recent evolution of global drought and projections for the twenty-first century with the hadley centre climate model. Journal of Hydrometeorology **7**:1113-1125.

Calder, I. R., and B. Aylward. 2006. Forest and floods: Moving to an evidence-based approach to watershed and integrated flood management. Water International **31**:87-99.

Campoe, O. C., J. L. Stape, J. P. Laclau, et al. 2012. Stand-level patterns of carbon fluxes and partitioning in a Eucalyptus grandis plantation across a gradient of productivity, in Sao Paulo State, Brazil. Tree Physiology **32**:696-706.

Cleveland, W. S. 1981. Lowess - a Program for Smoothing Scatterplots by Robust Locally Weighted Regression. American Statistician **35**:54-54.

Cochard, H., T. Holtta, S. Herbette, et al. 2009. New Insights into the Mechanisms of Water-Stress-Induced Cavitation in Conifers. Plant Physiology **151**:949-954.

Daszkowska-Golec, A., and I. Szarejko. 2013. Open or close the gate - stomata action under the control of phytohormones in drought stress conditions. Frontiers in Plant Science **4**.

Delzon, S., and D. Loustau. 2005. Age-related decline in stand water use: sap flow and transpiration in a pine forest chronosequence. Agricultural and Forest Meteorology **129**:105-119.

Du Toit, B. 2008. Effects of site management on growth, biomass partitioning and light use efficiency in a young stand of Eucalyptus grandis in South Africa. Forest Ecology and Management **255**:2324-2336.

Ducey, M. J. 2018. Design-unbiased point-to-object sampling on lines, with applications to areal sampling. European Journal of Forest Research **137**:367-383.

Dunn, G. M., and D. J. Connor. 1993. An Analysis of Sap Flow in Mountain Ash (Eucalyptus-Regnans) Forests of Different Age. Tree Physiology **13**:321-336.

Duursma, R. A., C. V. M. Barton, D. Eamus, et al. 2011. Rooting depth explains [CO2] × drought interaction in Eucalyptus saligna. Tree Physiology **31**:922-931.

Dye, P. J. 1996. Response of Eucalyptus grandis trees to soil water deficits. Tree Physiology **16**:233-238.

Engel, V., E. G. Jobbagy, M. Stieglitz, et al. 2005. Hydrological consequences of eucalyptus afforestation in the argentine pampas. Water Resources Research **41**.

England, J., and P. Attiwill. 2005. Changes in leaf morphology and anatomy with tree age and height in the broadleaved evergreen species, Eucalyptus regnans F. Muell.79-90

Everett, D. H., and F. W. Smith. 1954. A general approach to hysteresis. Part 2: Development of the domain theory. Transactions of the Faraday Society **50**:187-197.

Ewers, B. E., D. S. Mackay, S. T. Gower, et al. 2002. Tree species effects on stand transpiration in northern Wisconsin. Water Resources Research **38**.

Ewers, B. E., R. Oren, H. S. Kim, et al. 2007. Effects of hydraulic architecture and spatial variation in light on mean stomatal conductance of tree branches and crowns. Plant Cell and Environment **30**:483-496.

Fan, Y., G. Miguez-Macho, E. G. Jobbagy, et al. 2017. Hydrologic regulation of plant rooting depth. Proceedings of the National Academy of Sciences of the United States of America **114**:10572-10577.

Forrester, D. I. 2013. Growth responses to thinning, pruning and fertiliser application in Eucalyptus plantations: A review of their production ecology and interactions. Forest Ecology and Management **310**:336-347.

Forrester, D. I., J. J. Collopy, C. L. Beadle, and T. G. Baker. 2013. Effect of thinning, pruning and nitrogen fertiliser application on light interception and light-use efficiency in a young Eucalyptus nitens plantation. Forest Ecology and Management **288**:21-30.

Forrester, D. I., J. J. Collopy, C. L. Beadle, et al. 2012. Effect of thinning, pruning and nitrogen fertiliser application on transpiration, photosynthesis and water-use efficiency in a young Eucalyptus nitens plantation. Forest Ecology and Management **266**:286-300.

Forrester, D. I., J. J. Collopy, and J. D. Morris. 2010. Transpiration along an age series of Eucalyptus globulus plantations in southeastern Australia. Forest Ecology and Management **259**:1754-1760.

Giardina, F., A. G. Konings, D. Kennedy, et al. 2018. Tall Amazonian forests are less sensitive to precipitation variability. Nature Geoscience.

Goldstein, E., and G. E. Gutman. 2010. Biocombustibles y biotecnología. Contexto internacional, situación en Argentina. CEUR-CONICET, Buenos Aires, Argentina.

Granier, A. 1985. Une nouvelle méthode pour la mesure du flux de sève brute dans le tronc des arbres. Annals of Forest Science **42**:193-200.

Guswa, A. J., M. A. Celia, and I. Rodriguez-Iturbe. 2002a. Models of soil moisture dynamics in ecohydrology: A comparative study. Water Resources Research **38**.

Guswa, A. J., M. A. Celia, and I. Rodriguez-Iturbe. 2002b. Models of soil moisture dynamics in ecohydrology: A comparative study. Water Resources Research **38**:-.

Gutiérrez López, J. A. 2015. Construction of heat dissipation probes to estimate sap flow. Ecohydrology Laboratory - University of New Hampshire, Durham, New Hampshire. USA.

Gutiérrez Lopez, J. A., J. Licata, T. Pypker, and H. Asbjomsen. 2018. Analysis of changes in the current supplied to heat dissipation sensors using an improved tree-cut experiment on young Eucalyptus grandis trees. Tree Physiology.

Gutiérrez Lopez, J. A., T. Pypker, J. Licata, et al. In Prep. Maximum heat ratio: new method to extend the measuring range of sap flux density.

Haines, W. B. 1930. Studies in the physical properties of soil. V. The hysteresis effect in capillary properties, and the modes of moisture distribution associated therewith. The Journal of Agricultural Science **20**:97-116.

Han, Q. M. 2011. Height-related decreases in mesophyll conductance, leaf photosynthesis and compensating adjustments associated with leaf nitrogen concentrations in Pinus densiflora. Tree Physiology **31**:976-984.

Hubbard, R. M., J. Stape, M. G. Ryan, et al. 2010. Effects of irrigation on water use and water use efficiency in two fast growing Eucalyptus plantations. Forest Ecology and Management **259**:1714-1721.

INTA. 2014. Cartas de Suelos de Entre Ríos. http://geointa.inta.gov.ar/web/index.php/cartas-de-suelos-de-entre-rios/. Accessed date: July 16

Jassal, R. S., T. A. Black, C. Arevalo, et al. 2013. Carbon sequestration and water use of a young hybrid poplar plantation in north-central Alberta. Biomass & Bioenergy **56**:323-333.

Klomkliang, N., D. D. Do, and D. Nicholson. 2014. Hysteresis Loop and Scanning Curves of Argon Adsorption in Closed-End Wedge Pores. Langmuir **30**:12879-12887.

Kostner, B., E. Falge, and J. D. Tenhunen. 2002. Age-related effects on leaf area/sapwood area relationships, canopy transpiration and carbon gain of Norway spruce stands (Picea abies) in the Fichtelgebirge, Germany. Tree Physiology **22**:567-574.

Kozlowski, T. T., P. J. Kramer, and S. G. Pallardy. 1991. The physiological ecology of woody plants. Academic Press, San Diego.657 pp

Laclau, J. P., J. P. Arnaud M Fau - Bouillet, J. Bouillet Jp Fau - Ranger, and J. Ranger. 2001. Spatial distribution of Eucalyptus roots in a deep sandy soil in the Congo: relationships with the ability of the stand to take up water and nutrients.

Liu, W., J. Wu, H. Fan, et al. 2017. Estimations of evapotranspiration in an age sequence of Eucalyptus plantations in subtropical China. Plos One **12**:e0174208.

Lu, P., W. H. Outlaw, B. G. Smith, and G. A. Freed. 1997. A new mechanism for the regulation of stomatal aperture size in intact leaves - Accumulation of mesophyll-derived sucrose in the guard-cell wall of Vicia faba. Plant Physiology **114**:109-118.

Lu, P., S. Q. Zhang, W. H. Outlaw, and K. A. Riddle. 1995. Sucrose - a Solute That Accumulates in the Guard-Cell Apoplast and Guard-Cell Symplast of Open Stomata. Febs Letters **362**:180-184.

Lynch, T. B., D. Hamlin, M. J. Ducey, and B. E. Borders. 2018. Design-Unbiased Estimation and Alternatives for Sampling Trees on Plantation Rows. Forests **9**.

Ma, C., Y. Luo, M. Shao, et al. 2017. Environmental controls on sap flow in black locust forest in Loess Plateau, China. Scientific Reports **7**:13160.

Martin-StPaul, N. K., D. Longepierre, R. Huc, et al. 2014. How reliable are methods to assess xylem vulnerability to cavitation? The issue of 'open vessel' artifact in oaks. Tree Physiology **34**:894-905.

Meinzer, F. C., D. M. Johnson, B. Lachenbruch, et al. 2009. Xylem hydraulic safety margins in woody plants: coordination of stomatal control of xylem tension with hydraulic capacitance. Functional Ecology **23**:922-930.

Morris, J., N. N. Zhang, Z. J. Yang, et al. 2004. Water use by fast-growing Eucalyptus urophylla plantations in southern China. Tree Physiology **24**:1035-1044.

Myers, B. J., S. Theiveyanathan, N. D. OBrien, and W. J. Bond. 1996. Growth and water use of Eucalyptus grandis and Pinus radiata plantations irrigated with effluent. Tree Physiology **16**:211-219.

Naranjo, J. A. B., M. Weiler, and K. Stahl. 2011. Sensitivity of a data-driven soil water balance model to estimate summer evapotranspiration along a forest chronosequence. Hydrology and Earth System Sciences **15**:3461-3473.

Niu, D. K., M. G. Wang, and Y. F. Wang. 1997. Plant cellular osmotica. Acta Biotheoretica **45**:161-169.

Oguntunde, P. G. 2005. Whole-plant water use and canopy conductance of cassava under limited available soil water and varying evaporative demand. Plant and Soil **278**:371-383.

Otto, M. S. G., R. M. Hubbard, D. Binkley, and J. L. Stape. 2014. Dominant clonal Eucalyptus grandis×urophylla trees use water more efficiently. Forest Ecology and Management **328**:117-121.

Pavlakis, G., and L. Barden. 1972. Hysteresis in the moisture characteristics of clay soil. Journal of Soil Science **23**:350-361.

Pereira, J. S., M. M. Chaves, F. Fonseca, et al. 1992. Photosynthetic capacity of leaves of Eucalyptus globulus (Labill.) growing in the field with different nutrient and water supplies. Tree Physiology **11**:381-389.

Perez-Cruzado, C., A. Merino, and R. Rodriguez-Soalleiro. 2011. A management tool for estimating bioenergy production and carbon sequestration in Eucalyptus globulus and Eucalyptus nitens grown as short rotation woody crops in north-west Spain. Biomass & Bioenergy **35**:2839-2851.

Pfautsch, S. 2016. Hydraulic Anatomy and Function of Trees-Basics and Critical Developments. Current Forestry Reports **2**:236-248.

Porporato, A., E. Daly, and I. Rodriguez-Iturbe. 2004. Soil water balance and ecosystem response to climate change. American Naturalist **164**:625-632.

Quinones, M. A., Z. M. Lu, and E. Zeiger. 1996. Close correspondence between the action spectra for the blue light responses of the guard cell and coleoptile chloroplasts, and the spectra for blue light-dependent stomatal opening and coleoptile phototropism. Proceedings of the National Academy of Sciences of the United States of America **93**:2224-2228.

Renninger, H. J., N. Phillips, and D. R. Hodel. 2009. Comparative hydraulic and anatomic properties in palm trees (Washingtonia robusta) of varying heights: implications for hydraulic limitation to increased height growth. Trees-Structure and Function **23**:911-921.

Rozenberg, R., D. Saslavsky, and G. Svarzman. 2009. La industria de biocombustibles en la Argentina, in Ed. La Industria de Biocombustibles en el Mercosur. Red MERCOSUR. Montevideo, Uruguay.

Ryan, M. G., D. Binkley, and J. L. Stape. 2008. Why don't our stands grow even faster? Control of production and carbon cycling in eucalypt plantations. Southern Forests **70**:99-104.

SAGPYA. 2001. Sector forestal, anuario sobre régimen de promoción de plantaciones forestales. Government Document. Buenos Aires, Argentina

Salama, R. B., G. A. Bartle, and P. Farrington. 1994. Water-Use of Plantation Eucalyptus-Camaldulensis Estimated by Groundwater Hydrograph Separation Techniques and Heat Pulse Method. Journal of Hydrology **156**:163-180.

Sanchez Acosta, M. 2012. Caracterización de la madera del nuevo híbrido Eucalyptus grandis, Hill ex Maiden x Eucalyptus tereticornis, Smith, su aptitud de usos en Argentina. Universidad de Valladolid, Valladolid, Spain.

Schafer, K. V. R., R. Oren, and J. D. Tenhunen. 2000. The effect of tree height on crown level stomatal conductance. Plant Cell and Environment **23**:365-375.

SIGA. 2015. Sistema de información y gestión agrometereológico. http://siga2.inta.gov.ar/en/estadistica/. Accessed date: July 17

Soares, J. V., and A. C. Almeida. 2001. Modeling the water balance and soil water fluxes in a fast growing Eucalyptus plantation in Brazil. Journal of Hydrology **253**:130-147.

Stape, J. L., D. Binkley, and M. G. Ryan. 2004. Eucalyptus production and the supply, use and efficiency of use of water, light and nitrogen across a geographic gradient in Brazil. Forest Ecology and Management **193**:17-31.

Stape, J. L., D. Binkley, M. G. Ryan, et al. 2010. The Brazil Eucalyptus Potential Productivity Project: Influence of water, nutrients and stand uniformity on wood production. Forest Ecology and Management **259**:1684-1694.

Staple, W. J. 1965. Moisture tension diffusivity and conductivity of a loam soil during wetting and drying. Canadian Journal of Soil Science **45**:78-&.

Talbott, L. D., and E. Zeiger. 1996. Central roles for potassium and sucrose in guard-cell osmoregulation. Plant Physiology **111**:1051-1057.

Tallman, G. 2004. Are diurnal patterns of stomatal movement the result of alternating metabolism of endogenous guard cell ABA and accumulation of ABA delivered to the apoplast around guard cells by transpiration? Journal of Experimental Botany **55**:1963-1976.

Tyree, M. T. 2003. Hydraulic limits on tree performance: transpiration, carbon gain and growth of trees. Trees-Structure and Function **17**:95-100.

Ulla, T. 2015. El Niño floods in Argentina: a story of displacement and vulnerability. The State of Environmental Migration 2016: A review of 2015.

van Dam, J., A. P. C. Faaij, J. Hilbert, et al. 2009. Large-scale bioenergy production from soybeans and switchgrass in Argentina: Part A: Potential and economic feasibility for

national and international markets. Renewable and Sustainable Energy Reviews **13**:1710-1733.

Vandegehuchte, M. W., and K. Steppe. 2013. Sap-flux density measurement methods: working principles and applicability. Functional Plant Biology **40**:213-223.

Vangenuchten, M. T. 1980. A closed-form equation for predicting the hydraulic conductivity of unsaturated soils. Soil Science Society of America Journal **44**:892-898.

Vergeynst, L. L., M. W. Vandegehuchte, M. A. McGuire, et al. 2014. Changes in stem water content influence sap flux density measurements with thermal dissipation probes. Trees-Structure and Function **28**:949-955.

Virlouvet, L., T. J. Avenson, Q. Du, et al. 2018. Dehydration Stress Memory: Gene Networks Linked to Physiological Responses During Repeated Stresses of Zea mays. Frontiers in Plant Science **9**.

Virlouvet, L., and M. Fromm. 2015. Physiological and transcriptional memory in guard cells during repetitive dehydration stress. New Phytologist **205**:596-607.

Wang, K.-Y., S. Kellomäki, T. Zha, and H. Peltola. 2005. Annual and seasonal variation of sap flow and conductance of pine trees grown in elevated carbon dioxide and temperature. Journal of Experimental Botany **56**:155-165.

Ward, E. J., R. Oren, B. D. Sigurdsson, et al. 2008. Fertilization effects on mean stomatal conductance are mediated through changes in the hydraulic attributes of mature Norway spruce trees. Tree Physiology **28**:579-596.

Wheeler, J. K., B. A. Huggett, A. N. Tofte, et al. 2013. Cutting xylem under tension or supersaturated with gas can generate PLC and the appearance of rapid recovery from embolism. Plant Cell and Environment **36**:1938-1949.

Williams, M., B. J. Bond, and M. G. Ryan. 2001. Evaluating different soil and plant hydraulic constraints on tree function using a model and sap flow data from ponderosa pine. Plant Cell and Environment **24**:679-690.

Wilske, B., N. Lu, L. Wei, et al. 2009. Poplar plantation has the potential to alter the water balance in semiarid Inner Mongolia. Journal of Environmental Management **90**:2762-2770.

Winck, R. A., H. E. Fassola, S. R. Barth, et al. 2015. Modelos predictivos de biomasa aérea de Eucalyptus grandis para el Noreste de Argentina. Ciência Florestal **25**:595-606.

Xi, B. Y., N. Di, J. Q. Liu, et al. 2018. Hydrologic regulation of plant rooting depth: Pay attention to the widespread scenario with intense seasonal groundwater table fluctuation. Proceedings of the National Academy of Sciences of the United States of America **115**:E3863-E3864.

Zeiger, E. 2000. Sensory transduction of blue light in guard cells. Trends in Plant Science **5**:183-185.

Zeng, Y., S. J. Tan, D. D. Do, and D. Nicholson. 2016. Hysteresis and scanning curves in linear arrays of mesopores with two cavities and three necks: Classification of the scanning curves. Colloids and Surfaces A: Physicochemical and Engineering Aspects **496**:52-62.

Zeppel, M. J. B., B. R. Murray, C. Barton, and D. Eamus. 2004. Seasonal responses of xylem sap velocity to VPD and solar radiation during drought in a stand of native trees in temperate Australia. Functional Plant Biology **31**:461-470.

Zhang, Q., S. Manzoni, G. Katul, et al. 2014. The hysteretic evapotranspiration—Vapor pressure deficit relation. Journal of Geophysical Research: Biogeosciences **119**:125-140.

Zhang, Z. F. 2011. Soil Water Retention and Relative Permeability for Conditions from Oven-Dry to Full Saturation. Vadose Zone Journal **10**:1299-1308.

Zhu, J. X., R. Zeiger, and E. Zeiger. 1995. Structural and Functional-Properties of the Coleoptile Chloroplast - Photosynthesis and Photosensory Transduction. Photosynthesis Research **44**:207-219.

CHAPTER IV

GENERAL CONCLUSSIONS

Overarching goals of this study

My doctoral research was part of a large international interdisciplinary NSF-PIRE research project that examined the impacts, barriers and opportunities related to bioenergy production across the Americas (USA, Mexico, Brazil, Argentina). This dissertation is focused on two countries, USA and Argentina. The general goal of this research was to assess the potential ecohydrological impacts associated with the production of biomass for bioenergy from aspen (*Populus tremuloides* Mich.) in Wisconsin, USA, and eucalyptus (*Eucalyptus grandis*) plantations in Entre Rios, Argentina.

As part of this dissertation, we conducted a validation and calibration studies of two sap flow methods. First, we calibrated the heat dissipation (HD) method and assessed the effects of heater wattage on sap flux density (F_d) estimates. This paper was not included in this dissertation, but if has been published and it is fully available for readers (Gutierrez Lopez et al. 2018). We also estimated the measuring range of F_d for *E. grandis* and validated a new method that extended the measuring range of HR method and allowed us to measure low and inverse F_d with high precision; the maximum heat ratio (**MHR**) method. This later study was included in this dissertation and the results were used to estimate F_d in *E. grandis* trees. This conclusion, however, is focused on Chapters III and IV, which dealt with the potential ecohydrological impacts of the production of feedstocks for bioenergy under two environmentally different sites.

In our case studies in the USA and Entre Rios, Argentina, we set to determine if plantation age could be correlated to site *T*, which can be of great value to elaborate long-term modeling scenarios. Such modeling scenarios can help us determine the optimum rotation lengths to provide maximum timber growth, while minimizing potential negative ecohydrological impacts. The overarching objectives of this research were: (a) to determine how site transpiration (*T*, mm d^{-1}) changes both seasonally and at different plantation ages, (b) how different environmental variables such as precipitation (pp), soil saturation (S), air temperature (*AirT*), relative humidity (RH) and photosynthetic active radiation (PAR) and solar radiation affect *T* rates at different plantation ages. We tested different hypotheses at each site, based on their respective general management goals, and the environmental conditions that drive plant growth and water use at each site.

Wisconsin study site

To test if stand age and average water use relationships can be established in SRWC of *P. tremuloides*, the general goals of this study were: a) to estimate seasonal and daily *T* of three (Young, Mid-aged, and Mature, see next section for details) coppice plantations dominated by *Populus tremuloides* Mich., and b) determine how site effects can override the age effect on stand *T*. **Our first hypothesis** is that at the tree level, water use would be higher in the Mature site, compared to our Young site, while sap flux density would be higher for the latter. **Our second hypothesis** is that stand *T* will increase with stand age, primarily as a result increments of total leaf area and LAI, larger individual tree size and higher growth rates. **Our third hypothesis** is that site effects can override age effects on stand *T*, but addressing these differences can allow us to establish a relationship between age and stand *T*.

Summary of results for Wisconsin

According to our statistical analysis, estimated Mature stand *T* had a maximum of 5.5 m d^{-1} early in the growing season (seasonal average 2.7) and was higher than the Mid-aged and Young sites, which had both a maximum early-growing season *T* of 2.5 mm (seasonal average 1 and 0.3 mm, respectively). Modeled transpiration ($\boldsymbol{T_{mod}}$) under a *S*-limiting scenario reduced average transpiration rates by ~10% across sites, but these reductions were not significantly different from estimated *T*. T_{mod} under non-limiting *S* conditions resulted in significantly higher transpiration rates in the Young (+170%), but not in the Mid-aged (+34%) or Mature (+5%) sites. While not significantly different between the Mid-aged and Young sites, annual average *T* was positively correlated with stand age, and this relationship was maintained under both *S* scenarios. Dominant trees accounted for 76% of stand *T* in the Mature site, and 58% and 51% in Mid-aged and Young sites, respectively. In Young sites, our results highlight the important role of small-diameter trees. Our results indicate that site-specific differences can have an overriding effect on age, however, as long as site variability is addressed, stand age can be related to average stand *T*. Curves of expected water use with age can be of great valuable to the bioenergy industry, to elaborate potential scenarios of water use in aspen-dominated short rotation woody crops (**SRWC**). Finally, further research is needed under various environmental conditions to validate the existence of a water use curve in aspen-dominated or SRWC plantations.

Argentina study case

In Argentina our goal was to estimate whole-tree ($\boldsymbol{Q}$, L d^{-1}) and stand-level *T* in *Eucalyptus grandis* plantations of three different ages, 10, 4 and 1 years-old (**YO**) at regular density (**10YO**, **4YO**, **1YO**), one one-YO at a high (double) density (**1YOHD**), and reference crop evapotranspiration ($\boldsymbol{ET_k}$) in an adjacent fallow pasture site (common during rotation

cycles). In this site, the main objectives were: (a) first, to understand the relationship between plantation age, density, and tree and stand-level transpiration rates, and also (b) to assess the response of different plantations ages to variations in atmospheric and soil moisture stress, to understand resilience of eucalyptus plantations at different growing stages. We tested three main hypothesis, the **first hypothesis** was that stand *T* would increase from 1 to 4 YO, and decrease after that resulting in lower *T* in the older (10YO) site. **Our second hypothesis** was that older (4 an 10YO) plantations, would be less susceptible to environmental changes (*VPD* and soil moisture), which would be reflected in smaller hysteresis areas for *VPD* and PAR at low *S*, and in inflection points at higher *VPD* rates when soil moisture is limiting.

Summary of results for Argentina

We analyzed inflection points of sap flux density ($\boldsymbol{F_d}$, $cm^3\ cm^{-2}\ h^{-1}$) for *VPD* ($\boldsymbol{IP_{VPD}}$) and PAR ($\boldsymbol{IP_{PAR}}$) by fitting a local polynomial regression (LOESS) surface to the relationship between F_d and *AirT*, *VPD* or PAR. Additionally we studied hysteresis curves of F_d for *VPD* and PAR ($\boldsymbol{H_{VPD}}$ and $\boldsymbol{H_{PAR}}$, respectively) to assess the effects of stand age and density on tree response to environmental stress. In these sites, we tested and validated the maximum heat ratio method (**MHR**), which allowed us to extend the measuring range of the traditional heat ratio method, and a full chapter of this dissertation was dedicated for the validation of sap flow methods. F_d was then estimated with the MHR and used to estimated Q, which was later scaled up to estimate *T* using allometric equations developed between diameter and sapwood area.

In this site, *T* increased with age according to our first hypothesis from 1 to 4YO, and after that decreased significantly at 10YO. During the peak of the growing season, average *T* was 2.2, 5.2 and 3 mm d^{-1}, 1YO, 4YO and 10YO, respectively, in the regular-density sites. In the high-

density 1YO site, maximum T during the same period was 3.4 mm d^{-1}. We also observed that this site was the most responsive to precipitation inputs than the other sites.

Inflection points generated at varying soil moisture conditions, were more pronounced at lower *VPD* when soil moisture was low, suggesting that both soil moisture and *VPD* are important in controlling stomatal response to moisture stress. Our comparison across treatments showed that the older (10YO) site was less sensitive to changes in soil moisture and maintained relatively stable inflection points across a wide soil moisture ranges. Conversely, the 1YOHD showed the greatest variability, indicating more sensibility and at the same time more opportunistic water use behavior, increasing their water use rates when soil moisture was abundant, but reducing to similar rates of other sites of the same age when soil moisture was limiting. Our analysis of hysteresis areas showed that the hysteresis area for F_d -*VPD* ($\boldsymbol{H_{VPD}}$) were larger at lower soil moistures, despite F_d rates being lower at low soil moisture. Analyzed by soil moisture range a *butterfly*-shape curve for hysteresis areas between F_d and PAR (H_{PAR}) was observed at low soil water contents. Such *butterfly* patterns in the hysteresis graphs, which are associated to hydrologic stress, were observed in all sites except the 10YO. We associated the lack of *butterfly* patterns in hysteresis graphs in the 10YO site, to its ability to withstand higher hydrologic stress due to a combination of site characteristics and to its more developed root system, which might allow them to have access to a larger soil profile. In general, our results indicate that mature (10YO) *E. grandis* plantations, are more capable of regulating transpiration rates under high *VPD* and low soil moisture, reducing their risk for hydraulic failure, compared to younger sites.

General limitations of our study and recommendations for future studies

As discussed in their respective chapters, the study of site and watershed transpiration is commonly limited in both time and space. The limitations, however, are often related to the practicality of the measurements. In both the USA and Argentina, we relied on sap flow measurements to estimate *Q* and stand *T*. While sap flow sensors offer a higher precision in the measurements of tree water use, the number of sensors that can be maintained and deployed, often reduces the number of sites that can be monitored. To focus on our research question, we focused on deploying sensors across different site ages, and we tried to cover as much as possible the variability within each site.

In our study in Wisconsin, USA, site effects were found to significantly influence tree and stand-level water use rates. Various environmental variables such as photosynthetic active radiation (PAR), air temperature, relative humidity, precipitation and vapor pressure deficit (*VPD*) remained relatively stable across sites. However, soil properties differed across sites, which resulted in significant differences in soil moisture and soil saturation (**S**). Soil moisture has been considered a strong factor regulating *T* and growth rates in poplars and *P. tremuloides* trees (Bloemen et al. 2017, Chen et al. 2014, Larcheveque et al. 2011). According to our analysis, it also had strong effects on F_d.

In Entre Rios, Argentina, while the soil types were homogeneous cross sites, analysis of *S* showed that *S* was significantly different among sites. In this site, soil water in the top 40 cm (S_{40}) appeared to have a stronger influence on site *T*, but not on the diel patterns of F_d, which could be explained by the shape of the hysteresis curves we observed. Hysteresis graphs for *VPD* showed a compensation in F_d at low *VPD*'s, which explains the lack of statistical significance observed for site *T*, which considers the entire transpiration for a given day.

While we were able to monitor soil moisture to a depth of 100 cm in all sites, the modeling used to estimate site *T* makes two assumptions. First that *S* in the first 40 cm of soil has the strongest influence on *T*. While in fast growing plantations most of the fine roots are located in the top 50 cm of soil (Bouillet et al. 2002, Laclau et al. 2001), there are deeper roots can access water from deeper soil profiles (Toillon et al. 2013, Xi et al. 2013), and the root distribution is expected to be different at different plantations ages. The second assumption in our model is that changes in *S* are linearly related to F_d and stand *T*. According to Larcheveque et al. (2011), this relationship might be true within a volumetric water content range of 5-20%, but the slopes are different at high or low water contents. In modeling scenarios, the effects of *T* on soil moisture are expressed as a curve (extraction curve) (Guswa et al. 2002, Rodriguez-Iturbe et al. 2006, Rodriguez-Iturbe et al. 2001), with different slopes depending on the expected extraction rates (Rodriguez-Iturbe et al. 2001). *S* varied significant in the Mature site *S*, however, it was never lower than 0.14, and consequently, the slope estimated by our model might underestimate the effects of *S* in this site.

Two common limitations in sap flow studies are the sample size and the proper determination of stand-level A_S (Berry et al. 2018). Sample size is directly linked to equipment cost, and the spatial distribution of the species of interest. With wired sap flow stations, most studies limit the cable length between 10 and 15 m, to reduce to signal to noise ratio. This creates a radius around the sap flow station for the selection of the trees to be monitored, which can leave diametric categories or species of interest outside this radius. On single-species stands, Kume et al. (2012) recommended an optimal sample size of 15 measuring points to capture most of the tree-to-tree F_d variability. However, this recommendation was based om heat dissipation sensors with only one measuring point per sensor. As described in our methods section, we monitored a total of 24 measuring points distributed across 8 different trees, then while our

sample size was smaller, we captured the entire radial profile of all trees monitored. Proper determination of A_S and the F_d radial profile in large trees is difficulty, and can lead to major under or overestimations of tree and stand T (Alvarado-Barrientos et al. 2013, Ford et al. 2004, Gebauer et al. 2008, Kubota et al. 2005, Poyatos et al. 2007). To address sapwood depth radial variability, we collected two cores per tree to estimate A_S, and measured sapwood depth on four points per tree. Additionally, we installed trees in all four cardinal directions to cover the potential radial variations in F_d, and in all our trees the entire F_d radial profile was monitored. Finally, studies on *P. tremuloides* trees have reported diameters of 24 cm in 150 YO trees (Bond-Lamberty et al. 2002, 2014), thus we extended our sampling range for A_S to include trees up to 25 cm in diameter, and adjusted allometric equations for each site and predicted A_S with site-specific equations (see Table III-3). Species-specific allometric equations are of great value to scale up plant-to-stand level processes (Bond-Lamberty et al. 2002, Jenkins et al. 2003, Perala 1993), but adjusting equations for a specific site can reduce the error associated with the estimation of A_S.

Based on our experience, we make the following recommendations to future studies looking to estimate stand-level annual water balances or interested in modeling stand-level T. First, establish a weather station (with all the variables needed to estimate ET_0: air temperature, relative humidity, incoming short-waver radiation, outgoing long-wave radiation, wind speed. Additionally, soil moisture, precipitation, photosynthetically active radiation) earlier in the growing season, and in deciduous species, to install the weather station a month or two prior to the onset of transpiration. Next, track the development of LAI, and in evergreen species, measure it two or three times during the growing season, to address potential variability due to crown development. Monitor both throughfall and stemflow, considering that in *P. tremuloides* trees 15 cm in diameter, precipitation events under 30 mm (over two or three days) overfilled our

containers, which were designed to fit 10 L. For throughfall, a minimum of thirty collectors per site are recommended, which should also be designed to fit the precipitation expected for a monitoring period. Next, we strongly recommend stablishing replicates under different site conditions, and develop a site profile (i.e., soil characteristics, stand density, allometric equations, etc.) for each. If sap flow sensors are used to estimate F_d, under budgetary constraints, the design of the sensors can be modified to allow them to detach from the communication cables, and remain in the trees. This way, the same data logger and multiplexor (approx. 70% of the cost of a sap flow station) can be moved between sites (where sensors have been previously installed in the trees) at intervals of 10-15 days. With the site and environmental variables monitored at each site, it is possible to estimate stand-level transpiration for the periods where no F_d was not monitored at each site, using various gap-filling procedures (i.e., a linear mixed model) similar to the one used in our sites. If runoff is difficult to monitor, a model can be adjusted to the soil saturation of each site, and based in soil properties to estimate potential runoff and infiltration.

Recommended next steps

One of the goals of this study was to determine if stand age could be related to average transpiration. If such relationship can be established, it would be possible to established reliable long-term scenarios of water use, and consequently, assess the potential ecohydrological impacts of the production of bioenergy. As mentioned in the Chapter 1, one of the reasons behind the absence of strategies to address water-related issues in long-term bioenergy development plans (BETO 2013, Perlack et al. 2005), is the lack of continuous monitoring studies, particularly in fast growing plantations, which are essential to parameterize models.

As part of the long-term goal of this study, what we recommend as the next step for this research is to use the data collected and the models fitted in this study, to generate water use scenarios at different rotation lengths, including modeled biomass accumulations, as shown in Figure V-1. The major challenge in the next steps, will be to integrate the fitted water use models for each site, and biomass accumulation models for a given species (e.g., *P. tremuloides* and *E. grandis*), to test whether such long-term water use scenarios can yield similar results to those elaborated with mechanistic models alone or based on long-term mass balance approaches, where they are available. Some of the mechanistic methods mentioned in the introduction of this study were: Penman-Monteith (Allen et al. 1998), the Presley-Taylor (Priestley and Taylor 1972), and Eddy Covariance (Twine et al. 2000). Once the water use curve over time has been determined for a given species, and the long-term forecasted water use has been estimated (as in Figure V-1), the results can be compared with those estimated from those estimated from mechanistic models. In long-term ecological research stations, where site *T* is often estimated from water mass balance approaches over longer periods of time, estimates from both mechanistic models and water use curves over time can be validated. This approach of course will be limited in sites with high species diversity, if all dominant species are not considered to elaborate the expected water use curves of various rotation lengths. Finally, as mentioned in their respective chapters, temporal and spatial limitations of common sap flow studies need to be addressed in order to elaborate the described long-term water use scenarios.

Figures

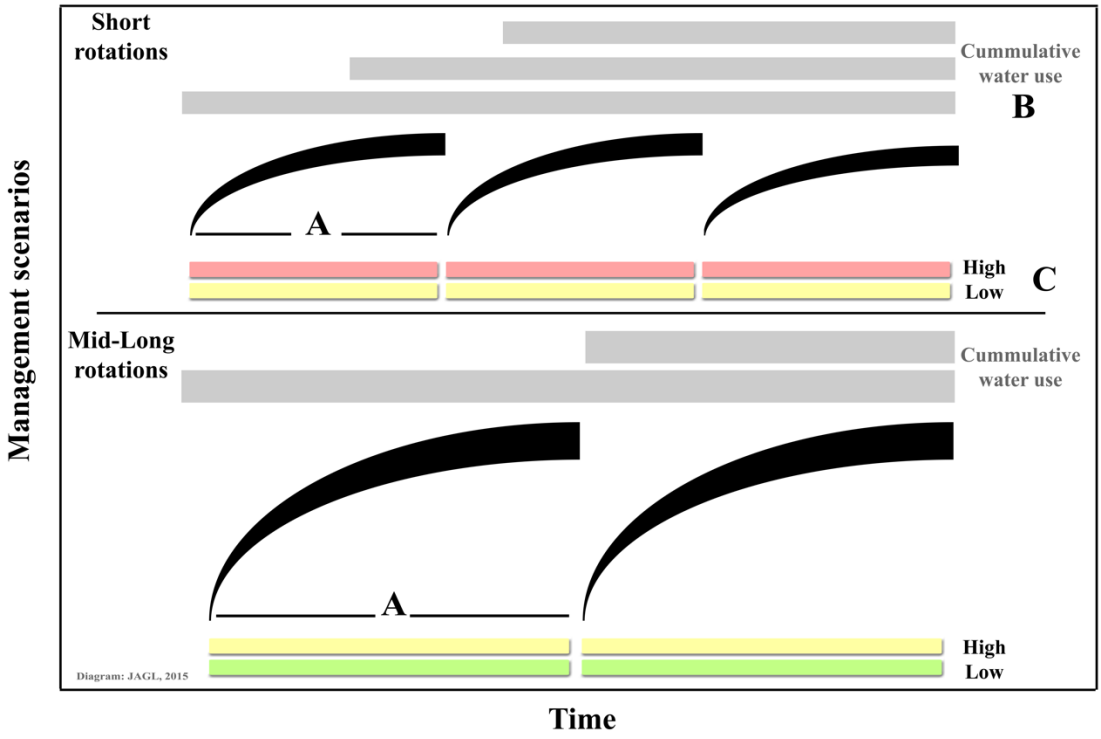

Figure V-1 Diagram showing to projected water use under two rotation scenarios

Multiple short rotations (top panel), and few rotations (bottom panel). The top panel represents a species where multiple short rotations result in higher cumulative water use than the same species under longer rotations (bottom panel). In this diagram: A) the rotation length, B) the cumulative water use, and C) the expected stress due to reductions in soil water availability.

References

Allen, R. G., L. S. Pereira, D. Raes, and M. Smith. 1998. Crop evapotranspiration: guidelines for computing crop water requiriments. Irrigation and drainage paper **56**.

Alvarado-Barrientos, M. S., V. Hernandez-Santana, and H. Asbjornsen. 2013. Variability of the radial profile of sap velocity in Pinus patula from contrasting stands within the seasonal cloud forest zone of Veracruz, Mexico. Agricultural and Forest Meteorology **168**:108-119.

Berry, Z. C., N. Looker, F. Holwerda, et al. 2018. Why size matters: the interactive influences of tree diameter distribution and sap flow parameters on upscaled transpiration. Tree Physiology **38**:263-275.

BETO. 2013. Multi-year program plan. Government Document. Bioenergy Technologies Office. DOE/EE-0915

Bloemen, J., R. Fichot, J. A. Horemans, et al. 2017. Water use of a multigenotype poplar short-rotation coppice from tree to stand scale. Global Change Biology Bioenergy **9**:370-384.

Bond-Lamberty, B., C. Wang, and S. T. Gower. 2002. Aboveground and belowground biomass and sapwood area allometric equations for six boreal tree species of northern Manitoba. Canadian Journal of Forest Research-Revue Canadienne De Recherche Forestiere **32**:1441-1450.

Bond-Lamberty, B., C. Wang, and S. T. Gower. 2014. Aboveground and belowground biomass and sapwood area allometric equations for six boreal tree species of northern Manitoba (vol 32, pg 1441, 2002). Canadian Journal of Forest Research-Revue Canadienne De Recherche Forestiere **44**:389-389.

Bouillet, J.-P., J.-P. Laclau, M. Arnaud, et al. 2002. Changes with age in the spatial distribution of roots of Eucalyptus clone in Congo: Impact on water and nutrient uptake. Forest Ecology and Management **171**:43-57.

Chen, L. X., Z. Q. Zhang, T. G. Zha, et al. 2014. Soil water affects transpiration response to rainfall and vapor pressure deficit in poplar plantation. New Forests **45**:235-250.

Ford, C. R., M. A. McGuire, R. J. Mitchell, and R. O. Teskey. 2004. Assessing variation in the radial profile of sap flux density in Pinus species and its effect on daily water use. Tree Physiology **24**:241-249.

Gebauer, T., V. Horna, and C. Leuschner. 2008. Variability in radial sap flux density patterns and sapwood area among seven co-occurring temperate broad-leaved tree species. Tree Physiology **28**:1821-1830.

Guswa, A. J., M. A. Celia, and I. Rodriguez-Iturbe. 2002. Models of soil moisture dynamics in ecohydrology: A comparative study. Water Resources Research **38**.

Gutierrez Lopez, J., J. Licata, T. Pypker, and H. Asbjornsen. 2018. Effects of heater wattage on sap flux density estimates using an improved tree-cut experiment.

Jenkins, J. C., D. C. Chojnacky, L. S. Heath, and R. A. Birdsey. 2003. National-scale biomass estimators for United States tree species. Forest Science **49**:12-35.

Kubota, M., J. Tenhunen, R. Zimmermann, et al. 2005. Influences of environmental factors on the radial profile of sap flux density in Fagus crenata growing at different elevations in the Naeba Mountains, Japan. Tree Physiology **25**:545-556.

Kume, T., K. Otsuki, S. Du, et al. 2012. Spatial variation in sap flow velocity in semiarid region trees: its impact on stand-scale transpiration estimates. Hydrological Processes **26**:1161-1168.

Laclau, J. P., J. P. Arnaud M Fau - Bouillet, J. Bouillet Jp Fau - Ranger, and J. Ranger. 2001. Spatial distribution of Eucalyptus roots in a deep sandy soil in the Congo: relationships with the ability of the stand to take up water and nutrients.

Larcheveque, M., M. Maurel, A. Desrochers, and G. R. Larocque. 2011. How does drought tolerance compare between two improved hybrids of balsam poplar and an unimproved native species? Tree Physiology **31**:240-249.

Perala, D. A. 1993. Allometric Biomass Estimators for Aspen-Dominated Ecosystems in the Upper Great-Lakes. Usda Forest Service North Central Forest Experiment Station Research Paper:1-&.

Perlack, R. D., L. L. Wright, A. F. Turhollow, et al. 2005. Biomass as feedstock for a bioenergy and bioproducts industry: the technical feasibility of a billion-ton annual supply. Technical Report, Oak Ridge National Laboratory, Oak Ridge, Tennessee.

Poyatos, R., J. Cermak, and P. Llorens. 2007. Variation in the radial patterns of sap flux density in pubescent oak (Quercus pubescens) and its implications for tree and stand transpiration measurements. Tree Physiology **27**:537-548.

Priestley, C. H. B., and R. J. Taylor. 1972. On the Assessment of Surface Heat Flux and Evaporation Using Large-Scale Parameters. Monthly Weather Review **100**:81-92.

Rodriguez-Iturbe, I., V. Isham, D. R. Cox, et al. 2006. Space-time modeling of soil moisture: Stochastic rainfall forcing with heterogeneous vegetation. Water Resources Research **42**.

Rodriguez-Iturbe, I., A. Porporato, F. Laio, and L. Ridolfi. 2001. Intensive or extensive use of soil moisture: plant strategies to cope with stochastic water availability. Geophysical Research Letters **28**:4495-4497.

Toillon, J., B. Rollin, E. Dalle, et al. 2013. Variability and plasticity of productivity, water-use efficiency, and nitrogen exportation rate in Salix short rotation coppice. Biomass & Bioenergy **56**:392-404.

Twine, T. E., W. P. Kustas, J. M. Norman, et al. 2000. Correcting eddy-covariance flux underestimates over a grassland. Agricultural and Forest Meteorology **103**:279-300.

Xi, B. Y., Y. Wang, L. M. Jia, et al. 2013. Characteristics of fine root system and water uptake in a triploid Populus tomentosa plantation in the North China Plain: Implications for irrigation water management. Agricultural Water Management **117**:83-92.

Alvarado-Barrientos, M. S., V. Hernandez-Santana, and H. Asbjornsen. 2013. Variability of the radial profile of sap velocity in Pinus patula from contrasting stands within the seasonal cloud forest zone of Veracruz, Mexico. Agricultural and Forest Meteorology **168**:108-119.

Berry, Z. C., N. Looker, F. Holwerda, et al. 2018. Why size matters: the interactive influences of tree diameter distribution and sap flow parameters on upscaled transpiration. Tree Physiology **38**:263-275.

BETO. 2013. Multi-year program plan. Government Document. Bioenergy Technologies Office. DOE/EE-0915

Bloemen, J., R. Fichot, J. A. Horemans, et al. 2017. Water use of a multigenotype poplar short-rotation coppice from tree to stand scale. Global Change Biology Bioenergy **9**:370-384.

Bond-Lamberty, B., C. Wang, and S. T. Gower. 2002. Aboveground and belowground biomass and sapwood area allometric equations for six boreal tree species of northern Manitoba. Canadian Journal of Forest Research-Revue Canadienne De Recherche Forestiere **32**:1441-1450.

Bond-Lamberty, B., C. Wang, and S. T. Gower. 2014. Aboveground and belowground biomass and sapwood area allometric equations for six boreal tree species of northern Manitoba (vol 32, pg 1441, 2002). Canadian Journal of Forest Research-Revue Canadienne De Recherche Forestiere **44**:389-389.

Bouillet, J.-P., J.-P. Laclau, M. Arnaud, et al. 2002. Changes with age in the spatial distribution of roots of Eucalyptus clone in Congo: Impact on water and nutrient uptake. Forest Ecology and Management **171**:43-57.

Chen, L. X., Z. Q. Zhang, T. G. Zha, et al. 2014. Soil water affects transpiration response to rainfall and vapor pressure deficit in poplar plantation. New Forests **45**:235-250.

Costanza, R., D. Duplisea, and U. Kautsky. 1998. Ecological modelling and economic systems with STELLA - Introduction. Ecological Modelling **110**:1-4.

Ford, C. R., M. A. McGuire, R. J. Mitchell, and R. O. Teskey. 2004. Assessing variation in the radial profile of sap flux density in Pinus species and its effect on daily water use. Tree Physiology **24**:241-249.

Gebauer, T., V. Horna, and C. Leuschner. 2008. Variability in radial sap flux density patterns and sapwood area among seven co-occurring temperate broad-leaved tree species. Tree Physiology **28**:1821-1830.

Guswa, A. J., M. A. Celia, and I. Rodriguez-Iturbe. 2002. Models of soil moisture dynamics in ecohydrology: A comparative study. Water Resources Research **38**.

Gutierrez Lopez, J., J. Licata, T. Pypker, and H. Asbjornsen. 2018. Effects of heater wattage on sap flux density estimates using an improved tree-cut experiment.

Jenkins, J. C., D. C. Chojnacky, L. S. Heath, and R. A. Birdsey. 2003. National-scale biomass estimators for United States tree species. Forest Science **49**:12-35.

Kubota, M., J. Tenhunen, R. Zimmermann, et al. 2005. Influences of environmental factors on the radial profile of sap flux density in Fagus crenata growing at different elevations in the Naeba Mountains, Japan. Tree Physiology **25**:545-556.

Kume, T., K. Otsuki, S. Du, et al. 2012. Spatial variation in sap flow velocity in semiarid region trees: its impact on stand-scale transpiration estimates. Hydrological Processes **26**:1161-1168.

Laclau, J. P., J. P. Arnaud M Fau - Bouillet, J. Bouillet Jp Fau - Ranger, and J. Ranger. 2001. Spatial distribution of Eucalyptus roots in a deep sandy soil in the Congo: relationships with the ability of the stand to take up water and nutrients.

Larcheveque, M., M. Maurel, A. Desrochers, and G. R. Larocque. 2011. How does drought tolerance compare between two improved hybrids of balsam poplar and an unimproved native species? Tree Physiology **31**:240-249.

Ouyang, Y., J. Zhang, T. D. Leininger, and B. R. Frey. 2015. A STELLA Model to Estimate Water and Nitrogen Dynamics in a Short-Rotation Woody Crop Plantation. Journal of Environmental Quality **44**:200-209.

Pallipparambil, G. R., S. Raghu, and R. N. Wiedenmann. 2015. Modeling the biomass production of the biofuel crop Miscanthus x giganteus, to understand and communicate benefits and risks in cultivation. Energy for Sustainable Development **27**:63-72.

Perala, D. A. 1993. Allometric Biomass Estimators for Aspen-Dominated Ecosystems in the Upper Great-Lakes. Usda Forest Service North Central Forest Experiment Station Research Paper:1-&.

Perlack, R. D., L. L. Wright, A. F. Turhollow, et al. 2005. Biomass as feedstock for a bioenergy and bioproducts industry: the technical feasibility of a billion-ton annual supply. Technical Report, Oak Ridge National Laboratory, Oak Ridge, Tennessee.

Poyatos, R., J. Cermak, and P. Llorens. 2007. Variation in the radial patterns of sap flux density in pubescent oak (Quercus pubescens) and its implications for tree and stand transpiration measurements. Tree Physiology **27**:537-548.

Richmond, B. 2004. An introduction to systems thinking. iSee Systems, Lebanon, NH, USA

Rodriguez-Iturbe, I., V. Isham, D. R. Cox, et al. 2006. Space-time modeling of soil moisture: Stochastic rainfall forcing with heterogeneous vegetation. Water Resources Research **42**.

Rodriguez-Iturbe, I., A. Porporato, F. Laio, and L. Ridolfi. 2001. Intensive or extensive use of soil moisture: plant strategies to cope with stochastic water availability. Geophysical Research Letters **28**:4495-4497.

Toillon, J., B. Rollin, E. Dalle, et al. 2013. Variability and plasticity of productivity, water-use efficiency, and nitrogen exportation rate in Salix short rotation coppice. Biomass & Bioenergy **56**:392-404.

Van Milgen, J., R. Boston, R. Kohn, and J. Ferguson. 1996. Comparison of available software for dynamic modeling. Annales de Zootechnie (Paris) **45**:257-273.

Xi, B. Y., Y. Wang, L. M. Jia, et al. 2013. Characteristics of fine root system and water uptake in a triploid Populus tomentosa plantation in the North China Plain: Implications for irrigation water management. Agricultural Water Management **117**:83-92.

Alvarado-Barrientos, M. S., V. Hernandez-Santana, and H. Asbjornsen. 2013. Variability of the radial profile of sap velocity in Pinus patula from contrasting stands within the seasonal cloud forest zone of Veracruz, Mexico. Agricultural and Forest Meteorology **168**:108-119.

Berry, Z. C., N. Looker, F. Holwerda, et al. 2018. Why size matters: the interactive influences of tree diameter distribution and sap flow parameters on upscaled transpiration. Tree Physiology **38**:263-275.

BETO. 2013. Multi-year program plan. Government Document. Bioenergy Technologies Office. DOE/EE-0915

Bloemen, J., R. Fichot, J. A. Horemans, et al. 2017. Water use of a multigenotype poplar short-rotation coppice from tree to stand scale. Global Change Biology Bioenergy **9**:370-384.

Bond-Lamberty, B., C. Wang, and S. T. Gower. 2002. Aboveground and belowground biomass and sapwood area allometric equations for six boreal tree species of northern Manitoba. Canadian Journal of Forest Research-Revue Canadienne De Recherche Forestiere **32**:1441-1450.

Bond-Lamberty, B., C. Wang, and S. T. Gower. 2014. Aboveground and belowground biomass and sapwood area allometric equations for six boreal tree species of northern Manitoba (vol 32, pg 1441, 2002). Canadian Journal of Forest Research-Revue Canadienne De Recherche Forestiere **44**:389-389.

Bouillet, J.-P., J.-P. Laclau, M. Arnaud, et al. 2002. Changes with age in the spatial distribution of roots of Eucalyptus clone in Congo: Impact on water and nutrient uptake. Forest Ecology and Management **171**:43-57.

Chen, L. X., Z. Q. Zhang, T. G. Zha, et al. 2014. Soil water affects transpiration response to rainfall and vapor pressure deficit in poplar plantation. New Forests **45**:235-250.

Costanza, R., D. Duplisea, and U. Kautsky. 1998. Ecological modelling and economic systems with STELLA - Introduction. Ecological Modelling **110**:1-4.

Ford, C. R., M. A. McGuire, R. J. Mitchell, and R. O. Teskey. 2004. Assessing variation in the radial profile of sap flux density in Pinus species and its effect on daily water use. Tree Physiology **24**:241-249.

Gebauer, T., V. Horna, and C. Leuschner. 2008. Variability in radial sap flux density patterns and sapwood area among seven co-occurring temperate broad-leaved tree species. Tree Physiology **28**:1821-1830.

Guswa, A. J., M. A. Celia, and I. Rodriguez-Iturbe. 2002. Models of soil moisture dynamics in ecohydrology: A comparative study. Water Resources Research **38**.

Gutierrez Lopez, J., J. Licata, T. Pypker, and H. Asbjornsen. 2018. Effects of heater wattage on sap flux density estimates using an improved tree-cut experiment.

Jenkins, J. C., D. C. Chojnacky, L. S. Heath, and R. A. Birdsey. 2003. National-scale biomass estimators for United States tree species. Forest Science **49**:12-35.

Kubota, M., J. Tenhunen, R. Zimmermann, et al. 2005. Influences of environmental factors on the radial profile of sap flux density in Fagus crenata growing at different elevations in the Naeba Mountains, Japan. Tree Physiology **25**:545-556.

Kume, T., K. Otsuki, S. Du, et al. 2012. Spatial variation in sap flow velocity in semiarid region trees: its impact on stand-scale transpiration estimates. Hydrological Processes **26**:1161-1168.

Laclau, J. P., J. P. Arnaud M Fau - Bouillet, J. Bouillet Jp Fau - Ranger, and J. Ranger. 2001. Spatial distribution of Eucalyptus roots in a deep sandy soil in the Congo: relationships with the ability of the stand to take up water and nutrients.

Larcheveque, M., M. Maurel, A. Desrochers, and G. R. Larocque. 2011. How does drought tolerance compare between two improved hybrids of balsam poplar and an unimproved native species? Tree Physiology **31**:240-249.

Ouyang, Y., J. Zhang, T. D. Leininger, and B. R. Frey. 2015. A STELLA Model to Estimate Water and Nitrogen Dynamics in a Short-Rotation Woody Crop Plantation. Journal of Environmental Quality **44**:200-209.

Pallipparambil, G. R., S. Raghu, and R. N. Wiedenmann. 2015. Modeling the biomass production of the biofuel crop Miscanthus x giganteus, to understand and communicate benefits and risks in cultivation. Energy for Sustainable Development **27**:63-72.

Perala, D. A. 1993. Allometric Biomass Estimators for Aspen-Dominated Ecosystems in the Upper Great-Lakes. Usda Forest Service North Central Forest Experiment Station Research Paper:1-&.

Perlack, R. D., L. L. Wright, A. F. Turhollow, et al. 2005. Biomass as feedstock for a bioenergy and bioproducts industry: the technical feasibility of a billion-ton annual supply. Technical Report, Oak Ridge National Laboratory, Oak Ridge, Tennessee.

Poyatos, R., J. Cermak, and P. Llorens. 2007. Variation in the radial patterns of sap flux density in pubescent oak (Quercus pubescens) and its implications for tree and stand transpiration measurements. Tree Physiology **27**:537-548.

Richmond, B. 2004. An introduction to systems thinking. iSee Systems, Lebanon, NH, USA

Rodriguez-Iturbe, I., V. Isham, D. R. Cox, et al. 2006. Space-time modeling of soil moisture: Stochastic rainfall forcing with heterogeneous vegetation. Water Resources Research **42**.

Rodriguez-Iturbe, I., A. Porporato, F. Laio, and L. Ridolfi. 2001. Intensive or extensive use of soil moisture: plant strategies to cope with stochastic water availability. Geophysical Research Letters **28**:4495-4497.

Toillon, J., B. Rollin, E. Dalle, et al. 2013. Variability and plasticity of productivity, water-use efficiency, and nitrogen exportation rate in Salix short rotation coppice. Biomass & Bioenergy **56**:392-404.

Van Milgen, J., R. Boston, R. Kohn, and J. Ferguson. 1996. Comparison of available software for dynamic modeling. Annales de Zootechnie (Paris) **45**:257-273.

Xi, B. Y., Y. Wang, L. M. Jia, et al. 2013. Characteristics of fine root system and water uptake in a triploid Populus tomentosa plantation in the North China Plain: Implications for irrigation water management. Agricultural Water Management **117**:83-92.

Alvarado-Barrientos, M. S., V. Hernandez-Santana, and H. Asbjornsen. 2013. Variability of the radial profile of sap velocity in Pinus patula from contrasting stands within the seasonal cloud forest zone of Veracruz, Mexico. Agricultural and Forest Meteorology **168**:108-119.

Berry, Z. C., N. Looker, F. Holwerda, et al. 2018. Why size matters: the interactive influences of tree diameter distribution and sap flow parameters on upscaled transpiration. Tree Physiology **38**:263-275.

BETO. 2013. Multi-year program plan. Government Document. Bioenergy Technologies Office. DOE/EE-0915

Bloemen, J., R. Fichot, J. A. Horemans, et al. 2017. Water use of a multigenotype poplar short-rotation coppice from tree to stand scale. Global Change Biology Bioenergy **9**:370-384.

Bond-Lamberty, B., C. Wang, and S. T. Gower. 2002. Aboveground and belowground biomass and sapwood area allometric equations for six boreal tree species of northern Manitoba. Canadian Journal of Forest Research-Revue Canadienne De Recherche Forestiere **32**:1441-1450.

Bond-Lamberty, B., C. Wang, and S. T. Gower. 2014. Aboveground and belowground biomass and sapwood area allometric equations for six boreal tree species of northern Manitoba (vol 32, pg 1441, 2002). Canadian Journal of Forest Research-Revue Canadienne De Recherche Forestiere **44**:389-389.

Bouillet, J.-P., J.-P. Laclau, M. Arnaud, et al. 2002. Changes with age in the spatial distribution of roots of Eucalyptus clone in Congo: Impact on water and nutrient uptake. Forest Ecology and Management **171**:43-57.

Chen, L. X., Z. Q. Zhang, T. G. Zha, et al. 2014. Soil water affects transpiration response to rainfall and vapor pressure deficit in poplar plantation. New Forests **45**:235-250.

Costanza, R., D. Duplisea, and U. Kautsky. 1998. Ecological modelling and economic systems with STELLA - Introduction. Ecological Modelling **110**:1-4.

Ford, C. R., M. A. McGuire, R. J. Mitchell, and R. O. Teskey. 2004. Assessing variation in the radial profile of sap flux density in Pinus species and its effect on daily water use. Tree Physiology **24**:241-249.

Gebauer, T., V. Horna, and C. Leuschner. 2008. Variability in radial sap flux density patterns and sapwood area among seven co-occurring temperate broad-leaved tree species. Tree Physiology **28**:1821-1830.

Guswa, A. J., M. A. Celia, and I. Rodriguez-Iturbe. 2002. Models of soil moisture dynamics in ecohydrology: A comparative study. Water Resources Research **38**.

Gutierrez Lopez, J., J. Licata, T. Pypker, and H. Asbjornsen. 2018. Effects of heater wattage on sap flux density estimates using an improved tree-cut experiment.

Jenkins, J. C., D. C. Chojnacky, L. S. Heath, and R. A. Birdsey. 2003. National-scale biomass estimators for United States tree species. Forest Science **49**:12-35.

Kubota, M., J. Tenhunen, R. Zimmermann, et al. 2005. Influences of environmental factors on the radial profile of sap flux density in Fagus crenata growing at different elevations in the Naeba Mountains, Japan. Tree Physiology **25**:545-556.

Kume, T., K. Otsuki, S. Du, et al. 2012. Spatial variation in sap flow velocity in semiarid region trees: its impact on stand-scale transpiration estimates. Hydrological Processes **26**:1161-1168.

Laclau, J. P., J. P. Arnaud M Fau - Bouillet, J. Bouillet Jp Fau - Ranger, and J. Ranger. 2001. Spatial distribution of Eucalyptus roots in a deep sandy soil in the Congo: relationships with the ability of the stand to take up water and nutrients.

Larcheveque, M., M. Maurel, A. Desrochers, and G. R. Larocque. 2011. How does drought tolerance compare between two improved hybrids of balsam poplar and an unimproved native species? Tree Physiology **31**:240-249.

Ouyang, Y., J. Zhang, T. D. Leininger, and B. R. Frey. 2015. A STELLA Model to Estimate Water and Nitrogen Dynamics in a Short-Rotation Woody Crop Plantation. Journal of Environmental Quality **44**:200-209.

Pallipparambil, G. R., S. Raghu, and R. N. Wiedenmann. 2015. Modeling the biomass production of the biofuel crop Miscanthus x giganteus, to understand and communicate benefits and risks in cultivation. Energy for Sustainable Development **27**:63-72.

Perala, D. A. 1993. Allometric Biomass Estimators for Aspen-Dominated Ecosystems in the Upper Great-Lakes. Usda Forest Service North Central Forest Experiment Station Research Paper:1-&.

Perlack, R. D., L. L. Wright, A. F. Turhollow, et al. 2005. Biomass as feedstock for a bioenergy and bioproducts industry: the technical feasibility of a billion-ton annual supply. Technical Report, Oak Ridge National Laboratory, Oak Ridge, Tennessee.

Poyatos, R., J. Cermak, and P. Llorens. 2007. Variation in the radial patterns of sap flux density in pubescent oak (Quercus pubescens) and its implications for tree and stand transpiration measurements. Tree Physiology **27**:537-548.

Richmond, B. 2004. An introduction to systems thinking. iSee Systems, Lebanon, NH, USA

Rodriguez-Iturbe, I., V. Isham, D. R. Cox, et al. 2006. Space-time modeling of soil moisture: Stochastic rainfall forcing with heterogeneous vegetation. Water Resources Research **42**.

Rodriguez-Iturbe, I., A. Porporato, F. Laio, and L. Ridolfi. 2001. Intensive or extensive use of soil moisture: plant strategies to cope with stochastic water availability. Geophysical Research Letters **28**:4495-4497.

Toillon, J., B. Rollin, E. Dalle, et al. 2013. Variability and plasticity of productivity, water-use efficiency, and nitrogen exportation rate in Salix short rotation coppice. Biomass & Bioenergy **56**:392-404.

Van Milgen, J., R. Boston, R. Kohn, and J. Ferguson. 1996. Comparison of available software for dynamic modeling. Annales de Zootechnie (Paris) **45**:257-273.

Xi, B. Y., Y. Wang, L. M. Jia, et al. 2013. Characteristics of fine root system and water uptake in a triploid Populus tomentosa plantation in the North China Plain: Implications for irrigation water management. Agricultural Water Management **117**:83-92.

Alvarado-Barrientos, M. S., V. Hernandez-Santana, and H. Asbjornsen. 2013. Variability of the radial profile of sap velocity in Pinus patula from contrasting stands within the seasonal cloud forest zone of Veracruz, Mexico. Agricultural and Forest Meteorology **168**:108-119.

Berry, Z. C., N. Looker, F. Holwerda, et al. 2018. Why size matters: the interactive influences of tree diameter distribution and sap flow parameters on upscaled transpiration. Tree Physiology **38**:263-275.

BETO. 2013. Multi-year program plan. Government Document. Bioenergy Technologies Office. DOE/EE-0915

Bloemen, J., R. Fichot, J. A. Horemans, et al. 2017. Water use of a multigenotype poplar short-rotation coppice from tree to stand scale. Global Change Biology Bioenergy **9**:370-384.

Bond-Lamberty, B., C. Wang, and S. T. Gower. 2002. Aboveground and belowground biomass and sapwood area allometric equations for six boreal tree species of northern Manitoba. Canadian Journal of Forest Research-Revue Canadienne De Recherche Forestiere **32**:1441-1450.

Bond-Lamberty, B., C. Wang, and S. T. Gower. 2014. Aboveground and belowground biomass and sapwood area allometric equations for six boreal tree species of northern Manitoba (vol 32, pg 1441, 2002). Canadian Journal of Forest Research-Revue Canadienne De Recherche Forestiere **44**:389-389.

Bouillet, J.-P., J.-P. Laclau, M. Arnaud, et al. 2002. Changes with age in the spatial distribution of roots of Eucalyptus clone in Congo: Impact on water and nutrient uptake. Forest Ecology and Management **171**:43-57.

Chen, L. X., Z. Q. Zhang, T. G. Zha, et al. 2014. Soil water affects transpiration response to rainfall and vapor pressure deficit in poplar plantation. New Forests **45**:235-250.

Costanza, R., D. Duplisea, and U. Kautsky. 1998. Ecological modelling and economic systems with STELLA - Introduction. Ecological Modelling **110**:1-4.

Ford, C. R., M. A. McGuire, R. J. Mitchell, and R. O. Teskey. 2004. Assessing variation in the radial profile of sap flux density in Pinus species and its effect on daily water use. Tree Physiology **24**:241-249.

Gebauer, T., V. Horna, and C. Leuschner. 2008. Variability in radial sap flux density patterns and sapwood area among seven co-occurring temperate broad-leaved tree species. Tree Physiology **28**:1821-1830.

Guswa, A. J., M. A. Celia, and I. Rodriguez-Iturbe. 2002. Models of soil moisture dynamics in ecohydrology: A comparative study. Water Resources Research **38**.

Gutierrez Lopez, J., J. Licata, T. Pypker, and H. Asbjornsen. 2018. Effects of heater wattage on sap flux density estimates using an improved tree-cut experiment.

Jenkins, J. C., D. C. Chojnacky, L. S. Heath, and R. A. Birdsey. 2003. National-scale biomass estimators for United States tree species. Forest Science **49**:12-35.

Kubota, M., J. Tenhunen, R. Zimmermann, et al. 2005. Influences of environmental factors on the radial profile of sap flux density in Fagus crenata growing at different elevations in the Naeba Mountains, Japan. Tree Physiology **25**:545-556.

Kume, T., K. Otsuki, S. Du, et al. 2012. Spatial variation in sap flow velocity in semiarid region trees: its impact on stand-scale transpiration estimates. Hydrological Processes **26**:1161-1168.

Laclau, J. P., J. P. Arnaud M Fau - Bouillet, J. Bouillet Jp Fau - Ranger, and J. Ranger. 2001. Spatial distribution of Eucalyptus roots in a deep sandy soil in the Congo: relationships with the ability of the stand to take up water and nutrients.

Larcheveque, M., M. Maurel, A. Desrochers, and G. R. Larocque. 2011. How does drought tolerance compare between two improved hybrids of balsam poplar and an unimproved native species? Tree Physiology **31**:240-249.

Ouyang, Y., J. Zhang, T. D. Leininger, and B. R. Frey. 2015. A STELLA Model to Estimate Water and Nitrogen Dynamics in a Short-Rotation Woody Crop Plantation. Journal of Environmental Quality **44**:200-209.

Pallipparambil, G. R., S. Raghu, and R. N. Wiedenmann. 2015. Modeling the biomass production of the biofuel crop Miscanthus x giganteus, to understand and communicate benefits and risks in cultivation. Energy for Sustainable Development **27**:63-72.

Perala, D. A. 1993. Allometric Biomass Estimators for Aspen-Dominated Ecosystems in the Upper Great-Lakes. Usda Forest Service North Central Forest Experiment Station Research Paper:1-&.

Perlack, R. D., L. L. Wright, A. F. Turhollow, et al. 2005. Biomass as feedstock for a bioenergy and bioproducts industry: the technical feasibility of a billion-ton annual supply. Technical Report, Oak Ridge National Laboratory, Oak Ridge, Tennessee.

Poyatos, R., J. Cermak, and P. Llorens. 2007. Variation in the radial patterns of sap flux density in pubescent oak (Quercus pubescens) and its implications for tree and stand transpiration measurements. Tree Physiology **27**:537-548.

Richmond, B. 2004. An introduction to systems thinking. iSee Systems, Lebanon, NH, USA

Rodriguez-Iturbe, I., V. Isham, D. R. Cox, et al. 2006. Space-time modeling of soil moisture: Stochastic rainfall forcing with heterogeneous vegetation. Water Resources Research **42**.

Rodriguez-Iturbe, I., A. Porporato, F. Laio, and L. Ridolfi. 2001. Intensive or extensive use of soil moisture: plant strategies to cope with stochastic water availability. Geophysical Research Letters **28**:4495-4497.

Toillon, J., B. Rollin, E. Dalle, et al. 2013. Variability and plasticity of productivity, water-use efficiency, and nitrogen exportation rate in Salix short rotation coppice. Biomass & Bioenergy **56**:392-404.

Van Milgen, J., R. Boston, R. Kohn, and J. Ferguson. 1996. Comparison of available software for dynamic modeling. Annales de Zootechnie (Paris) **45**:257-273.

Xi, B. Y., Y. Wang, L. M. Jia, et al. 2013. Characteristics of fine root system and water uptake in a triploid Populus tomentosa plantation in the North China Plain: Implications for irrigation water management. Agricultural Water Management **117**:83-92.

Alvarado-Barrientos, M. S., V. Hernandez-Santana, and H. Asbjornsen. 2013. Variability of the radial profile of sap velocity in Pinus patula from contrasting stands within the seasonal cloud forest zone of Veracruz, Mexico. Agricultural and Forest Meteorology **168**:108-119.

Berry, Z. C., N. Looker, F. Holwerda, et al. 2018. Why size matters: the interactive influences of tree diameter distribution and sap flow parameters on upscaled transpiration. Tree Physiology **38**:263-275.

BETO. 2013. Multi-year program plan. Government Document. Bioenergy Technologies Office. DOE/EE-0915

Bloemen, J., R. Fichot, J. A. Horemans, et al. 2017. Water use of a multigenotype poplar short-rotation coppice from tree to stand scale. Global Change Biology Bioenergy **9**:370-384.

Bond-Lamberty, B., C. Wang, and S. T. Gower. 2002. Aboveground and belowground biomass and sapwood area allometric equations for six boreal tree species of northern Manitoba. Canadian Journal of Forest Research-Revue Canadienne De Recherche Forestiere **32**:1441-1450.

Bond-Lamberty, B., C. Wang, and S. T. Gower. 2014. Aboveground and belowground biomass and sapwood area allometric equations for six boreal tree species of northern Manitoba (vol 32, pg 1441, 2002). Canadian Journal of Forest Research-Revue Canadienne De Recherche Forestiere **44**:389-389.

Bouillet, J.-P., J.-P. Laclau, M. Arnaud, et al. 2002. Changes with age in the spatial distribution of roots of Eucalyptus clone in Congo: Impact on water and nutrient uptake. Forest Ecology and Management **171**:43-57.

Chen, L. X., Z. Q. Zhang, T. G. Zha, et al. 2014. Soil water affects transpiration response to rainfall and vapor pressure deficit in poplar plantation. New Forests **45**:235-250.

Costanza, R., D. Duplisea, and U. Kautsky. 1998. Ecological modelling and economic systems with STELLA - Introduction. Ecological Modelling **110**:1-4.

Ford, C. R., M. A. McGuire, R. J. Mitchell, and R. O. Teskey. 2004. Assessing variation in the radial profile of sap flux density in Pinus species and its effect on daily water use. Tree Physiology **24**:241-249.

Gebauer, T., V. Horna, and C. Leuschner. 2008. Variability in radial sap flux density patterns and sapwood area among seven co-occurring temperate broad-leaved tree species. Tree Physiology **28**:1821-1830.

Guswa, A. J., M. A. Celia, and I. Rodriguez-Iturbe. 2002. Models of soil moisture dynamics in ecohydrology: A comparative study. Water Resources Research **38**.

Gutierrez Lopez, J., J. Licata, T. Pypker, and H. Asbjornsen. 2018. Effects of heater wattage on sap flux density estimates using an improved tree-cut experiment.

Jenkins, J. C., D. C. Chojnacky, L. S. Heath, and R. A. Birdsey. 2003. National-scale biomass estimators for United States tree species. Forest Science **49**:12-35.

Kubota, M., J. Tenhunen, R. Zimmermann, et al. 2005. Influences of environmental factors on the radial profile of sap flux density in Fagus crenata growing at different elevations in the Naeba Mountains, Japan. Tree Physiology **25**:545-556.

Kume, T., K. Otsuki, S. Du, et al. 2012. Spatial variation in sap flow velocity in semiarid region trees: its impact on stand-scale transpiration estimates. Hydrological Processes **26**:1161-1168.

Laclau, J. P., J. P. Arnaud M Fau - Bouillet, J. Bouillet Jp Fau - Ranger, and J. Ranger. 2001. Spatial distribution of Eucalyptus roots in a deep sandy soil in the Congo: relationships with the ability of the stand to take up water and nutrients.

Larcheveque, M., M. Maurel, A. Desrochers, and G. R. Larocque. 2011. How does drought tolerance compare between two improved hybrids of balsam poplar and an unimproved native species? Tree Physiology **31**:240-249.

Ouyang, Y., J. Zhang, T. D. Leininger, and B. R. Frey. 2015. A STELLA Model to Estimate Water and Nitrogen Dynamics in a Short-Rotation Woody Crop Plantation. Journal of Environmental Quality **44**:200-209.

Pallipparambil, G. R., S. Raghu, and R. N. Wiedenmann. 2015. Modeling the biomass production of the biofuel crop Miscanthus x giganteus, to understand and communicate benefits and risks in cultivation. Energy for Sustainable Development **27**:63-72.

Perala, D. A. 1993. Allometric Biomass Estimators for Aspen-Dominated Ecosystems in the Upper Great-Lakes. Usda Forest Service North Central Forest Experiment Station Research Paper:1-&.

Perlack, R. D., L. L. Wright, A. F. Turhollow, et al. 2005. Biomass as feedstock for a bioenergy and bioproducts industry: the technical feasibility of a billion-ton annual supply. Technical Report, Oak Ridge National Laboratory, Oak Ridge, Tennessee.

Poyatos, R., J. Cermak, and P. Llorens. 2007. Variation in the radial patterns of sap flux density in pubescent oak (Quercus pubescens) and its implications for tree and stand transpiration measurements. Tree Physiology **27**:537-548.

Richmond, B. 2004. An introduction to systems thinking. iSee Systems, Lebanon, NH, USA

Rodriguez-Iturbe, I., V. Isham, D. R. Cox, et al. 2006. Space-time modeling of soil moisture: Stochastic rainfall forcing with heterogeneous vegetation. Water Resources Research **42**.

Rodriguez-Iturbe, I., A. Porporato, F. Laio, and L. Ridolfi. 2001. Intensive or extensive use of soil moisture: plant strategies to cope with stochastic water availability. Geophysical Research Letters **28**:4495-4497.

Toillon, J., B. Rollin, E. Dalle, et al. 2013. Variability and plasticity of productivity, water-use efficiency, and nitrogen exportation rate in Salix short rotation coppice. Biomass & Bioenergy **56**:392-404.

Van Milgen, J., R. Boston, R. Kohn, and J. Ferguson. 1996. Comparison of available software for dynamic modeling. Annales de Zootechnie (Paris) **45**:257-273.

Xi, B. Y., Y. Wang, L. M. Jia, et al. 2013. Characteristics of fine root system and water uptake in a triploid Populus tomentosa plantation in the North China Plain: Implications for irrigation water management. Agricultural Water Management **117**:83-92.